ROLE OF MICRORNAS IN IMPROVED OSTEOGENICITY OF TOPOGRAPHICALLY MODIFIED TITANIUM IMPLANT SURFACES

Nishant Chakravorty

Bachelor of Medicine & Bachelor of Surgery (MBBS)
Master of Medical Science & Technology (MMST)

Submitted in fulfillment of the requirements for the degree of

Doctor of Philosophy

Institute of Health & Biomedical Innovation

Science & Engineering Faculty

Queensland University of Technology

July, 2014

Keywords

cell signaling, gene expression, microarray, microRNA, micro-roughened titanium surface, modSLA, SLA, osteogenesis, osteoprogenitor differentiation, titanium surface modification.

Abstract

Topographically modified micro-roughened titanium implants, like the clinically successful dental implants - sand-blasted, large grit, acid-etched (SLA) and its successor, the chemically modified hydrophilic SLA (modSLA) surfaces, are recognized to have improved osseointegration (*in vivo*) and osteogenic properties (*in vitro*). Micro-roughened surfaces are known to induce "contact osteogenesis", wherein osseointegration occurs via direct deposition of new bone on the implant surface itself, making the *in vitro* osteogenic differentiation process an appropriate reflection of the *in vivo* osseointegration process. Micro-roughened surfaces, as such provide us with a unique model to explore the molecular mechanisms involved in the process of osteogenesis and osseointegration. Previous studies on modSLA and SLA surfaces have described the differential expression of several genes and pathways compared with smooth polished (SMO) surfaces, and have hinted on an early regulation of osteogenic differentiation on these surfaces; however, a structured approach exploring the molecular events was lacking.

MicroRNA mediated RNA-interference mechanisms, are known to be vital regulators of cell differentiation by translational repression and gene silencing. This project hypothesized that an early modulation of molecular processes by microRNA-mediated mechanisms on micro-roughened surfaces, like the modSLA and SLA, leads to their improved osteogenic differentiation and osseointegration. A whole-genome transcriptome analysis of human osteoprogenitor cells, performed using Affymetrix Human Genome U133 Plus 2.0 arrays, following 3 and 24 hours exposure to SLA and SMO surfaces, confirmed an early pro-osteogenic response on micro-roughened titanium surfaces at 24 hours. An initial pro-angiogenic and immunomodulatory response, as seen on the SLA surfaces, was seen to condition them for the pro-osteogenic response. Subsequently, the microRNA expression profile of osteoprogenitor cells on modSLA and SLA surfaces at 24 hours revealed the differential expression of several microRNAs on these surfaces (compared with SMO). Relatively minor differences were observed between modSLA and SLA surfaces.

The microRNAs downregulated on modSLA and SLA surfaces (compared with SMO), were seen to have several putative targets in the TGFβ/BMP and Wnt/Ca^{2+} pathways (based on bioinformatics-based target predictions using TargetScan); indicating a possible activation of these pro-osteogenic cell signaling pathways. To confirm whether signaling pathways are activated within 24 hours of interaction with these surfaces, the expression of key genes of TGFβ, Wnt, FGF, Notch, and Hedgehog pathways was investigated. The study concluded that TGFβ/BMP, Wnt (especially the Wnt/Ca^{2+}), and Notch pathways show higher expression on SLA & modSLA (compared with SMO), as early as 24 hours. The study also demonstrated a relatively high expression of cell signaling genes at 24 hours compared to 72 hours, further highlighting the importance of the early interaction of cells with the micro-roughened surfaces.

The project further explored the role of two miRNAs, miR-26a and miR-17, that were observed to be downregulated on the modSLA and SLA surfaces (compared with SMO) and had putative targets in TGFβ/BMP and Wnt/Ca^{2+} pathways, during the process of osteogenic differentiation. Both of the miRNAs were found to have inhibitory effects on the TGFβ/BMP and Wnt/Ca^{2+} pathways; and over-expressing these miRNAs was seen to delay the process of osteogenesis. Empirical evidences also suggested a coordinated modulation of these two pathways, with the activation of the TGFβ/BMP having a stimulatory effect on the Wnt/Ca^{2+} pathway. To explore the plausibility of using miRNA modulators to regulate osteogenesis on implant surfaces, inhibitors of miR-26a (i-miR-26a) and miR-17 (i-miR-17) were used on smooth polished titanium surfaces. i-miR-26a and i-miR-17 transfected cells were seen to have superior osteogenic differentiation on SMO surfaces.

Taken together, the findings of the project strongly suggest a highly regulated microRNA-mediated control of molecular mechanisms during the process of osteogenesis, that may be responsible for the superior osseointegration and osteogenic differentiation properties on micro-roughened titanium implant surfaces. The conclusions derived from the project, indicate the possibility of using microRNA modulators to enhance osseointegration and bone formation in clinically demanding circumstances.

List of Publications

Published or accepted manuscripts relevant to the work performed in this PhD:

1. **Nishant Chakravorty**, Anjali Jaiprakash, Saso Ivanovski & Yin Xiao. "Implant surface modifications and osseointegration." In Li, Qing & Mai, Yiu-Wing (Ed.) Biomaterials for Implants and Scaffolds (Springer Series in Biomaterials Science and Engineering). *Springer Science+Business Media New York (accepted Nov, 2012)*
2. **Nishant Chakravorty**, Stephen Hamlet, Anjali Jaiprakash, Ross Crawford, Adekunle Oloyede, Mohammed Alfarsi, Yin Xiao & Saso Ivanovski. "Pro-osteogenic topographical cues promote early activation of osteoprogenitor differentiation via enhanced TGFβ, Wnt, and Notch signaling." *Clinical and Oral Implants Research. 2014;25(4):475-86. (doi: 10.1111/clr.12178)*
3. **Nishant Chakravorty**, Saso Ivanovski, Indira Prasadam, Ross Crawford, Adekunle Oloyede & Yin Xiao. "The microRNA expression signature on modified titanium implant surfaces influences genetic mechanisms leading to osteogenic differentiation." *Acta Biomaterialia. 2012;8(9):3516-23 (doi: 10.1016/j.actbio.2012.05.008)*

Manuscripts in preparation relevant to the work performed in this PhD:

1. **Nishant Chakravorty**, Saso Ivanovski & Yin Xiao. "Osteogenic differentiation on micro-roughened titanium surfaces: A review of current concepts and knowledge."
2. Saso Ivanovski[*], **Nishant Chakravorty**[*], Jamie Harle, Stephen Hamlet, Yin Xiao, Peter Brett & Maurizio Tonetti. "Genome-wide transcriptional analysis of early interactions of osteoprogenitor cells with micro-rough titanium implants." ([*]*Co-first authors*)
3. **Nishant Chakravorty,** Anjali Jaiprakash, Ross Crawford, Adekunle Oloyede, Saso Ivanovski & Yin Xiao. "The miR-26a and miR-17 mediated cell signaling cross-talks guide osteogenic differentiation and osseointegration."

Other publications

1. Yinghong Zhou, **Nishant Chakravorty**, Yin Xiao & Wenyi Gu. "Mesenchymal stem cells and nano-structured surfaces." In Turksen, Kurshad (Ed.) Stem Cell Nanotechnology: Methods and Protocols. *Springer Protocols, Humana Press Inc., New York. (Methods in Molecular Biology. 2013;1058:133-48) (doi: 10.1007/7651_2013_30)*
2. Indira Prasadam, **Nishant Chakravorty**, Ross Crawford & Yin Xiao. "Mesenchymal stem cell concepts in osteoarthritis therapy: Current status of theory, technology, and applications." In Xiao, Yin (Ed.) Mesenchymal Stem Cells. *Nova Science Publishers, Inc., Hauppauge, New York, 2012*

Research Grant

1. Yin Xiao, **Nishant Chakravorty** & Saso Ivanovski. "Role of micro-RNAs in improved osteogenicity of modified titanium implant surfaces". Funded by *Australian Dental Research Foundation*, 2012 ($10,101.60)

Table of Contents

List of Figures

List of Tables

List of Key Abbreviations

Ago	Argonaute
AFM	Atomic force microscopy
ALP	Alkaline phosphatase
BC	Bone-derived osteoprogenitor cells
BMP	Bone morphogenetic protein
CAMKII	Ca^{2+}/calmodulin-dependent protein kinases II
COL1	Collagen type I
DAVID	Database for Annotation, Visualization and Integrated Discovery
DMEM	Dulbecco's modified Eagle's medium
DKK	Dickkopf
ECM	Extra-cellular matrix
EDAX	Energy Dispersive Spectrometry
ELISA	Enzyme-linked immunosorbent assay
FBS	Fetal bovine serum
FC	Fold change
FGF	Fibroblast growth factor
FZD	Frizzled
GO	Gene ontology
HIF1A	Hypoxia-inducible factor 1-α
hPDL	Human periodontal ligament
HUVEC	Human umbilical vein endothelial cell
IBSP	Integrin-binding sialoprotein
IPA	Ingenuity Pathway Analysis
ITGA2	Integrin-α2
ITGB1	Integrin-β1
ITI	International Team for Implantology
KEGG	Kyoto Encyclopedia of Genes and Genomes
LRP	Low-density lipoprotein receptor-related protein
MAPK	Mitogen-activated protein kinase
miRNA	MicroRNA
modSLA	Chemically modified hydrophilic SLA

MSC	Mesenchymal stem cell
OCN	Osteocalcin
OPG	Osteoprotegerin
OSX	Osterix
PCP	Planar cell polarity
pri-miRNA	primary-miRNA
qPCR	Quantitative polymerase chain reaction
mRNA	Messenger ribonucleic acid
RISC	RNA-induced silencing complex
RUNX2	Runt-related transcription factor 2
SEM	Scanning electron microscope
siRNA	Small interfering RNA
SLA	Sand-blasted, large grit, acid-etched
SLActive	Chemically modified hydrophilic SLA
SMA	Sandblasted with medium grit and acid pickled
SMAD	Small mothers against decapentaplegic
SMO	Smooth polished
TCPS	Tissue culture plastic surface
TGFβ	Transforming growth factor-β
TNFα	Tumor necrosis factor-α
TPS	Titanium plasma-sprayed
UTR	Untranslated region
VEGF	Vascular endothelial growth factor
WNT	Wingless-type MMTV integration site family

Statement of Original Authorship

The work contained in this thesis has not been previously submitted to meet requirements for an award at this or any other higher education institution. To the best of my knowledge and belief, the thesis contains no material previously published or written by another person except where due reference is made.

QUT Verified Signature

Signature:

Date: 10th July, 2014

Acknowledgements

At the end of my PhD journey, I wish to convey my heartfelt gratitude to everyone who extended his/her selfless support and encouragement. Firstly, I wish to thank my principal supervisor, Professor Yin Xiao, for providing me with this PhD opportunity at the Institute of Health & Biomedical Innovation (IHBI), Queensland University of Technology (QUT). I am grateful to him for his constant support and directions during this project. I am deeply indebted to Professor Saso Ivanovski for his gracious supervision and guidance throughout. He has been an epitome of a "friend, philosopher and guide" throughout my journey and I am highly obliged to him. I wish to thank Professor Ross Crawford and Professor Adekunle Oloyede for their invaluable support, guidance and advice throughout my PhD.

I wish to acknowledge Dr. Stephen Hamlet for all his support and assistance. My appreciation also goes to Dr. Sanjleena Singh who helped me with my work at the Central Analytical Research Facility (CARF), QUT; Mr. Robert Simpson and Dr. Michael Nefedov at School of Chemistry and Molecular Biosciences, University of Queensland (UQ). I am thankful to Dr. Anna Taubenberger for helping me with Atomic Force Microscopy (AFM) visualization of the titanium discs. Thanks to Dr. Shane Stegeman and Mr. Samuel Perry for their technical suggestions and assistance for the molecular cloning and luciferase reporter assay experiments. Dr. Thor Friis has been a great friend who was always willing to help and his suggestions are highly appreciated.

I wish to thank the Queensland University of Technology for the QUT Postgraduate Research Award (QUTPRA) and tuition fee waiver scholarships; and Institute of Health & Biomedical Innovation (IHBI) for the IHBI Top-up scholarship. The professional staff members at the institute have been of great help during my work. I also wish to acknowledge the staff members at QUT and Science & Engineering Faculty, for gracefully extending a helping hand whenever needed. IHBI also provided me with world-class research facilities that helped me in completing my experimental studies.

I wish to thank all the members of the Bone group, at IHBI. Their friendship has been a strong support through this long journey. I would like to express my gratefulness to Ms. Anjali Jaiprakash, for being so supportive and helping me

throughout my project duration and also for keeping the “family of friends” in Brisbane together. Thanks to Yash, Pavan, Sumanth and Ranjay - you people have been amazing friends. I would like to thank all my friends back in India, and especially, Malay and Sneh, for extending their help and moral support throughout this journey. Finally, I wish to thank my adoring family - my parents, elder brother, sister-in-law, my cute little nephew, and my wife Rashmi, for their endless support and encouragement throughout my life and their constant belief in me.

Dedicated to my family

Chapter 1: Introduction

1.1 BACKGROUND

The use of metallic implants as a clinical modality for the treatment of damaged bone or teeth has been in practice for ages. Implants help in restoration of damaged body parts by providing a supporting framework for the healing bone. This process of healing requires the structural and functional integration of the implant with the surrounding bone – a biological phenomenon known as "osseointegration". Titanium (Ti) has been a material of choice clinically for a long time, owing to its potential to support bone regeneration with little evidence of rejection of the implant. Scientists working in the field of biomaterials have tried several modifications of the titanium implants to improve its bone regeneration properties. Empirical studies have revealed that surface modifications greatly influence the regenerative potential of these implants [1]. Rough surfaces have been found to have better osteogenic potential and osseointegration properties *in vivo*, when compared with smooth surfaces.

The clinically successful dental implants – the sand-blasted, large-grit, acid-etched (SLA) Ti implant and its successor, the chemically modified hydrophilic SLA (modSLA or SLActive®) are topographically modified micro-roughened implant surfaces designed by Institut Straumann AG (Waldenburg, Switzerland), that have proven superior osseointegration and osteogenic properties compared with their smooth counterparts [2-5]. The SLA implant surface remains the gold standard in implant dentistry, although recent studies claim the modSLA surface to have further improved osseointegration and stability at earlier time points when compared with SLA implants [6] and they have also been shown to reduce the healing period *in vivo* further when compared to SLA surfaces [5].

Osseointegration, as a biological process requires the differentiation of "osteogenic" cells to mineralized bone cells. The molecular mechanisms of cellular differentiation of progenitor cells have been a perplexing and challenging process to decrypt. In this context, it is worth noting that superior osteogenic properties of micro-roughened titanium implant surfaces, and especially their ability to induce "contact osteogenesis" [7], allow us to use them as physiologically relevant surfaces to study the possible molecular regulatory mechanisms orchestrating these properties. This will further allow us to gain in-depth insights into the osteogenic differentiation process without using chemically supplemented "osteogenic" media.

Numerous genes and proteins have been found to be involved in the regulation of osteogenic differentiation. Several signaling proteins and pathways have been found to be imperative in the regulation of osteogenesis and no single pathway is responsible for osteogenesis on its own. The interplay and crosstalk between cell signaling pathways is known to guide the process of osteogenesis of progenitor cells.

Micro-RNAs (miRNAs) are small RNA molecules that have been known to influence the pattern of gene expression by translational repression and gene silencing [8]; and are known to be vital regulators of the cell differentiation process. However, their role in the modulation of cell signaling pathways guiding osteogenesis *in vitro* and osseointegration *in vivo* on implant surfaces hasn't been explored in detail. Understanding the pattern of expression of miRNAs in progenitor cells cultured on osteogenic surfaces, will aid in deciphering the molecular basis of osteogenesis and the influence of implant surfaces on progenitor cells. This knowledge may further assist us in designing implants with faster and better osseointegration and also help us in achieving superior osseointegration in clinically demanding circumstances. Therefore, the overall aim of this project was to investigate the role of microRNAs in guiding the process of osteogenesis on topographically modified titanium implant surfaces through their influence on pro-osteogenic cell signaling pathways.

1.2 SCOPE OF THE PROJECT

This prime focus of this project has been on the early stages of osteogenic differentiation, for which it derives empirical cues from micro-roughened titanium implant surfaces. The project initially explores the pro-osteogenic response on micro-roughened surfaces and investigates the sequence of early events that lead to their pro-osteogenic response. The first part of the work identifies a pertinent time-point to study the early molecular events during osteogenesis on topographically modified surfaces. The pattern of microRNA expression on modSLA and SLA surfaces is subsequently explored. A potential correlation of this expression pattern with the stimulation of the pro-osteogenic TGFβ/BMP and Wnt/Ca^{2+} pathways is deduced using bioinformatic prediction models. The next part of the project attempts to further strengthen these findings and describes the stimulation of pro-osteogenic cell signaling pathways (especially the TGFβ/BMP and Wnt/Ca^{2+} pathways) on these surfaces. Finally, the role of microRNAs, miR-26a and miR-17, on the regulation of

the TGFβ/BMP and Wnt/Ca^{2+} pathways, during osteogenesis is further discussed and attempts to accelerate the rate of osteogenesis on polished titanium implant surfaces are described.

1.3 THESIS OUTLINE

- Hypothesis & Aims: This chapter discusses the hypothesis and key aims of the project. It also provides a brief overview of the different studies conducted to achieve the aims.
- Literature Review: The literature review is divided into three sub-parts.
  - The first part consists of excerpts from an accepted book chapter discussing implant surfaces and the phenomenon of osseointegration.

    (***Book chapter - accepted**:* Nishant Chakravorty et al. "Implant surface modifications and osseointegration." In Li, Qing & Mai, Yiu-Wing (Ed.) Biomaterials for Implants and Scaffolds. Springer Series in Biomaterials Science and Engineering).
  - The second part discusses the possible role of microRNAs in osteoblast differentiation.
  - The third part details the current concepts and knowledge regarding osteogenic differentiation on SLA and modSLA surfaces and is a review manuscript in preparation.

    (***Manuscript in preparation:*** Nishant Chakravorty et al. "Osteogenic differentiation on micro-roughened titanium surfaces: A review of current concepts and knowledge.").
- The microarray study: This chapter details the study conducted for Aim 1 of the project and is a manuscript in preparation.

  (***Manuscript in preparation:*** Saso Ivanovski, Nishant Chakravorty, et al. "Genome-wide transcriptional analysis of early interactions of osteoprogenitor cells with micro-rough titanium implants.").
- The microRNA profiling study: This chapter details the study conducted for Aim 2 of the project and is a published manuscript.

(***Published manuscript:*** Nishant Chakravorty et al. "The microRNA expression signature on modified titanium implant surfaces influences genetic mechanisms leading to osteogenic differentiation." *Acta Biomaterialia. 2012;8(9):3516-23*).

- Activation of cell signaling pathways on modified titanium surfaces: This chapter details the study conducted for Aim 3 of the project and is a published manuscript.

  (***Published manuscript:*** Nishant Chakravorty et al. "Pro-osteogenic topographical cues promote early activation of osteoprogenitor differentiation via enhanced TGFβ, Wnt, and Notch signaling." *Clinical and Oral Implants Research, 2014;25(4):475-86*).

- The microRNAs, miR-26a & miR-17 and TGFβ/BMP & Wnt/Ca^{2+} pathways: This chapter details the study conducted for Aim 4 of the project and is a manuscript in preparation.

  (***Manuscript in preparation:*** Nishant Chakravorty et al. "The miR-26a and miR-17 mediated cell signaling cross-talks guide osteogenic differentiation and osseointegration.").

- General Discussion: This chapter discusses the rationale for the studies conducted, the key findings and the limitations of the project.

- Concluding Remarks: Finishing comments for the project.

Referencing style: The references for each chapter (except for Chapter 6) are in numbered format (consistent with the format for the journal, *Acta Biomaterilia*, where Chapter 5 was published). Chapter 6 has references in accordance with the format for the journal, *Clinical Oral Implants Research*, where it has been published.

Ethics approvals for the PhD project

Primary human cells/tissues used/approved:

- Established human cell lines
- Human ethics (neglible-low risk), Queensland Univeristy of Technology

Gene Modified Organisms (GMO) ethics:

- GMO exempt dealing, Queensland University of Technology

1.4 REFERENCES

[1] Le Guehennec L, Soueidan A, Layrolle P, Amouriq Y. Surface treatments of titanium dental implants for rapid osseointegration. Dent Mater 2007;23:844-54.

[2] Buser D, Schenk RK, Steinemann S, Fiorellini JP, Fox CH, Stich H. Influence of surface characteristics on bone integration of titanium implants. A histomorphometric study in miniature pigs. J Biomed Mater Res 1991;25:889-902.

[3] Gotfredsen K, Wennerberg A, Johansson C, Skovgaard LT, Hjorting-Hansen E. Anchorage of TiO2-blasted, HA-coated, and machined implants: an experimental study with rabbits. J Biomed Mater Res 1995;29:1223-31.

[4] Vlacic-Zischke J, Hamlet SM, Friis T, Tonetti MS, Ivanovski S. The influence of surface microroughness and hydrophilicity of titanium on the up-regulation of TGFbeta/BMP signalling in osteoblasts. Biomaterials 2011;32:665-71.

[5] Buser D, Broggini N, Wieland M, Schenk RK, Denzer AJ, Cochran DL, et al. Enhanced bone apposition to a chemically modified SLA titanium surface. J Dent Res 2004;83:529-33.

[6] Abdel-Haq J, Karabuda CZ, Arisan V, Mutlu Z, Kurkcu M. Osseointegration and stability of a modified sand-blasted acid-etched implant: an experimental pilot study in sheep. Clin Oral Implants Res 2011; 22:265-74.

[7] Osborn J, Newesely H. Dynamic aspects of the implant-bone interface. In: Heimke G, editor. Dental implants: Materials and Systems: München: Carl Hanser Verlag; 1980. p. 111-23.

[8] Bartel DP. MicroRNAs: Target recognition and regulatory functions. Cell 2009;136:215-33.

Chapter 2: Hypothesis & Aims

2.1 HYPOTHESIS

MicroRNAs (miRNAs) are vital regulators of cell differentiation and are known to influence gene expression by translational repression and gene silencing. This project hypothesized that an early modulation of molecular processes by microRNA-mediated mechanisms on micro-roughened surfaces, like the SLA and modSLA, lead to their enhanced osteogenic differentiation and osseointegration properties. The overall aim of this project has been to explore the early molecular events guiding osteogenesis on micro-roughened titanium implant surfaces, with a particular focus on the role of microRNAs in guiding these responses. The observations from this project attempt to unravel the genetic control of osteogenesis using cues from a physiologically relevant micro-environment akin to the bone micro-architecture. The findings of this project could be translated to clinically relevant situations, like osteoporosis that demand enhanced osteogenesis.

2.2 AIMS OF THE PROJECT

The specific aims of the project were:

Aim 1: To study the sequence of early molecular events leading to a pro-osteogenic response on micro-roughened titanium implant surfaces and identify an early time-point to study the molecular mechanisms on micro-roughened titanium implant surfaces.

Aim 2: To study the differences in microRNA expression profiles on modSLA and SLA surfaces in comparison with the smooth polished (SMO) surfaces and predict the putative regulation of key pro-osteogenic cell signaling pathways, following 24 hours of exposure.

Aim 3: To confirm the activation of key pro-osteogenic cell signaling pathways on modSLA and SLA surfaces, following 24 hours of exposure.

Aim 4: To explore the role of miR-26a and miR-17 in the regulation of the pro-osteogenic TGFβ/BMP and Wnt/Ca^{2+} pathways during the process of osteogenesis.

2.3 OVERVIEW OF THE PROJECT

A flow-diagram explaining the sequence of the studies conducted for the project is showing in Figure 2-1.

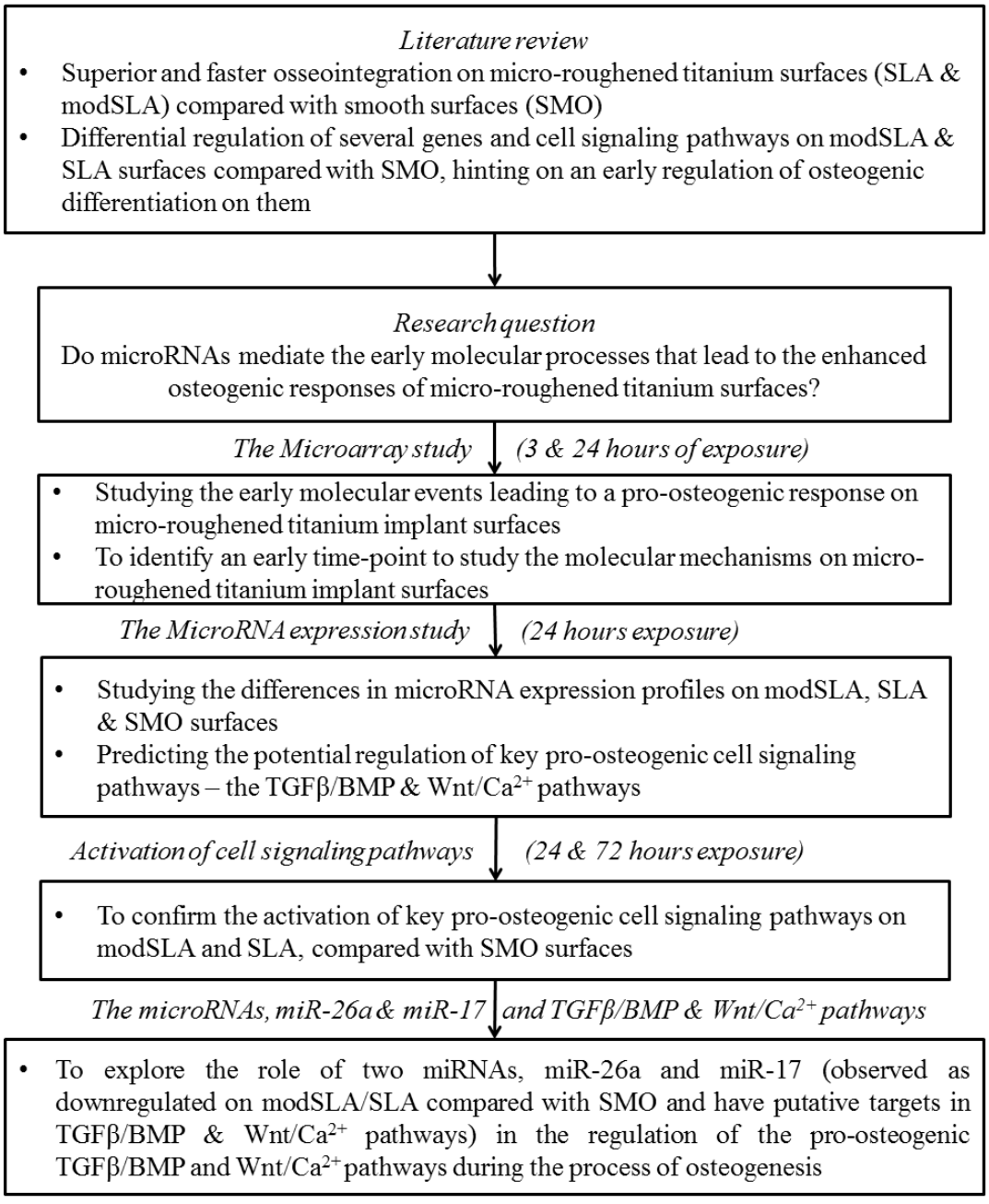

Figure 2-1: Flow-diagram describing the aims of the project

The project was designed as four separate studies, based on the aims as described above:

2.3.1 Study 1: The microarray study

Microarrays with their ability to comprehensively capture the expression of a large number of genes provide us with one of the best experimental methods to screen for the whole genome transcriptomic profile, and investigate the early molecular events on micro-roughened titanium implant surfaces. The study was designed as follows:

Mineralization properties of micro-roughened SLA surfaces

Human osteoprogenitor cells were cultured on SLA and smooth polished (SMO) surfaces and compared for their ability to induce osteogenic differentiation and mineral deposition.

Whole genome microarray expression profiling

A whole genome microarray expression profiling (Affymetrix Human Genome U133 Plus 2.0 arrays) was conducted, following exposure of human osteoprogenitor cells on SLA and SMO surfaces, for 3 and 24 hours, to study the early molecular responses on these surfaces. The comparative data analyses (between SLA and SMO, and the temporal comparisons) were performed using GeneSpring GX12.5 software.

Analysis of the microarray data using DAVID and IPA

To affirm the biological meaning of the data obtained from GeneSpring, functional clustering analysis was performed using the Database for Annotation, Visualization and Integrated Discovery (DAVID) and Ingenuity Pathways Analysis (IPA) tools. Molecular, physiological clusters and potential upstream regulators for the molecular processes enriched on SLA surfaces (compared with SMO) were extracted and conclusions were derived. A time-course analysis was also performed to explore the sequence of events.

2.3.2 Study 2: The microRNA expression profiling study

The expression pattern of microRNAs related to cell development and differentiation was assessed between modSLA, SLA, and SMO surfaces.

Effect of surface topography and hydrophilicity on the differential regulation of genes following 24 hours of exposure to titanium surfaces

The effect of modSLA and SLA surfaces on the differential regulation of BMP2, BMP6, ACVR1, FZD6, WNT5A, ITGB1, and ITGA2, following 24 hours of exposure of human osteoprogenitor cells was tested. These genes were found to be differentially regulated on micro-roughened surfaces compared with SMO at later time-points in previous studies.

The microRNA expression profiling

The differential regulation of microRNAs on modSLA, SLA, and SMO surfaces was assessed using Human Cell Development & Differentiation miRNA PCR Array (SABiosciences, Frederick, Maryland, USA), following 24 hours of exposure.

Target predictions for the differentially regulated miRNAs

Bioinformatics based target predictions for the differentially regulated miRNAs were performed using TargetScan. As previous studies had reported the activation of several genes of the TGFβ/BMP and Wnt/Ca^{2+} pathways, the potential regulation of these pathways by the differentially regulated miRNAs was assessed.

2.3.3 Study 3: Activation of cell signaling pathways on modSLA, SLA, and SMO surfaces

To confirm the correlation between the differential regulation of miRNAs (as observed in the previous part of the project) and cell signaling pathways, the activation of cell signaling pathways on modSLA, SLA, and SMO surfaces was tested. The study was designed as follows:

Surface imaging and phenotypic changes in cells cultured on micro-roughened surfaces

The surface topography of modSLA, SLA, and SMO surfaces was visualized using Atomic force microscopy (AFM) and Scanning electron microscope (SEM). The phenotypic variations in human osteoprogenitor cells cultured on micro-roughened surfaces and SMO surfaces was observed using SEM.

Cell signaling pathways activation on modSLA, SLA, and SMO surfaces

The differential regulation of key genes of the TGFβ/BMP, Wnt, FGF, Hedgehog, and Notch was evaluated on modSLA, SLA, and SMO surfaces using

Human Stem Cell Signaling PCR Array (SABiosciences, Frederick, MD, USA), following 24 and 72 hours of exposure.

Mineralization properties and expression of osteogenesis associated genes on modSLA, SLA, and SMO surfaces

The osteogenic differentiation potential of modSLA, SLA, and SMO surfaces was further explored using Alizarin Red S, ALP activity and expression analysis of osteogenesis associated genes.

2.3.4 Study 4: The microRNAs, miR-26a & miR-17 and TGFβ/BMP & Wnt/Ca^{2+} pathways relationship

The microRNAs, miR-26a and miR-17, were seen to be downregulated on modSLA and SLA surfaces (compared with SMO) in the first part of the project. They were also observed to have putative targets in the TGFβ/BMP and Wnt/Ca^{2+} pathways, which in turn were found to be stimulated on the micro-roughened surfaces. This study explored the role of miR-26a and miR-17 in the regulation of TGFβ/BMP and Wnt/Ca^{2+} pathways during osteogenesis.

Over-expression of miR-26a and miR-17

The miRNAs, miR-26a and miR-17, were confirmed to have lower expression on modSLA and SLA surfaces compared with SMO surfaces. This part of the project explored the role of miR-26a and miR-17 by transfecting synthetic miRNA mimics into SAOS-2 human osteoblast-like cells, and inducing osteogenic differentiation. The effects of over-expressing miR-26a and miR-17 on the TGFβ/BMP and Wnt/Ca^{2+} pathways were investigated at the gene and protein level.

Target validation experiments

Putative TGFβ/BMP and Wnt/Ca^{2+} pathway gene targets for miR-26a and miR-17 were cloned into pmirGLO Dual-Luciferase vector. Target validation experiments were performed after co-transfecting the target plasmids and miRNAs into Hep2 cells.

TGFβ/BMP and Wnt/Ca^{2+} pathway cross-talk

The influence of TGFβ/BMP and Wnt/Ca^{2+} pathways on each other was explored using recombinant human BMP2 and KN93 (inhibitor for Wnt/Ca^{2+} pathway).

Inhibition of miR-26a and miR-17 on SMO surfaces and osteogenesis

The impact of suppression of miR-26a and miR-17 on the osteogenic differentiation on SMO surfaces was investigated using Alizarin Red S staining and ALP activity.

Chapter 3: Literature Review

3.1 IMPLANT SURFACE MODIFICATIONS AND OSSEOINTEGRATION

Nishant Chakravorty, Anjali Jaiprakash, Saso Ivanovski & Yin Xiao

Accepted Book chapter: In Li, Qing & Mai, Yiu-Wing (Ed.) Biomaterials for Implants and Scaffolds (Springer Series in Biomaterials Science and Engineering). Springer Science+Business Media New York (accepted Nov, 2012)

Suggested Statement of Contribution of Co-Authors for Thesis by Publication

Contributors	Statement of contribution
Nishant Chakravorty	Involved in the conception and design of the manuscript. Wrote the manuscript.
Anjali Jaiprakash	Involved in critiquing the manuscript.
Saso Ivanovski	Involved in manuscript preparation and reviewing.
Yin Xiao	Involved in designing and preparation of the manuscript and reviewing.

Principal Supervisor Confirmation

I have sighted email or other correspondence from all co-authors confirming their certifying authorship

Prof. Yin Xiao		**10th July, 2014**
Name	**Signature**	**Date**

Excerpts from the book chapter follow

3.3 OSTEOGENIC DIFFERENTIATION ON MICRO-ROUGHENED TITANIUM SURFACES: A REVIEW OF CURRENT CONCEPTS AND KNOWLEDGE

Nishant Chakravorty, Saso Ivanovski & Yin Xiao

(Review manuscript in preparation)

Suggested Statement of Contribution of Co-Authors for Thesis by Publication

Contributors	Statement of contribution
Nishant Chakravorty	Involved in the conception and design of the manuscript. Wrote the manuscript.
Saso Ivanovski	Involved in manuscript preparation and reviewing.
Yin Xiao	Involved in manuscript preparation and reviewing.

Principal Supervisor Confirmation

I have sighted email or other correspondence from all co-authors confirming their certifying authorship

Prof. Yin Xiao		**10th July, 2014**
Name	**Signature**	**Date**

3.3.1 Introduction

The quest for superior osseointegration has lead researchers to experiment with surface modifications of titanium implants. Several studies and reviews have reported improved bone-to-implant contact with micro-roughened surfaces compared with smooth surfaces [5, 54-57]. Bone formation on implant surfaces occurs either via new bone deposition on the surface of existing bone (distance osteogenesis) or by direct osteoblastic activity on the implant surface itself (contact osteogenesis) as described by Osborn and Newesley (Figure 3-3) [58]. Osseointegration on machined (minimally rough) implant surfaces has been shown to occur by distance osteogenesis [59]. In contrast to this, rough (micro-roughened) implant surfaces are believed to integrate by contact osteogenesis [59-61].

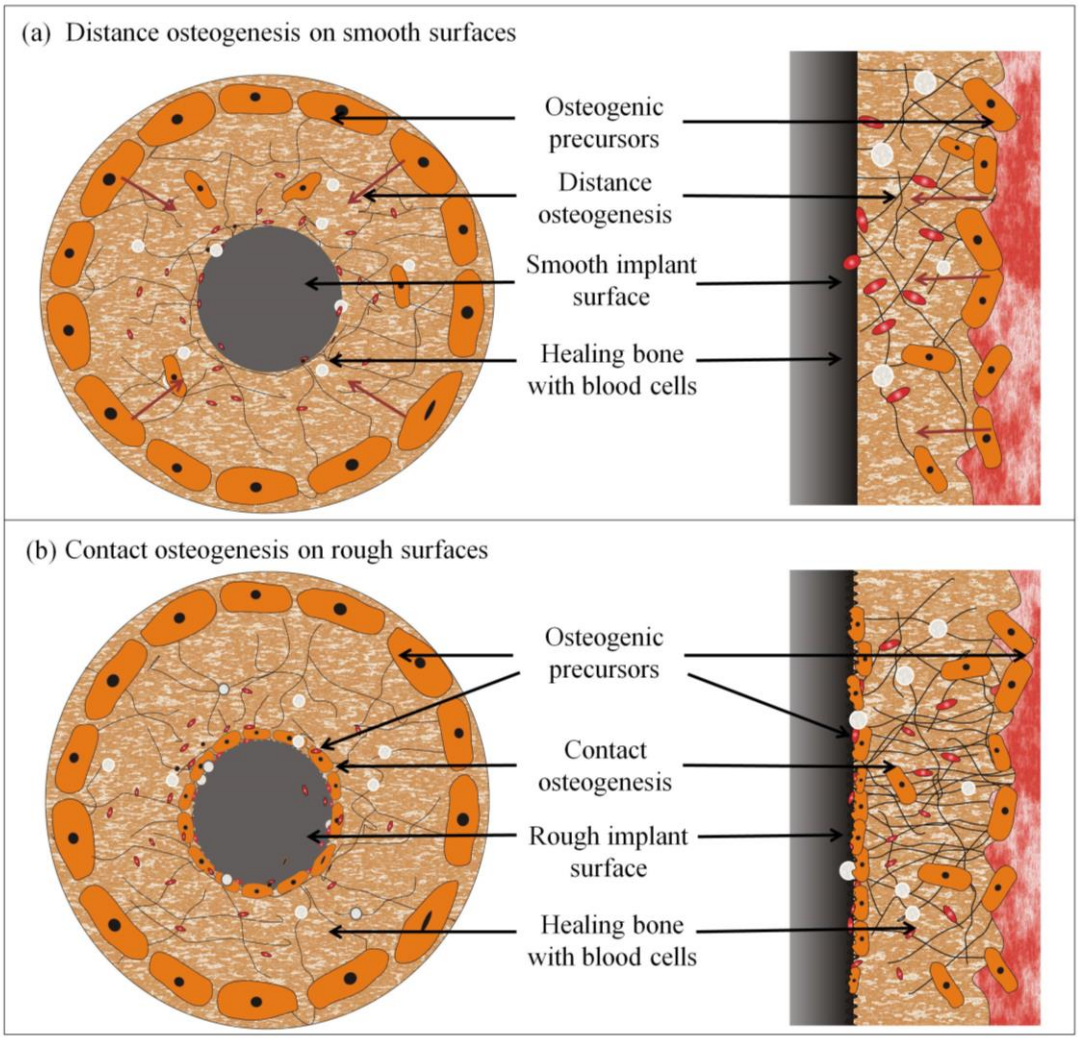

Figure 3-3: The concept of "distance osteogenesis" on smooth and "contact osteogenesis" on rough implant surfaces. Adapted from Davies et al. (2003) [59].

The molecular mechanisms regulating differentiation of stem cells and progenitor cells are known to be complex and difficult to interpret. Studying the molecular mechanisms of differentiation relies on *in vitro* experimentation and validation models. Traditional methods used to study osteogenic differentiation involve the use of chemical mediators like dexamethasone, β-glycerophosphate and L-ascorbic acid; and occasionally supplements such as vitamin D3, Transforming Growth Factor-beta (TGF-β) and bone morphogenetic proteins (BMPs). However, one of the major limitations of using such models is that they do not resemble the osteogenic conditions encountered *in vivo*. In contrast to this, micro-roughened implant surfaces by virtue of their characteristic contact osteogenesis phenomenon provide us with a unique model to explore the molecular mechanisms of osteogenic differentiation.

Newer implant surfaces have shown promising results for osteogenic differentiation of progenitor cells *in vitro* and superior *in vivo* osseointegration properties [62]. A chain of molecular events are initiated following the insertion of an implant and this ultimately leads to osteogenesis and new bone formation as depicted in Figure 3-4.

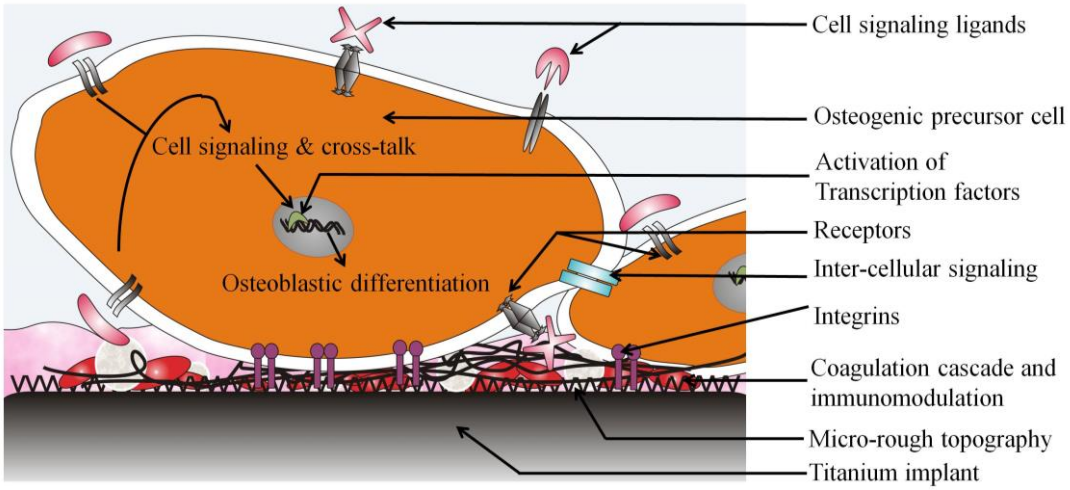

Figure 3-4: Osteogenic differentiation process on micro-roughened implant surfaces.

Osteoblasts have been shown to create an osteogenic microenvironment when cultured on topographically micro-roughened implant surfaces. *In vitro* testing of the interactions of osteogenic cells with implant surfaces is routinely employed for pre-clinical testing of their efficacy. This also provides an opportunity to use implant surfaces to study the molecular regulation of osteogenesis. In this context, the

topographically modified titanium dental implants - the sand blasted, large-grit, acid-etched (SLA) and its successor, the hydrophilic SLA (modSLA, also known as SLActive®), are worth mentioning. They are known to have excellent osseointegration properties, and have provided interesting insights into the processes of osteogenic differentiation and osseointegration. In fact, SLA surfaces, per se have been confirmed to induce "contact osteogenesis" [63]. These surfaces therefore, offer us excellent models to study the osteogenic differentiation process. The aim of this chapter is to explore the current concepts pertaining to the molecular mechanisms involved in osteogenesis, based on studies using these implant surfaces as prototypes for physiologically relevant substrates.

3.3.2 The topographically modified titanium implant surfaces

Sand-blasted, large grit, acid-etched (SLA) Ti implant is a micro-roughened implant surface designed by Institut Straumann AG (Waldenburg, Switzerland) that has proven superior osseointegration properties and supports osteogenesis [2, 4]. This was proven by Cochran et al. when they showed that the SLA surface provides better osseous contact at earlier time points when compared with a titanium plasma-sprayed (TPS) surface [64]. The SLA implant surface received FDA clearance in 1994 and has become a gold standard in implant dentistry [65].

Another modification of the SLA surface – modSLA (commercially known as SLActive®), also manufactured by Institut Straumann AG, has a higher wettability (hydrophilicity) compared to SLA. This implant surface has been shown to have better osseointegration and stability at earlier time points when compared with the SLA implants [66]. A faster and better structured bone formation *in vivo*, with greater vascularization and increased osteocalcin levels has been observed around modSLA implants when compared with SLA surfaces at 14 days [67]. This implant surface has also been shown to reduce the healing period further (compared with SLA) [68]. Further, it has been shown that the expression of osteogenic phenotype and differentiation of osteoblast-like cells (MG63 cells) co-cultured with human umbilical vein endothelial cells (HUVECs) is enhanced with hydrophilicity of Ti implant surfaces like modSLA [69]. A study by Vlacic-Zischke et al. suggested that the better osseointegration property of hydrophilic modSLA surfaces is possibly mediated through BMP signaling [24].

3.3.3 Microstructural characteristics of modSLA and SLA implants

The modSLA and SLA implants are essentially topographically (modSLA and SLA) and chemically (modSLA) modified titanium implant surfaces. Commercially pure (c.p.) grade II titanium (Institut Straumann AG, CH-4002, Basel, Switzerland) is the starting point for preparing these implant surfaces; from which the SLA surface is prepared by sandblasting using large grits of 0.25–0.50 mm and etching with hydrochloric/sulphuric acid [70]. The micro-rough topography is attributed to the sandblasting process. However, the acid-etching process imparts submicron scale roughness properties [71]. The SLA surface when rinsed under N_2 protection and stored in an isotonic saline (NaCl) solution again protected by N_2 filling, produces the modSLA surface [70]. Different studies have reported subtle differences in the micro-roughness of the topographically modified surfaces. The study by Buser et al. showed the S_a of modSLA and SLA (mean arithmetic deviation of surface) to be 1.15±0.05 µm [68]; whereas Vlacic-Zischke et al. reported it to be 1.8 µm [24] and Olivares-Navarrete et al. showed the R_a (the 2D counterpart of 3D descriptor S_a) to be of the order of 3.22 µm [72]. These differences may possibly be attributed to the variations in the techniques used in different studies. The topographical features of modSLA and SLA surfaces are fundamentally similar, showing surface micro-roughness in contrast to the topography of polished surfaces, that have a S_a value of approximately 0.33 µm [26]. The modSLA and SLA surfaces are known to show micron (10-50 µm) and submicron (1-2 µm) scale surface roughness [26]. Scanning electron microscopy (SEM) images show microstructures with cavities approximately 10 µm, which could be a result of the sand-blasting process [73]. Recent studies, using high resolution imaging techniques, have also reported the presence of nano-structures that are present only on modSLA surfaces in contrast to SLA and smooth (SMO) surfaces [74-76]. Nano-scale roughness superimposed on microrough surfaces has been demonstrated to improve osteoblastic differentiation and viability on SLA surfaces [77-79]. modSLA surfaces have a hydrophilic surface and the contact angle testing shows a contact angle of 0^0 as opposed to SLA surfaces that have contact angles in the range of 140^0 [70].

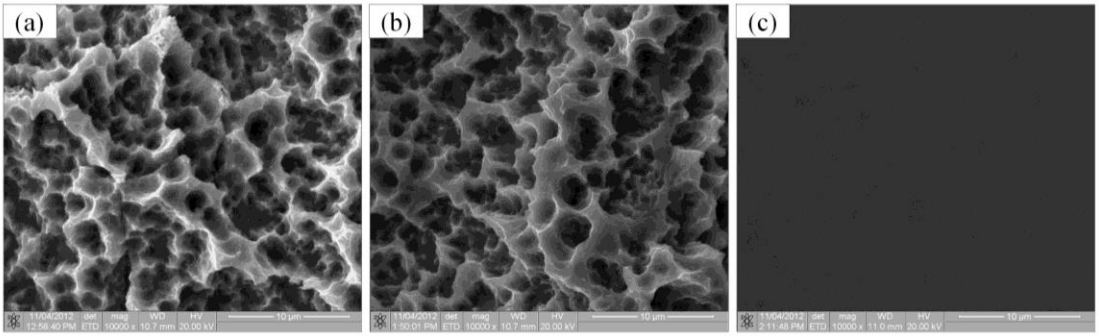

Figure 3-5: Scanning electron microscope images of (a) modSLA, (b) SLA and (c) SMO (smooth polished) Straumann titanium implant surfaces (10,000x magnification).

X-ray photoelectron spectroscopy analysis of modSLA and SLA surfaces has revealed similar spectra, with Ti, O, C, and N as the key elements for both of the surfaces [80]. Besides the key elements, traces of Cl [81] and Na [82] are also detectable on the modSLA surface. This is likely to be because these surfaces are stored in isotonic saline environment to preserve their hydrophilic property. There is an increased percentage of oxygen on modSLA surfaces when compared with SLA [68, 81]. The surface titanium dioxide coating formed on implant surfaces is responsible for the biocompatibility of titanium implants, and this gets contaminated when exposed to air forming hydrocarbons and carbonates, leading to a reduction in the surface free energy levels [70]. To preserve the surface free energy, the modSLA surfaces are stored in isotonic solution [70]. This could also attribute to the lower percentage of carbon observed on modSLA surfaces [68, 73, 83].

Micro-roughness and hydrophilicity of implant surfaces allow better physisorption and resultant enrichment of proteins on the implant surroundings (from blood and the bone cells), thereby enabling enrichment of factors essential for differentiation [84]. Further, dual acid etched surfaces are known to have better crosslinkage between fibrin and osteogenic cells [85]. Improved cellular attachment and adhesion properties of SLA and modSLA surfaces have also been explored using imaging techniques like scanning electron microscopy (SEM) in several studies. A study by Wall et al. had shown “stellate” shaped cells with extending cellular processes as opposed to rounded cells on their smooth (SMO) counterparts [86]. However, another study demonstrated a more flattened morphology of human osteoblasts on smooth surfaces when compared with the roughened surfaces [87]. This study also compared the difference in cellular morphology between modSLA and SLA surfaces-osteoblasts on SLA surfaces were more elongated. Several

lamellopodia (cytoskeletal projections composed of actin) were shown to be attaching to the micro-rough irregularities on the modSLA and SLA surfaces [87]. Another study by Zhao et al. had reported a more elongated and cuboid shaped morphology of MG63 (human osteosarcoma cell line) on modSLA and SLA surfaces [88]. They also reported that the cells prefer to nurture in the pits created on the surface due to the sand-blasting process and form attachments with the micropits. As described in other studies, they also did not observe any appreciable difference in the morphology of cells between modSLA and SLA surfaces.

3.3.4 Superior osseointegration on topographically modified titanium surfaces: *In vivo* and clinical evidences

The positive influence that the micro-rough SLA surface has on osseointegration was first shown by Buser et al. in 1991 [2]. The study found SLA surfaces to have the best bone-to-implant contact when comparisons were made between SLA, electropolished, sandblasted with medium grit and acid pickled (SMA), sandblasted with large grit (SL), and TPS surfaces, after 3 and 6 weeks of implantation into the metaphyses of the tibia and femur in miniature pigs. The SLA surface has also been seen to have higher removal torques in miniature pigs than the machined and acid-etched surface-Osteotite [89]. Histometric analysis of the junction between the implant (SLA and TPS) and gingiva in foxhounds, conducted by Cochran et al. (parameters like dimensions of junction epithelium, sulcal depth and contact with connective tissue) did not show any significant difference indicating that the topographically modified surface has a direct influence on osteoblasts and osteogenesis [90]. SLA surfaces are also known to have superior bone filling than in TPS and machined surfaces during post-implantitis healing as shown in a study conducted in beagle dogs [91]. Furthermore, no significant differences have been observed in terms of bone-to-implant contact ratios when standard SLA implants have been compared to their phosphate treated counterparts [92].

The improved osseointegration properties of SLA surface have been acknowledged clinically as well. A prospective clinical study by Cochran et al., demonstrated that ITI® implant screws having SLA endosseous surface could be restored in 6 weeks [65]. Another study by Roccuzzo et al. (one-year prospective study) on 32 patients also suggested similar early loading capabilities of the SLA implants [93]. These findings were further validated by Bornstein et al. in their three-

year prospective study where they tested the early loading of non-submerged (re-positioned mucoperiosteal flaps) ITI screws with SLA surfaces [94]. Successful osseointegration was observed in majority of the cases studied (only 2 out of 104 implants were considered as drop-outs/failure) after loading the implants following 6 weeks of healing. The success and efficacy of SLA surfaces was studied retrospectively by Buser et al [95]. Their 10-year long retrospective study on 303 partially edentulous patients fitted with SLA implants concluded on a 98.8% survival rate and 97% success rate. The modSLA surface was developed by Buser et al. in 2004 and they introduced it as a chemically modified SLA surface [68]. They observed significantly higher bone-to-implant contact ratios on modSLA compared to SLA surfaces in miniature pigs at 2 and 4 weeks, but not at 8 weeks suggesting that the modSLA surface facilitates bone formation during the early stages of osteogenesis. Several studies subsequently confirmed the improved osteogenic properties of modSLA surfaces [64, 96]. Similar results were demonstrated in a later study by Bornstein et al. in 2008 in American foxhounds at 2 weeks but not at 4 weeks [97]. Further, Lai et al. substantiated the Bornstein et al. sudy in 2009 [98].

Straumann introduced the modSLA surfaces for dental implantation in 2005 under the name "SLActive®" and marketed it as the "first hydrophilic surface". Straumann claims that the SLActive® surfaces reduce healing time to half of SLA surfaces. Schwarz et al. studied the early tissue reaction to modSLA and SLA surfaces and implanted them into the maxilla and mandibles of fox hounds [67]. Samples were taken at various time-points between 1 and 14 days. The positive influence of the modSLA surface was evidenced as early as day 4 through increased osteocalcin synthesis and observation of collagen dense connective tissue. The day 14 results from this study showed trabecular bone formation on SLA and mature woven bone arranged as parallel fibres were seen on the modSLA surfaces. In another study, Schwarz et al. further studied the bone regeneration capabilities of modSLA and SLA surfaces in dehiscence-type defects in the mandibular and maxillary pre-molar regions of beagle dogs and the results were assessed between 1 and 8 weeks [99]. This study showed lower "new bone height" and bone fill on the SLA surface.

Bone-implant interface is considered an important factor for the functional load bearing potential of implants. Ferguson et al. explored the interfacial shear strength

of modSLA and SLA implants in a miniature pig model [100]. modSLA and SLA implants were placed in miniature pigs maxillae and assessed after 2 to 8 weeks of healing. The results showed that modSLA was better at augmenting interfacial shear strength compared to SLA. Several prospective multicenter studies have demonstrated the early loading capabilities of the modSLA surfaces [101-104]. In fact, results with loading of modSLA surfaces immediately after placing them, have been seen to be similar to delayed loading [105]. The stability of modSLA and SLA implants have been explored in prospective randomized control trials as well. The prospective study by Schätzle et al. investigated the stability of implants using resonance frequency changes at the site of insertion of implants on 40 human subjects and showed faster stabilization of implants with the modSLA surfaces compared to SLA surfaces [106]. The modSLA implants showed improved stability at 12 weeks (77.8±1.9 in modSLA vs. 74.5±3.9 in SLA). Similar results were observed by Karabuda et al. when they prospectively explored the stability and bone losses in modSLA and SLA surfaces implanted in 22 human patients [107]. Several other animal models and human clinical studies have been conducted on the modSLA and SLA surfaces and all point towards superior bone formation on the modified surfaces.

The findings from the various *in vivo* and clinical studies suggest that modSLA and SLA surfaces have better osseointegration and osteogenic properties when compared with smooth surfaces. Collectively, the results indicate that the modified titanium implant surfaces have superior clinical success.

3.3.5 Effect of modSLA and SLA surfaces on cell proliferation

Studies exploring cellular proliferation characteristics on the micro-topographically modified surfaces have been fairly consistent in their reports. Initial reports of decreased proliferative capability of micro-topographically modified surfaces came from the studies conducted on the SLA surfaces. Lohmann and colleagues demonstrated this phenomenon on SLA surfaces compared to PT in 1999 [108, 109]. Reduced proliferation rates on SLA surfaces have been correlated with increased alkaline phosphatase (ALP) in several studies [108-112]. In 2011, Vlacic-Zischke et al. also reported decreased proliferation rates with surface modifications (modSLA surfaces showing the lowest proliferation rates) [24]. These results corroborate well with other studies; like the work by Mamalis et al. using human

mesenchymal stem cells [113]; and Zhao et al. (with MG63 osteoblast like cells) [88] where they described reduction in cell numbers on modSLA and SLA surfaces when compared with smooth polished titanium and plastic surfaces. Indeed, Zhao et al. also demonstrated a further 30% reduction on modSLA (compared with SLA). All these results are in agreement with one of the earlier studies by Martin et al. (reported in 1995), where they showed that cell proliferation was negatively related to the surface roughness of implants [114]. Decreased cell proliferation on SLA and modSLA for the first 7 days has been substantiated in other studies as well [115]. The study by Klein et al. observed the lowest proliferation rates on modSLA when compared with SLA and smooth surfaces [87]. A previous study by Klein et al. in 2010 had reported lowest cell numbers on modSLA up to 14 days of culture, although they had also observed that after 21 days, the growth rate increased only on modSLA surfaces [73]. Olivares-Navarrete et al. reason that the decreased proliferation on modSLA and SLA surface is a consequence of transition of the cells from a proliferative to a differentiating phenotype [72].

3.3.6 Molecular regulation of osteoblasts on micro-roughened titanium implant surfaces

Osseointegration and osteoconduction are attributes by which osteoprogenitor cells create a structural and functional connection between implants and the living system. Improved osteogenic properties of micro-roughened surfaces compared with smooth surfaces have allured researchers globally to explore the mechanisms responsible for their properties. The concept of contact osteogenesis on roughened implant surfaces as described by Osborn and Newesley [58], makes them an interesting model to study the molecular regulation and signaling cascades guiding the process of osteogenic differentiation.

Superior osteogenic differentiation on modified titanium surfaces: In vitro evidences

The interactions between osteogenic cells and topographically modified surfaces, at molecular and cellular levels play an important role in regulating the outcomes of these contacts. Several studies have focused on investigating these mechanistic interactions between osteogenic cells like mesenchymal stem cells, osteoprogenitor cells or human periodontal ligament (hPDL) cells and these implant surfaces. An increase in expression of osteogenic genes on the modified surfaces has

been observed in most studies on these surfaces [25, 73, 86-88, 113, 115-119]. The initial *in vitro* confirmation of the pro-osteogenic response of SLA surfaces came with studies performed by Boyan and colleagues. They demonstrated higher ALP and osteocalcin expression on sand-blasted and acid-etched surfaces compared with polished titanium and plastic surfaces [109, 120]. Boyan et al. had further shown that supplementation of dexamethasone to osteoblast cultures increased ALP activity on SLA and TPS, but not on smooth surfaces [121]. They also observed bone-like calcium/phosphorus ratio (2:1) only on SLA and TPS. Increased expression of osteogenic markers was verified in their subsequent work using MG63 cells [110, 111]. The level of ALP has been shown to decrease to base-line levels on SLA and TPS surfaces in presence of cycloxygenase inhibitors like indomethacin suggesting the role of prostaglandin mediators in their osteogenic effects [122]. A newer modification of SLA surface implanted with magnesium ions has been found to show higher cellular attachment and increased ALP activity and calcium deposition; however, elaborate experimental evidences for such findings are still lacking [123].

The modSLA surfaces have been shown to have better osteogenicity than SLA surfaces *in vivo* [68, 100]. An experimental model comparing different titanium surfaces (modSLA, SLA, TiOBlast™ and Osseospeed™) had documented highest ALP gene expression on the modSLA surface [124]. However, this study didn't show higher expression of other osteogenic markers like RUNX2, osterix and osteocalcin, although they did find higher expression of bone sialoprotein on modSLA and SLA than on plastic (modSLA>SLA). Another study examining the long-term response of a commercial human osteoblastic cell line, HOB-c (PromoCell, Heidelberg, Germany) on different titanium surfaces in media supplemented with dexamethasone and L-glutamine (standard osteoblast cultivation media), demonstrated higher levels of ALP activity on modSLA and SLA surfaces [73]. SPP1 and OCN gene levels were also elevated on modSLA and SLA surfaces at each time-point (Days 1, 2, 3, 7, 14 and 21). They concluded that modSLA and SLA surfaces helped in maturation of osteoprogenitors into post-mitotic osteoblasts. Microrough topographies have also been seen to increase the number and size of bone-like nodules when osteoblasts are cultured on SLA surfaces [125]. Further, Qu et al. have demonstrated early and improved formation of clusters of osteoblastic cells on modSLA compared to SLA surfaces and they have argued that this could be

an important factor responsible for improved expression of osteogenic genes on modSLA surfaces [126]. After culturing MG63 (human osteoblast-like) cells on modSLA, SLA, hydrophilic acid-etched (modA), hydrophobic acid-etched (A) and tissue culture plastic surface (TCPS) in normal expansion media, they observed cell cluster formation on modSLA just after 2 days of culture. Surface chemistry and topography have been seen to have a concerted effect on formation of bony nodules *in vitro* [127]. Moreover, combined micron and submicron topographical architecture has been shown to have a synergistic effect with the surface energy of modSLA surfaces on the osteoblastic response [71]. Surfaces lacking the micron scale roughness as seen in modSLA and SLA surfaces have been shown to have a reduced osteogenic response (reduced alkaline phosphatase activity and osteocalcin levels) [71]. Improved osteogenic outcomes have been demonstrated at molecular levels in several studies. For example, Wall et al. observed higher expression of the osteogenic markers, osteopontin (SPP1), Runt-related transcription factor 2 (RUNX2) and Bone sialoprotein (IBSP) on roughened surfaces (modSLA and SLA, with modSLA showing moderately higher response than SLA) [86]. They also demonstrated formation of calcified matrix at earlier time-points on the modified surfaces (no significant difference between modSLA and SLA). Furthermore, the expression of osteogenic markers like alkaline phosphatase (ALP), collagen type I (COL1), osteocalcin (OCN) and osteoprotegerin (OPG) has also been shown to be higher on modSLA surfaces [126]. OPG is known to inhibit the differentiation of osteoclast cells and therefore the increased expression of OPG on modSLA and SLA surfaces during osseointegration could play an important role in mediating the bone remodeling outcomes [128]. Studies have in fact, shown reduced osteoclast formation on modified titanium surfaces [129-131]. The study by Rausch-fan et al. also had demonstrated higher ALP activity on modSLA and SLA surfaces with MG63 cells [128]. They cultured MG63 cells on modSLA, SLA, modA, A and TCPS in normal expansion media and investigated the expression of osteocalcin, osteoprotegerin, TGFβ1 and VEGF using ELISA kits besides ALP. Their study revealed higher expression of these proteins on the modSLA and SLA surfaces compared with the smooth surfaces.

The *in vitro* studies on both of the micro-roughened surfaces (SLA and modSLA surfaces) have demonstrated their superior osteogenic differentiation

properties compared with smooth and polished surfaces. However, studies comparing between the modSLA and SLA surfaces in terms of molecular interactions with osteoblasts and osteoblast-like cells have managed to show only subtle differences between them, with essentially very similar osteo-regulatory patterns on both of the surfaces. This is in contrast to the *in vivo* reports demonstrating significantly higher osseointegration on modSLA compared with SLA surfaces, suggesting the role of "non-osteogenic" cells, like blood cells that are known to interact earlier than the mesenchymal stem cells and osteoblasts *in vivo*.

Coagulation cascade response on the modified titanium surfaces

The molecular mechanisms for the superior osteogenic properties of modSLA surfaces compared with SLA could possibly be due to reasons beyond the direct biological interactions of osteoprogenitor cells and osteoblasts. After implantation, the first tissue to come in contact with the implant surface is blood. This in turn leads to a series of cellular processes such as deposition of proteins, coagulation, inflammation, and tissue formation [132]. Therefore, the *in vitro* models studying the interactions of osteoblasts and osteoblast-like cells with modified surfaces tend to overlook the initial interactions that might play a key role in the process of new bone formation and osseointegration. SLA surfaces are known to retain the blood clot formed during the healing phase better compared with machined surfaces and show signs of new blood vessel formation as early as 3 days of implantation, as shown in an *in vivo* rabbit model [133]. Furthermore, modSLA surfaces have been shown to have increased thrombogenic properties compared with SLA as demonstrated by Hong et al. [134]. A substantial reduction (99% vs. 90%) in the platelet count and higher release of β-thromboglobulin was observed on modSLA surfaces compared with SLA surface. The study also observed higher activation of the coagulation system, as observed by increased thrombin-antithrombin complex (TAT). They also observed activation of the intrinsic coagulation cascade on the modSLA surface. These results therefore indicated higher thrombogenicity on modSLA surfaces through the activation of the intrinsic pathway. Activation of platelets and the coagulation cascade are well recognized precursors of osteogenesis [132, 135, 136]. Similar phenomena like platelet activation and cytokine release on micro-roughened surfaces have also been demonstrated by Kämmerer et al. [137]. They observed higher platelet consumption on SLA surfaces compared with polished titanium. Their

results however, did not reveal any substantial difference between the SLA and the modSLA surfaces, though a sharp decrease in platelet consumption after 30 mins was observed on the modSLA surface. VEGF and platelet-derived growth factor (PDGF)-αβ levels were higher on the micro-roughened surfaces as opposed to the polished surfaces supporting observations discussed previously in this chapter.

Immunomodulation on the modified titanium surfaces

Following protein adsorption and coagulation reactions, immunological response to the implant surface is important in the subsequent wound healing process and several studies have reported regulation of such responses on the modified surfaces. Murine macrophage-like cells, RAW 264.7 have been seen to express higher amounts of pro-inflammatory cytokines like tumor necrosis factor-α (TNFα) and interleukin-1β (IL1β) and IL6 on SLA compared with polished surfaces [138]. Additionally, observations from an *in vivo* study on male Sprague-Dawley rats have found immunological macrophages to be predominant cells accumulating on SLA surfaces (and not on smooth surfaces) after 1 week, and these cells were present in conjunction with early mineralization seen on SLA surfaces at 2 weeks [139]. In contrast to the observations on SLA surfaces, a recent study demonstrated downregulation of key pro-inflammatory genes, TNFα, IL1α, IL1β and CCL2 on modSLA surfaces compared with smooth and SLA surfaces when RAW 264.7 were cultured on these surfaces [81]. In a subsequent study using a human macrophage cell line, THP-1, Alfarsi et al. discussed the pro-inflammatory response of SLA surfaces as evidenced by upregulation of 16 key cytokines and chemokines [140]. In contrast to this, modSLA surface was seen to downregulate 10 key genes (including TNF, IL1β and IL1α) compared to SLA surfaces. In a separate study conducted by another group, Hyzy et al., described similar findings when they cultured MG63 osteoblast-like cells [141]. Lower expression of pro-inflammatory genes like, IL1β, IL6, IL7, IL8 an IL17 and higher expression of anti-inflammatory, IL10 were noted when modSLA surfaces were compared with SLA. Antigen-presenting cells (APCs) like dendritic cells are important regulators of the host cell response to any foreign substance and potentially play a key role in the subsequent osseointegration and osteoconduction properties. Kou et al. explored the response of dendritic cells to the modSLA, SLA and pre-treatment (PT) titanium surfaces [142]. PT and SLA surfaces were seen to induce a more mature phenotype of the dendritic cells (DCs) (increased

levels of maturation-associated markers like, CD86) in contrast to modSLA surfaces. The modSLA surfaces appear to result in a modulated inflammatory environment compared to SLA and PT surfaces. Though the study observed higher production of the chemokine, monocyte chemotactic protein-1 (MCP-1) on PT-treated DCs, higher levels of the anti-inflammatory cytokine, Interleukin 1 receptor antagonist (IL-1ra), was observed on PT-DCs. This has been argued as a response to mollify the pro-inflammatory response. Secretion of cytokines: Macrophage inflammatory protein-1α (MIP-1α), Tumor necrosis factor-α (TNFα) and IL-10 and IL-1ra was seen to be lower in modSLA-treated DCs especially when compared with SLA surfaces, however the differences were not statistically significant.

Angiogenic response on topographically modified surfaces

New blood vessel formation is an important process that precedes osseointegration. Increased expression of the predominant angiogenic molecule, vascular endothelial growth factor (VEGF) on the modified titanium surfaces at an *in vitro* level, could possibly indicate that the upregulated expression of angiogenic factors contribute to the improved osseointegration on these surfaces. In 2008, Rausch-fan et al. showed an increased expression of TGFβ1 and the angiogenic marker VEGF in alveolar osteoblast cells on modSLA and SLA (modSLA>SLA) surfaces compared to modA, A and TCPS [128]. A recent study has corroborated with similar findings after culturing endothelial progenitor cells on modified surfaces. Similarily, Ziebart et al. showed higher expression of VEGF-A on modSLA surfaces compared to SLA, modA and A surfaces [143]. As wound healing is an important aspect of successful dental implantation, and endothelial cells are important for mediation of angiogenic and inflammatory processes, An et al. explored the implications of modSLA and SLA surfaces on endothelial cells [144]. They cultured human umbilical vascular endothelial cells (HUVECs) on modSLA, SLA, modA and A surfaces. Angiogenic factors, like von Willebrand factor (VWF), thrombomodulin, endothelial cell protein C receptor, and adhesion molecules - intercellular adhesion molecule-1 (ICAM1) and E-selectin were most upregulated on modSLA. The role of endothelial cells was also explored by Zhang et al. in 2010 [69]. In this study, HUVEC and MG63 cells were co-cultured on A, modA, SLA and modSLA. The co-culture set-ups were observed to have higher expression of early differentiation markers and osteogenic factors on the titanium surfaces when

compared with cultures of single cell types. These properties were enhanced by both micro-rough topographies and hydrophilic surfaces. Their results showed that the effects are greater on the modSLA surfaces. Another study by Vlacic-Zischke et al. also demonstrated differential expression of angiogenic gene, KDR (VEGF receptor) on the modified surfaces [24]. Stringent regulation of angiogenesis during osteogenesis and osseointegration seems to play an important role on modified surfaces. Raines et al. did an in-depth exploration of the regulation of angiogenesis on modSLA and SLA surfaces [145]. They cultured primary human osteoblasts (HOB), MG63 cells and α2 integrin-silenced MG63 cells on different titanium discs (modSLA, SLA and SMO). They observed high levels of expression of secreted VEGF-A, basic fibroblast growth factor (FGF-2), epidermal growth factor (EGF) and angiopoietin-1 (Ang-1) on modSLA and SLA (modSLA>SLA) surfaces using sandwich ELISA assay techniques in unsilenced controls. The upregulation of angiogenic factors on modified titanium surfaces correlates well with the *in vivo* improved osseointegration and osteoconductive attributes of micro-roughened titanium surfaces, as increased blood vessel formation ensures better availability of osteogenic proteins and mediators.

Role of integrins and other associated molecules

Integrins are known to play an important role in the initial cell adhesion and attachment and an increased expression of α2 integrin subunit on modSLA and SLA surfaces as reported in different studies indicates a crucial role for the α2 integrin subunit in cellular attachment on micro-rough surfaces [146, 147]. A study by Raz et al. utilized MG63 cells cultured on SLA and polished titanium (PT) in the presence of 1,25-dihydroxyvitamin D3 (1α,25(OH)2D3) to study the expression of α2, α5, αv, β1 and β2 at different time-points [146]. The expression of α2 and β1 was observed to be consistently higher on the micro-rough titanium surfaces. α5 expression was seen to be downregulated on SLA, whereas αv and β2 levels remained unaffected. This study concluded that α2 is probably the favorable binding partner for β1 on titanium surfaces with micro-rough topographies. Integrin α5 subunit is known to influence interaction of cells with surfaces; however it does not have an effect on the differentiation characteristics of osteoblasts cultured on surfaces with micro-rough topographies [148]. The study by Raines et al. observed that α2 integrin-silenced MG63 cells cultured on titanium surfaces have ALP activity similar to normal MG63

cells cultured on TCPS [145]. α2 integrin-silencing did not show any effect on ALP activity on TCPS. The α2 integrin subunit is known to be important for the activation of the key osteogenic transcription factor, RUNX2 [149]. The importance of the β1 integrin subunit was confirmed further by Wang et al. [150]. In a later study, Lai et al. investigated whether cell adhesion is influenced by surface energy and observed higher attachment of alveolar osteoblasts on modSLA compared with SLA surfaces [151]. They also observed clearer actin filaments and higher expression of focal adhesion kinase (FAK) on modSLA surfaces. Another study exploring the osteoblastic commitment of MSCs on modSLA and SLA surfaces using co-culture experiments found that the soluble factors released from osteoblasts cultured on modSLA and SLA surfaces can induce osteogenic differentiation of MSCs [72]. They further observed increased expression of VEGF, TGFβ1, OCN and OPG in MSCs cultured in media enriched with soluble factors from osteoblasts cultured on modSLA and SLA. The levels of expression were more robust from cultures with factors from osteoblasts seeded on modSLA surfaces. α2 integrin-silencing studies performed by their group also confirmed that α2β1 signaling is required to mediate the paracrine effects of osteoblasts on MSCs [72]. Integrins α1, α2, α5, β1, and β3 are known to be responsive in mediating superior properties of SLA surfaces with induced hydrophilicity [152]. This study also suggested that integrin α3 does not play a major role in the osteogenic response of modified SLA surfaces. A recent study explored the implications of Rho GTPases regulated molecules, Rac and RhoA (through Rho Kinase - ROCK), and concluded that inhibition of the ROCK signaling pathway can stimulate osteogenic differentiation on micro-roughened titanium surfaces [153]. Earlier Galli et al. had demonstrated that inhibition of ROCK signaling on smooth surfaces stimulated Wnt/β-catenin pathway and promotes differentiation [154]. Further, Lumetti et al. have also shown that activation of small GTPase RhoA on microrough surfaces like SLA, affects the activation canonical Wnt/β-catenin pathway by modulation of myosin II (a molecule known to be important for internal cellular tension) [155].

Studies exploring the molecular mechanisms of improved osteogenic response on modSLA and SLA surfaces have shown cell signaling pathways to be differentially regulated on these surfaces.

Arachidonic acid cascade

The interest in the role of arachidonic acid cascade comes from early studies on roughened implant surfaces that observed higher expression of autocrine and paracrine mediators like latent TGFβ (LTGFβ) and prostaglandin E_2 [109, 120]. Boyan et al. had further demonstrated an improvement in the osteogenic response and expression of LTGFβ and PGE_2 on roughened surfaces when cultures of MG63 cells were supplemented with 1,25-dihydroxyvitamin D3 (1α,25(OH)2D3) [120]. However, this dependence was seen to be more specific with the maturation status of cells as shown by Lohmann et al., with immature osteoblastic cells showing higher response to 1α,25(OH)2D3 in terms of TGFβ1 and PGE_2 [109]. Subsequently, Lohmann et al. in 1999, demonstrated that osteoblastic differentiation and responsiveness to 1α,25(OH)2D3 on micro-roughened titanium surface (SLA) is mediated through Phospholipase A_2 [108]. Their study had shown that these effects are not mediated through protein kinase C (PKC) pathway. However, in a later report by Schwartz et al., they concluded the TGFβ1 expression on roughened titanium surfaces is mediated by the PKC instead of the PKA pathway, although they reiterated that TGFβ1 production via the 1α,25(OH)2D3 is independent of the PKC pathway [156]. They also reported that although the PGE_2 production is regulated by PKA; however, even this is not involved in the roughness-related increase in PGE_2. Earlier Batzer et al. in 1998 had implicated the role of prostaglandins in the roughness-response of MG63 cells [157]. Addition of indomethacin to the cultures had inhibited roughness-mediated increase in OCN and latent transforming growth factor-β (LTGFβ). A study by Boyan et al. on SLA surfaces in 2001 had revealed that cycloxygenase-1 (Cox-1) and Cox-2 were involved in production of prostaglandin E_2, transforming growth factor-β1 (TGFβ1) and OCN [122]. Later, in 2010, Fang et al. observed upregulation of osteogenic markers, OCN and OPG on modSLA and SLA surfaces and explored the role of phospholipase D (PLD) on the differentiation of osteoblasts on micro-roughened surfaces like modSLA and SLA [158]. They concluded that the improved cellular responses on these surfaces are mediated by PLD through protein-kinase C (PKC) dependent signaling. Phospholipases have been found to be important mediators of cellular differentiation; however, they do not seem to play any key role on the ALP response on SLA surface as seen in their study. Therefore, no conclusive evidence has been derived for the

role of prostaglandins on the osteogenic differentiation process on micro-rough surfaces.

Cell signaling pathways

Cell signaling pathways are coordinated chain of events that lead to a sequential activation of different genes and proteins, eventually leading to culmination of different cellular activities, maturation and differentiation. To understand the molecular mechanisms guiding osteogenic differentiation, it becomes important to explore the different cell signaling pathways that get modulated by virtue of the interactions of osteoblastic cells with the physiologically relevant surfaces like SLA and modSLA. Several groups globally have recently started investigating the regulation of different cellular signaling molecules (genes and proteins) on these substrates. An early report exploring the improved osteogenic responses with 1α,25(OH)2D3 on micro-roughened SLA surfaces concluded it to work through the activation of the Mitogen-activated protein kinase (MAPK) pathway [110]. However, Zhuang et al. reported that inhibition of the extracellular signal-regulated kinase 1/2 (ERK1/2) pathway (a well characterized MAPK pathway) may play a role in the enhanced osteogenic properties of SLA surfaces [159]. Similar findings have been reported by Jiang et al. [160]. In 2004, Brett et al. observed the differential regulation of several genes on SLA surfaces compared to SMO surfaces; however, this study didn't explore specific cell signaling pathways enriched [80]. Later, Galli et al. studied the activation of Wnt/β-catenin signaling pathway in mediation of cellular responses to SLA surfaces [161]. Their study described activation of the target genes of the Wnt pathway on SLA compared with polished surfaces. A higher Wnt/β-catenin pathway response along with lower expression of AXIN2 (important for degradation of β-catenin) was observed when WNT3A transfected C2C12 (murine cell line) were cultured on SLA surfaces (compared with polished). Their results were further consolidated when improved osteogenic responses of SLA surfaces were reversed upon inhibition of the β-catenin pathway. Their group has further shown that an alternate β-catenin mediated pathway (β-catenin/FoxB instead of conventional β-catenin/TCF) is activated on SLA surfaces when they need to prevent oxidative stresses by reactive oxygen species [162].

Researchers started focusing their attention further on the Wnt pathway and superior osteogenic response on modified surfaces subsequently. Wall et al. demonstrated higher expression of WNT5A (representative of the non-canonical Wnt/Ca^{2+} pathway) on modSLA and SLA surfaces (modSLA>SLA>SMO) [86]. Pathway analysis after a microarray based study on the modSLA and SLA surfaces by Vlacic-Zischke et al. in 2011 demonstrated upregulation of TGFβ/BMP and Wnt signaling cascades, when they performed a whole genome expression analysis after culturing human osteoblasts on modSLA and SLA surfaces for 72 hours [24]. They also observed differential regulation of genes associated with processes related to bone remodeling, like proteolysis, angiogenesis and osteoclast differentiation. Further, the Wnt pathway genes catenin (cadherin-associated protein), alpha 1 (CTNNA1), f-box and wd-40 domain protein 4 (FBXW4) and frizzled homolog 6 (drosophila) (FZD6) were observed to be upregulated on modSLA and SLA surfaces. The Wnt signaling pathway potentially plays a key role in modulation of the effects of modSLA and SLA on cells. These observations are in agreement with *in vivo* results as described by Donos et al. in 2011 [117]. Osteogenesis and angiogenesis associated genes have been shown to be upregulated after seven days of implantation of modSLA implants in humans and this seems to be regulated by the BMP and VEGF signaling pathway [117]. In another study, Ivanovski et al. studied the transcriptional profile during osseointegration in humans and described the role of TGFβ/BMP, Wnt and Notch pathways in the osteogenic phase of osseointegration [118]. This study performed a gene ontology (GO) analysis on the temporal profiles of transcriptional changes during osseointegration in humans. The GO analysis was performed using the online tool: DAVID - Database for Annotation, Visualization, and Integrated Discovery, which is an important tool used to decipher biological meaning from large datasets of gene expression [163]. Interestingly, the results indicated a maturing osteogenic process between 4-14 days of implantation. Cell signaling pathways are important regulators for cell fate transitions and several studies on the micro-roughened surfaces have indicated upregulation of pro-osteogenic and pro-angiogenic pathways during the process of osseointegration on these surfaces.

The role of canonical Wnt/β-catenin pathway in the early stages of differentiation of MG63 cells was described by Olivares-Navarrete et al. in 2010

[164]. Exogenous addition of canonical Wnt inhibitors Dickkopf-1 (Dkk1) and Dkk2 was shown to decrease osteogenic marker expression on the modified surfaces. They also demonstrated that Dkk1 and Dkk2 are important in the autocrine regulation of committed osteoblasts and have different effects on cells. Dkk2 was found to be important for the regulation of cells on smooth surfaces and Dkk1 for cells grown on micro-structured surfaces. Indeed, Dkk2 silencing was shown to decrease the expression of osteogenic markers like OCN. This study showed that Dkk2 may have an antagonistic role in the early stages and an agonistic role in the late stage of osteogenic differentiation. The role of canonical Wnt pathway on modSLA and SLA surfaces was also recently explored by Galli et al. [165]. Stimulation of the canonical Wnt pathway was shown to increase osteogenic differentiation on modified surfaces compared to controls. Recent studies have focused on the role of the non-canonical Wnt/Ca^{2+} pathway on micro-roughened surfaces. The Wnt/Ca^{2+} pathway was considered to be important in the late stage of differentiation on micro-roughened surfaces. Earlier, Wall et al. had indicated that activation of the WNT5A gene on modSLA possibly plays a key role in improved osteogenic differentiation [86]. The WNT5A gene is considered as a representative of the non-canonical Wnt/Ca^{2+} pathway [166]; and therefore upregulation of WNT5A is considered indicative of Wnt/Ca^{2+} pathway activation. The study by Olivares-Navarrete et al. in 2011 on these surfaces also corroborates with the previous reports on the role of the non-canonical Wnt pathway [26]. They demonstrated increased expression of WNT5A on micro-structured titanium surfaces which coincided with an increased osteogenic response. This study also explored the autocrine and paracrine effects of WNT3A (canonical Wnt/β-catenin pathway) and WNT5A (non-canonical Wnt/Ca^{2+} pathway). Human mesenchymal stem cells were cultured on titanium surfaces either with exogenous WNT3A and WNT5A or with antibodies against WNT3A and WNT5A. They observed a decrease in the level of OCN with exogenous WNT3A on all of the surfaces and an increase in the same with anti-WNT3A treatment. The findings were opposite in the WNT5A group. The levels of BMP2 and BMP4 were significantly higher on all the surfaces with exogenous WNT5A treatment when compared with the ones treated with anti-WNT5A. Their results tend to suggest that WNT3A has a negative influence on osteoblastogenesis on modified titanium surfaces. However, their findings also revealed an increase in the levels of VEGF-A and TGFβ1 expression with exogenous WNT3A. TGFβ1 (a member of the TGFβ/BMP pathway)

has been shown to be important in bone formation in several studies [167-169]. Similarly, VEGF upregulation has also been demonstrated in several reports on osteogenesis [170, 171]. Thus, increased levels of TGFβ1 and VEGF-A with WNT3A seem contradictory to the hypothesis that WNT3A is inhibitory to all aspects of osteogenic differentiation. The findings; however, substantiate the role of the non-canonical Wnt/Ca^{2+} pathway. The same group explored the role of the Wnt/Ca^{2+} pathway further in a subsequent study [25]. The study explored the expression pattern of genes related to the Wnt pathway (receptors, activators and inhibitors) after culturing MG63 cells on modSLA, SLA and smooth surfaces. WNT1, WNT3A, WNT7B, WNT10B (activators of Wnt/β-catenin pathway) were seen to be downregulated on the modified surfaces. WNT5A and WNT11 (non-canonical Wnt/Ca^{2+} pathway) were upregulated at the same time. They also observed upregulation of the classical inhibitor of the Wnt/β-catenin pathway, AXIN2 on these surfaces. This study further confirmed the observations as seen with exogenous addition of WNT3A and WNT5A, previously. However, they did not find any significant effect of WNT3A on the production of TGFβ1 and VEGF. In contrast, increased levels of BMP2, BMP4, VEGF, latent and active TGFβ1, and OPG were seen with the addition of WNT5A. These studies suggest that the non-canonical Wnt/Ca^{2+} pathway is essential for the induction of osteogenic differentiation of cells on micro-structured titanium surfaces. However, it is evident that much work is further needed to establish the role of this pathway in osteogenic differentiation. The difficulty in analysis of Wnt proteins by conventional Enzyme-linked immunosorbent assay (ELISA) and Western Blot techniques due to their hydrophobicity and affinity towards heparin and chondroitin sulphates makes efforts more challenging and research is still in progress [25, 172]. The current knowledge presented by different groups identifies an important role of the Wnt/Ca^{2+} pathway in osteogenic differentiation on micro-roughened surfaces. The role of PI3K/Akt signaling pathway on the modified titanium surfaces has been demonstrated by Gu et al. [173]. Their study suggests that the improved osteogenic response to modSLA and SLA surfaces could be due to the activity of the PI3K/Akt signaling pathway.

A chain of highly controlled and coordinated sequence of molecular events is known to modulate the process of bone formation on micro-roughened titanium implant surfaces, like the modSLA and SLA surfaces. Evidences from available

literature on the regulation of bone formation on modSLA and SLA surfaces reveal stimulation of several "pre-osteogenic" events like, response of blood cells, vascularization and cellular adhesions (Figure 3-6) that condition these surfaces for osteogenesis and bone formation.

The pre-conditioning of the modSLA and SLA surfaces, along with their ability to induce "contact osteogenesis" lead to superior bone formation *in vivo* and osteogenic differentiation *in vitro* on the modSLA and SLA surfaces and provide us with excellent *in vitro* models to study the complex mechanisms involved in the process of osteogenesis and osseointegration.

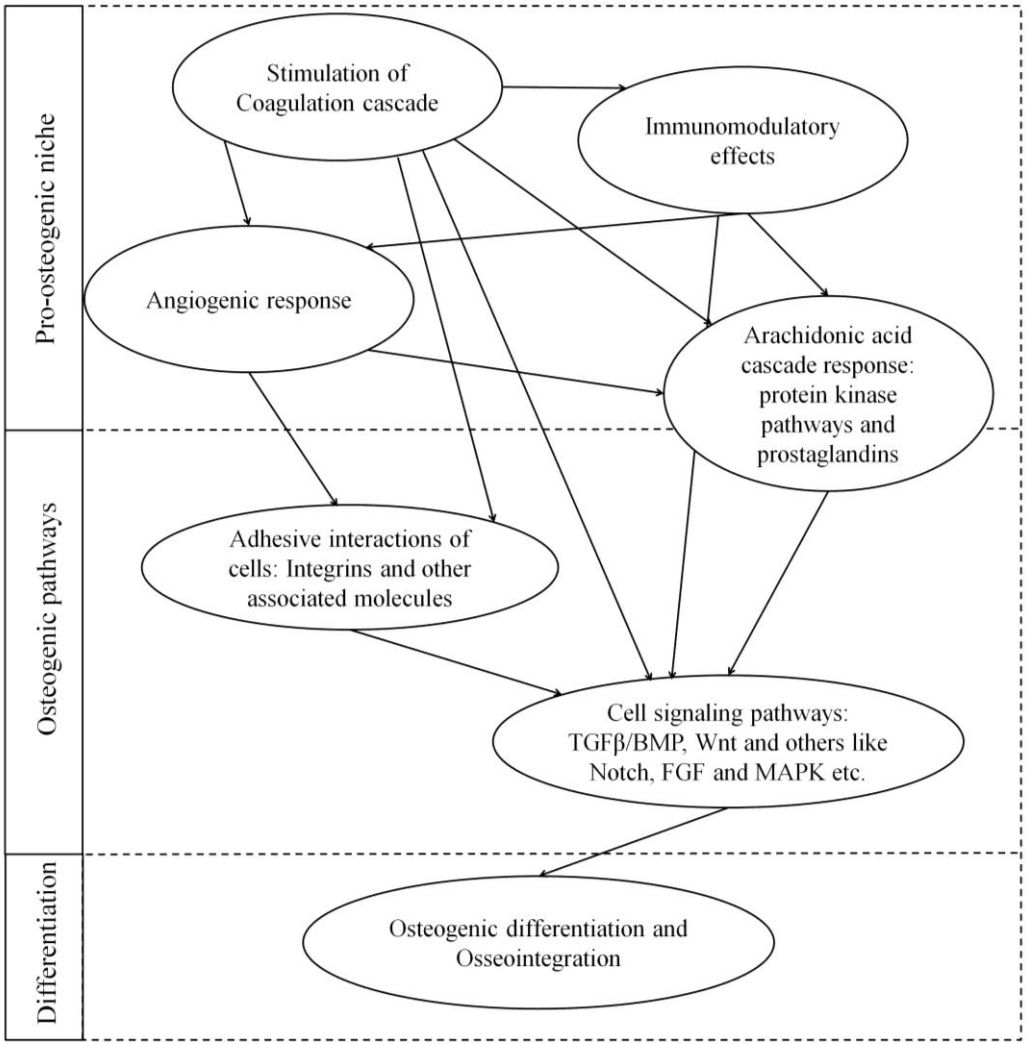

Figure 3-6: Sequence of events on modSLA and SLA surfaces promoting osteogenic differentiation and osseointegration.

3.4 SUMMARY

Osseointegration is a biological process that ensures a structural and functional integration of a foreign implant material and is dependent on the principles of osteogenesis and bone formation. Micro-roughened titanium implants, like the SLA and modSLA surfaces have been known to exhibit superior osseointegrative properties in comparison to their smoother counterparts and are considered to induce "contact osteogenesis". This chapter has attempted to summarize the available knowledge pertaining to the SLA and modSLA surfaces with a particular focus on the studies exploring the molecular mechanisms of osteogenesis and osseointegration on these surfaces. As is evident from the literature, studies on these surfaces have been investigating the "pre-osteogenic" and "pro-osteogenic" molecular events conditioning these surfaces for bone formation; however, none of the studies have focused on the role of small non-coding RNA molecules known as microRNAs that have been found to be critical in the development of tissues and organs with reports claiming that 40-70% of the human genes are potentially under the control of miRNAs. Therefore this present study focuses on investigating the role of microRNAs in modulating pro-osteogenic cell signaling pathways and thereby the process of osteogenic differentiation, extracting cues from the SLA and modSLA topographically modified titanium implant surfaces. Newer physically and chemically modified implant designs like electrochemical modification through potentiostatic anodization (ECH) and sandblasting, alkali heating, and etching (SMART), which are beginning to gain popularity are also expected to benefit from these findings [174]. It is believed that the inferences drawn from this study will aid us in designing tools to assess the clinical success of newer physically and chemically modified implant materials.

3.5 REFERENCES

[1] Brånemark R, Brånemark PI, Rydevik B, Myers RR. Osseointegration in skeletal reconstruction and rehabilitation: a review. J Rehabil Res Dev 2001;38:175-81.

[2] Buser D, Schenk RK, Steinemann S, Fiorellini JP, Fox CH, Stich H. Influence of surface characteristics on bone integration of titanium implants. A histomorphometric study in miniature pigs. J Biomed Mater Res 1991;25:889-902.

[3] Albrektsson T, Brånemark PI, Hansson HA, Lindstrom J. Osseointegrated titanium implants. Requirements for ensuring a long-lasting, direct bone-to-implant anchorage in man. Acta Orthop Scand 1981;52:155-70.

[4] Gotfredsen K, Wennerberg A, Johansson C, Skovgaard LT, Hjorting-Hansen E. Anchorage of TiO2-blasted, HA-coated, and machined implants: an experimental study with rabbits. J Biomed Mater Res 1995;29:1223-31.

[5] Wennerberg A, Albrektsson T, Johansson C, Andersson B. Experimental study of turned and grit-blasted screw-shaped implants with special emphasis on effects of blasting material and surface topography. Biomaterials 1996;17:15-22.

[6] Gotfredsen K, Nimb L, Hjorting-Hansen E, Jensen JS, Holmen A. Histomorphometric and removal torque analysis for TiO2-blasted titanium implants. An experimental study on dogs. Clin Oral Implants Res 1992;3:77-84.

[7] Muraglia A, Cancedda R, Quarto R. Clonal mesenchymal progenitors from human bone marrow differentiate in vitro according to a hierarchical model. J Cell Sci 2000;113:1161-6.

[8] Erlebacher A, Filvaroff EH, Gitelman SE, Derynck R. Toward a molecular understanding of skeletal development. Cell 1995;80:371-8.

[9] Friedenstein AJ, Chailakhjan RK, Lalykina KS. The development of fibroblast colonies in monolayer cultures of guinea pig bone marrow and spleen cells. Cell Tissue Kinet 1970;3:393-403.

[10] Friedenstein AJ. Precursor cells of mechanocytes. In: G.H. Bourne JFD, Jeon KW (Eds). International Review of Cytology: Academic Press;1976. p. 327-59.

[11] Friedenstein AJ, Chailakhyan RK, Gerasimov UV. Bone marrow osteogenic stem cells: in vitro cultivation and transplantation in diffusion chambers. Cell Tissue Kinet 1987;20:263-72.

[12] Ehrlich PJ, Lanyon LE. Mechanical strain and bone cell function: a review. Osteoporos Int 2002;13:688-700.

[13] Schenk RK, Buser D. Osseointegration: a reality. Periodontol 2000 1998;17:22-35.

[14] Frost HM. The biology of fracture healing. An overview for clinicians. Part II. Clin Orthop Relat Res 1989:294-309.

[15] Frost HM. The biology of fracture healing. An overview for clinicians. Part I. Clin Orthop Relat Res 1989:283-93.

[16] Aubin JE, Liu F, Malaval L, Gupta AK. Osteoblast and chondroblast differentiation. Bone 1995;17:77S-83S.

[17] Malaval L, Liu F, Roche P, Aubin JE. Kinetics of osteoprogenitor proliferation and osteoblast differentiation in vitro. J Cell Biochem 1999;74:616-27.

[18] Yamaguchi A, Komori T, Suda T. Regulation of osteoblast differentiation mediated by bone morphogenetic proteins, Hedgehogs, and Cbfa1. Endocr Rev 2000;21:393-411.

[19] von Bubnoff A, Cho KWY. Intracellular BMP signaling regulation in vertebrates: pathway or network? Dev Biol 2001;239:1-14.

[20] Krishnan V, Bryant HU, MacDougald OA. Regulation of bone mass by Wnt signaling. J Clin Invest 2006;116:1202-9.

[21] Gong Y, Slee RB, Fukai N, Rawadi G, Roman-Roman S, Reginato AM, et al. LDL Receptor-related Protein 5 (LRP5) affects bone accrual and eye development. Cell 2001;107:513-23.

[22] Tian E, Zhan F, Walker R, Rasmussen E, Ma Y, Barlogie B, et al. The role of the Wnt-signaling antagonist DKK1 in the development of osteolytic lesions in multiple myeloma. N Engl J of Med 2003;349:2483-94.

[23] Huelsken J, Behrens J. The Wnt signalling pathway. J Cell Sci 2002;115:3977-8.

[24] Vlacic-Zischke J, Hamlet SM, Friis T, Tonetti MS, Ivanovski S. The influence of surface microroughness and hydrophilicity of titanium on the up-regulation of TGFbeta/BMP signalling in osteoblasts. Biomaterials 2011;32:665-71.

[25] Olivares-Navarrete R, Hyzy SL, Hutton DL, Dunn GR, Appert C, Boyan BD, et al. Role of non-canonical Wnt signaling in osteoblast maturation on microstructured titanium surfaces. Acta Biomater 2011;7:2740-50.

[26] Olivares-Navarrete R, Hyzy SL, Park JH, Dunn GR, Haithcock DA, Wasilewski CE, et al. Mediation of osteogenic differentiation of human mesenchymal stem cells on titanium surfaces by a Wnt-integrin feedback loop. Biomaterials 2011;32:6399-411.

[27] Laufer E, Nelson CE, Johnson RL, Morgan BA, Tabin C. Sonic hedgehog and Fgf-4 act through a signaling cascade and feedback loop to integrate growth and patterning of the developing limb bud. Cell 1994;79:993-1003.

[28] Hojo H, Ohba S, Taniguchi K, Shirai M, Yano F, Saito T, et al. Hedgehog-Gli activators direct osteo-chondrogenic function of bone morphogenetic protein toward osteogenesis in the perichondrium. J Biol Chem 2013;288:9924-32

[29] Xiao G, Jiang D, Gopalakrishnan R, Franceschi RT. Fibroblast growth factor 2 induction of the osteocalcin gene requires MAPK activity and phosphorylation of the osteoblast transcription factor, Cbfa1/Runx2. J Biol Chem 2002;277:36181-7.

[30] Nobta M, Tsukazaki T, Shibata Y, Xin C, Moriishi T, Sakano S, et al. Critical regulation of bone morphogenetic protein-induced osteoblastic differentiation by Delta1/Jagged1-activated Notch1 signaling. J Biol Chem 2005;280:15842-8.

[31] Engin F, Yao Z, Yang T, Zhou G, Bertin T, Jiang MM, et al. Dimorphic effects of Notch signaling in bone homeostasis. Nat Med 2008;14:299-305.

[32] Bartel DP. MicroRNAs: target recognition and regulatory functions. Cell 2009;136:215-33.

[33] Xu P, Vernooy SY, Guo M, Hay BA. The Drosophila microRNA miR-14 suppresses cell death and is required for normal fat metabolism. Curr Biol 2003;13:790-5.

[34] Bentwich I, Avniel A, Karov Y, Aharonov R, Gilad S, Barad O, et al. Identification of hundreds of conserved and nonconserved human microRNAs. Nat Genet 2005;37:766-70.

[35] Lee RC, Feinbaum RL, Ambros V. The C. elegans heterochronic gene lin-4 encodes small RNAs with antisense complementarity to lin-14. Cell 1993;75:843-54.

[36] Reinhart BJ, Slack FJ, Basson M, Pasquinelli AE, Bettinger JC, Rougvie AE, et al. The 21-nucleotide let-7 RNA regulates developmental timing in Caenorhabditis elegans. Nature 2000;403:901-6.

[37] Rodriguez A, Griffiths-Jones S, Ashurst JL, Bradley A. Identification of mammalian microRNA host genes and transcription units. Genome Res 2004;14:1902-10.

[38] Lee Y, Kim M, Han J, Yeom K-H, Lee S, Baek SH, et al. MicroRNA genes are transcribed by RNA polymerase II. EMBO J 2004;23:4051-60.

[39] Gregory RI, Chendrimada TP, Shiekhattar R. MicroRNA biogenesis: isolation and characterization of the microprocessor complex. Methods Mol Biol 2006; 342:33-47.

[40] Hutvagner G, Simard MJ. Argonaute proteins: key players in RNA silencing. Nat Rev Mol Cell Biol 2008;9:22-32.

[41] Valencia-Sanchez MA, Liu J, Hannon GJ, Parker R. Control of translation and mRNA degradation by miRNAs and siRNAs. Genes Dev 2006;20:515-24.

[42] Lewis BP, Burge CB, Bartel DP. Conserved seed pairing, often flanked by adenosines, indicates that thousands of human genes are microRNA targets. Cell 2005;120:15-20.

[43] Friedman RC, Farh KK-H, Burge CB, Bartel DP. Most mammalian mRNAs are conserved targets of microRNAs. Genome Res 2009;19:92-105.

[44] Li Z, Hassan MQ, Volinia S, van Wijnen AJ, Stein JL, Croce CM, et al. A microRNA signature for a BMP2-induced osteoblast lineage commitment program. Proc Natl Acad Sci U S A 2008;105:13906-11.

[45] Itoh T, Nozawa Y, Akao Y. MicroRNA-141 and -200a are involved in bone morphogenetic protein-2-induced mouse pre-osteoblast differentiation by targeting distal-less homeobox 5. J Biol Chem 2009;284: 19272-9.

[46] Li Z, Hassan MQ, Jafferji M, Aqeilan RI, Garzon R, Croce CM, et al. Biological functions of miR-29b contribute to positive regulation of osteoblast differentiation. J Biol Chem 2009;284:15676-84.

[47] Mizuno Y, Yagi K, Tokuzawa Y, Kanesaki-Yatsuka Y, Suda T, Katagiri T, et al. miR-125b inhibits osteoblastic differentiation by down-regulation of cell proliferation. Biochem Biophys Res Commun 2008;368:267-72.

[48] Huang J, Zhao L, Xing L, Chen D. MicroRNA-204 regulates Runx2 protein expression and mesenchymal progenitor cell differentiation. Stem Cells 2010;28:357-64.

[49] Kapinas K, Kessler CB, Delany AM. miR-29 suppression of osteonectin in osteoblasts: regulation during differentiation and by canonical Wnt signaling. J Cell Biochem 2009;108:216-24.

[50] Inose H, Ochi H, Kimura A, Fujita K, Xu R, Sato S, et al. A microRNA regulatory mechanism of osteoblast differentiation. Proc Natl Acad Sci U S A 2009;106:20794-9.

[51] Mizuno Y, Tokuzawa Y, Ninomiya Y, Yagi K, Yatsuka-Kanesaki Y, Suda T, et al. miR-210 promotes osteoblastic differentiation through inhibition of ACVR1B. FEBS Lett 2009;583:2263-8.

[52] Li H, Xie H, Liu W, Hu R, Huang B, Tan YF, et al. A novel microRNA targeting HDAC5 regulates osteoblast differentiation in mice and contributes to primary osteoporosis in humans. J Clin Invest 2009;119:3666-77.

[53] Kim YJ, Bae SW, Yu SS, Bae YC, Jung JS. miR-196a regulates proliferation and osteogenic differentiation in mesenchymal stem cells derived from human adipose tissue. J Bone Miner Res 2009;24:816-25.

[54] Wennerberg A, Albrektsson T. Effects of titanium surface topography on bone integration: a systematic review. Clin Oral Implants Res 2009;20:172-84.

[55] Wennerberg A, Albrektsson T, Andersson B, Krol JJ. A histomorphometric and removal torque study of screw-shaped titanium implants with three different surface topographies. Clin Oral Implants Res 1995;6:24-30.

[56] Shalabi MM, Gortemaker A, Van't Hof MA, Jansen JA, Creugers NH. Implant surface roughness and bone healing: a systematic review. J Dent Res 2006;85:496-500.

[57] Lang NP, Jepsen S. Implant surfaces and design (Working Group 4). Clin Oral Implants Res 2009;20 Suppl 4:228-31.

[58] Osborn J, Newesely H. Dynamic aspects of the implant-bone interface. In: Heimke G, editor. Dental implants: Materials and Systems: München: Carl Hanser Verlag; 1980. p. 111-23.

[59] Davies JE. Understanding peri-implant endosseous healing. J Dent Educ 2003;67:932-49.

[60] Amor N, Geris L, Vander Sloten J, Van Oosterwyck H. Computational modelling of biomaterial surface interactions with blood platelets and osteoblastic cells for the prediction of contact osteogenesis. Acta Biomater 2011;7:779-90.

[61] Yamaki K, Kataoka Y, Ohtsuka F, Miyazaki T. Micro-CT evaluation of in vivo osteogenesis at implants processed by wire-type electric discharge machining. Dent Mater J 2012;31:427-32.

[62] Letic-Gavrilovic A, Scandurra R, Abe K. Genetic potential of interfacial guided osteogenesis in implant devices. Dent Mater J 2000;19:99-132.

[63] Berglundh T, Abrahamsson I, Lang NP, Lindhe J. De novo alveolar bone formation adjacent to endosseous implants. Clin Oral Implants Res 2003;14:251-62.

[64] Cochran DL, Schenk RK, Lussi A, Higginbottom FL, Buser D. Bone response to unloaded and loaded titanium implants with a sandblasted and acid-etched surface: a histometric study in the canine mandible. J Biomed Mater Res 1998;40:1-11.

[65] Cochran DL, Buser D, Ten Bruggenkate CM, Weingart D, Taylor TM, Bernard J-P, et al. The use of reduced healing times on ITI® implants with a sandblasted and acid-etched (SLA) surface. Clin Oral Implants Res 2002;13:144-53.

[66] Abdel-Haq J, Karabuda CZ, Arisan V, Mutlu Z, Kurkcu M. Osseointegration and stability of a modified sand-blasted acid-etched implant: an experimental pilot study in sheep. Clin Oral Implants Res 2011;22:265-74.

[67] Schwarz F, Herten M, Sager M, Wieland M, Dard M, Becker J. Histological and immunohistochemical analysis of initial and early subepithelial connective tissue attachment at chemically modified and conventional SLA®titanium implants. A pilot study in dogs. Clin Oral Investig 2007;11:245-55.

[68] Buser D, Broggini N, Wieland M, Schenk RK, Denzer AJ, Cochran DL, et al. Enhanced bone apposition to a chemically modified SLA titanium surface. J Dent Res 2004;83:529-33.

[69] Zhang Y, Andrukhov O, Berner S, Matejka M, Wieland M, Rausch-Fan X, et al. Osteogenic properties of hydrophilic and hydrophobic titanium surfaces evaluated with osteoblast-like cells (MG63) in coculture with human umbilical vein endothelial cells (HUVEC). Dent Mater 2010;26:1043-51.

[70] Rupp F, Scheideler L, Olshanska N, de Wild M, Wieland M, Geis-Gerstorfer J. Enhancing surface free energy and hydrophilicity through chemical modification of microstructured titanium implant surfaces. J Biomed Mater Res A 2006;76:323-34.

[71] Zhao G, Raines AL, Wieland M, Schwartz Z, Boyan BD. Requirement for both micron- and submicron scale structure for synergistic responses of osteoblasts to substrate surface energy and topography. Biomaterials 2007;28:2821-9.

[72] Olivares-Navarrete R, Hyzy SL, Hutton DL, Erdman CP, Wieland M, Boyan BD, et al. Direct and indirect effects of microstructured titanium substrates on the induction of mesenchymal stem cell differentiation towards the osteoblast lineage. Biomaterials 2010;31:2728-35.

[73] Klein MO, Bijelic A, Toyoshima T, Gotz H, von Koppenfels RL, Al-Nawas B, et al. Long-term response of osteogenic cells on micron and submicron-scale-structured hydrophilic titanium surfaces: sequence of cell proliferation and cell differentiation. Clin Oral Implants Res 2010;21:642-9.

[74] Gittens RA, McLachlan T, Olivares-Navarrete R, Cai Y, Berner S, Tannenbaum R, et al. The effects of combined micron-/submicron-scale surface roughness and nanoscale features on cell proliferation and differentiation. Biomaterials 2011;32:3395-403.

[75] Wennerberg A, Svanborg LM, Berner S, Andersson M. Spontaneously formed nanostructures on titanium surfaces. Clin Oral Implants Res 2013;24:203-9.

[76] Wennerberg A, Galli S, Albrektsson T. Current knowledge about the hydrophilic and nanostructured SLActive surface. Clin Cosmet Investig Dent 2011;3:59-67.

[77] Lin YH, Peng PW, Ou KL. The effect of titanium with electrochemical anodization on the response of the adherent osteoblast-like cell. Implant Dent 2012;21:344-9.

[78] Zhuang XM, Zhou B, Ouyang JL, Sun HP, Wu YL, Liu Q, et al. Enhanced MC3T3-E1 preosteoblast response and bone formation on the addition of nano-needle and nano-porous features to microtopographical titanium surfaces. Biomed Mater 2014;9:045001.

[79] Meng W, Zhou Y, Zhang Y, Cai Q, Yang L, Wang B. Effects of hierarchical micro/nano-textured titanium surface features on osteoblast-specific gene expression. Implant Dent 2013;22:656-61.

[80] Brett PM, Harle J, Salih V, Mihoc R, Olsen I, Jones FH, et al. Roughness response genes in osteoblasts. Bone 2004;35:124-33.

[81] Hamlet S, Alfarsi M, George R, Ivanovski S. The effect of hydrophilic titanium surface modification on macrophage inflammatory cytokine gene expression. Clin Oral Implants Res 2012;23:584-90.

[82] Zinelis S, Silikas N, Thomas A, Syres K, Eliades G. Surface characterization of SLActive dental implants. Eur J Esthet Dent 2012;7:72-92.

[83] Li S, Ni J, Liu X, Zhang X, Yin S, Rong M, et al. Surface characteristics and biocompatibility of sandblasted and acid-etched titanium surface modified by ultraviolet irradiation: an in vitro study. J Biomed Mater Res B Appl Biomater 2012;100:1587-98.

[84] Anselme K. Biomaterials and interface with bone. Osteoporos Int 2011;22:2037-42.

[85] Katona B, Daroczi L, Jenei A, Bako J, Hegedus C. Comperative study of implant surface characteristics. Fogorv Sz 2013;106:135-43.

[86] Wall I, Donos N, Carlqvist K, Jones F, Brett P. Modified titanium surfaces promote accelerated osteogenic differentiation of mesenchymal stromal cells in vitro. Bone 2009;45:17-26.

[87] Klein MO, Bijelic A, Ziebart T, Koch F, Kammerer PW, Wieland M, et al. Submicron scale-structured hydrophilic titanium surfaces promote early osteogenic gene response for cell adhesion and cell differentiation. Clin Implant Dent Relat Res 2013;15:166-75.

[88] Zhao G, Schwartz Z, Wieland M, Rupp F, Geis-Gerstorfer J, Cochran DL, et al. High surface energy enhances cell response to titanium substrate microstructure. J Biomed Mater Res A 2005;74:49-58.

[89] Buser D, Nydegger T, Hirt HP, Cochran DL, Nolte LP. Removal torque values of titanium implants in the maxilla of miniature pigs. Int J Oral Maxillofac Implants 1998;13:611-9.

[90] Cochran DL, Hermann JS, Schenk RK, Higginbottom FL, Buser D. Biologic width around titanium implants. A histometric analysis of the implanto-gingival junction around unloaded and loaded nonsubmerged implants in the canine mandible. J Periodontol 1997;68:186-98.

[91] Wetzel AC, Vlassis J, Caffesse RG, Hammerle CH, Lang NP. Attempts to obtain re-osseointegration following experimental peri-implantitis in dogs. Clin Oral Implants Res 1999;10:111-9.

[92] Derksen RB, Kontogiorgos ED, Dechow PC, Opperman LA. A pilot histologic comparison of bone-to-implant contact between phosphate-coated and control titanium implants in the canine model. Int J Oral Maxillofac Implants 2014;29:203-10.

[93] Roccuzzo M, Bunino M, Prioglio F, Bianchi SD. Early loading of sandblasted and acid-etched (SLA) implants: a prospective split-mouth comparative study. Clin Oral Implants Res 2001;12:572-8.

[94] Bornstein MM, Lussi A, Schmid B, Belser UC, Buser D. Early loading of nonsubmerged titanium implants with a sandblasted and acid-etched (SLA) surface: 3-year results of a prospective study in partially edentulous patients. Int J Oral Maxillofac Implants 2003;18:659-66.

[95] Buser D, Janner SF, Wittneben JG, Bragger U, Ramseier CA, Salvi GE. 10-year survival and success rates of 511 titanium implants with a sandblasted and acid-etched surface: a retrospective study in 303 partially edentulous patients. Clin Implant Dent Relat Res 2012;14:839-51.

[96] Buser D, Nydegger T, Oxland T, Cochran DL, Schenk RK, Hirt HP, et al. Interface shear strength of titanium implants with a sandblasted and acid-etched surface: a biomechanical study in the maxilla of miniature pigs. J Biomed Mater Res 1999;45:75-83.

[97] Bornstein MM, Valderrama P, Jones AA, Wilson TG, Seibl R, Cochran DL. Bone apposition around two different sandblasted and acid-etched titanium implant

surfaces: a histomorphometric study in canine mandibles. Clin Oral Implants Res 2008;19:233-41.

[98] Lai HC, Zhuang LF, Zhang ZY, Wieland M, Liu X. Bone apposition around two different sandblasted, large-grit and acid-etched implant surfaces at sites with coronal circumferential defects: an experimental study in dogs. Clin Oral Implants Res 2009;20:247-53.

[99] Schwarz F, Sager M, Ferrari D, Herten M, Wieland M, Becker J. Bone regeneration in dehiscence-type defects at non-submerged and submerged chemically modified (SLActive) and conventional SLA titanium implants: an immunohistochemical study in dogs. J Clin Periodontol 2008;35:64-75.

[100] Ferguson SJ, Broggini N, Wieland M, de Wild M, Rupp F, Geis-Gerstorfer J, et al. Biomechanical evaluation of the interfacial strength of a chemically modified sandblasted and acid-etched titanium surface. J Biomed Mater Res A 2006;78:291-7.

[101] Nicolau P, Korostoff J, Ganeles J, Jackowski J, Krafft T, Neves M, et al. Immediate and early loading of chemically modified implants in posterior jaws: 3-year results from a prospective randomized multicenter study. Clin Implant Dent Relat Res 2013;15:600-12.

[102] Ganeles J, Zollner A, Jackowski J, ten Bruggenkate C, Beagle J, Guerra F. Immediate and early loading of Straumann implants with a chemically modified surface (SLActive) in the posterior mandible and maxilla: 1-year results from a prospective multicenter study. Clin Oral Implants Res 2008;19:1119-28.

[103] Zollner A, Ganeles J, Korostoff J, Guerra F, Krafft T, Bragger U. Immediate and early non-occlusal loading of Straumann implants with a chemically modified surface (SLActive) in the posterior mandible and maxilla: interim results from a prospective multicenter randomized-controlled study. Clin Oral Implants Res 2008;19:442-50.

[104] Morton D, Bornstein MM, Wittneben JG, Martin WC, Ruskin JD, Hart CN, et al. Early loading after 21 days of healing of nonsubmerged titanium implants with a chemically modified sandblasted and acid-etched surface: two-year results of a prospective two-center study. Clin Implant Dent Relat Res 2010;12:9-17.

[105] Linares A, Mardas N, Dard M, Donos N. Effect of immediate or delayed loading following immediate placement of implants with a modified surface. Clin Oral Implants Res 2011;22:38-46.

[106] Schatzle M, Mannchen R, Balbach U, Hammerle CH, Toutenburg H, Jung RE. Stability change of chemically modified sandblasted/acid-etched titanium palatal implants. A randomized-controlled clinical trial. Clin Oral Implants Res 2009;20:489-95.

[107] Karabuda ZC, Abdel-Haq J, Arisan V. Stability, marginal bone loss and survival of standard and modified sand-blasted, acid-etched implants in bilateral edentulous spaces: a prospective 15-month evaluation. Clin Oral Implants Res 2011;22:840-9.

[108] Lohmann CH, Sagun R, Jr., Sylvia VL, Cochran DL, Dean DD, Boyan BD, et al. Surface roughness modulates the response of MG63 osteoblast-like cells to 1,25-(OH)(2)D(3) through regulation of phospholipase A(2) activity and activation of protein kinase A. J Biomed Mater Res 1999;47:139-51.

[109] Lohmann CH, Bonewald LF, Sisk MA, Sylvia VL, Cochran DL, Dean DD, et al. Maturation state determines the response of osteogenic cells to surface roughness and 1,25-dihydroxyvitamin D3. J Bone Miner Res 2000;15:1169-80.

[110] Schwartz Z, Lohmann CH, Vocke AK, Sylvia VL, Cochran DL, Dean DD, et al. Osteoblast response to titanium surface roughness and 1alpha,25-(OH)(2)D(3) is mediated through the mitogen-activated protein kinase (MAPK) pathway. J Biomed Mater Res 2001;56:417-26.

[111] Sisk MA, Lohmann CH, Cochran DL, Sylvia VL, Simpson JP, Dean DD, et al. Inhibition of cyclooxygenase by indomethacin modulates osteoblast response to titanium surface roughness in a time-dependent manner. Clin Oral Implants Res 2001;12:52-61.

[112] Lohmann CH, Tandy EM, Sylvia VL, Hell-Vocke AK, Cochran DL, Dean DD, et al. Response of normal female human osteoblasts (NHOst) to 17beta-estradiol is modulated by implant surface morphology. J Biomed Mater Res 2002;62:204-13.

[113] Mamalis AA, Silvestros SS. Analysis of osteoblastic gene expression in the early human mesenchymal cell response to a chemically modified implant surface: an in vitro study. Clin Oral Implants Res 2011;22:530-7.

[114] Martin JY, Schwartz Z, Hummert TW, Schraub DM, Simpson J, Lankford J, Jr., et al. Effect of titanium surface roughness on proliferation, differentiation, and protein synthesis of human osteoblast-like cells (MG63). J Biomed Mater Res 1995;29:389-401.

[115] Khan MR, Donos N, Salih V, Brett PM. The enhanced modulation of key bone matrix components by modified Titanium implant surfaces. Bone 2012;50:1-8.

[116] Lang NP, Salvi GE, Huynh-Ba G, Ivanovski S, Donos N, Bosshardt DD. Early osseointegration to hydrophilic and hydrophobic implant surfaces in humans. Clin Oral Implants Res 2011;22:349-56.

[117] Donos N, Hamlet S, Lang NP, Salvi GE, Huynh-Ba G, Bosshardt DD, et al. Gene expression profile of osseointegration of a hydrophilic compared with a hydrophobic microrough implant surface. Clin Oral Implants Res 2011;22:365-72.

[118] Ivanovski S, Hamlet S, Salvi GE, Huynh-Ba G, Bosshardt DD, Lang NP, et al. Transcriptional profiling of osseointegration in humans. Clin Oral Implants Res 2011;22:373-81.

[119] Donos N, Retzepi M, Wall I, Hamlet S, Ivanovski S. In vivo gene expression profile of guided bone regeneration associated with a microrough titanium surface. Clin Oral Implants Res 2011;22:390-8.

[120] Boyan BD, Batzer R, Kieswetter K, Liu Y, Cochran DL, Szmuckler-Moncler S, et al. Titanium surface roughness alters responsiveness of MG63 osteoblast-like cells to 1 alpha,25-(OH)2D3. J Biomed Mater Res 1998;39:77-85.

[121] Boyan BD, Bonewald LF, Paschalis EP, Lohmann CH, Rosser J, Cochran DL, et al. Osteoblast-mediated mineral deposition in culture is dependent on surface microtopography. Calcif Tissue Int 2002;71:519-29.

[122] Boyan BD, Lohmann CH, Sisk M, Liu Y, Sylvia VL, Cochran DL, et al. Both cyclooxygenase-1 and cyclooxygenase-2 mediate osteoblast response to titanium surface roughness. J Biomed Mater Res 2001;55:350-9.

[123] Kim BS, Kim JS, Park YM, Choi BY, Lee J. Mg ion implantation on SLA-treated titanium surface and its effects on the behavior of mesenchymal stem cell. Mater Sci Eng C Mater for Biol Appl 2013;33:1554-60.

[124] Masaki C, Schneider GB, Zaharias R, Seabold D, Stanford C. Effects of implant surface microtopography on osteoblast gene expression. Clin Oral Implants Res 2005;16:650-6.

[125] Wieland M, Textor M, Chehroudi B, Brunette DM. Synergistic interaction of topographic features in the production of bone-like nodules on Ti surfaces by rat osteoblasts. Biomaterials 2005;26:1119-30.

[126] Qu Z, Rausch-Fan X, Wieland M, Matejka M, Schedle A. The initial attachment and subsequent behavior regulation of osteoblasts by dental implant surface modification. J Biomed Mater Res A 2007;82:658-68.

[127] Perizzolo D, Lacefield WR, Brunette DM. Interaction between topography and coating in the formation of bone nodules in culture for hydroxyapatite- and titanium-coated micromachined surfaces. J Biomed Mater Res 2001;56:494-503.

[128] Rausch-fan X, Qu Z, Wieland M, Matejka M, Schedle A. Differentiation and cytokine synthesis of human alveolar osteoblasts compared to osteoblast-like cells (MG63) in response to titanium surfaces. Dent Mater 2008;24:102-10.

[129] Mamalis AA, Markopoulou C, Vrotsos I, Koutsilirieris M. Chemical modification of an implant surface increases osteogenesis and simultaneously reduces osteoclastogenesis: an in vitro study. Clin Oral Implants Res 2011;22:619-26.

[130] Lossdorfer S, Schwartz Z, Wang L, Lohmann CH, Turner JD, Wieland M, et al. Microrough implant surface topographies increase osteogenesis by reducing osteoclast formation and activity. J Biomed Mater Res A 2004;70:361-9.

[131] Bang SM, Moon HJ, Kwon YD, Yoo JY, Pae A, Kwon IK. Osteoblastic and osteoclastic differentiation on SLA and hydrophilic modified SLA titanium surfaces. Clin Oral Implants Res 2014; 25:831-7.

[132] Kuzyk PR, Schemitsch EH. The basic science of peri-implant bone healing. Indian J Orthop 2011;45:108-15.

[133] Orsini E, Salgarello S, Martini D, Bacchelli B, Quaranta M, Pisoni L, et al. Early healing events around titanium implant devices with different surface microtopography: a pilot study in an in vivo rabbit model. ScientificWorldJournal 2012;2012:349842.

[134] Hong J, Kurt S, Thor A. A hydrophilic dental implant surface exhibit thrombogenic properties in vitro. Clin Implant Dent Relat Res 2013;15:105-12.

[135] Nurden AT. Platelets, inflammation and tissue regeneration. Thromb Haemost 2011;105 Suppl 1:S13-33.

[136] Aukhil I. Biology of wound healing. Periodontol 2000 2000;22:44-50.

[137] Kammerer PW, Gabriel M, Al-Nawas B, Scholz T, Kirchmaier CM, Klein MO. Early implant healing: promotion of platelet activation and cytokine release by topographical, chemical and biomimetical titanium surface modifications in vitro. Clin Oral Implants Res 2012;23:504-10.

[138] Refai AK, Textor M, Brunette DM, Waterfield JD. Effect of titanium surface topography on macrophage activation and secretion of proinflammatory cytokines and chemokines. J Biomed Mater Res A 2004;70:194-205.

[139] Chehroudi B, Ghrebi S, Murakami H, Waterfield JD, Owen G, Brunette DM. Bone formation on rough, but not polished, subcutaneously implanted Ti surfaces is preceded by macrophage accumulation. J Biomed Mater Res A 2010;93:724-37.

[140] Alfarsi MA, Hamlet SM, Ivanovski S. Titanium surface hydrophilicity modulates the human macrophage inflammatory cytokine response. J Biomed Mater Res A 2014;102:60-7.

[141] Hyzy SL, Olivares-Navarrete R, Hutton DL, Tan C, Boyan BD, Schwartz Z. Microstructured titanium regulates interleukin production by osteoblasts, an effect modulated by exogenous BMP-2. Acta Biomater 2013;9:5821-9.

[142] Kou PM, Schwartz Z, Boyan BD, Babensee JE. Dendritic cell responses to surface properties of clinical titanium surfaces. Acta Biomater 2011;7:1354-63.

[143] Ziebart T, Schnell A, Walter C, Kammerer PW, Pabst A, Lehmann KM, et al. Interactions between endothelial progenitor cells (EPC) and titanium implant surfaces. Clin Oral Investig 2013;17:301-9.

[144] An N, Schedle A, Wieland M, Andrukhov O, Matejka M, Rausch-Fan X. Proliferation, behavior, and cytokine gene expression of human umbilical vascular endothelial cells in response to different titanium surfaces. J Biomed Mater Res A 2010;93:364-72.

[145] Raines AL, Olivares-Navarrete R, Wieland M, Cochran DL, Schwartz Z, Boyan BD. Regulation of angiogenesis during osseointegration by titanium surface microstructure and energy. Biomaterials 2010;31:4909-17.

[146] Raz P, Lohmann CH, Turner J, Wang L, Poythress N, Blanchard C, et al. 1 alpha,25(OH)(2)D-3 Regulation of integrin expression is substrate dependent. J Biomed Mater Res A 2004;71:217-25.

[147] Olivares-Navarrete R, Raz P, Zhao G, Chen J, Wieland M, Cochran DL, et al. Integrin alpha2beta1 plays a critical role in osteoblast response to micron-scale surface structure and surface energy of titanium substrates. Proc Natl Acad Sci U S A 2008;105:15767-72.

[148] Keselowsky BG, Wang L, Schwartz Z, Garcia AJ, Boyan BD. Integrin alpha(5) controls osteoblastic proliferation and differentiation responses to titanium substrates presenting different roughness characteristics in a roughness independent manner. J Biomed Mater Res A 2007;80:700-10.

[149] Xiao G, Wang D, Benson MD, Karsenty G, Franceschi RT. Role of the alpha2-integrin in osteoblast-specific gene expression and activation of the Osf2 transcription factor. J Biol Chem 1998;273:32988-94.

[150] Wang L, Zhao G, Olivares-Navarrete R, Bell BF, Wieland M, Cochran DL, et al. Integrin beta1 silencing in osteoblasts alters substrate-dependent responses to 1,25-dihydroxy vitamin D3. Biomaterials 2006;27:3716-25.

[151] Lai HC, Zhuang LF, Liu X, Wieland M, Zhang ZY. The influence of surface energy on early adherent events of osteoblast on titanium substrates. J Biomed Mater Res A 2010;93:289-96.

[152] Park JH, Wasilewski CE, Almodovar N, Olivares-Navarrete R, Boyan BD, Tannenbaum R, et al. The responses to surface wettability gradients induced by chitosan nanofilms on microtextured titanium mediated by specific integrin receptors. Biomaterials 2012;33:7386-93.

[153] Prowse PD, Elliott CG, Hutter J, Hamilton DW. Inhibition of Rac and ROCK signalling influence osteoblast adhesion, differentiation and mineralization on titanium topographies. PLoS One 2013;8:e58898.

[154] Galli C, Piemontese M, Lumetti S, Ravanetti F, Macaluso GM, Passeri G. Actin cytoskeleton controls activation of Wnt/beta-catenin signaling in mesenchymal cells on implant surfaces with different topographies. Acta Biomater 2012;8:2963-8.

[155] Lumetti S, Mazzotta S, Ferrillo S, Piergianni M, Piemontese M, Passeri G, et al. RhoA Controls Wnt Upregulation on Microstructured Titanium Surfaces. BioMed Res Int 2014;2014:401859.

[156] Schwartz Z, Lohmann CH, Sisk M, Cochran DL, Sylvia VL, Simpson J, et al. Local factor production by MG63 osteoblast-like cells in response to surface roughness and 1,25-(OH)2D3 is mediated via protein kinase C- and protein kinase A-dependent pathways. Biomaterials 2001;22:731-41.

[157] Batzer R, Liu Y, Cochran DL, Szmuckler-Moncler S, Dean DD, Boyan BD, et al. Prostaglandins mediate the effects of titanium surface roughness on MG63 osteoblast-like cells and alter cell responsiveness to 1 alpha,25-(OH)2D3. J Biomed Mater Res 1998;41:489-96.

[158] Fang M, Olivares-Navarrete R, Wieland M, Cochran DL, Boyan BD, Schwartz Z. The role of phospholipase D in osteoblast response to titanium surface microstructure. J Biomed Mater Res A 2010;93:897-909.

[159] Zhuang LF, Jiang HH, Qiao SC, Appert C, Si MS, Gu YX, et al. The roles of extracellular signal-regulated kinase 1/2 pathway in regulating osteogenic differentiation of murine preosteoblasts MC3T3-E1 cells on roughened titanium surfaces. J Biomed Mater Res A 2012;100:125-33.

[160] Jiang HH, Dong K, Liu ST, Liu ZH. Role of extracellular signal-regulated kinase in osteoblast differentiation on roughened titanium surfaces.Shanghai Kou Qiang Yi Xue 2014;23:39-45.

[161] Galli C, Passeri G, Ravanetti F, Elezi E, Pedrazzoni M, Macaluso GM. Rough surface topography enhances the activation of Wnt/beta-catenin signaling in mesenchymal cells. J Biomed Mater Res A 2010;95:682-90.

[162] Galli C, Macaluso GM, Piemontese M, Passeri G. Titanium topography controls FoxO/beta-catenin signaling. J Dent Res 2011;90:360-4.

[163] Dennis G, Jr., Sherman BT, Hosack DA, Yang J, Gao W, Lane HC, et al. DAVID: Database for Annotation, Visualization, and Integrated Discovery. Genome Biol 2003;4:P3.

[164] Olivares-Navarrete R, Hyzy S, Wieland M, Boyan BD, Schwartz Z. The roles of Wnt signaling modulators Dickkopf-1 (Dkk1) and Dickkopf-2 (Dkk2) and cell maturation state in osteogenesis on microstructured titanium surfaces. Biomaterials 2010;31:2015-24.

[165] Galli C, Piemontese M, Lumetti S, Manfredi E, Macaluso GM, Passeri G. GSK3b-inhibitor lithium chloride enhances activation of Wnt canonical signaling and osteoblast differentiation on hydrophilic titanium surfaces. Clin Oral Implants Res 2013;24:921-7.

[166] Nishita M, Yoo SK, Nomachi A, Kani S, Sougawa N, Ohta Y, et al. Filopodia formation mediated by receptor tyrosine kinase Ror2 is required for Wnt5a-induced cell migration. J Cell Biol 2006;175:555-62.

[167] Lammens J, Liu Z, Aerssens J, Dequeker J, Fabry G. Distraction bone healing versus osteotomy healing: a comparative biochemical analysis. J Bone Miner Res 1998;13:279-86.

[168] Sato M, Ochi T, Nakase T, Hirota S, Kitamura Y, Nomura S, et al. Mechanical tension-stress induces expression of bone morphogenetic protein (BMP)-2 and BMP-4, but not BMP-6, BMP-7, and GDF-5 mRNA, during distraction osteogenesis. J Bone Miner Res 1999;14:1084-95.

[169] Kim IS, Song YM, Hwang SJ. Osteogenic responses of human mesenchymal stromal cells to static stretch. J Dent Res 2010;89:1129-34.

[170] Zelzer E, McLean W, Ng YS, Fukai N, Reginato AM, Lovejoy S, et al. Skeletal defects in VEGF(120/120) mice reveal multiple roles for VEGF in skeletogenesis. Development 2002;129:1893-904.

[171] Jiang J, Fan CY, Zeng BF. Osteogenic differentiation effects on rat bone marrow-derived mesenchymal stromal cells by lentivirus-mediated co-transfection of human BMP2 gene and VEGF165 gene. Biotechnol Lett 2008;30:197-203.

[172] Kummitha CM, Mayle KM, Christman MA, 2nd, Deosarkar SP, Schwartz AL, McCall KD, et al. A sandwich ELISA for the detection of Wnt5a. J Immunol Methods 2010;352:38-44.

[173] Gu YX, Du J, Si MS, Mo JJ, Qiao SC, Lai HC. The roles of PI3K/Akt signaling pathway in regulating MC3T3-E1 preosteoblast proliferation and differentiation on SLA and SLActive titanium surfaces. J Biomed Mater Res A 2013;101:748-54.

[174] Chen WC, Chen YS, Ko CL, Lin Y, Kuo TH, Kuo HN. Interaction of progenitor bone cells with different surface modifications of titanium implant. Mater Sci Eng C Mater for Biol Appl 2014;37:305-13.

Chapter 4: The Microarray Study

Genome-wide transcriptional analysis of early interactions of osteoprogenitor cells with micro-rough titanium implants

Saso Ivanovski[*], Nishant Chakravorty[*], Jamie Harle,

Stephen Hamlet, Yin Xiao, Peter Brett & Maurizio Tonetti

(Manuscript in preparation)

Suggested Statement of Contribution of Co-Authors for Thesis by Publication

Contributors	Statement of contribution
Saso Ivanovski[*]	Involved in the conception and design of the project. Performed laboratory experiments and reviewed the manuscript.
Nishant Chakravorty[*]	Performed pathway and network analysis using functional genomics. Data analysis and interpretation. Wrote the manuscript.
Jamie Harle	Involved in the design of the project. Performed laboratory experiments.
Stephen Hamlet	Assisted in technical guidance and reviewing the manuscript.
Yin Xiao	Involved in designing the project, manuscript preparation and reviewing.
Peter Brett	Involved in the conception and design of the project.
Maurizio Tonetti	Involved in the conception and design of the project.

[*]*Co-first authors*

Principal Supervisor Confirmation

I have sighted email or other correspondence from all co-authors confirming their certifying authorship

Prof. Yin Xiao		**10th July, 2014**
Name	**Signature**	**Date**

Abstract

Topographically modified micro-roughened titanium implant surfaces are known to have superior osseointegration properties when compared with their polished counterparts. Osseointegration is the biological process integrating an implant structurally and functionally with the surrounding bone, and involves a series of molecular processes culminating in new bone formation around the implant. The aim of this study was to investigate the early molecular events following exposure to micro-roughened sand-blasted, large grit, acid-etched (SLA) surfaces that lead to their enhanced osteogenic properties in comparison with smooth polished (SMO) implants. Whole genome transcriptional analysis was performed using Affymetrix Human Genome U133 Plus 2.0 arrays following the exposure of primary human osteoprogenitor cells to SLA and SMO surfaces for 3 and 24 hours. A clear pro-osteogenic response was observed on SLA surfaces compared with SMO surfaces following 24 hours of exposure. The bone morphogenetic protein, BMP2 (fold-change: FC >5.7) and the key osteogenic transcription factor, RUNX2 (FC=2.2) were seen to have higher expression on SLA compared with SMO within 24 hours. Analysis using the Database for Annotation, Visualization and Integrated Discovery (DAVID) and Ingenuity Pathways Analysis (IPA) tool, revealed clusters related to skeletal system development as the earliest physiological clusters enriched on SLA surfaces. Assessment of the immediate response to SLA and SMO surfaces, showed differential expression of clusters related to cell-mediated immune response, immune cell trafficking and nervous system development between them after 3 hours of exposure. An immediate pro-angiogenic and immunomodulatory response on SLA surfaces as demonstrated by a time-course analysis (3 hours vs. base-line) possibly lays the foundation for the pro-osteogenic niche provided by the SLA surface, as confirmed by higher mineralization on SLA surfaces. These results describe a sequential pattern of molecular events that may be responsible for the enhanced osseointegration observed on micro-roughened surfaces and emphasize the biological relevance of studying the early cellular response to micro-roughened titanium implant surfaces.

4.1 INTRODUCTION

Titanium surfaces are established as dental and orthopedic implant surfaces owing to their superior osseointegration and osteointegrative properties. The key challenge in implantology is the early structural and functional restoration of body parts. Researchers have been constantly exploring physical and chemical alterations to implant surfaces and have come up with several modifications. The topographically modified titanium dental implant surface - sand blasted, large-grit, acid-etched (SLA), has been a clinically successful dental implant with superior osseointegration and osteogenic properties compared with smooth (SMO) surfaces [1-5].

The bone matrix formed by mineralization of osteoid deposited by osteoblastic activity, has a multi-dimensional micro-rough architecture and this makes the micro-rough SLA surface an interesting substrate to study osteogenesis. Moreover, Osborn and Newesley have described osteogenesis on micro-roughened surfaces as "contact osteogenesis", wherein new bone is deposited by direct osteoblastic activity on the surface of the implant [6]. The micro-roughened structure of topographically modified titanium surfaces as such, provides a substrate akin to the native bone architecture. Therefore, it is reasonable to consider the use of such surfaces to study the mechanistic regulation of osteogenesis instead of conventional techniques inducing osteogenic differentiation using chemical methods.

The transcriptome of a living organism is the repository of genetic information necessary for the growth and development of various organs and physiological systems. Activation and repression of different mRNA molecules in the genome regulate different biological processes like cell and tissue differentiation. Whole genome transcriptome analysis tools like microarrays, provides us with a powerful instrument to study the inter-relationship between different messenger molecules. Osteogenic differentiation and osseointegration are biological processes guided by series of molecular events resulting in activation of signaling pathways. These processes eventually lead to matrix deposition, mineralization and finally a structural and functional integration of implant with the surrounding bone. Several studies have used the micro-roughened SLA surface as a physiologically relevant model to explore the molecular mechanisms of osteogenic differentiation and osseointegration *in vitro* [1, 2, 7-9]. Studies have revealed an early modulation of gene expression and

have also shown differential expression of cell signaling pathways on these surfaces [2, 3, 9]. Although, these surfaces have been frequently used to study the osteo-differentiation process, none of the studies have confirmed whether such surfaces can actually be substantial models to study the process of osteogenesis and osseointegration and neither have they identified a time-course of events that lead to the pro-osteogenic mechanisms. The aim of this study was to explore the genetic mechanisms and biological processes regulated on micro-roughened surfaces that lead to their superior osseointegration properties compared to smooth/polished surfaces.

4.2 MATERIALS AND METHODS

4.2.1 Titanium discs

The SLA and SMO discs were supplied by Institut Straumann (Basel, Switzerland). They were prepared from grade II commercially pure titanium (15 mm in diameter, 1 mm in thickness). The SLA surfaces were prepared by blasting the titanium surface with 250-500 µm corundum grit and acid etching with a hot solution of hydrochloric/sulfuric acids. Polished smooth titanium surfaces (SMO) were used as control surfaces for the study.

4.2.2 Cell culture

Alveolar bone derived primary osteoprogenitor cells (BCs) were obtained from three human volunteers. The cells were established after culturing redundant tissues obtained following third molar extraction surgery using methods described in previous studies from our research group [10-12]. The BCs were seeded at a density of 5×10^4 cells/titanium disc placed in 24 well tissue culture plates (BD Falcon, North Ryde, NSW, Australia), and incubated at 37 °C in a 5% CO_2 atmosphere in Dulbecco's modified Eagle's medium (DMEM) (Invitrogen, Mt Waverley, VIC, Australia) supplemented with fetal bovine serum (FBS) (Thermo, In Vitro Technologies, Nobel Park, VIC, Australia) and antibiotics (100 U/ml penicillin/100 µg/ml streptomycin). Six discs of each kind per sample per time point were used for the study.

4.2.3 Mineralization study

Mineral deposition on the SLA and SMO titanium surfaces by BCs cultured in either standard (SM) or osteogenic supplemented media (DEX+: SM supplemented

with 100 nM dexamethasone). Supplementation of low doses of dexamethasone to standard culture has been known to stimulate osteogenesis for a long time now [13]. This helps in relative quantification of mineral deposition by alleviating the response. The cultures were assessed for mineralization up to 4 weeks, using Alizarin Red S staining. This staining was carried out using a modification of the method described by Reinholz et al. [14]. Briefly, after removing the media and washing the cells with phosphate buffered saline (PBS), the cells were first fixed with 10% neutral buffered formalin and then stained with 40 mM Alizarin Red S for 10 min at room temperature. The excess stain was then removed by washing with ultrapure water and the samples were allowed to air dry before photographing. Semi-quantitative assessment of mineralization was achieved by destaining for 15 min with 10% (w/v) cetylpyridinium chloride in 10 mM sodium phosphate pH 7.0. The extracted stain was transferred to a 96-well plate and the absorbance at 570 nm measured using a plate reader/spectrophotometer. The calcium and phosphorus content was further assessed using Energy Dispersive Spectrometry (EDAX).

4.2.4 Microarray analysis

Microarray whole genome analysis was performed following 3 and 24 hours of exposure of osteoblasts to the SLA and SMO surfaces. Affymetrix Human Genome U133 Plus 2.0 arrays (Affymetrix, Santa Clara, California) containing 54675 probes for analysis, were used for the study. Total RNA was isolated (RNAqueous, Ambion) and cDNA was synthesized using the Affymetrix one cycle cDNA kit. Pseudo-uridine labeled probes were prepared by synthesizing cRNA (Affymetrix IVT kit) before hybridization onto the microarrays. Data analysis was performed using the trial version of GeneSpring GX12.5 (Agilent Technologies, Inc., developed on avadis^{TM} platform by Strand Life Science Pvt. Ltd.).

Comparisons between the expression profile on SLA and SMO surfaces were performed at each time-point (3 and 24 hours) using Student's *t*-test. Correlations were also made between the two time-points and with the base-line expression (0 hour) for each of the surfaces (SLA and SMO). Functional classification of the differentially expressed genes was subsequently performed, and pathway and network enrichments were further assessed using the Database for Annotation, Visualization and Integrated Discovery (DAVID) [15] and Ingenuity Pathways

Analysis (IPA) tool (Ingenuity® Systems, www.ingenuity.com, Redwood City, CA, USA) [16].

4.3 RESULTS

4.3.1 Mineralization assay

Human BCs were seen to induce more mineral deposition on SLA surfaces compared to SMO (Figure 4-1). The differences were observed to become significant after two weeks of culture. Osteoblasts were seen to induce mineral deposition even in the absence of osteogenic supplementation (in SM); however, the deposition was always higher in DEX+ than SM media. Increased deposition is seen throughout the 4 weeks for all cultures. EDAX analysis confirmed increased mineralization at week 4. Higher deposition of calcium and phosphorus was detected on the SLA surfaces than on the SMO surfaces, both in the presence (DEX+) or absence (SM) of osteogenic supplement, although the deposition was significantly higher with cells cultured using DEX+ (Figure 4-1).

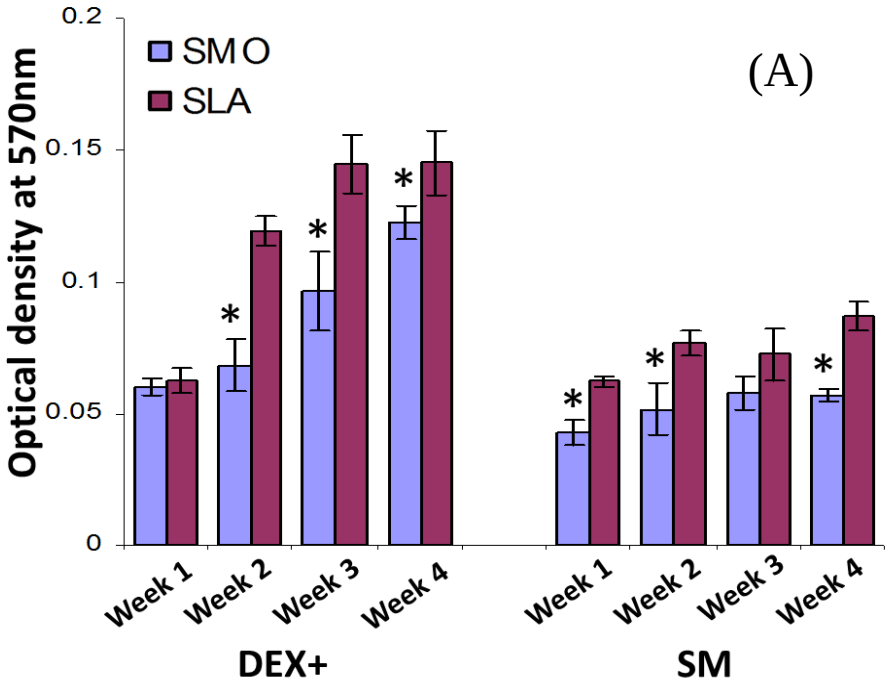

Figure 4-1 A: Spectrophotometric quantification of Alizarin Red S staining.

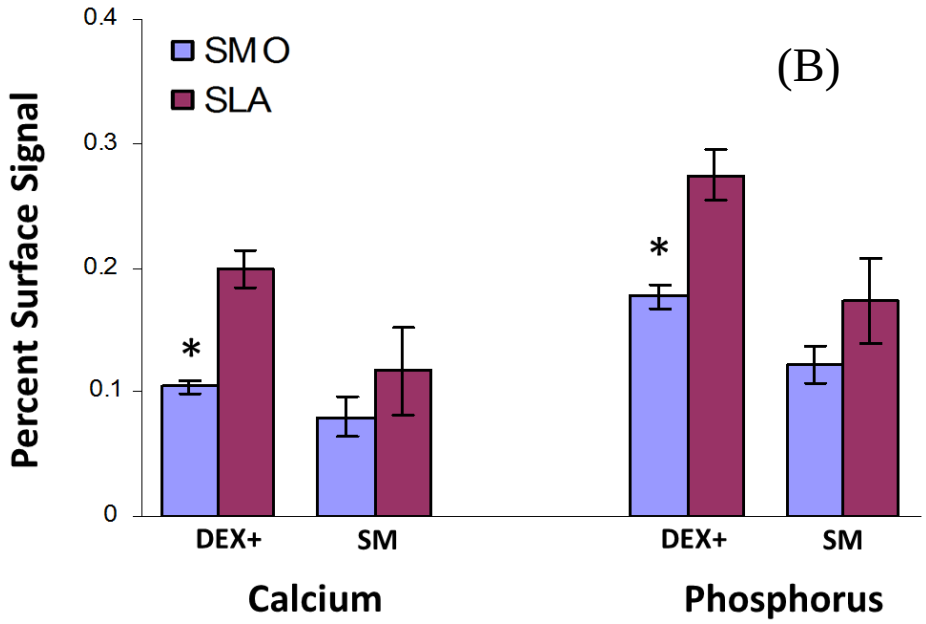

Figure 4-1 B: Energy Dispersive Spectrometry (EDAX) quantification.

Figure 4-1: Mineralization study on SLA and SMO surfaces: (A) Spectrophotometric quantification of Alizarin Red S staining after culturing alveolar bone derived primary osteoprogenitor cells (BCs) on SLA and SMO surfaces (with osteogenic supplementation: DEX+ and standard media: SM), showing higher staining on SLA than SMO surfaces. (B) Energy Dispersive Spectrometry (EDAX) quantification (expressed as percent surface signal) of calcium and phosphorus content after 4 weeks culture of osteoprogenitor cells on SLA and SMO surfaces showing higher intensities on SLA surfaces compared with SMO surfaces (both Ca and P)(significant in osteogenic cultures)(*: p-value <0.05, SLA vs. SMO).

4.3.2 Whole genome expression analysis

Affymetrix Human Genome U133 Plus 2.0 array (Affymetrix, Santa Clara, California) were used to assess whole genome expression profile of osteoblasts following 3 and 24 hours of exposure to SLA and SMO surfaces.

4.3.3 Differentially regulated genes

After three hours of exposure of the BCs to the two different titanium surfaces, 90 genes (37 upregulated and 53 downregulated) were seen to qualify the statistical stringency (p-value cutoff 0.05). Out of these 90 genes, 15 (9 upregulated and 6 downregulated) genes showed fold change (FC) beyond +/-1.5. The number of differentially expressed genes on SLA compared with SMO surface escalated to 636 after 24 hours of exposure to the surfaces (381 upregulated and 255 downregulated) out of which 242 (136 upregulated and 106 downregulated) genes had FC beyond +/-

1.5 (Figure 4-2 and Table 4-1). Table 4-2 shows the top ten up- and downregulated genes at 3 and 24 hours.

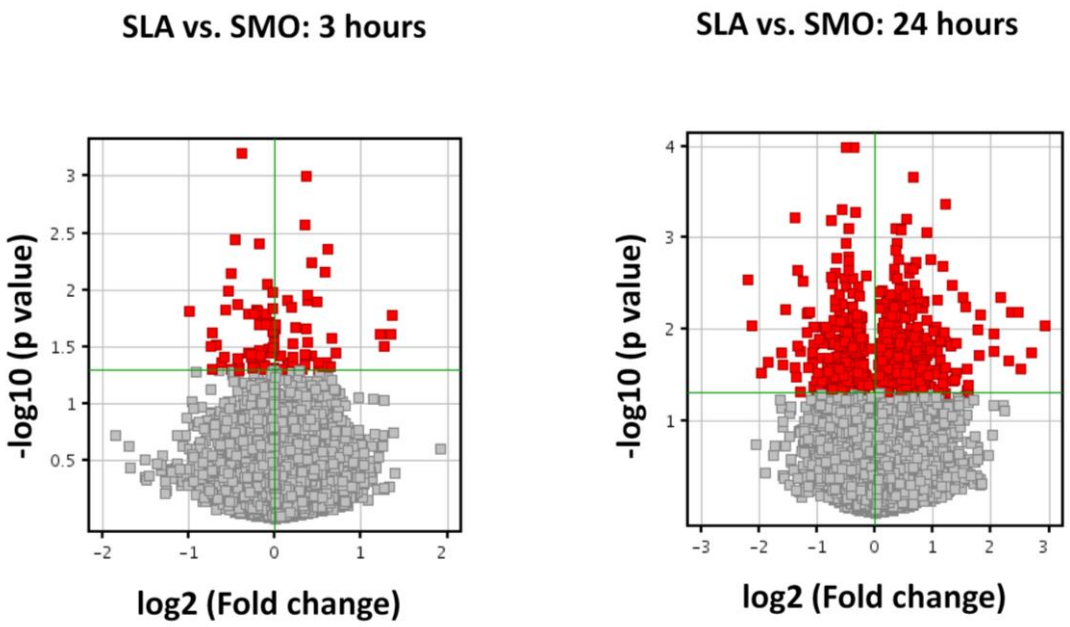

Figure 4-2: Volcano plots showing comparisons between SLA and SMO following 3 and 24 hours exposure. The statistically significant genes are shown in red. A clearly evident increase in the number of differentially regulated genes was observed between 24 and 3 hours.

Table 4-1: Number of genes differentially regulated on micro-roughened SLA and polished titanium surfaces (SMO) (after 3 and 24 hours of exposure of BCs).

Comparisons		FC cut-off: 1			FC cut-off: 1.5			FC cut-off: 2			FC cut-off: 3		
		Up	Down	Total	Up	Down	Total	Up	Down	Total	Up	Down	Total
SLA vs. SMO	3 hr	37	53	90	9	6	15	4	0	4	0	0	0
	24 hr	381	255	636	136	106	242	46	27	73	14	6	20
SLA	3 hr vs. 0 hr	1636	1335	2971	1430	1084	2514	1060	684	1744	569	336	905
	24 hr vs. 0 hr	2703	1649	4352	2294	1387	3681	1609	909	2518	769	389	1158
	24 hr vs. 3 hr	1282	1274	2556	1051	1104	2155	742	762	1504	439	386	825
SMO	3 hr vs. 0 hr	1575	1252	2827	1371	1079	2450	1025	766	1791	547	404	951
	24 hr vs. 0 hr	2750	2232	4982	2410	1914	4324	1745	1274	3019	862	560	1422
	24 hr vs. 3 hr	1659	1302	2961	1434	1100	2534	1053	795	1848	627	414	1041

Table 4-2: List of top ten upregulated and downregulated genes on SLA surfaces compared with SMO surfaces at 3 and 24 hours time-points (FC: fold change).

SLA vs. SMO					
3 hours			24 hours		
Gene symbol	FC	p-value	Gene symbol	FC	p-value
Top 10 Upregulated genes			Top 10 Upregulated genes		
CEP78	2.55	0.017	FOSB	7.52	0.009
KIF3C	2.52	0.024	RRAD	6.44	0.018
GSTO2	2.39	0.031	BMP2	5.70	0.027
PIGM	2.33	0.024	TPPP3	5.46	0.006
RHOB	1.62	0.035	RGCC	4.92	0.022
NR1D1	1.58	0.026	C8orf4	4.44	0.004
AP1S2	1.56	0.047	GPR183	4.11	0.017
CENPA	1.52	0.004	CRIP1	4.11	0.011
HPS1	1.51	0.043	KLF9	3.50	0.007
LIN7B	1.49	0.007	NUPR1	3.44	0.019
Top 10 Downregulated genes			Top 10 Downregulated genes		
ZNF426	-1.99	0.015	MKI67	-4.61	0.003
CNNM2	-1.68	0.031	ACTG2	-3.90	0.029
KLHL7	-1.66	0.049	CENPE	-3.63	0.023
HFE	-1.65	0.023	PLK1	-3.06	0.018
SCAF4	-1.61	0.030	TPM1	-2.96	0.006
PHF3	-1.54	0.042	KRT19	-2.63	0.001
CNIH4	-1.50	0.039	DEPDC1	-2.60	0.025
C2orf27A/C2orf27B	-1.49	0.015	AUNIP	-2.58	0.033
TBRG4	-1.47	0.010	ARHGAP22	-2.53	0.015
SRSF1	-1.43	0.007	GTSE1	-2.47	0.049

Centrosomal protein 78 kDa (CEP78), a gene with little known function, showed the highest upregulation on SLA surface compared with SMO (FC=2.554, p-value=0.0165) within 3 hours of exposure. The other genes showing FCs beyond +2 at 3 hours were: Kinesin family member 3C (KIF3C) (FC=2.516, p-value=0.024), glutathione S-transferase omega 2 (GSTO2) (FC=2.385, p-value=0.0311) and phosphatidylinositol glycan anchor biosynthesis, class M (PIGM) (FC=2.329, p-value=0.0244). KIF3C is a member of the KIF3 family - class of microtubule-dependent motors that is important for cell division and intracellular transport [17]. Among the other two genes - GSTO2 possibly plays a vital role in cellular signaling [18] and PIGM is involved in the synthesis of glycosylphosphatidylinositol (GPI)-anchor that helps to anchor proteins to the surface of cells [19].

The FBJ murine osteosarcoma viral oncogene homolog B (FOSB) gene (FC=7.52, p-value=0.00915) was seen to be the most highly upregulated gene on the SLA surface (compared with SMO surface) after 24 hours. The FOS proteins are known to be associated with regulation of cellular proliferation and differentiation. Ras-related associated with diabetes (RRAD) gene showed the second highest fold-

change (FC=6.441, p-value=0.0179). This gene is seen to have roles in cell cycle progression and differentiation.

A characteristic feature observed at the 3 hours time-point was increased expression of the gene RHOB (FC=1.62, p-value=0.0355) which is known to be important for attachment of fibroblastic cells. PRKDC was observed to be downregulated (FC=-1.308, p-value=0.000615). This gene is known to affect G1/S phase transition arrest of fibroblast cell lines. Bone morphogenetic protein 2 (BMP2) emerged as a highly upregulated gene (FC=5.697, p-value=0.0268). The BMP2 protein is one of the key ligands responsible for activation and functioning of the BMP signaling pathway. The BMP pathway is known to play an instrumental role in the osteogenic differentiation process.

4.3.4 Functional clustering of differentially regulated genes

Functional grouping and clustering of the differentially regulated genes at 3 and 24 hours were performed using the Database for Annotation, Visualization and Integrated Discovery (DAVID) [15] and Ingenuity Pathways Analysis tool [16]. Functional annotation using DAVID revealed higher distribution of Gene ontology (GO) terms related to biological processes at both time-points (65.22% at 3 hours and 57.34% at 24 hours) (Figure 4-3).

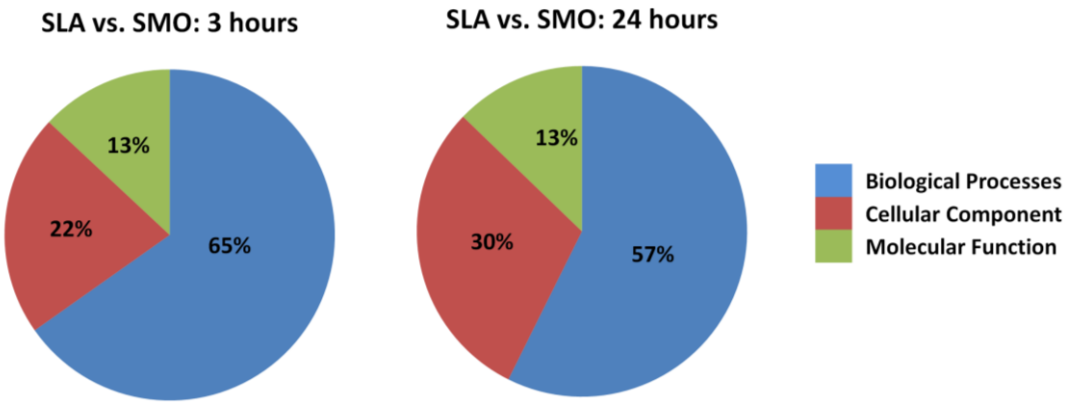

Figure 4-3: Summary of key gene ontology (GO) terms enriched on SLA surfaces compared with SMO following 3 and 24 hours of culture . GO clustering analysis was performed using Database for Annotation, Visualization and Integrated Discovery (DAVID) and considering the GOTERM_BP_FAT, GOTERM_CC_FAT and GOTERM_MF_FAT, which are summarized versions of the Biological Processes, Cellular Components and Molecular Functions, respectively in the gene ontology (medium classification stringency).

Cellular component terms showed 20-30% enrichment (21.74% at 3 hours and 29.86% at 24 hours) and molecular function terms were seen to have ~13% enrichment (13.04% at 3 hours and 12.80% at 24 hours). To ascertain the biological meaning of the GO categories enriched, a further clustering analysis was performed on DAVID and the enrichment score cutoff was set at 1.3 (corresponds to non-log geometric mean of p-value=0.05 [20]) (Table 4-3). Only one annotation cluster passed the stringent criteria set at the three hours time-point. This cluster was primarily related to GO terms associated with nucleic acid processing and nuclear functions. In contrast to this, 12 annotation clusters qualified after twenty-four hours. The maximally enriched clusters at the 24 hours time-point were related to microtubular and cytoskeletal architecture, and also with cell organelle. The first physiological system related cluster to get highlighted at 24 hours between SLA and SMO surfaces was associated with skeletal system development (Table 4-3).

Comparative analysis of the microarray expression profile at three hours and twenty-hours between SLA and SMO surfaces was performed using IPA (Figure 4-4). The analysis revealed differential expression of clusters related to cell-mediated immune response, immune cell trafficking and nervous system development as early as 3 hours. Skeletal and muscular system development clusters were observed as the most differentially regulated clusters at the 24 hours time-point. "Connective tissue development and function" cluster was the second one to get highlighted at 24 hours. Six upregulated genes (FOS, RUNX2, PTHLH, HEXA, MMP14 and WNT9A) on the SLA surface at 24 hours time-point clustered together towards the "length of bone" functional annotation (activation z-score=2.4, p-value=0.0021).

Table 4-3: Functional Annotation Clustering using DAVID showing Gene Ontology (GO) annotation clusters with enrichment scores ≥1.3 (non-log geometric mean of p-values=0.05) for differentially regulated genes in BCs following 3 and 24 hours exposure to SLA and SMO surfaces (Numbers in parentheses indicate number of genes from the dataset matching the GO term).

SLA vs SMO 3 hours
Annotation Cluster 1: Enrichment Score: 1.30
GO:0008380-RNA splicing (6), GO:0006396-RNA processing (8), GO:0006397-mRNA processing (6), GO:0016071-mRNA metabolic process (6), GO:0044451-Nucleoplasm part (7), GO:0005654-Nucleoplasm (9), GO:0031981-Nuclear lumen (12), GO:0070013-Intracellular organelle lumen (12), GO:0043233-Organelle lumen (12), GO:0031974-Membrane-enclosed lumen (12), GO:0000375-RNA splicing, via transesterification reactions (3), GO:0000377-RNA splicing (3), via transesterification reactions with bulged adenosine as nucleophile (3), GO:0000398-Nuclear mRNA splicing, via spliceosome (3), GO:0016604-Nuclear body (3), GO:0005730-Nucleolus (5)

Table 4-3 (continued)

SLA vs SMO 24 hours
Annotation Cluster 1: Enrichment Score: 6.97
GO:0015630- Microtubule cytoskeleton (43), GO:0043228-Non-membrane-bounded organelle (121), GO:0043232-Intracellular non-membrane-bounded organelle (121), GO:0005856-Cytoskeleton (72), GO:0005874-Microtubule (25), GO:0044430-Cytoskeletal part (52)
Annotation Cluster 2: Enrichment Score: 5.25
GO:0015630-Microtubule cytoskeleton (43), GO:0000279-M phase (28), GO:0000278-Mitotic cell cycle (30), GO:0022402-Cell cycle process (39), GO:0022403-Cell cycle phase (32), GO:0007049-Cell cycle (48), GO:0000280-nuclear division (21), GO:0007067-Mitosis (21), GO:0000087-M phase of mitotic cell cycle (21), GO:0048285-Organelle fission (21), GO:0007017-Microtubule-based process (22), GO:0051301-Cell division (21), GO:0005819-Spindle (13)
Annotation Cluster 3: Enrichment Score: 4.25
GO:0015630-Microtubule cytoskeleton (43), GO:0000226-Microtubule cytoskeleton organization (14), GO:0005813-Centrosome (16), GO:0005815-Microtubule organizing center (17)
Annotation Cluster 4: Enrichment Score: 2.82
GO:0031974-Membrane-enclosed lumen (79), GO:0070013-Intracellular organelle lumen (75), GO:0031981-Nuclear lumen (63), GO:0043233-Organelle lumen (75), GO:0005730-nucleolus (34), GO:0005654-Nucleoplasm (34)
Annotation Cluster 5: Enrichment Score: 2.23
GO:0005739-Mitochondrion (49), GO:0031967-Organelle envelope (32), GO:0031975-Envelope (32), GO:0019866-Organelle inner membrane (20), GO:0005743-Mitochondrial inner membrane (18), GO:0031090-Organelle membrane (46), GO:0005740-Mitochondrial envelope (22), GO:0031966-Mitochondrial membrane (19), GO:0044429-Mitochondrial part (26)
Annotation Cluster 6: Enrichment Score: 2.16
GO:0005773-Vacuole (16), GO:0005764-Lysosome (14),GO:0000323-Lytic vacuole (14)
Annotation Cluster 7: Enrichment Score: 2.03
GO:0003777-Microtubule motor activity (9), GO:0005875-Microtubule associated complex (10), GO:0003774-Motor activity (11), GO:0007018-Microtubule-based movement (7)
Annotation Cluster 8: Enrichment Score: 1.74
GO:0001958-Endochondral ossification (4), GO:0060348-Bone development (10), GO:0060350-Endochondral bone morphogenesis (4), GO:0060349-Bone morphogenesis (4), GO:0001503-Ossification (9), GO:0001501-Skeletal system development (17), GO:0048705-Skeletal system morphogenesis (7)
Annotation Cluster 9: Enrichment Score: 1.71
GO:0042641-Actomyosin (5), GO:0001725-Stress fiber (4), GO:0032432-Actin filament bundle (4)
Annotation Cluster 10: Enrichment Score: 1.40
GO:0000793-Condensed chromosome (11), GO:0000775-Chromosome, centromeric region (10), GO:0034508- centromere complex assembly (3), GO:0000776-Kinetochore (7), GO:0005694-Chromosome (21), GO:0000777-Condensed chromosome kinetochore (5), GO:0000779-Condensed chromosome, centromeric region (5), GO:0044427-Chromosomal part (16), GO:0065004-Protein-DNA complex assembly (4)
Annotation Cluster 11: Enrichment Score: 1.39
GO:0050684-Regulation of mRNA processing (4), GO:0048024-Regulation of nuclear mRNA splicing, via spliceosome (3), GO:0043484-Regulation of RNA splicing (3)
Annotation Cluster 12: Enrichment Score: 1.36
GO:0051384-Response to glucocorticoid stimulus (8), GO:0031960-Response to corticosteroid stimulus (8), GO:0009719-Response to endogenous stimulus (19), GO:0048545-Response to steroid hormone stimulus (11), GO:0009725-Response to hormone stimulus (17), GO:0010033-Response to organic substance (25)

(A)

Figure 4-4 A: Functional clustering analysis (Systemic processes) of differentially regulated genes between SLA and SMO after 3 hours of culture. (IPA analysis)

(B)

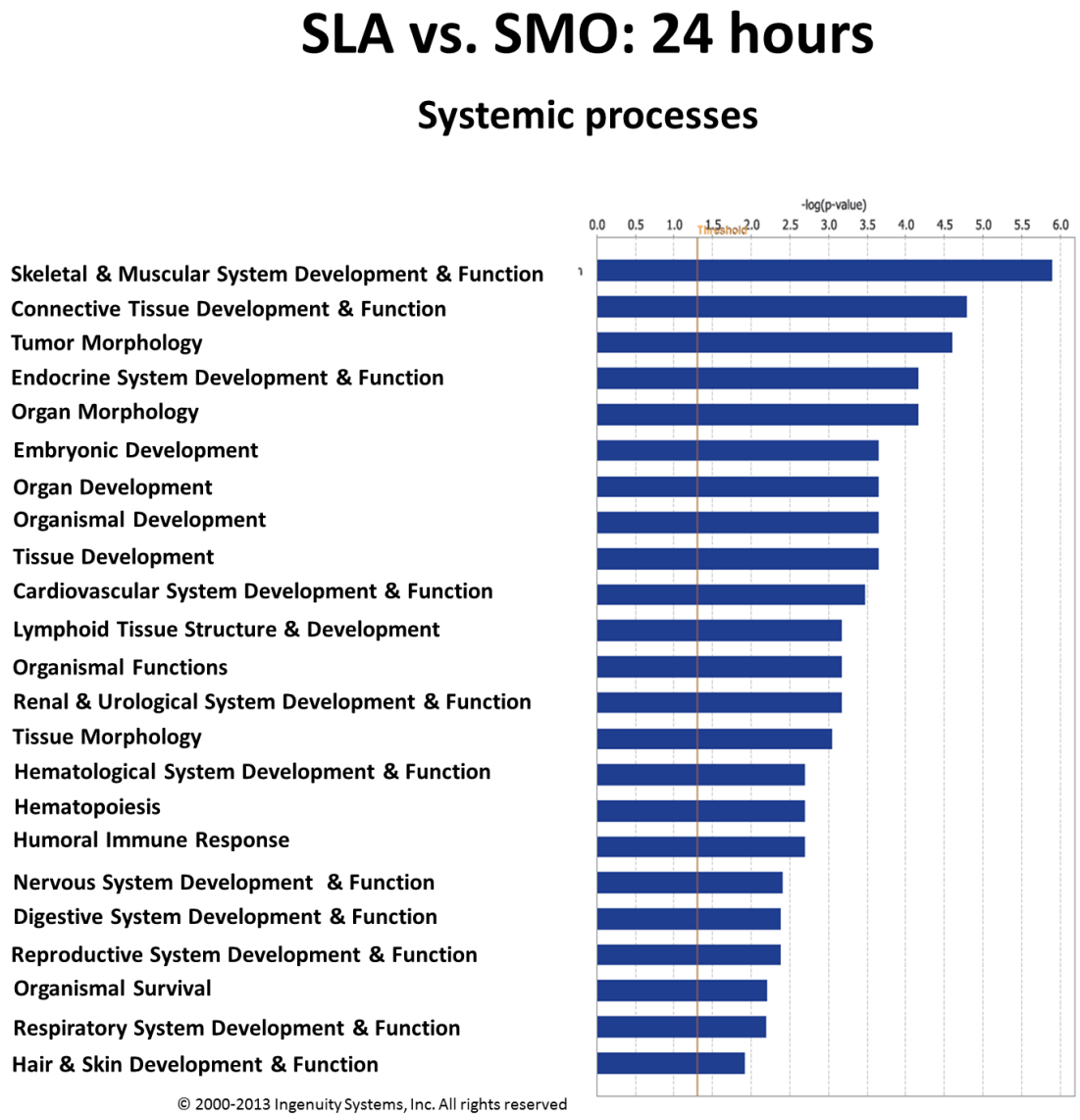

Figure 4-4 B: Functional clustering analysis (Systemic processes) of differentially regulated genes between SLA and SMO after 24 hours of culture. (IPA analysis)

(C)

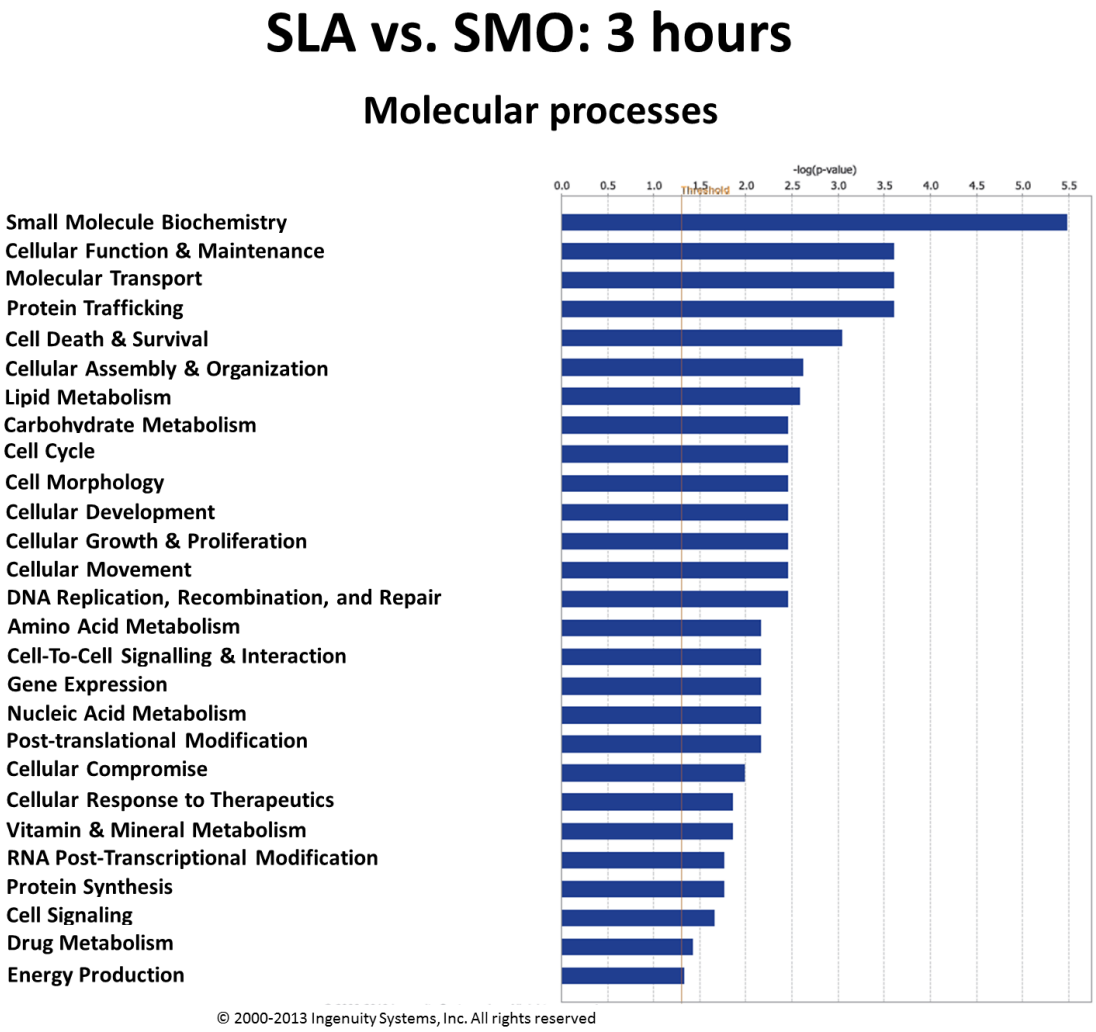

Figure 4-4 C: Functional clustering analysis (Molecular processes) of differentially regulated genes between SLA and SMO after 3 hours of culture. (IPA analysis)

(D)

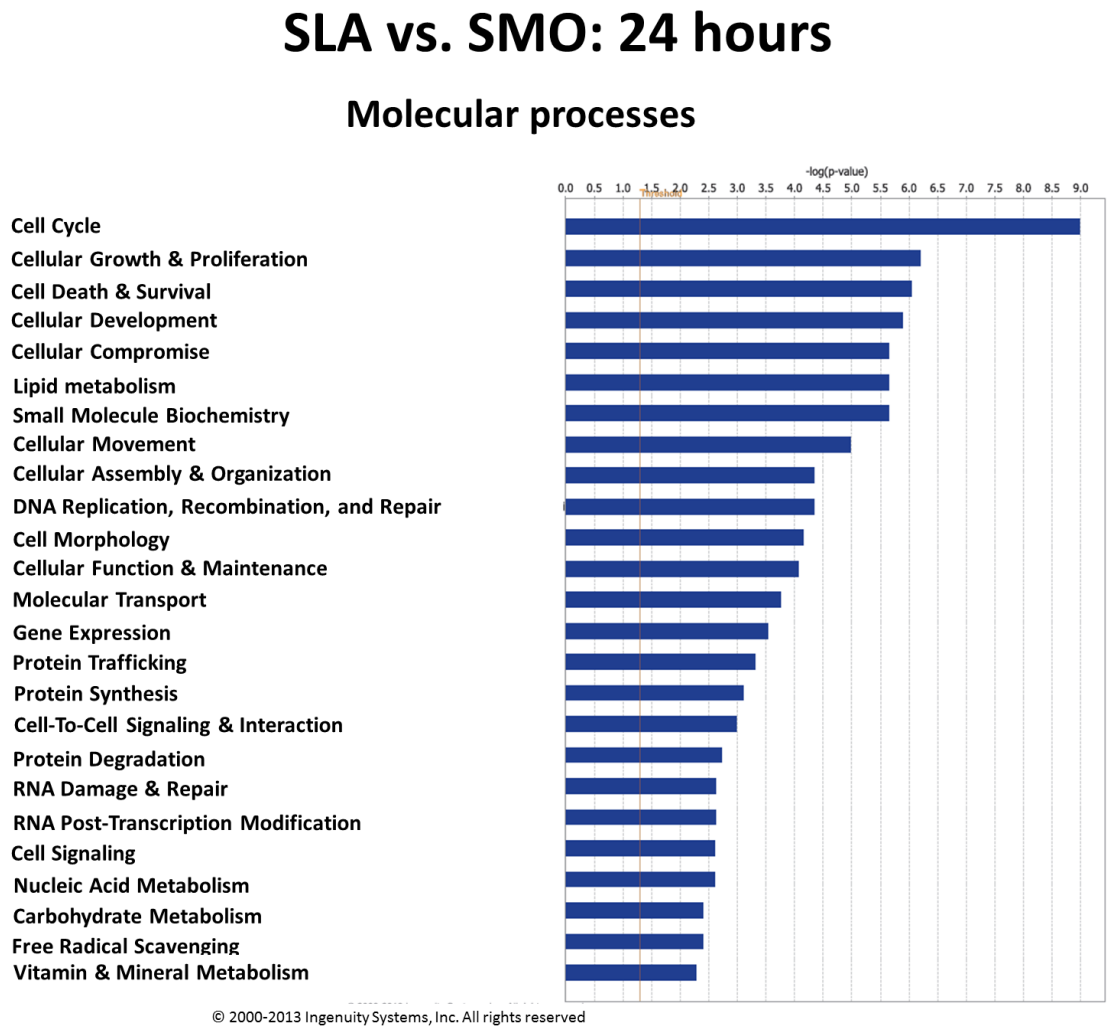

Figure 4-4 D: Functional clustering analysis (Molecular processes) of differentially regulated genes between SLA and SMO after 24 hours of culture. (IPA analysis)

Figure 4-4 (A-D): Functional clustering analysis of differentially regulated genes between SLA and SMO after 3 and 24 hours of culture (Analysis performed using Ingenuity Pathway Analysis: IPA).

4.3.5 Time-course analysis for functional pathways

Functional clustering analysis of the differentially regulated genes on SLA and SMO over the time-course (0, 3 and 24 hours) was performed using IPA. IPA's hierarchical classification organizes functional pathways on the basis of high-level categories. Based on activation z-score analysis of IPA, scores beyond +/- 1.5 were considered as significantly regulated clusters (z>+1.5: increased and z<-1.5: decreased). More functional clusters were seen to have increased z-scores on both SLA and SMO surfaces in the 3 hours vs. 0 hour (base-line) comparison (SLA=110 and SMO=75), than 24 hours vs. 3 hours comparison (SLA=33 and SMO=53). In

contrast to this, fewer clusters were seen to have decreased z-scores on both SLA and SMO surfaces in the 3 hours vs. 0 hour comparison (SLA=30 and SMO=14), than 24 hours vs. 3 hours comparison (SLA=59 and SMO=40). Relevant clusters are highlighted in Table 4-4. A categorical analysis of the comparisons has been shown as a heatmap map analysis in Figure 4-5.

Increased Activation Score	SLA 3 vs. 0 hr	SLA 24 vs. 3 hr	SMO 3 vs. 0 hr	SMO 24 vs. 3 hr	SLA 3 vs. 0 hr	SLA 24 vs. 3 hr	SMO 3 vs. 0 hr	SMO 24 vs. 3 hr	Decreased Activation Score
Categories (Seen to have both increased and decreased activation scores)									
Cancer	10	1	8	7	4	12	1	13	Cancer
Cardiovascular System Development and Function	4	1	1	0	0	1	0	0	Cardiovascular System Development and Function
Cell Cycle	3	12	5	27	1	4	0	5	Cell Cycle
Cell Death and Survival	9	1	15	1	3	8	3	8	Cell Death and Survival
Cell Morphology	1	1	1	0	0	1	0	1	Cell Morphology
Cellular Assembly and Organization	4	2	3	7	0	3	0	2	Cellular Assembly and Organization
Cellular Compromise	2	0	0	0	0	0	0	2	Cellular Compromise
Cellular Development	23	0	8	2	2	10	0	2	Cellular Development
Cellular Growth and Proliferation	9	0	5	3	1	2	1	0	Cellular Growth and Proliferation
Connective Tissue Development and Function	2	0	0	2	1	0	0	0	Connective Tissue Development and Function
Connective Tissue Disorders	1	0	3	0	3	0	1	0	Connective Tissue Disorders
Developmental Disorder	0	7	0	0	10	0	3	0	Developmental Disorder
DNA Replication, Recombination, and Repair	1	4	0	11	0	1	0	4	DNA Replication, Recombination, and Repair
Embryonic Development	5	0	2	0	1	2	0	2	Embryonic Development
Gastrointestinal Disease	0	0	0	3	2	0	1	0	Gastrointestinal Disease
Gene Expression	10	0	8	0	0	1	0	5	Gene Expression
Hematological Disease	2	0	0	0	0	0	0	9	Hematological Disease
Hematological System Development and Function	19	0	3	0	0	0	0	1	Hematological System Development and Function
Hematopoiesis	12	0	3	0	0	0	0	1	Hematopoiesis
Hepatic System Disease	0	0	0	3	1	0	1	0	Hepatic System Disease
Immunological Disease	1	0	0	2	2	0	0	4	Immunological Disease
Infectious Disease	14	0	11	0	0	2	0	0	Infectious Disease
Inflammatory Response	1	0	0	0	1	0	0	0	Inflammatory Response
Organ Morphology	2	0	0	0	2	0	0	0	Organ Morphology
Organismal Development	3	0	1	0	1	2	0	0	Organismal Development
Organismal Injury and Abnormalities	4	0	1	0	3	0	0	0	Organismal Injury and Abnormalities
Organismal Survival	0	2	0	0	2	2	2	1	Organismal Survival
Renal and Urological Disease	1	0	1	0	1	0	1	0	Renal and Urological Disease
Skeletal and Muscular Disorders	1	0	3	0	4	0	2	0	Skeletal and Muscular Disorders
Tissue Development	5	0	2	0	0	1	0	0	Tissue Development
Tissue Morphology	8	0	0	0	2	7	0	1	Tissue Morphology
Unique categories (either to have increased or decreased activation scores)									
Carbohydrate Metabolism	1	0	0	0	0	0	0	1	Cellular Response to Therapeutics
Cell-mediated Immune Response	2	0	0	0	1	0	0	0	Hair and Skin Development and Function
Cell-To-Cell Signaling and Interaction	1	0	1	0	3	0	1	0	Neurological Disease
Cellular Function and Maintenance	6	0	4	0	0	1	2	0	RNA Post-Transcriptional Modification
Cellular Movement	8	0	0	4					
Dermatological Diseases and Conditions	1	0	1	0					
Digestive System Development and Function	1	0	0	0					
Drug Metabolism	1	0	1	0					
Endocrine System Development and Function	1	0	2	0					
Hepatic System Development and Function	1	0	0	0					
Humoral Immune Response	1	0	0	0					
Immune Cell Trafficking	1	0	0	0					
Lipid Metabolism	1	0	1	0					
Lymphoid Tissue Structure and Development	3	1	1	2					
Molecular Transport	2	0	5	0					
Nervous System Development and Function	2	0	0	0					
Nucleic Acid Metabolism	0	0	0	1					
Post-Translational Modification	1	0	1	0					
Protein Synthesis	2	0	2	0					
Renal and Urological System Development and Function	1	0	0	0					
Reproductive System Development and Function	0	0	1	0					
Reproductive System Disease	1	0	1	0					
RNA Trafficking	0	0	3	0					
Skeletal and Muscular System Development and Function	1	0	1	0					
Small Molecule Biochemistry	2	0	2	1					
Tumor Morphology	2	0	0	0					

Figure 4-5: Heat-map of significantly regulated categories of functional clusters differentially regulated on SLA and SMO surfaces over the time-course of analysis (base-line-0 hour, 3 hours and 24 hours) based on the activation z-score analysis on IPA (scores beyond +/- 1.5).

Large number of clusters belonging to the categories: cell development (n=23), hematological system development and function (n=19), hematopoiesis (n=12), gene expression (n=10), cell death & survival (n=9), cell movement categories (n=8) and tissue morphology (n=8) were observed as activated after 3 hours exposure to SLA surfaces. In contrast, the SMO surface exposure showed higher number of clusters belonging to the categories: cell death & survival (n=15), gene expression (n=8) and cellular development (n=8). Other categories showing high numbers of activated clusters on the titanium surfaces after 3 hours were: infectious disease (n=14 on SLA and n=11 on SMO) and cancer (n=10 on SLA and n=8 on SMO). The comparisons made between 24 hours and 3 hours on both of the surfaces revealed large number of clusters categorized as belonging to "cell cycle" on both surfaces (n=12 on SLA and n=27). Unmatched categories on SLA and SMO surfaces showed developmental disorders category as having 7 activated clusters on SLA surface (24 hours vs. 3 hours), whereas DNA replication, recombination and repair showed 11 activated clusters on SMO.

The developmental disorders category was seen to have the highest number of clusters (n=10) that showed inhibition after 3 hours of exposure to SLA surfaces. Categories "cell death and survival" and "developmental disorders" were seen to be inhibited on SMO surfaces (n=3 for both). "Skeletal and muscular disorders clusters" (n=4) were also seen to be inhibited on SLA surfaces (3 hours vs. 0 hour). Numerous categories were seen to be inhibited when comparisons were made between 24 hours and 3 hours for both SLA and SMO surfaces. The inhibited categories worth mentioning were "cell death and survival" (n=8 on both SLA and SMO), "cellular development" (n=10 on SLA) and hematological diseases (n=9 on SMO).

Several unique functional annotation clusters were depicted by IPA upon analysis of the genes differentially regulated in 3 hours vs. base-line and 24 hours vs. 3 hours comparisons. The most relevant clusters have been shown in Table 4-4. Higher numbers of relevant clusters were found to be activated when compared to inhibited clusters after 3 hours on both SLA and SMO. In contrast to this, more clusters were seen to be inhibited in 24 hours vs. 3 hours comparison.

Table 4-4: Relevant functional annotation clusters as depicted by IPA upon analysis of the genes showing differential regulation in 3 hours vs. base-line and 24 hours vs. 3 hours comparisons on SLA and SMO surfaces.

SLA 3 hr vs. 0 hr		SLA 24 hr vs. 3 hr		SMO 3 hr vs. 0 hr		SMO 24 hr vs. 3 hr	
Functions Annotation	z	Functions Annotation	z	Functions	z	Functions	z
Increased activation z-score (>+1.5)							
Transcription	3.87	Congenital anomaly of skeletal bone	3.19	Nuclear export	1.98	Association of chromosome components	3.25
Transcription of RNA	3.77	Congenital anomaly of musculoskeletal system	3.04	Nuclear export of molecule	1.75	Association of chromatin	2.79
Expression of RNA	3.70	Craniofacial abnormality	2.61	Nuclear export of mRNA	1.75	Stabilization of chromosomes	2.47
Transactivation	3.55	Association of chromosome components	2.79	Transactivation	3.54	Excision repair	2.36
Expression of DNA	3.03	Association of chromatin	2.61	Transcription	2.55	Alignment of chromosomes	2.33
Transcription of DNA	2.95	Alignment of chromosomes	2.14	Expression of RNA	2.54	Segregation of chromosomes	2.01
Activation of DNA endogenous promoter	2.61	Mismatch repair of DNA	1.96	Transcription of RNA	2.52	Binding of chromosomes	1.98
Initiation of transcription	2.14	Metabolism of DNA	1.78	Activation of protein	2.22	Chromosomal congression of chromosomes	1.91
Repression of RNA	2.42	Chromosomal congression of chromosomes	1.66	Expression of DNA	2.07	Conformational modification of DNA	1.63
DNA damage response of cells	1.98	Cycling of centrosome	2.54	Transcription of DNA	2.03	Hydrolysis of nucleotide	1.61
Binding of DNA	1.51	Replication of cells	2.31	Repression of RNA	1.98	Repair of DNA	1.51
Development of cardiovascular system	3.37	Checkpoint control	2.08	Activation of DNA endogenous promoter	1.75	Mismatch repair of DNA	1.96
Vasculogenesis	2.96	Repair of cells	1.57	Transport of mRNA	1.73	Interphase of connective tissue cells	3.14
Migration of endothelial cells	1.99	Hypoplasia	2.65	Export of mRNA	1.69	Interphase of fibroblasts	2.98
Cell movement of endothelial cells	1.84	Hypoplasia of organ	1.98	Metabolism of protein	1.91	Cycling of centrosome	2.70
Development of hematopoietic cells	2.39	Interphase of connective tissue cells	2.31	Synthesis of protein	1.72	Checkpoint control	2.59
Development of leukocytes	2.34	Re-entry into cell cycle progression	2.29	Organization of cytoskeleton	2.88	Proliferation of cells	2.39
Development of blood cells	2.28	G1 phase of fibroblasts	2.24	Organization of cytoplasm	2.86	S phase of connective tissue cells	2.34
Differentiation of blood cells	2.26	S phase of bone cancer cell lines	2.16	Microtubule dynamics	2.62	Interphase	2.25
Quantity of lymphocytes	2.03	Interphase of fibroblasts	2.08	Proliferation of cells	2.21	S phase of fibroblasts	2.12
Differentiation of red blood cells	2.00	Interphase of bone cancer cell lines	1.60	M phase	2.14	S phase of bone cancer cell lines	1.94
Differentiation of leukocytes	2.00	Morphology of hematopoietic progenitor cells	2.22	Cell cycle progression	2.06	S phase	1.93
Quantity of B lymphocytes	2.00	Formation of neointima	1.94	Re-entry into S phase	1.51	Cytokinesis	1.91
Differentiation of hematopoietic progenitor cells	1.81	Morphology of lymphatic system component	1.72	Development of connective tissue	3.20	Cytokinesis of tumor cell lines	1.81
Differentiation of mononuclear leukocytes	1.80			Differentiation of cells	3.07	S phase checkpoint control	1.76
Accumulation of myeloid cells	1.75			Development of leukocytes	1.75	Re-entry into cell cycle progression	1.74

Table 4-4 (continued): Relevant functional annotation clusters (Activation z-score >+1.5)

SLA 3 hr vs. 0 hr		SLA 24 hr vs. 3 hr		SMO 3 hr vs. 0 hr		SMO 24 hr vs. 3 hr	
Quantity of mononuclear leukocytes	1.75			Differentiation of endothelial cells	1.74	Replication of cells	1.74
Formation of fibronectin matrix	1.73			Development of blood cells	1.69	G1 phase of fibroblast cell lines	1.57
Quantity of blood cells	1.64			Apoptosis of hematopoietic cell lines	1.65	G1/S phase	1.53
Development of lymphocytes	1.61			Differentiation of erythroid progenitor cells	1.52	Cell transformation	1.51
T cell development	1.59			Proliferation of hematopoietic cell lines	1.51	Invasion of cells	1.59
Differentiation of lymphocytes	1.59			Cell survival	2.78	Entry into interphase	1.50
Differentiation of hematopoietic cells	1.58			Cell viability	2.45	Formation of vessel component	2.36
T cell homeostasis	1.57			Cell viability of embryonic stem cell lines	1.99		
Metabolism of protein	2.27			Cytostasis	2.37		
Synthesis of protein	2.07			Cell cycle progression of tumor cell lines	1.74		
Shock response	2.03			Contact growth inhibition	1.73		
Polyubiquitination	1.98			Self-renewal of cells	1.59		
Synthesis of glycosaminoglycan	1.91			Sprouting	1.62		
Differentiation of cells	4.26			Differentiation of connective tissue cells	2.37		
Cell survival	3.68			Differentiation of osteoblasts	2.36		
Cell viability	3.19			Bone cancer	1.94		
Formation of cells	2.69			Tumorigenesis of osteosarcoma	1.63		
Proliferation of cells	2.62						
Quantity of cells	2.56						
Cell cycle progression	2.30						
M phase	2.14						
Proliferation of stem cells	2.09						
Cytostasis	2.09						
Growth of plasma membrane projections	2.55						
Nuclear export	1.75						
Nuclear export of molecule	1.51						
Endoplasmic reticulum stress response	1.71						
Endoplasmic reticulum stress response of cells	1.71						
Self-renewal of embryonic stem cells	1.95						
Proliferation of embryonic stem cells	1.67						
Differentiation of connective tissue cells	1.90						
Bone cancer	1.72						
Differentiation of osteoblasts	1.65						

Table 4-4 (continued): Relevant functional annotation clusters (Activation z-score <-1.5)

SLA 3 hr vs. 0 hr		SLA 24 hr vs. 3 hr		SMO 3 hr vs. 0 hr		SMO 24 hr vs. 3 hr	
Functions annotation	z	Functions annotation	z	Functions annotation	z	Functions annotation	z
Decreased activation z-score (<-1.5)							
Organismal death	-5.79	Repression of RNA	-2.73	Organismal death	-5.06	DNA damage	-3.03
Growth failure	-3.3	Breakage of chromosomes	-2.67	Splicing of mRNA	-2.17	Sister chromatid exchange	-2.80
Hypoplasia of organ	-3.04	Missegregation of chromosomes	-1.98	Processing of mRNA	-1.71	Transactivation	-2.26
Hypoplasia	-2.53	Processing of RNA	-1.91	Neuromuscular disease	-1.98	Activation of DNA endogenous promoter	-1.97
Cell death	-1.88	Proliferation of leukocyte cell lines	-2.81	Congenital anomaly of skeletal bone	-1.76	Transcription of DNA	-1.85
Apoptosis	-1.54	Proliferation of hematopoietic cell lines	-2.75			Expression of DNA	-1.79
Congenital anomaly of musculoskeletal system	-2.93	Quantity of hematopoietic progenitor cells	-2.14			Repression of DNA	-1.64
Congenital anomaly of skeletal bone	-2.82	Quantity of mononuclear leukocytes	-2.06			Missegregation of chromosomes	-1.63
Craniofacial abnormality	-2.14	Quantity of bone marrow cells	-2.05			Differentiation of cells	-2.35
Adipogenesis of fibroblast cell lines	-1.71	Quantity of blood cells	-2.01			Differentiation of embryonic cells	-2.04
Morphology of connective tissue	-1.63	Quantity of lymphocytes	-1.94			Sensitivity of cells	-2.13
Interphase of fibroblasts	-1.52	Quantity of leukocytes	-1.92			Delay in mitosis	-2.10
Chronic inflammation	-1.67	Differentiation of lymphocytes	-1.84			Cell death of antigen presenting cells	-1.94
Morphology of vessel	-1.94	Differentiation of mononuclear leukocytes	-1.83			Apoptosis of antigen presenting cells	-1.81
		Differentiation of embryonic cells	-2.45			Cell death of macrophages	-1.54
		Differentiation of cells	-2.17			Quantity of mitotic spindle	-1.71
		Development of connective tissue	-2.08			Binucleation of cells	-1.66
		Differentiation of connective tissue cells	-1.87			Bone marrow cancer	-1.77
		Organization of cytoplasm	-1.86				
		Organization of cytoskeleton	-1.86				
		Delay in initiation of M phase	-1.80				
		Development of cardiovascular system	-1.82				
		Development of bone marrow	-1.81				
		Development of bone marrow cells	-1.80				
		Lymphopoiesis	-1.76				
		Development of lymphatic system component	-1.71				
		Differentiation of hematopoietic progenitor cells	-1.66				
		Differentiation of blood cells	-1.62				
		Development of blood cells	-1.50				

Table 4-4 (continued): Relevant functional annotation clusters (Activation z-score <-1.5)

SLA 3 hr vs. 0 hr	SLA 24 hr vs. 3 hr		SMO 3 hr vs. 0 hr	SMO 24 hr vs. 3 hr
	Cell death of fibroblast cell lines	-1.74		
	Formation of mitotic spindle	-1.73		
	Senescence of fibroblasts	-1.64		
	Apoptosis of fibroblast cell lines	-1.62		
	Senescence of fibroblast cell lines	-1.55		

The most relevant cluster that showed the highest activation score on SLA surface in 3 hours vs. base-line comparison was “differentiation of cells” (z=4.26), whereas “transactivation” was the most relevant cluster on SMO surface (z=3.56). Several clusters related to nucleic acid processing, gene expression and protein metabolism were seen to be activated on SLA and SMO surfaces within 3 hours of exposure. Clusters related to cell differentiation (including differentiation of osteoblasts and connective tissue cells) were also observed as activated on both SLA and SMO surfaces. The SLA surface demonstrated activation of several clusters related to development of vascular networks and stimulation of blood cell formation in 3 hours. The SMO surface also showed activation of some clusters related to differentiation of endothelial and blood cells. However, the SMO surface was also seen to activate the "apoptosis of hematopoietic cell lines” (z=1.65). Clusters related to cytoplasmic organization and cell cycle were activated on SMO surfaces. Clusters relevant to bone formation and skeletogenesis (congenital anomaly of skeletal bone, congenital anomaly of musculoskeletal system and craniofacial abnormality) were seen to be activated on SLA surface (24 hours vs. 3 hours). The same clusters were observed as inhibited in the 3 hours vs. base-line comparison on SLA surface. No such clusters were seen to be regulated on the SMO surfaces either at 3 hours or in the 24 hours vs. 3 hours comparison. Chromosomal associations and organization clusters were seen to be activated on both SLA and SMO surfaces after 3 hours (24 hours vs. 3 hours). Cell cycle related clusters were activated on both SLA and SMO surfaces in both comparisons. “Morphology of hematopoietic progenitor cells” (z=2.22), “formation of neointima” (z=1.94) and “morphology of lymphatic system components” (z=1.72) clusters were activated on SLA at 24 hours (24 hours vs. 3 hours comparison). The cluster “formation of vessel component” (z=2.36), was found to be activated on the SMO surface in the 24 hours vs. 3 hours comparison.

A few numbers of clusters were seen to be inhibited on both SLA and SMO surfaces at 3 hours. Most of the clusters inhibited were related to cellular death and failure of growth. One cluster, "chronic inflammation" (z=-1.67) was inhibited on the SLA surface after 3 hours. Several clusters related to quantity of blood cells and differentiation and development of the cardiovascular system were inhibited on the SLA surface as observed in the 24 hours vs. 3 hours comparison. The SMO surface was found to inhibit several pathways related to DNA processing and defense cells (antigen presenting cells and macrophages).

4.3.6 Up-stream regulators

The IPA analysis was used to explore the list of potential upstream regulators with predicted activation scores (z-scores). Genes with predicted activation (z-score>0) or inhibition (z-score<0) were further screened for their fold changes in the available data-set. Table 4-5 shows the list of genes (described as "correlated upstream regulators" henceforth) whose expression patterns (fold changes) positively correlated with their activation scores as predicted by IPA (upregulation for activation and downregulation for inhibition). Although, there were no correlated upstream regulators when SLA was compared to SMO after 3 hours; however, NUPR1 (Nuclear Protein, Transcriptional Regulator, 1) upstream regulator was predicted as activated (z-score=2.0). The SLA vs. SMO comparison at 24 hours revealed 8 correlated upstream regulators (6 activated and 2 inhibited). NUPR1 was observed as the gene showing highest activation z-score (3.8). The fold change for this gene was 3.4 (SLA vs. SMO at 24 hours). BMP2 and RUNX2 were amongst the 8 correlated upstream regulators (predicted as activated).

Table 4-5: Upstream regulators showing similar trends for activation z-scores and fold changes on SLA and SMO surfaces (SLA vs. SMO comparisons at 3 hours did not reveal any such upstream regulator) (IPA analysis of microarray data).

(A) Activated

SLA vs. SMO: 24 hr			SLA: 3 hr vs. 0 hr			SLA:24 hr vs. 3 hr			SMO: 3 hr vs. 0 hr			SMO: 24 hr vs. 3 hr		
Regulator	**z**	**FC**	**Regulator**	**z**	**FC**	**Regulator**	**z**	**FC**	**Regulator**	**z**	**FC**	**Regulator**	**z**	**FC**
NUPR1	3.8	3.4	VEGFA	4.5	4.6	E2F1	5.5	3.5	VEGFA	4.2	5.0	E2F1	5.5	4.5
PTEN	2.0	1.5	HIF1A	3.7	1.2	E2F2	4.1	1.0	EIF4E	3.3	1.8	E2F2	4.0	1.4
MITF	1.9	1.2	CREM	3.3	7.1	TFDP1	2.0	2.0	CREM	3.2	6.6	FOXM1	3.5	7.3
SQSTM1	1.9	2.3	TGFB3	2.7	4.6	CHEK1	1.8	2.9	MYC	2.4	4.4	TFDP1	2.2	2.2
BMP2	1.0	5.7	CYR61	2.6	1.9	CCND3	1.7	5.4	CYR61	2.0	2.2	CCND3	1.7	5.0
RUNX2	0.7	2.2	MYC	2.5	4.9	DDX58	1.7	10.3	TGFB3	1.9	2.7	COPS8	1.6	1.3
			ATF4	2.5	2.3	XIAP	1.6	1.8	ATF4	1.9	2.3	CHEK1	1.5	3.6
			AREG/AREGB	2.4	28.9	PLK4	1.6	10.4	MAP2K1	1.8	1.9	SPARC	1.1	1.5
			SRF	2.4	2.6	CDKN1B	1.6	5.3	MAPK1	1.5	1.5	FN1	1.1	12.6
			MAP2K1	2.2	1.6	CDK2	1.5	5.3	AREG/AREGB	1.5	24.0	CDK2	1.0	5.3
			ELAVL1	2.0	2.2	ITGA2	1.4	2.8	FOXO3	1.3	6.1	CDKN1B	1.0	7.5
			F2RL1	1.9	6.5	EIF2S1	1.3	1.6	GDNF	1.2	6.5	CKS1B	1.0	2.8
			KAT5	1.1	1.4	KIAA1524	1.1	6.0	SRF	1.1	2.8	SKP2	0.9	7.2
			WWTR1	1.0	3.4	TOPBP1	1.0	2.4	WWTR1	1.0	2.6	ADAM12	0.9	6.9
			ETS1	0.9	13.9	CKS1B	1.0	2.9	S1PR2	0.8	2.8	TYMS	0.8	2.9
			NR3C1	0.8	1.4	EIF2AK2	0.9	2.2	RIPK1	0.5	5.3	ATR	0.7	2.6
			EGR1	0.7	2.5	COPS8	0.8	1.6	JUNB	0.2	3.9	EGFR	0.5	2.3
			TGFB2	0.6	3.6	CCNE1	0.8	2.8				CCNE1	0.3	3.6
			FGF1	0.5	3.3	CDK1	0.8	23.9						
			GNB2L1	0.4	3.1	MYBL2	0.2	2.5						
			PTGS2	0.4	4.2									
			JUNB	0.3	4.0									
			FOXO3	0.2	4.2									

Table 4-5 (continued): Upstream regulators showing similar trends for activation z-scores and fold changes on SLA and SMO surfaces

(B) Inhibited

SLA vs. SMO: 24 hr			SLA: 3 hr vs. 0 hr			SLA:24 hr vs. 3 hr			SMO: 3 hr vs. 0 hr			SMO: 24 hr vs. 3 hr		
Regulator	**z**	**FC**	**Regulator**	**z**	**FC**	**Regulator**	**z**	**FC**	**Regulator**	**z**	**FC**	**Regulator**	**z**	**FC**
FAS	-0.6	-1.1	DICER1	-0.3	-3.0	ETS1	-0.2	-2.6	CASP8	-0.1	-2.0	PPARD	-0.1	-2.6
FOXM1	-1.8	-2.1	TAF4	-1.8	-2.1	PPARD	-0.4	-2.3	KIAA1524	-1.7	-1.6	RASSF5	-0.1	-2.5
						SMAD3	-0.5	-2.0				RHOB	-0.2	-2.4
						KITLG	-0.6	-1.8				ETS1	-0.2	-2.8
						CEBPB	-0.6	-2.5				CEBPB	-0.5	-3.5
						FOXO3	-0.7	-2.8				MXI1	-0.6	-2.4
						VGLL3	-0.8	-3.0				GNB2L1	-0.6	-2.3
						ATF6	-0.9	-1.7				INHBA	-0.8	-3.7
						ST8SIA1	-1.0	-7.3				PIM1	-0.8	-3.9
						FGFR1	-1.0	-1.7				PPARG	-0.9	-6.9
						REL	-1.0	-3.5				PRKCE	-0.9	-2.0
						NR3C1	-1.2	-3.5				LGALS3	-0.9	-1.5
						VEGFA	-1.4	-2.1				SPRY2	-1.0	-4.9
						PIM1	-1.5	-4.1				RND3	-1.0	-1.3
						PPARG	-1.6	-7.1				SAT1	-1.0	-4.8
						ATF3	-1.7	-5.2				IGF1R	-1.0	-2.9
						TGFB3	-1.8	-5.4				KITLG	-1.1	-1.9
						F2RL1	-1.9	-4.9				EGR2	-1.2	-3.8
						ITGB1	-2.2	-13.2				VEGFA	-1.3	-3.0
						CDKN1A	-2.4	-2.4				F2RL1	-1.5	-5.2
						CREM	-2.8	-4.5				NR3C1	-1.5	-2.5
						TCF3	-3.1	-1.9				TGFB3	-1.6	-2.7
												PTEN	-1.9	-1.7
												PPRC1	-1.9	-2.9
												BAG1	-2.0	-2.2
												FOXO3	-2.6	-2.5
												CREM	-2.6	-4.7
												CDKN1A	-2.7	-2.9
												ATF4	-3.2	-2.8
												NUPR1	-9.4	-7.4

Time-course analysis (3 hours vs. base-line and 24 hours vs. 3 hours comparisons) was also performed on both of the surfaces. The 3 hours vs. base-line (0 hour) comparison revealed VEGFA, CREM, TGFB3, CYR61, MYC, ATF4, AREG/AREGB, SRF, MAP2K1, WWTR1, JUNB and FOXO3 among the correlated upstream regulators on both SLA and SMO surfaces (3 hours vs. base-line). HIF1A, ELAVL1, F2RL1, KAT5, ETS1, NR3C1, EGR1, TGFB2, FGF1, GNB2L1 and PTGS2 were only seen on SLA surface and EIF4E, MAPK1, GDNF, S1PR2 and RIPK1 were observed on SMO after 3 hours of exposure. The 24 hours vs. 3 hours comparisons on both SLA and SMO surfaces showed E2F1, E2F2, TFDP1, CHEK1, CCND3, CDKN1B, CDK2, CKS1B, COPS8 and CCNE1 as common activated upstream regulators. DDX58, XIAP, PLK4, ITGA2, EIF2S1, KIAA1524, TOPBP1, EIF2AK2, CDK1 and MYBL2 were seen as activated only on SLA surface (and not on SMO) when 24 hours expression was compared with 3 hours. FOXM1, SPARC, FN1, SKP2, ADAM12, TYMS, ATR and EGFR were observed as activated on SMO only (and not on SLA) upon 24 hours vs. 3 hours comparisons. ETS1, PPARD, KITLG, CEBPB, FOXO3, NR3C1, VEGFA, PIM1, PPARG, TGFB3, F2RL1, CDKN1A and CREM were genes found to be inhibited on both SLA and SMO surfaces on the 24 hours vs. 3 hours comparison. The molecules SMAD3, VGLL3, ATF6, ST8SIA1, FGFR1, REL, ATF3, ITGB1 and TCF3 were inhibited only on SLA surface, while RASSF5, RHOB, MXI1, GNB2L1, INHBA, PRKCE, LGALS3, SPRY2, RND3, SAT1, IGF1R, EGR2, PTEN, PPRC1, BAG1, ATF4 and NUPR1 were inhibited on SMO surfaces (24 hours vs. 3 hours).

4.4 DISCUSSION

Per-Ingvar Brånemark's discovery of the phenomenon of osseointegration in the late 1950s [21], heralded the drive to use titanium implants for restoring structural parts of the body. This also led researchers to start investigating implant design modifications that may have superior osseointegrative properties. In 1991, Buser et al. reported a positive correlation between implant micro-roughness and osseointegration, when they demonstrated superior osseointegration on SLA surfaces compared with electropolished and sand-blasted, medium-grit surfaces [1]. Ever since then, the improved osseointegrative property of micro-roughened titanium surfaces, like SLA has been a subject of intense research over the past few years and

several studies have validated the findings in terms of expression of osteogenic genes and markers [22-25].

The phenomenon of osseointegration is dependent on the process of osteogenic differentiation. Micro-roughened implant surfaces, like the SLA surface, by virtue of their property of "contact osteogenesis" [6], provide us with an *in vitro* substrate akin to the physiological micro-rough osteogenic niche. Several groups have been investigating the molecular mechanisms involved in the superior osseointegrative properties of micro-roughened surfaces compared with smooth surfaces. Superior osteogenic effects of micro-roughened surfaces have been substantiated in this report as well (Figure 4-1). Investigating the molecular dynamics of osteoprogenitor and osteoblast cells on SLA surfaces, and comparing them with the expression patterns on polished titanium (SMO) at the same instance, allow us to study the genetic mechanisms involved in the process of osteogenic differentiation and osseointegration. A time-course analysis of the gene expression pattern on both of the surfaces and a comparative assessment provides an opportunity to study the trail of genetic events that make the micro-roughened surface more conducive to osteogenic differentiation. Osteogenic differentiation has been conventionally known as a process wherein osteogenic cells undergo a series of molecular and morphological changes, leading to the formation of a calcified matrix and expression of markers like collagen type I, alkaline phosphatase, osteonectin, osteopontin, and osteocalcin [26]. However, the early molecular mechanisms that lead to these manifestations still remain elusive. Previous reports have described differential modulation of genes following early exposure to micro-roughened surfaces [2, 3, 9, 27, 28]. In this study, a whole genome microarray expression approach was used to ensure a comprehensive capture of the molecular changes in BCs following exposure to SLA and SMO titanium surfaces. To assess the time-course of changes on SLA and SMO surfaces, the study included microarray based gene expression analyses at three time-points: base-line (or 0 hour-before exposure to either SLA or SMO surfaces), 3 hours and 24 hours.

Analysis of the microarray gene expression profiles on SLA and SMO surfaces and the comparisons between them at 3 hours and 24 hours showed a cascade of gene modulations resulting in upregulation and downregulation of several genes at both of the time-points. The GO clusters belonging to "biological processes"

domain were enriched between SLA and SMO surfaces at both 3 and 24 hours. The GO domain "biological processes", tries to interpret a sequence of molecular functions that may lead to a particular biological process. Sixty-five percent of the clusters at 3 hours and 57% at 24 hours were categorized in the "biological processes" GO domain (SLA vs. SMO). A chain of genetic mechanisms leading to different physiological processes are triggered when bone cells are exposed to SLA surfaces as documented by Ivanovski et al. [25]. The number of genes differentially regulated between SLA and SMO surfaces was seen to increase over the period of assessment (between base-line and 3 hours and between 3 and 24 hours), indicating a sequential pattern of molecular events that lead to the course of biological processes. The genes, Rho GTP-binding protein family (RHOB) and Hermansky-Pudlak syndrome 1 (HPS1) were among the top ten genes showing higher expression on SLA surfaces compared to SMO after 3 hours exposure. RHOB is known to promote angiogenesis [29], cell adhesion of macrophages especially by regulation of integrins [30], and platelet activation [31]. It is known to be involved in signal transduction by the non-canonical Wnt/Ca^{2+} ligand WNT5A [32]. The Lin-7 Homolog B (LIN7B) gene and Kelch-Like Family Member 7 (KLHL7) genes are known to be involved in protein metabolism. The LIN7B helps in protein binding, whereas KLHL7 is known to assist in protein ubiquitination and degradation [33-35]. Higher expression of LIN7B and downregulation of KLHL7 on SLA surfaces (compared to SMO) indicates an early promotion of anabolic activity on SLA surfaces.

A clearly evident pro-osteogenic response was manifested on the SLA surfaces when compared with SMO surfaces, following 24 hours of exposure. The bone morphogenetic protein, BMP2 gene was seen to be highly upregulated (FC=5.70) on SLA surfaces compared to SMO surfaces at 24 hours (Table 4-2). The BMP2 protein was discovered by its ability to induce bone formation ectopically [36, 37], and stimulation of the TGFβ/BMP pathway is known to be of prime importance in osteogenesis [38]. Therefore, higher expression of the BMP2 gene on SLA surfaces is a strong indication of the early modulation of pro-osteogenic cell signaling on these surfaces. Besides, the simultaneous upregulation of RUNX2 on SLA surfaces at 24 hours (FC=2.2), together with a positive activation z-score, strengthens our proposition. The gene showing highest upregulation on SLA surfaces (compared to SMO) at 24 hours was FBJ murine osteosarcoma viral oncogene

homolog B (FOSB) (FC=7.52). Overexpression of DeltaFOSB is known to increase osteoblastogenesis [39]. Regulator of Cell Cycle (RGCC) and C8orf4 were also seen to be upregulated on SLA (compared with SMO) after 24 hours. RGCC is known to be a negative regulator of angiogenesis and cytokine secretion [40, 41]. Higher expression of RGCC after 24 hours indicates a shift in the molecular processes from a pro-angiogenic phase (as observed at 3 hours time-point) to a pro-osteogenic phase. RGCC gene is also known to help in collagen synthesis [42], and thereby initiates the foundation of the mineralized matrix. Analysis of the functional clusters and upstream regulators also point towards the same phenomenon. Clusters related to "development of blood cells" and "differentiation of connective tissues" were repressed between 24 hours and 3 hours. The time-course analysis pattern also described similar findings. Clusters related to skeletogenesis were upregulated on SLA surfaces (24 hours vs. 3 hours on SLA) (Table 4-4). No such clusters were seen on the SMO surfaces. In fact, the first organogenesis cluster enriched using gene ontology analysis with DAVID was related to endochondral ossification, bone and skeletal development when gene expression between SLA and SMO at 24 hours was compared. The relevant genes differentially expressed between SLA and SMO surfaces and their correlation with the GO skeletal tissue development terms are shown in Figure 4-6.

Figure 4-6: 2D view of associations between genes differentially regulated on SLA (compared with SMO) and GO terms related to skeletal and bone formation (DAVID analysis – SLA vs. SMO following 24 hours of culture of osteoprogenitor cells).

Cell signaling pathways together with cytoskeletal organization, cell proliferation and cell survival pathways seem to be modulated early on the SLA surface. C8orf4, a gene known to be a positive regulator of the Wnt pathway was upregulated on the SLA surface at 24 hours [43]. Increased response of the TGFβ/BMP pathway was demonstrated by the higher expression of BMP2. Integrin-α2 (ITGA2) was one of the upstream regulators found to be activated on SLA (24 hours vs. 3 hours) and not on the SMO surface. ITGA2, is a key integrin molecule that is known to play an important role in osteogenesis on SLA surfaces through a WNT5A mediated response [44]. Another integrin molecule, Integrin-β1 (ITGB1)

was however found to be inhibited between 24 hours and 3 hours on SLA surfaces. Previous studies have reported an increased expression of ITGB1 on modified titanium surfaces [8, 44]; however, the interpretations in these studies have been based on comparison of modified surfaces with smooth surfaces and not as a time-course pattern. Moreover, micro-topography mediated increase of ITGB1 is known to be obliterated by ITGA2 knock-downs indicating a greater role of ITGA2 than ITGB1 [45]. Clusters related to microtubule organization and motor activities were enriched between SLA and SMO surfaces at 24 hours. We further evaluated whether there was a tendency towards upregulation/downregulation of the genes for such processes. The differentially regulated genes belonging to the GO categories "microtubule cytoskeleton, cytoskeleton and microtubule motor activity" were extracted from the list and assigned a score of either +1 (if upregulated on SLA) or -1 (if downregulated on SLA) and a sum was calculated. A net negative sum was observed for all the clusters. A possible inhibition of microtubular and cytoskeletal changes correlated with the pro-osteogenic response.

Activation of E2F1 and E2F2 genes was observed on both SLA and SMO surfaces (24 hours vs. 3 hours). The E2F transcription factors are responsible for cells to enter the S phase of cell cycle and thereafter undergo division [46]. Cellular development, proliferation and cell cycle related pathways were activated on both SLA and SMO surfaces over the time-course. Proliferation and cell cycle are integral part of the developmental process and are known to be important particularly in the early phase of development as seen in embryonic cells [47]. The transcription factor, ETS1 which is known to be expressed in dividing preosteoblastic cells was potentially inhibited on both of the SLA and SMO surfaces (24 hours vs. 3 hours) suggesting a shift towards maturation and differentiation of osteoprogenitor cells on both of the surfaces [48]. The co-inhibition of the pro-adipogenic PPARG indicates the same. However, the inhibition of PPARD, which is known as an inhibitor of PPARG activity [49] was also observed. This could possibly indicate a modulatory effect striking a balance between the different biological pathways.

The 3 hours assessments between SLA and SMO surfaces indicated an early activity on the SLA surface that leads to the creation of a pro-osteogenic niche. Gene ontology analysis using DAVID showed significant enrichment of clusters (enrichment scores ≥ 1.3) related to nucleic acid processing and mRNA conditioning

for signal transduction (Table 4-3). This effect was reflected upon analyzing the pattern of gene expression over a time-course: base-line, 3 hours and 24 hours. Although activation of clusters related to nucleic acid processing was observed on both SLA and SMO surfaces, clusters related to protein metabolism and glycosaminoglycans were more highlighted on the SLA surfaces within 3 hours indicating a preparatory phase before the actual process of osteogenesis is initiated. The SLA time-course analysis revealed several activated clusters related to development and differentiation of blood cells and vascularization (Table 4-4) within 3 hours of exposure. High activation scores for vascular endothelial growth factor A (VEGFA) and hypoxia-inducible factor 1-alpha (HIF1A) identified them as the top two upstream regulators on SLA (3 hours vs. base-line) surfaces. Interestingly, both of the genes were themselves seen as upregulated at 3 hours. Although, VEGFA was also seen as the top upstream regulator on SMO surface; however, HIF1A wasn't evident. Hypoxia inducible factors (HIFs) have been recently identified as key components inducing VEGFs and angiogenesis and they are known to be important for angiogenesis-osteogenesis coupling [50]. Recent research has shown that HIF1A expression from osteoblasts promotes blood vessel formation and osteogenesis [51]. High activation score coupled with a statistically significant upregulation strengthens the pro-angiogenic effects of SLA surface. Implant osseointegration is a process similar to any wound healing process. The process is initiated with the preparation of the implant bed and insertion of the implant. Blood with all its components (organic and in-organic) is the first tissue that interacts with the implant. Among the other genes identified as upstream regulators only on SLA surfaces (3 hours vs. base-line) were F2RL1, ETS1 and FGF1 and each of them are known to positively regulate angiogenic effects [52-54].

The expression of clusters associated with immunological processes (e.g. lymphoid tissue structure and development, humoral cell trafficking, immune cell trafficking and cell mediated immune response, see Figure 4-4) was significantly higher on SLA surfaces than SMO surfaces at 3 hours. Immunological responses and inflammatory modulators are known to be of prime importance in bone healing and repair after a fracture. As mentioned before, implant insertion and osseointegration process is very similar to the process of fracture healing and the *in vivo* peri-implant hematoma is analogous to the fracture-hematoma [55]. Immunomodulatory factors

found in peri-implant hematoma are believed to be important for initiating a cascade of reactions leading to the migration of mesenchymal stem cells and osteoprogenitor cells towards the site of bone repair [55]. However, the immediate expression of immunomodulatory clusters in osteoprogenitor cells as observed on SLA surfaces indicates a larger role beyond the initial recruitment of osteogenic cells. Such molecules and their signaling networks possibly prepare the niche for the initiation of an osteogenic response, which was evident after 24 hours of exposure. This concept is further strengthened by the inhibition of "chronic inflammatory" cluster as observed on SLA surface (3 hours vs. base-line) suggesting stimulation of an acute immunomodulatory response in concert with suppression of chronic inflammation.

4.5 CONCLUSION

A complex sequence of biological responses occur upon exposure of osteogenic cells to micro-roughened SLA surfaces and this eventually leads to the improved osteogenic differentiation *in vitro* and osseointegration *in vivo*. This study aimed to explore the early changes in alveolar bone-derived osteoprogenitor cells following exposure to SLA surfaces and comparing them with SMO surfaces, with intent to divulge the events that lead to improved osteogenic properties. The initial time-point of comparison (3 hours) revealed a pro-angiogenic and immunomodulatory response on the SLA surface, that wasn't observed on the SMO surface. Our results also demonstrated an early pro-osteogenic response on the SLA surface compared to SMO surfaces (24 hours). The initial cascade of gene modulation potentially lays the foundation for the pro-osteogenic niche provided by the SLA surface and this response starts immediately post-exposure to the surfaces. The findings from the study elaborate the biological relevance of studying the immediate and early cellular response to micro-roughened titanium implant surfaces.

4.6 REFERENCES

[1] Buser D, Schenk RK, Steinemann S, Fiorellini JP, Fox CH, Stich H. Influence of surface characteristics on bone integration of titanium implants. A histomorphometric study in miniature pigs. J Biomed Mater Res 1991;25:889-902.

[2] Vlacic-Zischke J, Hamlet SM, Friis T, Tonetti MS, Ivanovski S. The influence of surface microroughness and hydrophilicity of titanium on the up-regulation of TGFbeta/BMP signalling in osteoblasts. Biomaterials 2011;32:665-71.

[3] Brett PM, Harle J, Salih V, Mihoc R, Olsen I, Jones FH, et al. Roughness response genes in osteoblasts. Bone 2004;35:124-33.

[4] Olivares-Navarrete R, Hyzy SL, Hutton DL, Erdman CP, Wieland M, Boyan BD, et al. Direct and indirect effects of microstructured titanium substrates on the induction of mesenchymal stem cell differentiation towards the osteoblast lineage. Biomaterials 2010;31:2728-35.

[5] Buser D, Nydegger T, Oxland T, Cochran DL, Schenk RK, Hirt HP, et al. Interface shear strength of titanium implants with a sandblasted and acid-etched surface: a biomechanical study in the maxilla of miniature pigs. J Biomed Mater Res 1999;45:75-83.

[6] Osborn J, Newesely H. Dynamic aspects of the implant-bone interface. In: Heimke G, editor. Dental implants: Materials and Systems: München: Carl Hanser Verlag; 1980. p. 111-23.

[7] Olivares-Navarrete R, Hyzy S, Wieland M, Boyan BD, Schwartz Z. The roles of Wnt signaling modulators Dickkopf-1 (Dkk1) and Dickkopf-2 (Dkk2) and cell maturation state in osteogenesis on microstructured titanium surfaces. Biomaterials 2010;31:2015-24.

[8] Chakravorty N, Ivanovski S, Prasadam I, Crawford R, Oloyede A, Xiao Y. The microRNA expression signature on modified titanium implant surfaces influences genetic mechanisms leading to osteogenic differentiation. Acta Biomater 2012;8:3516-23.

[9] Chakravorty N, Hamlet S, Jaiprakash A, Crawford R, Oloyede A, Alfarsi M, et al. Pro-osteogenic topographical cues promote early activation of osteoprogenitor differentiation via enhanced TGFbeta, Wnt, and Notch signaling. Clin Oral Implants Res 2014;25:475-86.

[10] Haase HR, Ivanovski S, Waters MJ, Bartold PM. Growth hormone regulates osteogenic marker mRNA expression in human periodontal fibroblasts and alveolar bone-derived cells. J Periodontal Res 2003;38:366-74.

[11] Xiao Y, Haase H, Young WG, Bartold PM. Development and transplantation of a mineralized matrix formed by osteoblasts in vitro for bone regeneration. Cell Transplant 2004;13:15-25.

[12] Xiao Y, Qian H, Young WG, Bartold PM. Tissue engineering for bone regeneration using differentiated alveolar bone cells in collagen scaffolds. Tissue Eng 2003;9:1167-77.

[13] Tenenbaum HC, Heersche JNM. Dexamethasone stimulates osteogenesis in chick periosteum in vitro. Endocrinology 1985;117:2211-7.

[14] Reinholz GG, Getz B, Pederson L, Sanders ES, Subramaniam M, Ingle JN, et al. Bisphosphonates directly regulate cell proliferation, differentiation, and gene expression in human osteoblasts. Cancer Res 2000;60:6001-7.

[15] Dennis G, Jr., Sherman BT, Hosack DA, Yang J, Gao W, Lane HC, et al. DAVID: Database for Annotation, Visualization, and Integrated Discovery. Genome Biol 2003;4:P3.

[16] Van Vaerenbergh I, Van Lommel L, Ghislain V, In't Veld P, Schuit F, Fatemi HM, et al. In GnRH antagonist/rec-FSH stimulated cycles, advanced endometrial maturation on the day of oocyte retrieval correlates with altered gene expression. Hum Reprod 2009;24:1085-91.

[17] Yang Z, Goldstein LS. Characterization of the KIF3C neural kinesin-like motor from mouse. Mol Biol Cell 1998;9:249-61.

[18] Wang L, Xu J, Ji C, Gu S, Lv Y, Li S, et al. Cloning, expression and characterization of human glutathione S-transferase Omega 2. Int J Mol Med 2005;16:19-27.

[19] Almeida AM, Murakami Y, Layton DM, Hillmen P, Sellick GS, Maeda Y, et al. Hypomorphic promoter mutation in PIGM causes inherited glycosylphosphatidylinositol deficiency. Nat Med 2006;12:846-51.

[20] Huang da W, Sherman BT, Lempicki RA. Systematic and integrative analysis of large gene lists using DAVID bioinformatics resources. Nat Protoc 2009;4:44-57.

[21] Brånemark PI. Vital microscopy of bone marrow in rabbit. Scand J Clin Lab Invest 1959;11:1-82.

[22] Bosshardt DD, Salvi GE, Huynh-Ba G, Ivanovski S, Donos N, Lang NP. The role of bone debris in early healing adjacent to hydrophilic and hydrophobic implant surfaces in man. Clin Oral Implants Res 2011;22:357-64.

[23] Lang NP, Salvi GE, Huynh-Ba G, Ivanovski S, Donos N, Bosshardt DD. Early osseointegration to hydrophilic and hydrophobic implant surfaces in humans. Clin Oral Implants Res 2011;22:349-56.

[24] Donos N, Hamlet S, Lang NP, Salvi GE, Huynh-Ba G, Bosshardt DD, et al. Gene expression profile of osseointegration of a hydrophilic compared with a hydrophobic microrough implant surface. Clin Oral Implants Res 2011;22:365-72.

[25] Ivanovski S, Hamlet S, Salvi GE, Huynh-Ba G, Bosshardt DD, Lang NP, et al. Transcriptional profiling of osseointegration in humans. Clin Oral Implants Res 2011;22:373-81.

[26] Strauss PG, Closs EI, Schmidt J, Erfle V. Gene expression during osteogenic differentiation in mandibular condyles in vitro. J Cell Biol 1990;110:1369-78.

[27] Wall I, Donos N, Carlqvist K, Jones F, Brett P. Modified titanium surfaces promote accelerated osteogenic differentiation of mesenchymal stromal cells in vitro. Bone 2009;45:17-26.

[28] Donos N, Retzepi M, Wall I, Hamlet S, Ivanovski S. In vivo gene expression profile of guided bone regeneration associated with a microrough titanium surface. Clin Oral Implants Res 2011;22:390-8.

[29] Adini I, Rabinovitz I, Sun JF, Prendergast GC, Benjamin LE. RhoB controls Akt trafficking and stage-specific survival of endothelial cells during vascular development. Genes Dev 2003;17:2721-32.

[30] Wheeler AP, Ridley AJ. RhoB affects macrophage adhesion, integrin expression and migration. Exp Cell Res 2007;313:3505-16.

[31] Huang M, Satchell L, Duhadaway JB, Prendergast GC, Laury-Kleintop LD. RhoB links PDGF signaling to cell migration by coordinating activation and localization of Cdc42 and Rac. J Cell Biochem 2011;112:1572-84.

[32] Katoh M. Transcriptional mechanisms of WNT5A based on NF-kappaB, Hedgehog, TGFβ, and Notch signaling cascades. Int J Mol Med 2009;23:763-9.

[33] Kitano J, Yamazaki Y, Kimura K, Masukado T, Nakajima Y, Nakanishi S. Tamalin is a scaffold protein that interacts with multiple neuronal proteins in distinct modes of protein-protein association. J Biol Chem 2003;278:14762-8.

[34] Jo K, Derin R, Li M, Bredt DS. Characterization of MALS/Velis-1, -2, and -3: a family of mammalian LIN-7 homologs enriched at brain synapses in association with the postsynaptic density-95/NMDA receptor postsynaptic complex. J Neurosci 1999;19:4189-99.

[35] Kigoshi Y, Tsuruta F, Chiba T. Ubiquitin ligase activity of Cul3-KLHL7 protein is attenuated by autosomal dominant retinitis pigmentosa causative mutation. J Biol Chem 2011;286:33613-21.

[36] Urist MR. Bone: Formation by autoinduction. Science 1965;150:893-9.

[37] Wozney JM. The bone morphogenetic protein family and osteogenesis. Mol Reprod Dev 1992;32:160-7.

[38] Wu C-J, Lu H-K. Smad Signal Pathway in BMP-2-induced Osteogenesis-A Mini Review. J Dent Sci 2008;3:13-21.

[39] Sabatakos G, Sims NA, Chen J, Aoki K, Kelz MB, Amling M, et al. Overexpression of DeltaFosB transcription factor(s) increases bone formation and inhibits adipogenesis. Nat Med 2000;6:985-90.

[40] An X, Jin Y, Guo H, Foo SY, Cully BL, Wu J, et al. Response gene to complement 32, a novel hypoxia-regulated angiogenic inhibitor. Circulation 2009;120:617-27.

[41] Fosbrink M, Cudrici C, Tegla CA, Soloviova K, Ito T, Vlaicu S, et al. Response gene to complement 32 is required for C5b-9 induced cell cycle activation in endothelial cells. Exp Mol Pathol 2009;86:87-94.

[42] Huang WY, Li ZG, Rus H, Wang X, Jose PA, Chen SY. RGC-32 mediates transforming growth factor-beta-induced epithelial-mesenchymal transition in human renal proximal tubular cells. J Biol Chem 2009;284:9426-32.

[43] Jung Y, Bang S, Choi K, Kim E, Kim Y, Kim J, et al. TC1 (C8orf4) enhances the Wnt/beta-catenin pathway by relieving antagonistic activity of Chibby. Cancer Res 2006;66:723-8.

[44] Olivares-Navarrete R, Hyzy SL, Park JH, Dunn GR, Haithcock DA, Wasilewski CE, et al. Mediation of osteogenic differentiation of human mesenchymal stem cells on titanium surfaces by a Wnt-integrin feedback loop. Biomaterials 2011;32:6399-411.

[45] Olivares-Navarrete R, Raz P, Zhao G, Chen J, Wieland M, Cochran DL, et al. Integrin alpha2beta1 plays a critical role in osteoblast response to micron-scale surface structure and surface energy of titanium substrates. Proc Natl Acad Sci U S A 2008;105:15767-72.

[46] Berman SD, Yuan TL, Miller ES, Lee EY, Caron A, Lees JA. The retinoblastoma protein tumor suppressor is important for appropriate osteoblast differentiation and bone development. Mol Cancer Res 2008;6:1440-51.

[47] Cooper G. Cell proliferation in development and differentiation. In: GM C, editor. The Cell: A Molecular Approach. 2nd ed. Sunderland (MA): Sinauer Associates; 2000.

[48] Raouf A, Seth A. Ets transcription factors and targets in osteogenesis. Oncogene 2000;19:6455-63.

[49] Shi Y, Hon M, Evans RM. The peroxisome proliferator-activated receptor delta, an integrator of transcriptional repression and nuclear receptor signaling. Proc Natl Acad Sci U S A 2002;99:2613-8.

[50] Schipani E, Maes C, Carmeliet G, Semenza GL. Regulation of osteogenesis-angiogenesis coupling by HIFs and VEGF. J Bone Miner Res 2009;24:1347-53.

[51] Wang Y, Wan C, Deng LF, Liu XM, Cao XM, Gilbert SR, et al. The hypoxia-inducible factor a pathway couples angiogenesis to osteogenesis during skeletal development. J Clin Invest 2007;117:1616-26.

[52] Zhang XT, Wang WB, Mize GJ, Takayama TK, True LD, Vessella RL. Protease-activated receptor 2 signaling upregulates angiogenic growth factors in renal cell carcinoma. Exp Mol Pathol 2013;94:91-7.

[53] Iwasaka C, Tanaka K, Abe M, Sato Y. Ets-1 regulates angiogenesis by inducing the expression of urokinase-type plasminogen activator and matrix metalloproteinase-1 and the migration of vascular endothelial cells. J Cell Physiol 1996;169:522-31.

[54] Ding I, Liu WM, Sun JZ, Paoni SF, Hernady E, Fenton BM, et al. FGF1 and VEGF mediated angiogenesis in KHT tumor-bearing mice. Adv Exp Med Biol 2003;530:603-9.

[55] Kuzyk PR, Schemitsch EH. The basic science of peri-implant bone healing. Indian J Orthop 2011;45:108-15.

Chapter 5: The MicroRNA Expression Profiling Study

The microRNA expression signature on modified titanium implant surfaces influences genetic mechanisms leading to osteogenic differentiation

Nishant Chakravorty, Saso Ivanovski, Indira Prasadam, Ross Crawford,

Adekunle Oloyede & Yin Xiao

(Published manuscript)

Citation: *Chakravorty N, Ivanovski S, Prasadam I, Crawford R, Oloyede A, Xiao Y. The microRNA expression signature on modified titanium implant surfaces influences genetic mechanisms leading to osteogenic differentiation. Acta Biomater 2012;8:3516-23.*

Suggested Statement of Contribution of Co-Authors for Thesis by Publication

Contributors	Statement of contribution
Nishant Chakravorty	Involved in the conception and design of the project. Performed laboratory experiments and wrote the manuscript.
Saso Ivanovski	Involved in the conception and design of the project, manuscript preparation and reviewing.
Indira Prasadam	Assisted in performing the experiments.
Ross Crawford	Involved in the conception and design of the project. Assisted in reviewing the manuscript.
Adekunle Oloyede	Involved in the conception and design of the project. Assisted in reviewing the manuscript.
Yin Xiao	Involved in the conception and design of the project, manuscript preparation and reviewing.

Principal Supervisor Confirmation

I have sighted email or other correspondence from all co-authors confirming their certifying authorship

Prof. Yin Xiao		**10th July, 2014**
Name	**Signature**	**Date**

Abstract

Topographically and chemically modified titanium implants are recognized to have improved osteogenic properties; however, the molecular regulation of this process remains unknown. This study aimed to determine the microRNA profile and the potential regulation of osteogenic differentiation following early exposure of osteoprogenitor cells to sand-blasted, large-grit acid-etched (SLA) and hydrophilic SLA (modSLA) surfaces. Firstly, the osteogenic characteristics of the primary osteoprogenitor cells were confirmed using ALP activity and Alizarin Red S staining. The effect of smooth (SMO), SLA and modSLA surfaces on the TGFβ/BMP (BMP2, BMP6, ACVR1) and non-canonical Wnt/Ca^{2+} (WNT5A, FZD6) pathways, as well as the integrins ITGB1 and ITGA2, was determined. It was revealed that the modified titanium surfaces could induce the activation of TGFβ/BMP and non canonical Wnt/Ca^{2+} signaling genes. The expression pattern of microRNAs (miRNAs) related to cell differentiation was evaluated. Statistical analysis of the differentially regulated miRNAs indicated that 35 and 32 miRNAs were down-regulated on the modSLA and SLA surfaces respectively, when compared with smooth surface (SMO). Thirty-one miRNAs that were down-regulated were common to both modSLA and SLA. There were 10 miRNAs up-regulated on modSLA and 9 on SLA surfaces, amongst which eight were the same as observed on modSLA. TargetScan predictions for the down-regulated miRNAs revealed genes of the TGFβ/BMP and non-canonical Wnt/Ca^{2+} pathways as targets. This study demonstrated that modified titanium implant surfaces induce differential regulation of miRNAs, which potentially regulate the TGFβ/BMP and Wnt/Ca^{2+} pathways during osteogenic differentiation on modified titanium implant surfaces.

5.1 INTRODUCTION

Titanium has long been considered the preferred material for implants in dentistry and orthopedics owing to its physical, chemical and biocompatibility features. Increasing clinical use of implants has necessitated the need for improved healing, especially in sites where bone quality and quantity is less than ideal. Surface topography and chemistry have been shown to be important factors influencing the osteogenic properties of implant surfaces [1, 2].

Micro-roughened surfaces such as the widely studied sand-blasted, large grit, acid-etched (SLA) titanium surfaces, potentially mimic the micro-rough biological bone tissue environment. The activities and characteristics of progenitor cells are influenced by their interaction with the implant surfaces [3]. Chemical modification of SLA, resulting in a hydrophilic surface (modSLA), has been shown to further improve osteogenic differentiation *in vitro* and osseointegration *in vivo* [4-11]. Investigation of the underlying molecular mechanisms responsible for the enhanced osteogenic properties of modified surfaces has been the focus of significant recent attention, and *in vivo* and *in vitro* gene expression studies have revealed differences in osteogenesis associated gene expression in response to SLA and modSLA [12-16]. Furthermore, studies investigating the associated biological mechanisms suggest that the TGFβ/BMP and Wnt signaling pathways are triggered early in the interaction between osteoprogenitors and implant surfaces [2, 13, 14, 17]. However, the detailed molecular mechanisms that regulate osteogenesis on these surfaces are still elusive and require further investigation.

The activation and de-activation of key regulatory genes is crucial to the process of differentiation of progenitor cells. Micro-RNAs (miRNAs) have been shown to influence the pattern of gene expression by translational repression and gene silencing [18] and are vital regulators of the differentiation process [19]. MiRNAs have been found to be critical in the development of organisms and show differential expression profiles in different tissues [20]. It is believed that 40-70% of human genes are under the regulation of miRNAs [21]. Recent studies have identified the role of several miRNAs as regulators of a variety of osteogenic genes, including transcription factors, signaling molecules and their receptors [22].

The expression of miRNAs has not been investigated in relation to the modulation of osteogenic gene expression by the SLA and modSLA surfaces. Therefore, the present study aimed to compare the early pattern of expression of a panel of miRNAs associated with human cell development and differentiation in osteoprogenitor cells cultured on three titanium implant surfaces (modSLA, SLA and smooth polished) and assesses their prospective regulation of the initial molecular interactions on modified titanium implant surfaces.

5.2 MATERIALS AND METHODS

5.2.1 Titanium discs

This study utilized discs (15 mm in diameter and 1 mm in thickness) of grade II commercially pure titanium which were supplied by Institut Straumann (Basel, Switzerland). Three different surfaces were studied – smooth polished (SMO), SLA and modSLA. The SLA surface modification was obtained by blasting the SMO surface with 250-500 μm corundum grit and acid etching with a hot solution of hydrochloric/sulfuric acids (Sa, arithmetic mean deviation of the surface=1.8 μm). The modSLA surface was obtained by rinsing the SLA discs under N_2 protection and stored in an isotonic saline solution at pH 4-6. The surface topography for modSLA, SLA and SMO was visualized using Atomic Force Microscopy (AFM) (JPK Instruments AG, Berlin, Germany) as shown in Figure 5-1. The rms roughness values for modSLA, SLA ranged between 1.6 and 2.1 μm and SMO was between 0.006-0.009 μm.

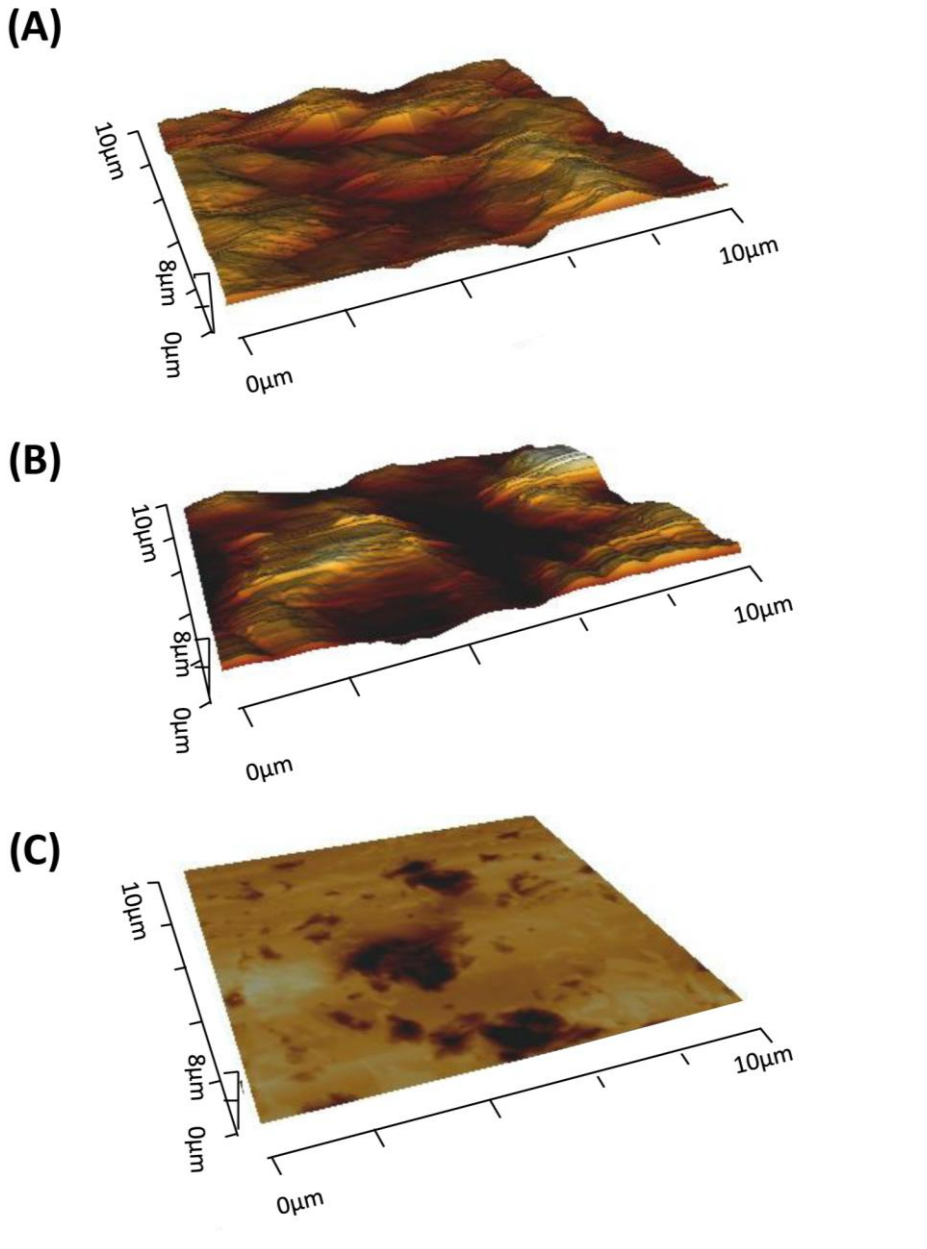

Figure 5-1: AFM visualization of surface topography of (A) modSLA, (B) SLA and (C) SMO.

5.2.2 Cell culture

Primary human osteoprogenitor cells established from redundant alveolar bone tissues obtained following third molar extraction surgery as previously described [23], were cultured in Dulbecco's Modified Eagle's Medium (DMEM) (Invitrogen, Mt Waverley, VIC, Australia) supplemented with 10% fetal bovine serum (FBS) (Thermo, In Vitro Technologies, Nobel Park, VIC, Australia) and antibiotics (100 U/ml penicillin/100 µg/ml streptomycin).

The cells were confirmed as osteoprogenitors by characterizing their osteogenic differentiation potential. Briefly, the cells were seeded at a density of 5×10^4 cells/well in 24-well tissue culture plates and osteogenic differentiation was induced by supplementing the culture media with 100 nM dexamethasone, 0.2 mM L-ascorbic acid and 10 mM β-glycerophosphate for 21 days. Intracellular ALP activity was determined with the Quantichrom™ Alkaline Phosphatase Assay Kit (Gentaur Belgium BVBA, Kampenhout, Belgium), a p-nitrophenyl phosphate (pNP-PO_4) based assay. Briefly, the cells were rinsed twice with PBS, and lysed in 500µl of 0.2% Triton X-100 in MilliQ water, followed by 20 minutes agitation at room temperature. A 50 µl sample was then mixed with a 100 µl working solution and absorbance was measured after 5 min at 405 nm in a microplate reader. Extracellular matrix deposition was determined by fixing the cells in 4% paraformaldehyde and staining with a 1% Alizarin Red S solution.

Following characterization, the osteoprogenitor cells were seeded at a density of 5×10^4 cells/titanium disc placed in 24 well tissue culture plates (BD Falcon, North Ryde, NSW, Australia) and incubated in non-osteogenic media. The cells were allowed to interact with the surfaces for 24 hours. After 24 hours of incubation, the media was removed and the discs were washed with Phosphate buffered saline (PBS) once. They were subsequently processed for extraction of miRNAs.

5.2.3 RNA isolation

After 24 hours of incubation on the three titanium surfaces, the cells were washed with PBS and lysed using QIAzol lysis reagent (Qiagen Pty Ltd, Doncaster, VIC, Australia). Total RNA (including miRNA fraction) was isolated using the miRNeasy mini kit (Qiagen Pty Ltd, Doncaster, VIC, Australia) as per the manufacturer's instructions. The kit allows purification of all RNA molecules with a minimum size threshold of 18 nucleotides, and is therefore suitable for analysis of both mRNA and miRNA expression. RNA integrity and concentration was measured using RNA 6000 Nano Chips and the Agilent Bioanalyzer 2100 System (Agilent Tech Inc., Santa Clara, USA).

5.2.4 Quantitative real-time PCR

cDNA was prepared from 1µg RNA templates by reverse transcription using DyNAmo^{TM} cDNA Synthesis Kit (Finnzymes Oy., Vantaa, Finland) according to the

manufacturer's protocol. The mRNA expression of BMP2, BMP6, ACVR1, FZD6, WNT5A, ITGB1, and ITGA2 was investigated after 24 hours of culture on the different titanium discs. Primers were obtained from GeneWorks Pty Ltd (Hindmarsh, SA, Australia) and are summarized in Table 5-1. Quantitative real time PCR (qPCR) reactions were performed using the ABI Prism 7000 Sequence Detection System (Applied Biosystems). The system enables direct detection of PCR products by measuring the increase in fluorescence caused by the binding of SYBR Green dye to double-stranded (ds) DNA. The reactions were incubated at 95 °C for 10 minutes; and then 95 °C for 15 seconds and 60 °C for 1 minute for 40 cycles. PCR reactions were validated by observing the presence of a single peak in the dissociation curve analysis. The housekeeping gene glyceraldehyde-3-phosphate-dehydrogenase (GAPDH) was used as an endogenous reference gene for analysis using the Comparative Ct (Cycle of threshold) value method.

Table 5-1: Primer sequences used for real-time PCR analysis of gene expression.

Gene name	Forward primer	Reverse primer
BMP2	CGCAGCTTCCACCATGAAGAATC	CCTGAAGCTCTGCTGAGGTG
BMP6	CAGGAGCATCAGCACAGAGAC	GCTGAAGCCCCATGTTATGCTG
ACVR1	AGTCATGGTTCAGGGAAACGG	ACCACAGCTGGGTACTGGAG
FZD6	GCGGAGTGAAGGAAGGATTAG	ACAAGCAGAGATGTGGAACC
WNT5A	TCTCAGCCCAAGCAACAAGG	GCCAGCATCACATCACAACAC
ITGB1	GCCTGTTTACAAGGAGCTGAA	CTGACAATTTGCCGTTTTCC
ITGA2	CAAGGCTGGTGACATCAGTTG	CAGGAAGCAGTTCTGCAGTTC
GAPDH	TCAGCAATGCCTCCTGCAC	TCTGGGTGGCAGTGATGGC

5.2.5 Real-time PCR-based miRNA expression profiling

The expression profile of 88 miRNAs known to be associated with different stages of development, from stem cells to terminal differentiation, was assessed using the Human Cell Development & Differentiation miRNA PCR Array (SABiosciences, Frederick, Maryland, USA). The full list of miRNAs included on this array is available at http://www.sabiosciences.com/mirna_pcr_product/HTML/MAH-103A.html. For real time PCR amplification, 0.5µg of total RNA was initially used to convert miRNAs into first strand cDNA by using the RT^2 miRNA First Strand Kit (SABiosciences, Frederick, Maryland, USA) as per the manufacturer's

protocol. Real time PCR was subsequently performed using the RT^2 SYBR Green qPCR Master Mix (SABiosciences, Frederick, Maryland, USA) and the ABI 7900 Sequence Detection System (Applied Biosystems). The reactions were incubated at 95 °C for 10 minutes for 1 cycle, and then 95 °C (15 seconds), 60 °C (for 30 seconds) and 72 °C (for 30 seconds) for 40 cycles. PCR reactions were validated by observing the presence of a single peak in the dissociation curve analysis. The miRNA expression was normalized using the endogenous references: SNORD47, SNORD44, and RNU6-2.

In order to identify potential targets for the differentially regulated miRNAs, computational predictions were performed using the online tool TargetScan [24]. The predictions are based on the identification of potential miRNA binding sites in the mRNA 3' UTR region and thereby assigning a context score. TargetScan enables classifying a particular miRNA (within a miRNA family) with the lowest total context score as the "representative miRNA" for a target. To increase the probability of the target prediction we have specifically considered the representative miRNAs for the purpose of analyses in this study. As microRNAs function by translational repression or gene silencing, miRNAs potentially targeting genes associated with osteogenic differentiation should be down-regulated during the differentiation process. Therefore, the predicted targets for down-regulated miRNAs were further screened for genes colligated to the osteogenic differentiation process, and in particular the TGFβ/BMP and non-canonical Wnt/Ca^{2+} pathways, which have been shown to be regulated by titanium surface modification [2, 13, 14].

For the miRNA/mRNA expression, any sample having Ct values more than 33 was not included in the analysis. The melting temperature of all the miRNAs were in the range 74-77.5 °C. The arrays used also had positive control miRNA and they had similar dissociation curves and melting temperatures. The melting temperatures for mRNAs analyzed were in the range 75.5 to 81.8 °C.

5.2.6 Statistical analysis

The experiments were carried out in triplicates. The relative levels of expression of mRNAs and miRNAs were compared between the cells cultured on modSLA, SLA and polished titanium discs using Student's *t* test. The ΔC_T value was obtained by subtracting the average Ct value of the endogenous references selected from the test mRNA or miRNA Ct value of the same samples. The $\Delta\Delta C_T$ was

determined by subtracting the ΔC_T of the control sample from the ΔC_T of the target sample. The relative mRNA or miRNA quantification of the target gene was calculated by $2^{-\Delta\Delta CT}$. Down-regulated miRNA values were calculated as the negative reciprocal of the $2^{-\Delta\Delta CT}$ score. A value of $p<0.05$ was considered significant.

5.3 RESULTS

5.3.1 Osteogenic potential of primary human osteoprogenitor cells

There was a significant increase in the ALP activity of the cells cultured with osteogenic differentiation media as compared to standard media (Figure 5-2A). The osteogenic culture media also induced positive Alizarin Red S staining (Figure 5-2B). These assays confirmed that the primary alveolar bone derived cell cultures contain efficient osteoprogenitor cells.

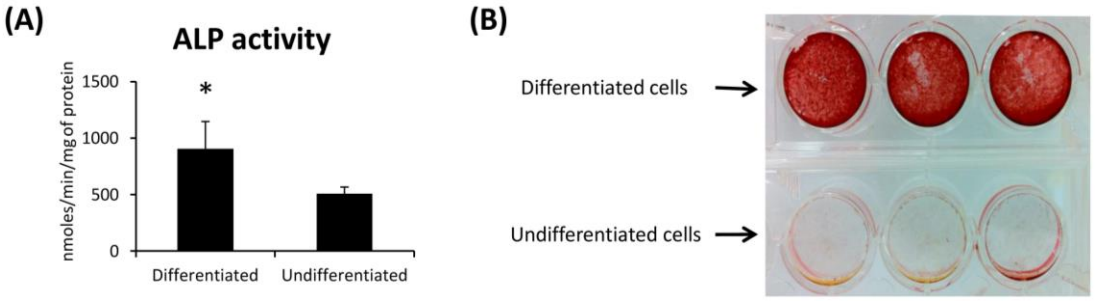

Figure 5-2: Osteogenic differentiation of alveolar bone-derived osteoblasts (n=3): (A) ALP activity observed after 21 days of culture in osteogenic media was significantly increased compared with the culture in growth media; (B) Osteoprogenitor cells after 21 days of culture in osteogenic media showed positive staining with Alizarin Red S.

5.3.2 Effect of surface topography and hydrophilicity on the expression of BMP2, BMP6, ACVR1, FZD6, WNT5A, ITGB1, and ITGA2

Previous studies showed that BMP2, BMP6, ACVR1, FZD6, WNT5A were differentially expressed by osteoprogenitor cells cultured on modSLA, SLA and SMO surfaces [13, 15]. In this study, the expression of BMP2, BMP6, ACVR1, FZD6, WNT5A, ITGB1, and ITGA2 was measured after 24 hours of culture on modSLA, SLA and SMO. A consistent pattern of expression was found for all of the genes under investigation with the highest level of expression found in response to modSLA, followed by SLA and SMO. BMP2, BMP6, ACVR1 and FZD6 were significantly up-regulated on the modSLA surface compared to the SMO surface. BMP6 was also significantly increased on the SLA compared with the SMO surface, whereas ACVR1 had significantly higher expression on modSLA compared with

SLA. WNT5A, ITGB1 and ITGA2 also showed up-regulation on the modified surfaces, although this was not statistically significant (Figure 5-3).

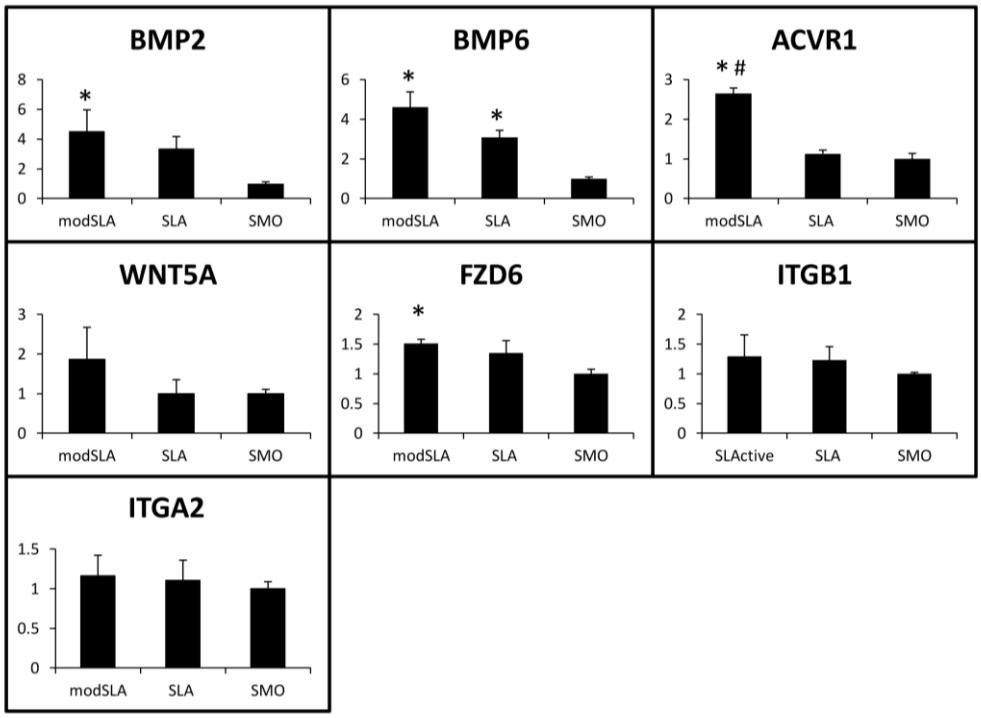

Figure 5-3: Fold-change in expression of BMP2, BMP6, ACVR1, WNT5A, FZD6, ITGB1, ITGA2 on modSLA and SLA surfaces compared with expression on SMO surface. Relative expression of the genes was higher on modSLA and SLA surfaces as compared to SMO after 24 hours of culture (*p < 0.05, when modSLA and SLA were compared with SMO surface; #p < 0.05, when modSLA was compared with SLA surface).

5.3.3 miRNA expression profile

Eighty-eight miRNAs associated with stem cell differentiation were studied using the Human Cell Development & Differentiation miRNA PCR Array (SABiosciences, Frederick, Maryland, USA). The expression of miRNAs on modSLA and SLA surfaces were compared with the control SMO surfaces (Figure 5-4) and the statistically significant changes in expression were considered for analyses. In comparison to the SMO surface, 39 miRNAs were significantly down-regulated and 11 miRNAs were significantly up-regulated (Figure 5-4 A&B) on the modSLA surface. Thirty-eight miRNAs were down-regulated and 10 miRNAs were significantly up-regulated on the SLA surface (Figure 5-4 C&D). Further systemic analysis of the expression profile using stringent criteria (fold change ≤-2.0, p-value <0.05) revealed 35 miRNAs down-regulated on the modSLA surface (Table 5-2A)

and 32 miRNAs were down-regulated on SLA surfaces (Table 5-2A). Similar stringent criteria for up-regulation (fold change ≥+2.0, p-value <0.05), revealed 10 miRNAs to be up-regulated on modSLA (Table 5-2B) and nine miRNAs on SLA surfaces (Table 5-2B), each compared to SMO. Notably, 31 miRNAs that were down-regulated were common to both modSLA and SLA (miR-215, miR-10a, miR-125b, miR-1, miR-218, miR-10b, miR-21, miR-126, miR-16, miR-195, miR-146b-5p, miR-194, miR-7, miR-192, miR-99a, miR-100, miR-125a-5p, miR-137, miR-146a, miR-424, miR-23b, miR-20b, miR-155, miR-378, miR-20a, miR-132, miR-17, miR-26a, miR-134, miR-452, miR-24). The miRNAs down-regulated on modSLA only were miR-503, miR-214 (fold change <-2.0), and miR-185 (fold change >-2.0). Meanwhile, let-7f (fold change <-2.0) and let-7a (fold change >-2.0) were seen to be down-regulated only on SLA. Among the up-regulated miRNAs (fold-change >+2 and p<0.05), eight were common to both modSLA and SLA (miR-33a, miR-222, miR-127-5p, miR-15a, miR-210, miR-130a, miR-22, miR-181a), while let-7i and let-7b were seen to be more than 2 fold up-regulated only on modSLA, and miR-18b was more than 2 fold up-regulated on SLA. A general trend of down-regulation of miRNAs was noted on modSLA surface compared with the SLA surface. 18 miRNAs (miR-106b, miR-22, miR-92a, miR-93, miR-301a, miR-18a, miR-103, miR-424, miR-222, miR-18b, miR-345, miR-17, miR-185, miR-128, miR-130a, miR-127-5p, let-7g, miR-142-3p) were down-regulated significantly and one miRNA (miR-16) was up-regulated significantly on modSLA compared with SLA surfaces; however all of the differences were within the twofold threshold (Figure 5-4 E&F).

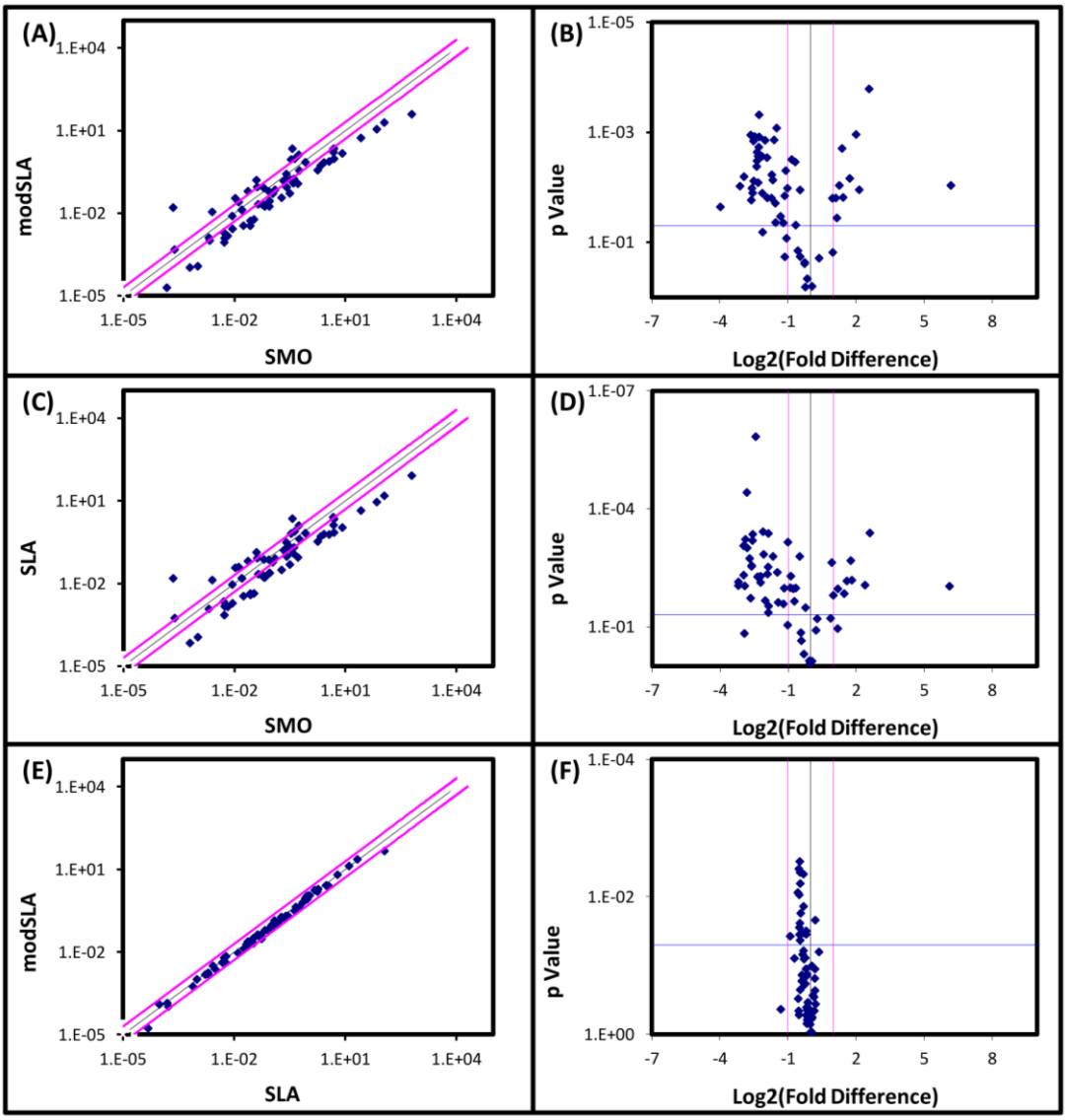

Figure 5-4: Relative miRNA expression profile of human osteoprogenitor cells on modSLA, SLA and SMO surfaces after 24 hours of culture: (A) relative expression – modSLA vs. SMO; (B) volcano plot – modSLA vs. SMO; (C) relative expression – SLA vs. SMO; (D) volcano plot – SLA vs. SMO; (E) relative expression – modSLA vs. SLA; (F) volcano plot – modSLA vs. SLA. The pink line indicates twofold change and the horizontal blue line in the graph indicates p-value = 0.05.

Table 5-2: miRNAs showing differential expression on different surfaces (modSLA, SLA and SMO) after 24 hours of culture. (A) miRNAs down-regulated on modified surfaces – modSLA and SLA when compared to SMO (fold change, p-value <0.05); and on modSLA compared to SLA (p-value <0.05); (B): miRNAs up-regulated on modified surfaces – modSLA and SLA when compared to SMO (fold change, p-value <0.05); and on modSLA compared to SLA. The miRNAs showing differential regulation either on modSLA or SLA (but not both) when compared with SMO are highlighted in italics.

(A) miRNAs down-regulated on modified surfaces – modSLA and SLA when compared to SMO.

miRNA ID	T-TEST p value	Fold Change modSLA/SMO	miRNA ID	T-TEST p value	Fold Change SLA/SMO	miRNA ID	T-TEST p value	Fold Change modSLA/SLA
miR-503	0.0229	-15.76	**miR-215**	0.0091	-9.18	**miR-18b**	0.0376	-1.86
miR-215	0.0096	-8.65	**miR-10b**	0.0073	-9.14	**miR-92a**	0.0087	-1.48
miR-10a	0.0064	-7.65	**miR-125b**	0.0009	-7.79	**miR-127-5p**	0.0039	-1.43
miR-125b	0.0011	-6.24	**miR-126**	0.0049	-7.78	**miR-185**	0.0094	-1.41
miR-1	0.0172	-6.12	**miR-16**	0.0009	-7.72	**miR-128**	0.0281	-1.41
miR-218	0.0104	-6.00	**miR-1**	0.0092	-7.53	**miR-103**	0.0356	-1.40
miR-10b	0.0127	-5.88	**miR-21**	0.0006	-7.38	**miR-142-3p**	0.0031	-1.39
miR-21	0.0014	-5.72	**miR-194**	0.0000	-7.06	**miR-301a**	0.0243	-1.39
miR-126	0.0077	-5.68	**miR-195**	0.0010	-7.00	**miR-345**	0.0044	-1.38
miR-16	0.0012	-5.55	**miR-218**	0.0018	-6.50	**miR-93**	0.0431	-1.38
miR-195	0.0042	-5.19	**miR-10a**	0.0189	-6.30	**let-7g**	0.0064	-1.37
miR-146b-5p	0.0033	-5.14	**miR-146b-5p**	0.0028	-6.10	**miR-106b**	0.0174	-1.35
miR-194	0.0023	-5.12	**miR-125a-5p**	0.0029	-6.10	**miR-17**	0.0339	-1.30
miR-7	0.0083	-4.98	**miR-100**	0.0006	-5.93	**miR-18a**	0.0047	-1.24
miR-192	0.0027	-4.97	**miR-137**	0.0004	-5.90	**miR-130a**	0.0138	-1.24
miR-99a	0.0019	-4.87	**miR-99a**	0.0000	-5.38	**miR-222**	0.0337	-1.22
miR-100	0.0005	-4.82	**miR-192**	0.0054	-5.09	**miR-22**	0.0314	-1.15
miR-125a-5p	0.0012	-4.81	**miR-146a**	0.0075	-4.64	**miR-424**	0.0353	-1.14
miR-137	0.0027	-4.42	**miR-155**	0.0052	-4.64			
miR-146a	0.0129	-4.38	**miR-23b**	0.0004	-4.31			
miR-424	0.0014	-4.02	**miR-424**	0.0015	-4.23			
miR-23b	0.0029	-3.79	**miR-20b**	0.0217	-4.03			
miR-20b	0.0156	-3.76	**miR-378**	0.0046	-3.75			
miR-155	0.0158	-3.30	**miR-132**	0.0030	-3.68			
miR-378	0.0060	-3.27	***let-7f***	0.0440	-3.66			
miR-20a	0.0074	-3.17	**miR-7**	0.0004	-3.65			
miR-132	0.0014	-3.05	**miR-26a**	0.0301	-3.63			
miR-17	0.0196	-2.93	**miR-20a**	0.0016	-3.17			
miR-26a	0.0440	-2.91	**miR-134**	0.0042	-2.78			
miR-134	0.0008	-2.82	**miR-17**	0.0242	-2.71			
miR-452	0.0340	-2.50	**miR-452**	0.0264	-2.31			
miR-214	0.0447	-2.30	**miR-24**	0.0106	-2.25			
miR-24	0.0144	-2.21						
miR-93	0.0050	-2.14						
miR-92a	0.0105	-2.03						

Table 5-2B: miRNAs up-regulated on modified surfaces – modSLA and SLA when compared to SMO.

(B) miRNA ID	T-TEST p value	Fold Change modSLA/SMO	miRNA ID	T-TEST p value	Fold Change SLA/SMO	miRNA ID	T-TEST p value	Fold Change modSLA/SLA
miR-33a	0.0093	72.89	**miR-33a**	0.0094	69.65	**miR-16**	0.0219	1.16
miR-222	0.0002	5.99	**miR-222**	0.0004	6.09			
miR-127-5p	0.0111	4.42	**miR-127-5p**	0.0088	5.26			
miR-15a	0.0011	4.01	**miR-210**	0.0066	3.51			
miR-210	0.0069	3.31	**miR-15a**	0.0021	3.40			
miR-130a	0.0154	2.70	**miR-18b**	0.0069	3.02			
let-7b	0.0020	2.62	**miR-130a**	0.0145	2.79			
miR-22	0.0093	2.41	**miR-22**	0.0109	2.29			
let-7i	0.0363	2.24	**miR-181a**	0.0160	2.00			
miR-181a	0.0157	2.16						

5.3.4 Target predictions for differentially regulated miRNAs

Target predictions for the differentially regulated miRNAs using the online tool, TargetScan [24], revealed several potential targets for these miRNAs. miR-215 and miR-125b were among the most highly down-regulated miRNAs on both the SLA and modSLA surfaces. Osteogenic genes like COL5A1, RUNX1, FOXN1, IGF1 were potential targets for miR-215. Similarly, TargetScan also predicted SCARB1, MAP2K7, VDR, NCOR2, BMPR1B, SEL1L, SMAD2, SMAD4, PPP2CA, COL4A3 genes as possible targets for miR-125b. The miRNAs, miR-503 and miR-214 were significantly down-regulated on modSLA surface, and not on SLA surface (fold change $\leq$-2.0, p-value <0.05). Notably, several potential osteogenic targets were identified for miR-503 (CCND2, CCND1, CCNE1, DIXDC1, BTRC, HIPK2, IGF1R, BMPR1A, WNT3A, VEGFA, WNT4, CCND3, IGF1, FOSL1, ACVR2A) and miR-214 (CBL, FGFR1, CTNNB1, SENP2, CDH11, NOTCH2, NBL1, RUNX1, KREMEN1). TargetScan also predicted a number of genes as potential targets for the up-regulated miRNAs and these were screened for key inhibitors of osteogenesis. Several inhibitors were found to be targets for the up-regulated miRNAs, e.g. miR-33a potentially targets CDK6, SMAD7, TWIST1 and miR-22 is predicted to target HDAC4.

Previous studies have reported that the TGFβ/BMP and the non-canonical Wnt/Ca^{2+} signaling pathways are involved in the process of differentiation on modSLA and SLA surfaces [2, 13, 15]. Therefore, we further explored whether genes of the TGFβ/BMP and non-canonical Wnt/Ca^{2+} pathway were among the predicted targets for the down-regulated miRNAs. The Kyoto Encyclopedia of Genes

and Genomes (KEGG) pathway database, which records networks of molecular interactions in cells [25] was used to extract the list of genes associated with the TGFβ/BMP and non-canonical Wnt/Ca^{2+} pathways. The list of predicted targets for the significantly down-regulated miRNAs was matched for the genes of these pathways. Several genes for both the TGFβ/BMP and non-canonical Wnt/Ca^{2+} pathways were identified as potential targets for the miRNAs. The KEGG pathway database enables visualizing cell signaling networks as wire diagrams linking related genes [26] and therefore we adapted the two pathway maps from the KEGG database and listed the miRNAs which may be potential targets for the genes of these pathways (Figure 5-5).

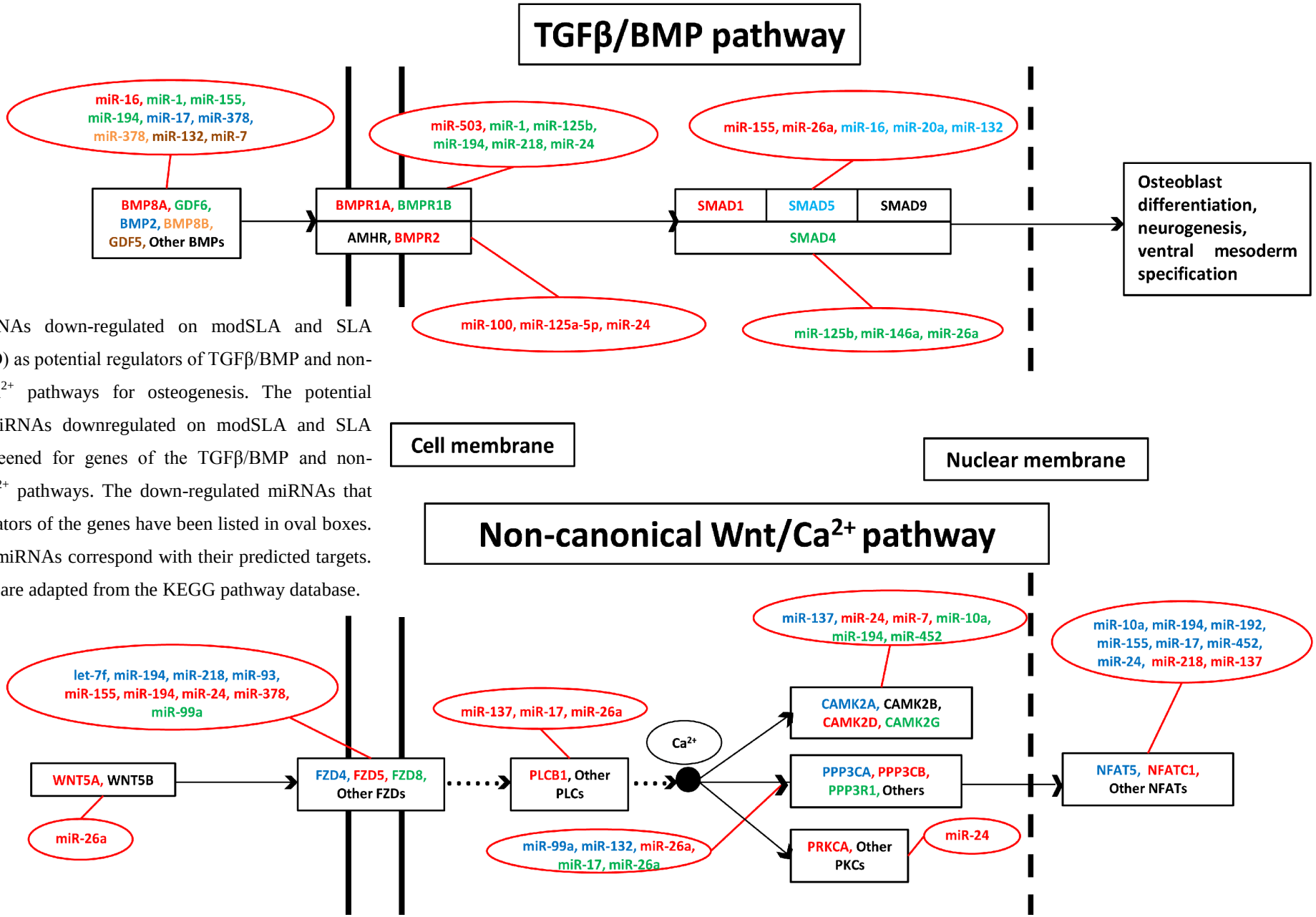

Figure 5-5: miRNAs down-regulated on modSLA and SLA (compared to SMO) as potential regulators of TGFβ/BMP and non-canonical Wnt/Ca^{2+} pathways for osteogenesis. The potential targets for the miRNAs downregulated on modSLA and SLA surfaces were screened for genes of the TGFβ/BMP and non-canonical Wnt/Ca^{2+} pathways. The down-regulated miRNAs that are potential regulators of the genes have been listed in oval boxes. The colors of the miRNAs correspond with their predicted targets. Pathway diagrams are adapted from the KEGG pathway database.

5.4 DISCUSSION

Topographically modified titanium implant surfaces have been found to have improved osteogenic properties [1]. It has also been shown that additional chemical modification resulting in increased hydrophilicity leads to improved osseointegration *in vivo* [4, 6] and osteogenic properties *in vitro* [8-11]. The modSLA and SLA surfaces have been shown to have augmented osteogenic lineage commitment and differentiation [27]. However, the biological mechanisms responsible for these findings are not well elucidated, with TGFβ/BMP and Wnt signaling both implicated [2, 13, 15]. Although *in vivo* studies of gene expression during the osseointegration of dental implants have shown that it involves a variety of overlapping biological processes including inflammation, osteogenesis, angiogenesis and neurogenesis [12, 17, 28], bone formation is the key phenotypic variable which is manipulated by surface modification, and hence the effect of titanium surface modification on osteoblasts and their progenitors has been the subject of considerable attention in the literature. To this end, the well characterized SLA surface has emerged as a widely used model that is believed to mimic the native microenvironment encountered by osteoprogenitor cells *in vivo*. It has been shown that cells differentiating in response to these substrates behave very differently compared with cells that are grown on culture plastic and are chemically differentiated using β-glycerophosphate/dexamethasone. Hence, these surfaces are not only useful as *in vitro* models of clinical relevance to dentistry and orthopedics, but can be used more generally as physiologically relevant substrates for the study of important biological mechanisms responsible for differentiation along the osteogenic lineage. In this study, we report on the influence of surface topography on the expression of miRNAs, which are a group of relatively novel molecules which are known to regulate gene expression, by osteoprogenitor cells.

Primary alveolar bone derived cells, rather than an engineered cell line, were used in this study in order to more closely replicate a physiologically relevant system. The osteogenic potential of the cells was confirmed by enhanced ALP expression and Alizarin Red S staining in response to osteogenic media. Furthermore, the responsiveness of the osteoprogenitor cells to the different implant surfaces was assessed in relation to the expression of a panel of genes (BMP2,

BMP6, ACVR1, FZD6, WNT5A, ITGB1 and ITGA2) that have been implicated as determinants of the response to surface modification [2, 13, 15]. More specifically, the TGFβ/BMP signaling pathway members BMP2, BMP6 and ACVR1 were all shown to have increased expression in osteoprogenitor cells using whole genome analysis [13]. Similarly, Olivares-Navarrete et al. [14] demonstrated the up-regulation of the non-canonical Wnt signaling pathway genes WNT5A and FZD6 by osteoblasts in response to SLA and modSLA. Finally, the integrin α2β1 has been suggested to play an important role in the early response to the modified titanium surfaces and our study also found increased expression of ITGB1 and ITGA2 following exposure to SLA and modSLA [29, 30]. The pattern of expression characterized by increased expression on modSLA, followed by SLA and SMO, is in agreement with previous reports, confirming that the response of these osteoprogenitor cells is consistent with the currently established literature.

MicroRNAs are known to influence the gene regulation pattern by translational repression and gene silencing [18]. We explored the pattern of expression of 88 micro-RNAs, known to be associated with stem cell differentiation, in well-characterized primary osteoprogenitor cells following 24 hours exposure to modSLA, SLA and SMO titanium surfaces. Several studies have shown that gene expression is regulated during the early response to modified surfaces, and as regulators of gene expression, the miRNA expression was assessed at this early time-point. A total of 31 miRNAs were seen to be significantly down-regulated and eight miRNAs were found to be up-regulated (beyond twofold change and p-value <0.05) on the modified surfaces compared with the polished titanium surfaces. Notably, only minor differences were observed on comparing the modSLA with SLA surface. This was consistent with the findings of a whole genome analysis comparing the response of similar primary osteoprogenitor cells to SMO, SLA and modSLA, whereby the magnitude of the difference between either SLA or modSLA and SMO were much greater than between SLA and modSLA [13].

Osteogenic differentiation has been reported to be regulated by miRNAs in various studies [22]. It is interesting to note that several miRNAs identified to be differentially regulated on the modified titanium surfaces correspond to findings in other studies investigating the effect of miRNAs on osteogenic differentiation. Mizuno et al. [31] showed that miR-125b inhibits osteogenic differentiation, and our

study also revealed critical down-regulation of this miRNA on modSLA and SLA surfaces. miR-16 has been found to be under-expressed in osteogenic differentiation [32]. This miRNA was observed to be significantly down-regulated (fold-change <-5.0) on the modified surfaces. miR-26a has been reported to target SMAD1, and osteogenic differentiation of human adipose tissue-derived stem cells (hADSCs) is enhanced upon inhibiting miR-26a [33]. miR-1 and miR-21 have been documented to regulate myogenic [34] and adipogenic [35] differentiation respectively. These were also observed to be under-expressed on modSLA and SLA surfaces. miR-218 was also seen to be down-regulated in our study. This miRNA potentially targets the RUNX2 gene; however, Zhang et al.'s study did not reveal a significant influence on osteogenic differentiation by this miRNA [36]. It is likely that a network of miRNAs work in synergy in order to influence the differentiation process.

Implant surfaces like titanium have been predicted to influence osteoblastic translational process [37]. Physical and chemical modifications of titanium surfaces have been shown to induce differential regulation of miRNAs in osteoblast-like cells [38, 39]. Palmieri et al. had demonstrated several miRNAs to be differentially regulated in osteoblast-like MG63 (human osteosarcoma cell line) when cultured on discs coated with nano-TiO_2 (anatase) on titanium surfaces and compared with machined grade 3 titanium, suggesting the molecular implications of surface micro- and nano-architecture [39]. The results of our study reveal the differential regulation of miRNAs as a consequence of modifications to surface chemistry and topography of titanium implants. miR-22, miR-93 and miR-17 were among the significantly down-regulated miRNAs when modSLA was compared with SLA and these miRNAs were also observed to be down-regulated in anatase treated titanium [39]. Further, miR-210 was up-regulated on both modSLA and SLA surfaces as seen on anatase-treated titanium surfaces [39].

The findings of this study are in line with previous reports showing the influence of titanium surface modification on the differential regulation of several genes related to early osteogenic differentiation [13, 40]. In particular, several genes of the TGFβ/BMP and non-canonical Wnt pathways were identified as likely targets of the miRNAs that were down-regulated in response to the modSLA and SLA surfaces. Key genes of the TGFβ/BMP pathway which are likely to be under the regulatory control of miRNAs are BMPs, BMPRs and SMADs (Figure 5-5). Several

genes of the non-canonical Wnt/Ca^{2+} pathway, like WNT5A, CAMK2 family and the NFAT family of transcription factors were also potential targets (Figure 5-5), further corroborating with Olivares-Navarrete et al.'s [14] finding that the non-canonical Wnt/Ca^{2+} signaling pathway plays an important role in osteoblast maturation on these surfaces.

In this present study, we identified a number of predicted target genes for the differentially regulated miRNAs which were associated with osteogenesis and in particular the TGFβ/BMP and non-canonical Wnt pathways. This finding corroborates previous reports showing that osteogenic genes are up-regulated on modified titanium surfaces [13, 14, 41]. Since these target genes are only predictions, these molecular mechanisms need to be validated with further studies.

5.5 CONCLUSION

This study shows that the expression profile of microRNAs in osteoprogenitor cells is influenced by the exposure to topographically (SLA) and chemically (modSLA) modified titanium surfaces. The majority of miRNAs were down-regulated in response to the SLA and modSLA surfaces compared to the smooth surfaces, with only relatively minor changes found between SLA and modSLA. These findings were consistent with the previous findings that surface modification can influence osteogenic differentiation *in vitro* and bone formation *in vivo*. Screening of the predicted gene targets for the differentially regulated miRNAs revealed several osteogenic genes as potential targets. Several genes of the TGFβ/BMP and non-canonical Wnt/Ca^{2+} pathway were predicted as targets for the down-regulated miRNAs. These results indicate that the expression of miRNAs influence the genetic mechanisms leading to osteogenic differentiation on modified titanium implant surfaces.

5.6 REFERENCES

[1] Wennerberg A, Albrektsson T. Effects of titanium surface topography on bone integration: a systematic review. Clin Oral Implants Res 2009;20:172-84.

[2] Wall I, Donos N, Carlqvist K, Jones F, Brett P. Modified titanium surfaces promote accelerated osteogenic differentiation of mesenchymal stromal cells in vitro. Bone 2009;45:17-26.

[3] Bagno A, Piovan A, Dettin M, Chiarion A, Brun P, Gambaretto R, et al. Human osteoblast-like cell adhesion on titanium substrates covalently functionalized with synthetic peptides. Bone 2007;40:693-9.

[4] Buser D, Broggini N, Wieland M, Schenk RK, Denzer AJ, Cochran DL, et al. Enhanced bone apposition to a chemically modified SLA titanium surface. J Dent Res 2004;83:529-33.

[5] Bosshardt DD, Salvi GE, Huynh-Ba G, Ivanovski S, Donos N, Lang NP. The role of bone debris in early healing adjacent to hydrophilic and hydrophobic implant surfaces in man. Clin Oral Implants Res 2011;22:357-64.

[6] Lang NP, Salvi GE, Huynh-Ba G, Ivanovski S, Donos N, Bosshardt DD. Early osseointegration to hydrophilic and hydrophobic implant surfaces in humans. Clin Oral Implants Res 2011;22:349-56.

[7] Abdel-Haq J, Karabuda CZ, Arisan V, Mutlu Z, Kurkcu M. Osseointegration and stability of a modified sand-blasted acid-etched implant: an experimental pilot study in sheep. Clin Oral Implants Res 2011;22: 265-74.

[8] Qu Z, Rausch-Fan X, Wieland M, Matejka M, Schedle A. The initial attachment and subsequent behavior regulation of osteoblasts by dental implant surface modification. J Biomed Mater Res A 2007;82A:658-68.

[9] Rausch-fan X, Qu Z, Wieland M, Matejka M, Schedle A. Differentiation and cytokine synthesis of human alveolar osteoblasts compared to osteoblast-like cells (MG63) in response to titanium surfaces. Dent Mater 2008;24:102-10.

[10] Zhao G, Raines AL, Wieland M, Schwartz Z, Boyan BD. Requirement for both micron- and submicron scale structure for synergistic responses of osteoblasts to substrate surface energy and topography. Biomaterials 2007;28:2821-9.

[11] Masaki C, Schneider GB, Zaharias R, Seabold D, Stanford C. Effects of implant surface microtopography on osteoblast gene expression. Clin Oral Implants Res 2005;16:650-6.

[12] Donos N, Hamlet S, Lang NP, Salvi GE, Huynh-Ba G, Bosshardt DD, et al. Gene expression profile of osseointegration of a hydrophilic compared with a hydrophobic microrough implant surface. Clin Oral Implants Res 2011;22:365-72.

[13] Vlacic-Zischke J, Hamlet SM, Friis T, Tonetti MS, Ivanovski S. The influence of surface microroughness and hydrophilicity of titanium on the up-regulation of TGF-beta/BMP signalling in osteoblasts. Biomaterials 2011;32:665-71.

[14] Olivares-Navarrete R, Hyzy SL, Hutton DL, Dunn GR, Appert C, Boyan BD, et al. Role of non-canonical Wnt signaling in osteoblast maturation on microstructured titanium surfaces. Acta Biomater 2011;7:2740-50.

[15] Olivares-Navarrete R, Hyzy SL, Park JH, Dunn GR, Haithcock DA, Wasilewski CE, et al. Mediation of osteogenic differentiation of human mesenchymal stem cells on titanium surfaces by a Wnt-integrin feedback loop. Biomaterials 2011;32:6399-411.

[16] Brett PM, Harle J, Salih V, Mihoc R, Olsen I, Jones FH, et al. Roughness response genes in osteoblasts. Bone 2004;35:124-33.

[17] Ivanovski S, Hamlet S, Salvi GE, Huynh-Ba G, Bosshardt DD, Lang NP, et al. Transcriptional profiling of osseointegration in humans. Clin Oral Implants Res 2011;22:373-81.

[18] Bartel DP. MicroRNAs: target recognition and regulatory functions. Cell 2009;136:215-33.

[19] Shivdasani RA. MicroRNAs: regulators of gene expression and cell differentiation. Blood 2006;108:3646-53.

[20] Xu P, Vernooy SY, Guo M, Hay BA. The Drosophila microRNA miR-14 suppresses cell death and is required for normal fat metabolism. Curr Biol 2003;13:790-5.

[21] Bentwich I, Avniel A, Karov Y, Aharonov R, Gilad S, Barad O, et al. Identification of hundreds of conserved and nonconserved human microRNAs. Nat Genet 2005;37:766-70.

[22] Hu R, Li H, Liu W, Yang L, Tan YF, Luo XH. Targeting miRNAs in osteoblast differentiation and bone formation. Expert Opin Ther Targets 2010;14:1109-20.

[23] Haase HR, Ivanovski S, Waters MJ, Bartold PM. Growth hormone regulates osteogenic marker mRNA expression in human periodontal fibroblasts and alveolar bone-derived cells. J Periodontal Res 2003;38:366-74.

[24] Lewis BP, Burge CB, Bartel DP. Conserved seed pairing, often flanked by adenosines, indicates that thousands of human genes are microRNA targets. Cell 2005;120:15-20.

[25] Kanehisa M, Goto S. KEGG: Kyoto encyclopedia of genes and genomes. Nucleic Acids Res 2000;28:27-30.

[26] Kanehisa M, Goto S, Hattori M, Aoki-Kinoshita KF, Itoh M, Kawashima S, et al. From genomics to chemical genomics: new developments in KEGG. Nucleic Acids Res 2006;34:D354-7.

[27] Khan MR, Donos N, Salih V, Brett PM. The enhanced modulation of key bone matrix components by modified Titanium implant surfaces. Bone 2012;50(1):1-8.

[28] Donos N, Retzepi M, Wall I, Hamlet S, Ivanovski S. In vivo gene expression profile of guided bone regeneration associated with a microrough titanium surface. Clin Oral Implants Res 2011;22:390-8.

[29] Rezania A, Healy KE. Integrin subunits responsible for adhesion of human osteoblast-like cells to biomimetic peptide surfaces. J Orthop Res 1999;17:615-23.

[30] Olivares-Navarrete R, Hyzy SL, Hutton DL, Erdman CP, Wieland M, Boyan BD, et al. Direct and indirect effects of microstructured titanium substrates on the

induction of mesenchymal stem cell differentiation towards the osteoblast lineage. Biomaterials 2010;31:2728-35.

[31] Mizuno Y, Yagi K, Tokuzawa Y, Kanesaki-Yatsuka Y, Suda T, Katagiri T, et al. miR-125b inhibits osteoblastic differentiation by down-regulation of cell proliferation. Biochem Biophys Res Commun 2008;368:267-72.

[32] Gao J, Yang T, Han J, Yan K, Qiu X, Zhou Y, et al. MicroRNA expression during osteogenic differentiation of human multipotent mesenchymal stromal cells from bone marrow. J Cell Biochem 2011;112:1844-56.

[33] Luzi E, Marini F, Sala SC, Tognarini I, Galli G, Brandi ML. Osteogenic differentiation of human adipose tissue-derived stem cells is modulated by the miR-26a targeting of the SMAD1 transcription factor. J Bone Miner Res 2008;23:287-95.

[34] Chen JF, Mandel EM, Thomson JM, Wu Q, Callis TE, Hammond SM, et al. The role of microRNA-1 and microRNA-133 in skeletal muscle proliferation and differentiation. Nat Genet 2006;38:228-33.

[35] Kim YJ, Hwang SJ, Bae YC, Jung JS. MiR-21 regulates adipogenic differentiation through the modulation of TGF-beta signaling in mesenchymal stem cells derived from human adipose tissue. Stem Cells, 2009;27:3093-102.

[36] Zhang Y, Xie RL, Croce CM, Stein JL, Lian JB, van Wijnen AJ, et al. A program of microRNAs controls osteogenic lineage progression by targeting transcription factor Runx2. Proc Natl Acad Sci U S A 2011;108:9863-8.

[37] Palmieri A, Pezzetti F, Avantaggiato A, Lo Muzio L, Scarano A, Rubini C, et al. Titanium acts on osteoblast translational process. J Oral Implantol 2008;34:190-5.

[38] Palmieri A, Pezzetti F, Brunelli G, Arlotti M, Lo Muzio L, Scarano A, et al. Anatase nanosurface regulates microRNAs. J Craniofac Surg 2008;19:328-33.

[39] Palmieri A, Brunelli G, Guerzoni L, Lo Muzio L, Scarano A, Rubini C, et al. Comparison between titanium and anatase miRNAs regulation. Nanomedicine 2007;3:138-43.

[40] Zhao G, Schwartz Z, Wieland M, Rupp F, Geis-Gerstorfer J, Cochran DL, et al. High surface energy enhances cell response to titanium substrate microstructure. J Biomed Mater Res A 2005;74A:49-58.

[41] Schwartz Z, Olivares-Navarrete R, Wieland M, Cochran DL, Boyan BD. Mechanisms regulating increased production of osteoprotegerin by osteoblasts cultured on microstructured titanium surfaces. Biomaterials 2009;30:3390-6.

5.7 ACKNOWLEDGEMENTS

Dr. Nishant Chakravorty is supported by QUT scholarship. The modSLA, SLA, and SMO discs were supplied by Institut Straumann. This project is partly supported by the ITI foundation. We thank Dr. Anna Taubenberger for helping us with the AFM visualization of the discs.

Chapter 6: Activation of cell signaling pathways on modified titanium surfaces

Pro-osteogenic topographical cues promote early activation of osteoprogenitor differentiation via enhanced TGFβ, Wnt, and Notch signaling

Nishant Chakravorty, Stephen Hamlet, Anjali Jaiprakash, Ross Crawford,
Adekunle Oloyede, Mohammed Alfarsi, Yin Xiao & Saso Ivanovski

(Published manuscript)

Citation: *Chakravorty N, Hamlet S, Jaiprakash A, Crawford R, Oloyede A, Alfarsi M, Xiao Y, Ivanovski S. Pro-osteogenic topographical cues promote early activation of osteoprogenitor differentiation via enhanced TGFβ, Wnt, and Notch signaling. Clin Oral Implants Res 2014;25:475-86.*

Suggested Statement of Contribution of Co-Authors for Thesis by Publication

Contributors	Statement of contribution
Nishant Chakravorty	Involved in the conception and design of the project. Performed laboratory experiments and wrote the manuscript.
Stephen Hamlet	Assisted in materials and data acquisition, analysis and critiquing the manuscript.
Anjali Jaiprakash	Assisted in experiments and critiquing the manuscript.
Ross Crawford	Involved in the conception and design of the project and critiquing the manuscript.
Adekunle Oloyede	Involved in the conception and design of the project and critiquing the manuscript.
Mohammed Alfarsi	Assisted in data acquisition, analysis and critiquing the manuscript.
Yin Xiao	Involved in the conception and design of the project, manuscript preparation and reviewing.
Saso Ivanovski	Involved in the conception and design of the project, manuscript preparation and reviewing.

Principal Supervisor Confirmation

I have sighted email or other correspondence from all co-authors confirming their certifying authorship

Prof. Yin Xiao		**10th July, 2014**
Name	**Signature**	**Date**

Abstract

Objectives: Titanium implants surfaces with modified topographies have improved osteogenic properties *in vivo*. However, the molecular mechanisms remain obscure. This study explored the signaling pathways responsible for the pro-osteogenic properties of micro-roughened (SLA) and chemically/nanostructurally (modSLA) modified titanium surfaces on human alveolar bone-derived osteoprogenitor cells (BCs) *in vitro*.

Materials & Methods: The activation of stem-cell signaling pathways (TGFβ/BMP, Wnt, FGF, Hedgehog, Notch) was investigated following early exposure (24 and 72 hours) of BCs to SLA and modSLA surfaces in the absence of osteogenic cell culture supplements.

Results: Key regulatory genes from the TGFβ/BMP (TGFBR2, BMPR2, BMPR1B, ACVR1B, SMAD1, SMAD5), Wnt (Wnt/β-catenin and Wnt/Ca^{2+}) (FZD1, FZD3, FZD5, LRP5, NFATC1, NFATC2, NFATC4, PYGO2, LEF1) and Notch (NOTCH1, NOTCH2, NOTCH4, PSEN1, PSEN2, PSENEN) pathways were upregulated on the modified surfaces. These findings correlated with a higher expression of osteogenic markers bone sialoprotein (IBSP) and osteocalcin (BGLAP), and bone differentiation factors BMP2, BMP6, and GDF15, as observed on the modified surfaces.

Conclusions: These findings demonstrate that the activation of the pro-osteogenic cell signaling pathways by modSLA and SLA surfaces leads to enhanced osteogenic differentiation as evidenced after 7 and 14 days culture in osteogenic media and provide a mechanistic insight into the superior osseointegration on the modified surfaces observed *in vivo*.

6.1 INTRODUCTION

The clinical success of implants depends on their osteogenic and osseointegrative properties. A number of studies have addressed the importance of the physical and chemical properties of the titanium implant surface in the phenotypic and functional regulation of osteoblast cells (Galli et al. 2012). Topographically modified titanium implant surfaces, such as the sand-blasted, large grit, acid-etched (SLA) titanium surface, and the chemically modified form of SLA (modSLA), have been shown to improve osteogenic properties, which lead to accelerated osseointegration and reduced healing times (Buser et al. 1991, 1999, 2004; Roccuzzo et al. 2001; Bornstein et al. 2008; Lai et al. 2009; Bosshardt et al. 2011; Donos et al. 2011b; Lang et al. 2011). Both SLA and modSLA surfaces exhibit a micro-roughened topography, while recent reports suggest that the modSLA surface also has a nano-structured topography (Wennerberg et al. 2011; Wennerberg et al. 2013). The modSLA and SLA surfaces have been widely utilized to study the interaction of modified titanium implants with osteogenic cells and have been shown to enhance osteoblastic differentiation compared to smooth surfaces (Schwartz et al. 2001; Brett et al. 2004; Wieland et al. 2005; Zinger et al. 2005; Zhao et al. 2007; Olivares-Navarrete et al. 2011a,b; Vlacic-Zischke et al. 2011). As such, these surfaces represent a valuable model for the study of the cellular and molecular mechanisms of osteoblastic differentiation that may more closely replicate physiological responses compared to commonly utilized *in vitro* models incorporating chemically induced osteogenic differentiation.

The suitability of the micro-environment to promote osteogenic differentiation is crucial for appropriate osseointegration *in vivo*. However, the molecular mechanisms leading to the enhanced osteogenic differentiation following exposure to the SLA and modSLA surfaces are not fully elucidated. Several whole transcriptome profiling studies have revealed a differential gene expression profile of osteoprogenitor cells between 3 hours and 72 hours (Brett et al. 2004; Wall et al. 2009; Vlacic-Zischke et al. 2011) of exposure to modSLA and SLA compared to smooth surfaces, suggesting that topographically induced cues exert an early influence on biological mechanisms that ultimately lead to enhanced osseointegration. Therefore, determining the early response of osteoprogenitor cells

to topographical cues is critical for understanding the cascade of events that ultimately leads to enhanced differentiation.

Several signaling proteins and pathways are known to be important in the regulation of osteogenesis. The interplay and crosstalk between cell signaling pathways like TGFβ/BMP, Wnt, Notch (Zamurovic et al. 2004), Hedgehog (St-Jacques et al. 1999; Mak et al. 2006) and FGF (Tsutsumi et al. 2001; Ito et al. 2008) guides osteogenic differentiation of progenitor cells. Recent studies have shown that both TGFβ/BMP and Wnt signaling are activated during *in vivo* guided bone regeneration (Ivanovski et al. 2011b) and are involved in the osteogenic response to SLA and modSLA surfaces (Donos et al. 2011b; Ivanovski et al. 2011a; Olivares-Navarrete et al. 2011b; Vlacic-Zischke et al. 2011). The aim of the present study was to investigate the effect of pro-osteogenic topographical cues from modified titanium surfaces on the early response of key cell signaling pathways (TGFβ, Wnt, FGF, Notch, Hedgehog) that are important in regulating osteoprogenitor differentiation.

6.2 MATERIALS AND METHODS

6.2.1 Titanium discs

All titanium discs used in this study were manufactured from Grade II commercially pure titanium (15 mm in diameter, 1 mm in thickness) and supplied by Institut Straumann (Basel, Switzerland). SLA surfaces were prepared by blasting the surface with 250-500 µm corundum grit and acid etching with a hot solution of hydrochloric/sulfuric acids. The modSLA surface was obtained by rinsing SLA discs under N_2 protection and storage in isotonic saline solution at pH 4-6. This treatment has been shown to generate a chemically modified hydrophilic surface with reduced carbon surface contamination (Hamlet et al. 2012). Smooth/polished (SMO) titanium discs were used as the control surface for the study.

6.2.2 Surface imaging

The surface topography of the three titanium surfaces, modSLA, SLA, and SMO, was analyzed by scanning electron microscopy (SEM) (FEI Quanta 3D Focused Ion Beam SEM) and atomic force microscopy (AFM) (BMT Multiscan AFM, Karlsruher, Germany). The modSLA surfaces were removed from the isotonic saline solution, washed with deionised water and dried with a jet of argon gas for imaging using SEM and AFM. SEM imaging was performed in high vacuum

conditions using the Everhart-Thornley Detector. AFM imaging of the surfaces was performed in tapping mode using silicon AFM probes with a natural frequency of 300 kHz at a scan rate of 0.2 Hz (Innovative Solutions Bulgaria Ltd., Sofia, Bulgaria). High-resolution thermal field emission scanning electron microscopy (JSM-7001F, Joel, French's Forest, NSW, Australia) was used to assess the nano-structure of the surfaces.

6.2.3 Cell culture

Primary alveolar bone derived osteoprogenitor cell (BCs) obtained from three healthy human volunteers were used for the study. These cells were established after culturing redundant tissues obtained following third molar extraction surgery using methods described previously (Haase et al. 2003; Xiao et al. 2003, 2004). The BCs were seeded at a density of 5×10^4 cells/titanium disc placed in 24 well tissue culture plates (BD Falcon, North Ryde, NSW, Australia), and incubated at 37 °C in a 5% CO_2 atmosphere in Dulbecco's modified Eagle's medium (DMEM) (Invitrogen, Mt Waverley, VIC, Australia) supplemented with fetal bovine serum (FBS) (Thermo, In Vitro Technologies, Nobel Park, Vic., Australia) and antibiotics (100 U/ml penicillin/100 μg/ml streptomycin).

6.2.4 Cell morphology

The morphology of osteoblastic cells on the modSLA, SLA, and SMO was studied using SEM. Cells were cultured in complete expansion media on the different surfaces for 24 hours and 72 hours as described above. After 24 and 72 hours of culture, the media was removed and the cells were fixed with 2% glutaraldehyde in 0.1M sodium cacodylate buffer overnight. The samples were subsequently washed with 0.1M sodium cacodylate buffer for 10 minutes, and post-fixed with 1% osmium tetroxide for 1 hour. The samples were then washed with distilled water twice (10 minutes each time) and gradually dehydrated in ethanol with increasing concentration (50%, 70%, 90%, and 100%). Finally, the samples were dried using critical point drying apparatus. To view the fixed cells with SEM they were coated with gold using a gold sputter coater. SEM imaging was performed under high vacuum as described previously (Mao et al. 2009).

6.2.5 RNA isolation and osteogenic gene expression pattern

Total RNA was extracted using an Ambion RNAqueous kit (GeneWorks, Thebarton, SA, Australia) as per the manufacturer's instructions, and RNA concentrations were assessed using a Nanodrop spectrometer (Thermo Scientific, Scoresby, Vic., Australia). Expression of the osteogenic genes bone sialoprotein (IBSP) and osteocalcin (BGLAP) was evaluated and compared between the modSLA, SLA, and SMO surfaces after exposing the cells to the titanium discs for 1, 3, 7 and 28 days. cDNA was prepared from 100 ng RNA template using the DyNAmo^{TM} cDNA Synthesis Kit (Finnzymes Oy., Vantaa, Finland) according to the manufacturer's protocol. The expression pattern of bone morphogenetic proteins, BMP2, BMP6, and GDF15, was also assessed at 24 and 72 hours. Taqman primers and probes were purchased from Applied Biosystems (Assay on demand, Applied Biosystems, Mulgrave, Vic., Australia). Quantitative real time PCR (qRT-PCR) reactions were performed using ABI Prism 7000 Sequence Detection System (Applied Biosystems) using TaqMan® Universal PCR Master Mix (Invitrogen Australia Pty Limited, Vic., Australia). The reactions were incubated at 50 °C for 2 min, followed by 10 min at 95 °C to activate the polymerase, and subsequently at 95 °C (15 seconds) and 60 °C (for 1 minute) for 40 cycles.

6.2.6 Gene expression profiling for stem cell signaling pathways

The expression profile of 84 key genes involved in signal transduction pathways for maintenance and differentiation of immature cell types (TGFβ, Wnt, FGF, Notch, and Hedgehog) was assessed using the Human Stem Cell Signaling PCR Array (SABiosciences, Frederick, MD, USA). The full list of genes included on this array is available at http://www.sabiosciences.com/rt_pcr_product/HTML/PAHS-047A.html. cDNA was prepared from 100 ng RNA templates by reverse transcription using the RT^2 First Strand Kit (SABiosciences) according to the manufacturer's protocol and our previous work (Liu et al. 2009; Mareddy et al. 2010). Quantitative real time PCR (qPCR) reactions were performed using the ABI Prism 7900HT Sequence Detection System (Applied Biosystems). The reactions were incubated at 95 °C for 10 minutes for one cycle, and then 95 °C (15 seconds), 60 °C (for 1 minute) for 40 cycles. PCR reactions were validated by observing the presence of a single peak in the dissociation curve analysis. The endogenous reference genes used to normalize the calculations by comparative Ct (Cycle of

threshold) value method were β-2-microglobulin (B2M), hypoxanthine phosphoribosyltransferase 1 (HPRT1), ribosomal protein L13a (RPL13A), glyceraldehyde-3-phosphate-dehydrogenase (GAPDH), and β-actin (ACTB).

6.2.7 Alizarin Red S staining and Calcium assay

Extracellular matrix deposition on the titanium surfaces after culturing cells in osteogenic media (standard media supplemented with 100 nM dexamethasone, 0.2 mM L-ascorbic acid, and 10 mM β-glycerophosphate) was assessed using Alizarin Red S staining. Briefly, after 7 and 14 days of culture, the media was removed and the cells were washed with PBS. The cells were then fixed using 4% paraformaldehyde and subsequently stained with 1% Alizarin Red S solution. Excess Alizarin Red stain was washed with ultrapure water; the samples were allowed to dry and then imaged with a Leica M125 stereo microscope (Leica Microsystems GmbH, Wetzlar, Germany). The Alizarin Red S staining was further assessed semi-quantitatively using a colorimetric technique (Gregory et al. 2004). Briefly, the samples were incubated in 10% acetic acid for 30 minutes, mixed with mineral oil, and heated to 85 °C for 10 minutes and immediately transferred to ice. They were subsequently centrifuged, mixed with 10% ammonium hydroxide and the absorbance was measured at 405 nm. To quantify the calcium content after 7 and 14 days of culture in osteogenic media, calcium was extracted by incubating the samples in 0.6N hydrochloric acid overnight and subsequently quantified using the Quantichrome^{TM} calcium assay kit (Gentaur Belgium BVBA, Kampenhout, Belgium) according to the manufacturer's protocol (Han et al. 2012). The absorbance was measured at 612 nm.

6.2.8 Statistical analysis

The relative levels of expression of mRNAs were compared between the cells cultured on modSLA, SLA, and SMO titanium discs using the Student's *t*-test. The critical value for significance was set at $p<0.05$. The ΔC_T value was obtained by subtracting the average Ct value of the endogenous references selected from the test mRNA Ct value of the same samples. The $\Delta\Delta C_T$ was determined by subtracting the ΔC_T of the control sample from the ΔC_T of the target sample. The relative mRNA quantification of the target gene was calculated by $2^{-\Delta\Delta CT}$. Downregulated mRNA values were calculated as the negative reciprocal of the $2^{-\Delta\Delta CT}$ score. The Ct values for each biological replicate were considered for analysis. Only the genes which

showed statistically significant difference in the level of expression on the surfaces for all the patients were considered as positive results.

6.3 RESULTS

6.3.1 Surface analysis

The micro-textured structure of modSLA and SLA surfaces was clearly demonstrated on the SEM images (Figure 6-1a-c). No significant difference in the micro-topographical level architecture was observed when the modSLA surface was compared with the SLA surfaces. Micro-scale irregularities ranging between 3 and 5 µm were commonly observed on both modSLA and SLA surfaces. These pit-shaped irregularities are the likely result of the sand-blasting procedure. The SMO surfaces exhibited a smooth architecture and do not show any micro-scale irregularities. The main topographical difference between the modSLA and SLA surfaces was the presence of nano-structures on the modSLA surface which could be detected using high-magnification SEM images. Clearly defined nano-structures were visible only on the modSLA surfaces, while SLA and SMO surfaces were devoid of any nano-scale features (Figure 6-1d-i).

Atomic force microscopy measurements of the surfaces also demonstrated similar micro-scale morphology on the modSLA and SLA, but not the SMO surface (Figure 6-2a-c). The BMT Multiscan AFM has the potential to scan z-axis deviations close to 50 µm. It revealed varying degrees of roughness on the modSLA and SLA surfaces (some peaks >±3 µm), but essentially they demonstrated very similar structural features. The root mean square (rms) roughness for both modSLA and SLA showed wide variations (0.8 µm-2 µm), due to the limitation in the total area that could be scanned with AFM. The z-axis visualization of the SMO surface did not show any sharp peaks. The rms roughness for the SMO surface ranged between 0.006 and 0.015 µm.

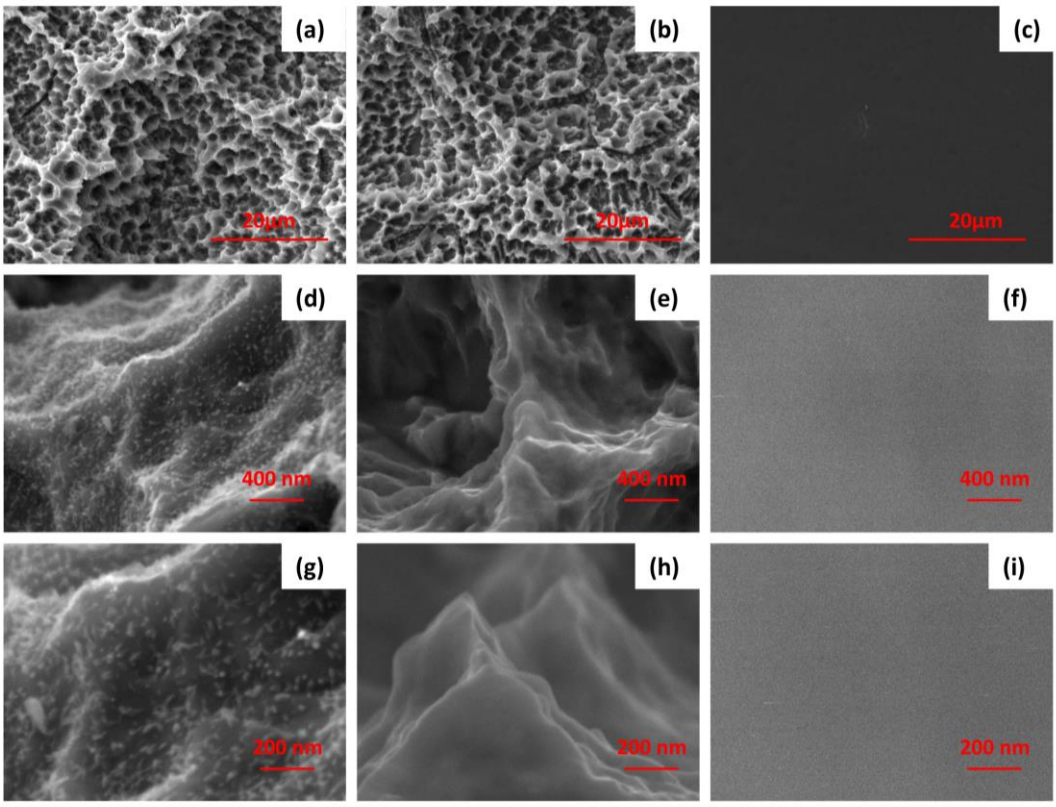

Figure 6-1: Scanning electron microscope (SEM) images of (a) modSLA; (b) SLA; (c) SMO (Magnification-5,000x) showing micro-rough topography of modSLA and SLA surfaces; (d-i): SEM images at 50,000x magnification [(d) modSLA; (e) SLA; (f) SMO], and 100,000x [(g) modSLA; (h) SLA; (i) SMO] showing the presence of nano-structures only modSLA surfaces.

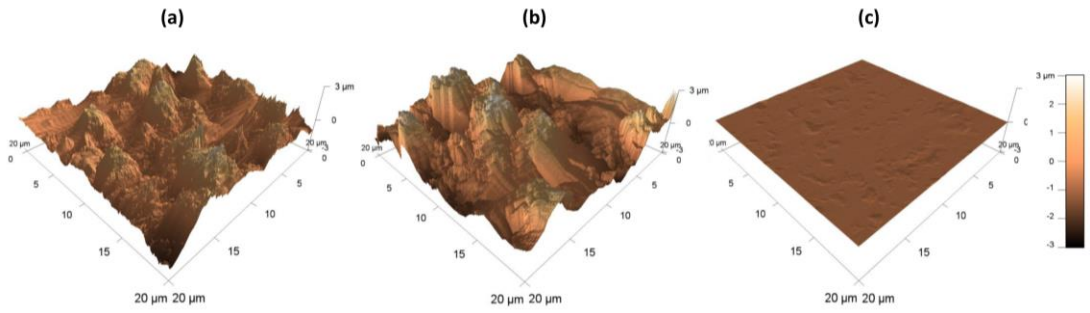

Figure 6-2: Atomic force microscopy images of (a) modSLA, (b) SLA, and (c) SMO.

6.3.2 Cell morphology on the discs

Cellular morphology was significantly different between the micro-roughened (SLA and modSLA) surfaces compared with the smooth surface. Cells showed a more flattened morphology on the SMO surface when compared with the modSLA

and SLA surfaces at both 24 and 72 hours. In comparison with the SMO surface, the cells on the SLA and modSLA surfaces showed a more elevated appearance with cellular processes extending to the pits and the neighbouring cells. The cells exhibited more surface granules on the modSLA and SLA discs, possibly due to increased protein secretion in response to these surfaces. The granules and processes on the cells were seen to increase between 24 hours and 72 hours (Figure 6-3).

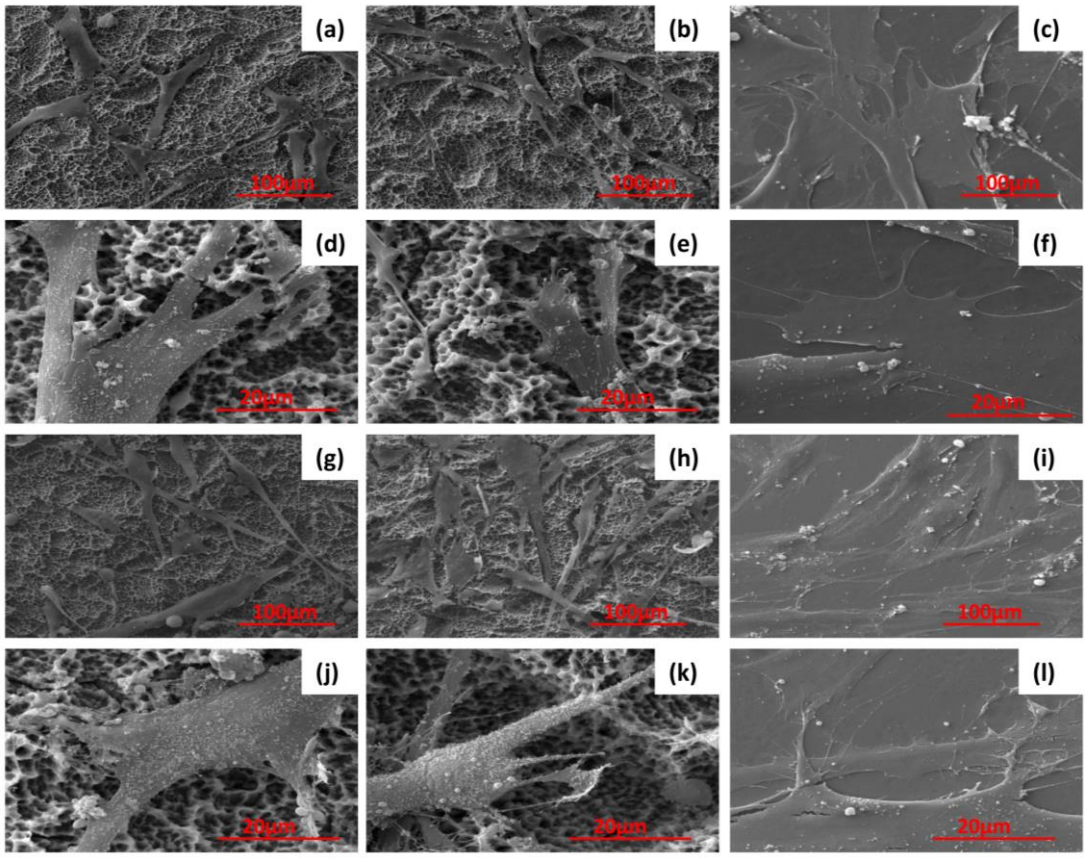

Figure 6-3: Cell morphology on modSLA, SLA, and SMO. Scanning electron microscope (SEM) images of human alveolar bone-derived cells on (a) modSLA-24h (Magnification-800x); (b) SLA-24h (Magnification-800x); (c) SMO-24h (Magnification-800x); (d) modSLA-24h (Magnification-5000x); (e) SLA-24h (Magnification-5000x); (f) SMO-24h (Magnification-5000x); (g) modSLA-72h (Magnification-800x); (h) SLA-72h (Magnification-800x); (i) SMO-72h (Magnification-800x); (j) modSLA-72h (Magnification-5000x); (k) SLA-72h (Magnification-5000x); (l) SMO-72h (Magnification-5000x).

6.3.3 Signaling pathways

A total of 84 key genes involved in major signal transduction pathways (Fibroblast Growth Factor (FGF), Hedgehog, Notch, TGFβ, and Wnt) were assessed. The expression of these genes on the three surfaces (modSLA, SLA, and SMO) was compared at two early time-points (24 and 72 hours). Furthermore, the relative

expression of genes for each type of disc at 72 hours was compared with the expression at 24 hours.

Twenty-four hours comparison

A total of 16 genes were found to be significantly upregulated ($p<0.05$) on the modSLA, and 17 genes on the SLA surface compared to the SMO surface (Table 6-1). No genes were downregulated between the modified surfaces and the smooth surface. Several genes of the Wnt, Notch, and TGFβ pathways showed significantly higher expression on these surfaces after 24 hours of exposure, with the majority of the upregulated molecules belonging to the Wnt signaling pathway (7/16 on modSLA and 9/17 on SLA). Furthermore, TGFβ signaling (4/16 and 2/17 upregulated genes on modSLA and SLA, respectively) and Notch signaling (4/16 and 5/17 upregulated genes on modSLA and SLA, respectively) were also activated on the modified surfaces after 24 hours. Only one gene (TCF7) showed increased expression on the modSLA compared to the SLA surface (Table 6-1). NFATC2 (Wnt pathway) showed the highest fold change (FC=9.03) when modSLA was compared with SMO (p-value=0.05). Indeed, NFATC2 also showed the highest fold change (8.23) (p-value=0.01) on the SLA surface (compared with SMO).

Seventy-two hours comparison

Ten genes were significantly upregulated on the modSLA surface and 18 genes on the SLA surface. Similar to the trend at 24 hours, the modSLA and SLA surfaces showed increased expression of genes of the Wnt (5/10 on modSLA and 4/18 on SLA), Notch (4/10 on modSLA and 6/18 on SLA), and TGFβ (1/10 on modSLA and 6/18 on SLA) pathways. Only genes PSENEN (Notch) and SMAD3 (TGFβ) were observed to be significantly downregulated on the modSLA compared with the SLA surface (Table 6-1). FZD9 (Wnt pathway) was the gene showing the highest statistically significant ($p<0.05$) fold change on modSLA (FC=3.77) and SLA (FC= 2.87).

Table 6-1: Cell signaling pathway genes showing statistically significant difference in expression pattern of human alveolar bone derived cells on modSLA, SLA, and SMO titanium surfaces after 24 hours and 72 hours of culture (n=3).

modSLA vs SMO 24 h			modSLA vs SMO 72 h			SLA vs SMO 24 h			SLA vs SMO 72 h			modSLA vs SLA 24 hrs			modSLA vs SLA 72 h		
Gene symbol	p-value	Fold-change	Gene symbol	p-value	Fold-change	Gene symbol	p-value	Fold-change	Gene symbol	p-value	Fold-change	Gene symbol	p-value	Fold-change	Gene symbol	p-value	Fold-change
TGFβ/BMP pathway																	
ACVR1B	0.011	1.76	TGFBR2	0.041	1.49	BMPR2	0.047	1.51	ACVRL1	0.013	1.47				SMAD3	0.043	-1.24
BMPR2	0.015	1.56				TGFBR2	0.036	1.33	ENG	0.016	1.62						
LTBP3	0.029	1.89							SMAD3	0.027	1.41						
SMAD1	0.030	1.68							SMAD6	0.001	2.85						
									TGFBR2	0.014	1.48						
									TGFBR3	0.004	1.44						
Wnt pathway																	
FZD1	0.043	1.83	FZD6	0.030	1.55	FZD1	0.003	1.84	FZD1	0.026	1.54	TCF7	0.010	2.24			
LEF1	0.018	1.96	FZD9	0.041	3.77	FZD3	0.017	2.90	FZD8	0.039	1.83						
LRP5	0.022	1.69	NFATC1	0.027	2.29	FZD5	0.002	2.38	FZD9	0.010	2.87						
NFATC1	0.007	3.22	NFATC4	0.033	1.80	LRP5	0.016	1.49	PYGO2	0.044	2.23						
NFATC2	0.005	9.03	PYGO2	0.012	2.89	NFATC1	0.015	2.14									
NFATC4	0.008	2.77				NFATC2	0.012	8.23									
PYGO2	0.005	3.50				NFATC3	0.035	1.18									
TCF7	0.003	2.47				PYGO2	0.042	3.42									
						VANGL2	0.045	2.67									
Notch pathway																	
NOTCH2	0.011	1.48	NOTCH1	0.031	2.36	NOTCH4	0.005	2.26	NOTCH1	0.019	2.59				PSENEN	0.010	-1.42
PSEN1	0.031	1.87	NOTCH2	0.033	1.57	PSEN1	0.003	1.93	NOTCH2	0.027	1.60						
PSEN2	0.012	2.07	PSEN1	0.011	1.88	PSEN2	0.001	2.15	NOTCH4	0.035	1.62						
PSENEN	0.040	2.01	PSENEN	0.005	1.78	PSENEN	0.007	1.86	PSEN1	0.012	1.84						
						RBPJL	0.01	2.36	PSEN2	0.005	2.22						
									PSENEN	0.001	2.53						
FGF pathway																	
						CDX2	0.018	3.18									
Pluripotency Maintenance Pathway																	
IL6ST	0.023	1.51							IL6ST	0.021	1.59						
									LIFR	0.024	1.83						

Seventy-two hours vs. twenty-four hours comparison

The relative expression of genes on the modSLA, SLA, and SMO discs was compared between the two time-points (72 hours vs. 24 hours) (Table 6-2). Most of the genes (7 on modSLA, 8 on SLA, and 10 on SMO) were significantly down regulated at 72 hours when compared with 24 hours. Only two genes (SMAD3 on SLA and CXD2 on SMO) were upregulated at 72 hours. Three of the seven genes (ACVR1, BMPR2, SMAD1) downregulated on modSLA were part of the TGFβ superfamily, two (TCF7, BCL9L) belonged to the Wnt pathway and one (NOTCH2) to the Notch pathway. The genes that were downregulated on SLA included members of the TGFβ (2 of 8) (BMPR2, SMAD7), Wnt (4 of 8) (FZD1, LEF1, NFATC2, NFATC3) and Notch (1 of 8) (NOTCH4) pathways. Five of the 10 genes (ACVR1, BMPR1B, ENG, SMAD7, TGFBR3) differentially regulated on SMO were from the TGFβ pathway, three from the Wnt (FZD1, NFATC2, BCL9L), one (NOTCH3) from Notch. TCF7 and NFATC2, both from the Wnt pathway, were the most significantly downregulated on modSLA and SLA surfaces respectively at 72 hours (-4.77 and -5.51, respectively).

Table 6-2: Cell signaling pathway genes showing statistically significant difference in expression pattern of human alveolar bone derived cells at 72 hours (compared with 24 hours) on modSLA, SLA, and SMO titanium surfaces after 24 hours and 72 hours of culture (n=3).

modSLA: 72 h vs 24 h			SLA: 72 h vs 24 h			SMO: 72 h vs 24 h		
Gene symbol	p-value	Fold-change	Gene symbol	p-value	Fold-change	Gene symbol	p-value	Fold-change
TGFβ/BMP pathway								
ACVR1	0.025	-1.98	BMPR2	0.024	-1.54	ACVR1	0.018	-1.99
BMPR2	0.024	-1.74	SMAD3	0.045	1.61	BMPR1B	0.002	-2.16
SMAD1	0.012	-2.04	SMAD7	0.013	-3.28	ENG	0.009	-1.52
						SMAD7	0.002	-3.03
						TGFBR3	0.034	-1.25
Wnt pathway								
TCF7	0.005	-4.77	FZD1	0.004	-1.77	FZD1	0.023	-1.49
BCL9L	0.029	-1.86	LEF1	0.024	-2.17	NFATC2	0.043	-2.13
			NFATC2	0.017	-5.51	BCL9L	0.028	-1.88
			NFATC3	0.032	-1.49			
Notch pathway								
NOTCH2	0.036	-1.36	NOTCH4	0.027	-1.63	NOTCH3	0.044	-3.08
FGF pathway								
						CDX2	0.034	2.56
Pluripotency Maintenance Pathway								
IL6ST	0.019	-1.62						

Notch, Wnt, and TGFβ/BMP pathway

Notch, Wnt, and TGFβ pathway molecules were observed to be consistently upregulated on modSLA and SLA surfaces at both time-points. Figure 6-4 highlights the expression pattern of some of the key differentially regulated genes of the TGFβ (TGFBR2, BMPR2, BMPR1B, ACVR1B, SMAD1, and SMAD5), Wnt (FZD1, FZD3, FZD5, LRP5, NFATC1, NFATC2, NFATC4, PYGO2, and LEF1), and Notch pathways (NOTCH1, NOTCH2, NOTCH4, PSEN1, PSEN2 and PSENEN). Most of

the genes showed similar trends (expression on modSLA≥SLA>SMO). When modSLA was compared with SLA, very few genes showed statistically significant changes, although there was a general trend for higher expression associated with modSLA.

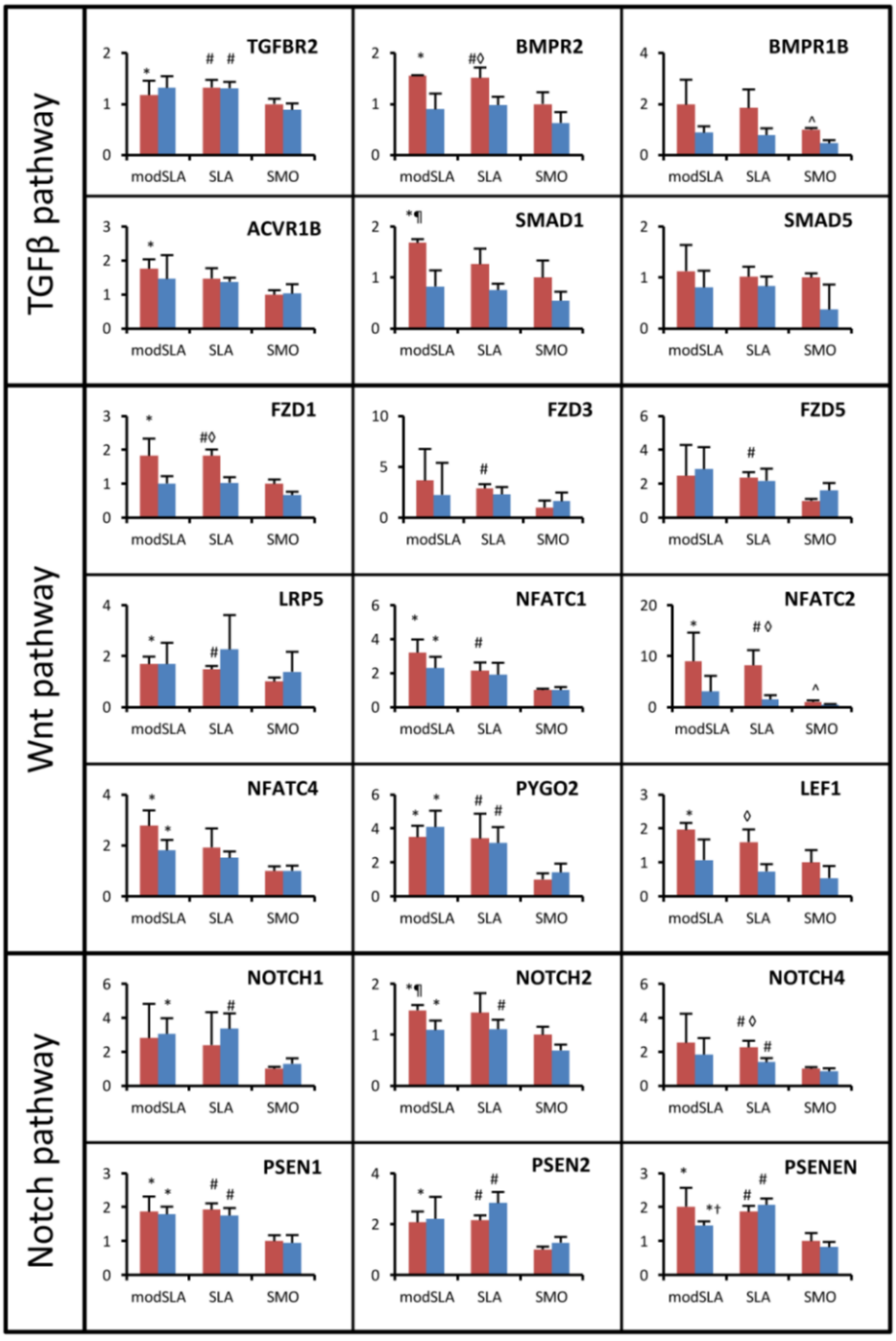

Figure 6-4: Relative gene expression profile of key genes of TGFβ, Wnt, and Notch pathways on modSLA, SLA, and SMO titanium surfaces (Fold changes to SMO Day 1; *: p<0.05, modSLA vs. SMO; #: p<0.05, SLA vs. SMO; †: p-value<0.05, modSLA vs. SLA; ¶: p<0.05 modSLA 24 hours vs. 72 hours; ◊: p<0.05, SLA 24 hours vs. 72 hours; ^: p<0.05, SMO 24 hours vs. 72 hours). (■ 24 hours ■ 72 hours).

Notch signaling

The Human Stem Cell Signaling PCR array contains 9 genes of the Notch pathway (8 receptors/co-receptors and 1 transcription factor). Four of the nine genes of the Notch pathway were upregulated on the modSLA surface at each time-point. The SLA surface showed upregulation of 5/9 genes of the Notch pathway at 24 hours and 6/9 genes at 72 hours. The Notch pathway receptor/co-receptor genes that were upregulated on modSLA were as follows: NOTCH2, PSEN1, PSENEN (both at 24 and 72 hours); PSEN2 (at 24 hours); and NOTCH1 (at 72 hours). The receptor/co-receptor genes (Notch pathway) highly expressed on SLA surface were as follows: PSEN1, PSEN2, PSENEN (both at 24 and 72 hours); NOTCH4 (at 24 hours); NOTCH1, NOTCH2, NOTCH4 (at 72 hours). The transcription factor RBPJL was seen to be upregulated only on the SLA surface (compared with SMO) at 24 hours.

Wnt signaling

The Human Stem Cell Signaling PCR array contains 25 genes of the Wnt pathway (12 receptors and 13 transcription factors and co-factors). The transcription factors of the Wnt signaling molecules that showed increased expression on modSLA were as follows: NFATC1, NFATC4, PYGO2 (both at 24 and 72 hours); LEF1 and TCF7 (at 24 hours). The receptors upregulated on modSLA were FZD1, LRP5 (at 24 hours), FZD6, and FZD9 (at 72 hours). Wnt molecules upregulated on the SLA surface both at 24 and 72 hours were as follows: FZD1 (receptor) and PYGO2. The genes upregulated only at 24 hours were as follows: FZD3, FZD5, LRP5, VANGL2 (receptors); NFATC1, NFATC2, NFATC3 (transcription factors/co-factors). The co-receptors FZD8 and FZD9 were upregulated on SLA at 72 hours.

TGFβ signaling pathway

The array used for this study included 20 receptors (and co-receptors) and 15 transcription factors (and co-factors) of the TGFβ superfamily. A number of genes of the TGFβ/BMP pathway were upregulated on the modified surfaces: the receptors/co-receptors ACVR1B, BMPR2, LTBP3 (upregulated on modSLA at 24 hours); BMPR2 (upregulated on SLA at 24 hours); ACVRL1, ENG, TGFBR3 (upregulated on SLA at 72 hours), TGFBR2 (upregulated on modSLA and SLA at 24 hours and on SLA at 72 hours), and the transcription factors and co-factors SMAD1 (upregulated on modSLA at 24 hours), SMAD3 and SMAD6 (upregulated on SLA at

72 hours). Only three genes were seen to be differentially regulated when modSLA was compared with SLA (TCF7 was upregulated on modSLA at 24 hours, and PSENEN and SMAD were downregulated on modSLA at 72 hours).

6.3.4 Mineralization properties and osteogenesis associated gene expression

Higher Alizarin Red S staining and calcium deposition was observed on the modSLA and SLA surfaces compared with the SMO surface (modSLA>SLA>SMO) at days 7 and 14 (Figure 6-5a-e) following culture in osteogenic media.

The temporal expression pattern of the osteogenesis-associated genes IBSP and BGLAP on the three surfaces was assessed after 1, 3, 7, and 28 days of culture in standard expansion media (Figure 6-5f-g). IBSP showed significant increase in gene expression on the modified titanium surfaces (modSLA and SLA) with increasing time. There was a higher expression of IBSP on the modSLA and SLA compared with the SMO surfaces at each time-point (Figure 6-5f). The relative expression of BGLAP was also observed to be higher on the modSLA and SLA compared with SMO surfaces (especially at days 7 and 28 days) (Figure 6-5g). The expression of the bone morphogenetic proteins, BMP2 and BMP6, was also higher on the modSLA and SLA compared with the SMO surfaces, and the expression was higher at 24 hours compared with 72 hours on all surfaces (Figure 6-6), pointing to a role of BMPs in stimulating osteogenic differentiation of progenitor cells in the early phase of differentiation. The expression of GDF15 did not vary greatly between the surfaces or over time, although significantly higher expression was noted on modSLA at 72 hours.

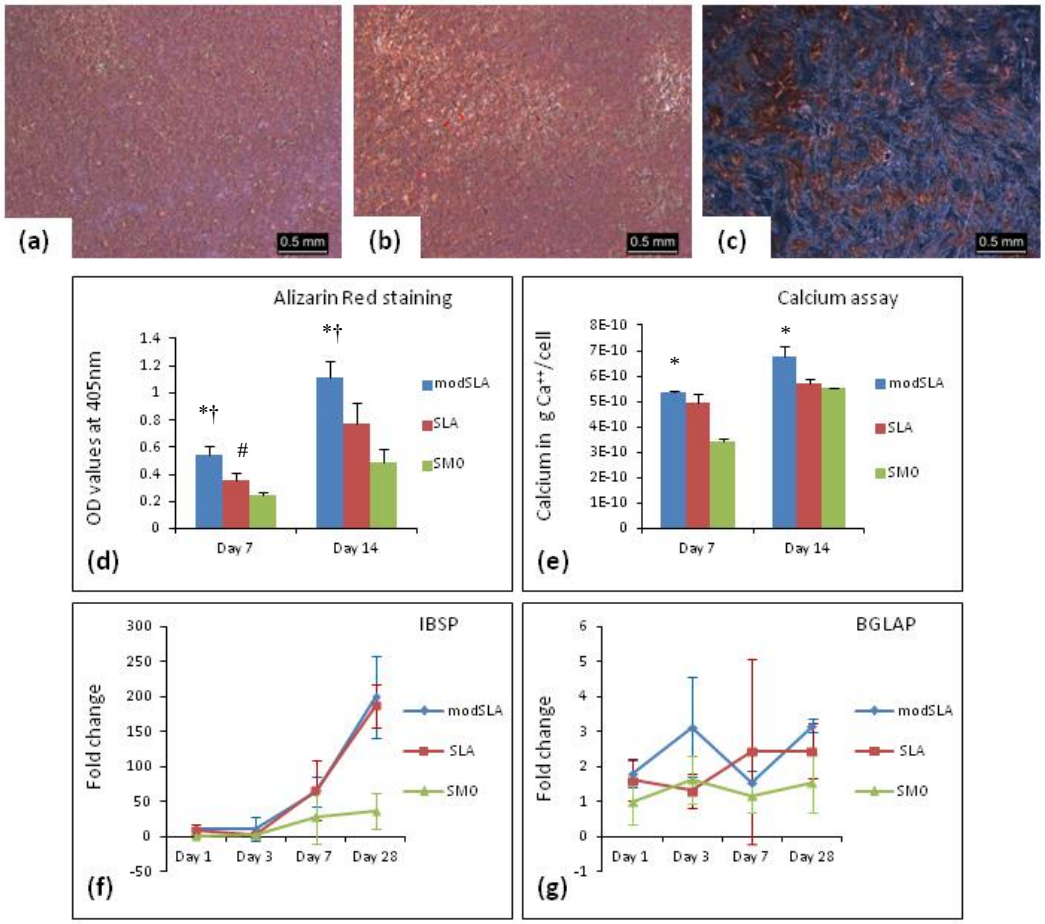

Figure 6-5: Osteogenic properties of modSLA and SLA surfaces. (a, b, c) Alizarin Red S staining after 14 days of culture in osteogenic media on (a) modSLA, (b) SLA, and (c) SMO showing higher mineralization on modSLA and SLA surfaces compared with SMO. (d) Quantification of Alizarin Red S staining on modSLA, SLA, and SMO surfaces after 7 and 14 days of culture in osteogenic media. (e) Calcium assay after 7 and 14 days of culture in osteogenic media on modSLA, SLA, and SMO surfaces showing calcium levels (modSLA>SLA>SMO). (*: p<0.05, modSLA vs. SMO; #: p<0.05, SLA vs. SMO; †: p<0.05, modSLA vs. SLA). (f) & (g) Temporal gene expression (IBSP and BGLAP) profile on modSLA, SLA, and SMO surfaces after 1, 3, 7, and 28 days of culture in complete expansion media (fold changes relative to SMO day 1) showing higher expression of genes on modSLA and SLA surfaces. p-value < 0.05 for following pairs: IBSP – modSLA vs. SMO (Day 1, 3 and 28); SLA vs. SMO (Day 1 and 28); modSLA (Day 28 vs. Day 1 & Day 3; Day 7 vs. Day 3 & Day 1); SLA (Day 28 vs. Day 1, 3 & 7; Day 7 vs. Day 3 & 1) BGLAP – modSLA (Day 28 vs. Day 7 & 1).

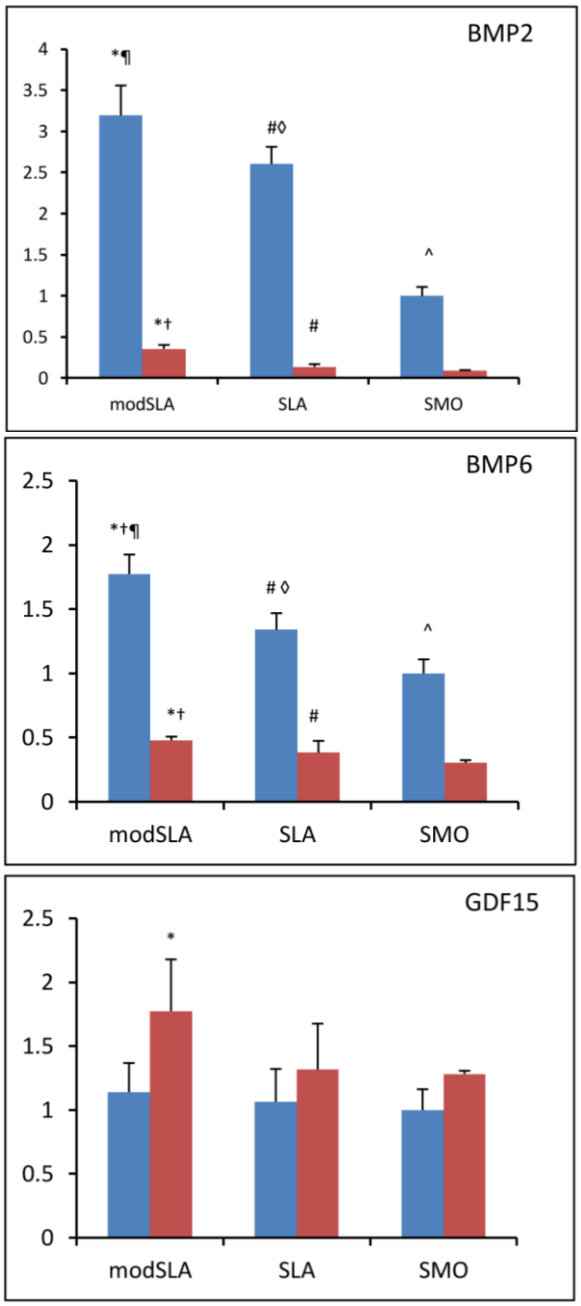

Figure 6-6: Relative gene expression profile (BMP2-Bone morphogenetic protein-2, BMP6-Bone morphogenetic protein-6, GDF15-Growth differentiation factor 15) of human alveolar bone derived cells on modSLA, SLA, and SMO titanium surfaces after 24 and 72 hours of culture (n=3). (*: $p<0.05$, modSLA vs. SMO; #: $p<0.05$, SLA vs. SMO; †: $p<0.05$, modSLA vs. SLA, ¶: $p<0.05$ modSLA 24 hours vs. 72 hours; ◊: $p<0.05$, SLA 24 hours vs. 72 hours; ^: $p<0.05$, SMO 24 hours vs. 72 hours) (■ 72 hours ■ 24 hours).

6.4 DISCUSSION

Osteogenic differentiation is a process guided by activation and interaction of several cell signaling pathways (Lin & Hankenson 2011), namely TGFβ/BMP, Wnt, Notch (Zamurovic et al. 2004), Hedgehog (St-Jacques et al. 1999; Mak et al. 2006),

and FGF (Tsutsumi et al. 2001; Ito et al. 2008). These pathways are known to interact, but the precise nature of these interactions during osteogenic differentiation is unknown. *In vitro* osteogenic differentiation studies traditionally used to study cell and molecular mechanisms usually incorporate chemical mediators like β-glycerophosphate, dexamethasone, and L-ascorbic acid into the culture media. However, the *in vivo* environment is not accurately replicated with this chemical method. Micro-roughened implant surfaces provide a favorable osteogenic environment and influence the differentiation potential of progenitor cells (Bagno et al. 2007). The well characterized SLA surface has emerged as a widely used model that is believed to mimic the microenvironment encountered by osteoblast cells *in vivo,* and hence represents an alternative, physiologically relevant model for studying osteogenic differentiation. The use of the modSLA surface in clinical dentistry has further reduced healing time associated with dental implants (Buser et al. 2004; Lang et al. 2011), and it has been shown to promote biological mechanisms associated with osteogenesis in both *in vitro* and *in vivo* studies (Buser et al. 1991, 2004; Donos et al. 2011a; Vlacic-Zischke et al. 2011). This surface is manufactured and stored under conditions resulting in a hydrophilic surface with reduced surface contamination. In this study, we found that this surface has a nano-structured topography, which is in agreement with a recent report of spontaneous nanostructure formation on the modSLA surface (Wennerberg et al. 2013).

This study aimed to determine the effects of the pro-osteogenic environment created by modified titanium surfaces (modSLA and SLA) on the expression of cell signaling pathways during the early exposure of primary human BCs. The mRNA expression for several genes of the Wnt, Notch, and TGFβ/BMP, but not FGF or Hedgehog, signaling pathways was modulated by the titanium surface modification. These findings are supported by previous reports that have suggested that the TGFβ/BMP and Wnt signaling pathways are triggered early in the interaction between osteoblasts and implant surfaces (Wall et al. 2009; Ivanovski et al. 2011a; Olivares-Navarrete et al. 2011a; Vlacic-Zischke et al. 2011). A novel finding of the study is that Notch is an additional pathway that is triggered early in the response to these surfaces. TGFβ/BMP, Wnt, and Notch pathways have been known to be key cell signaling pathways involved in the process of osteogenesis (Zamurovic et al.

2004) and *in vivo* bone formation and healing (Ivanovski et al. 2011a,b), and these findings are in agreement with our observations.

The Notch pathway associated presenilin molecules (PSEN1 and PSEN2), and Presenilin enhancer 2 (PSENEN) were constantly upregulated on both of the modified implant surfaces at both time-points. Presenilin molecules form part of the γ-secretase complex that is involved in the cleavage of Notch receptors (Taniguchi et al. 2002; Hemming et al. 2008), and the PSENEN product is a regulatory component of that complex (Kaether et al. 2006). Presenilin knockout models have demonstrated the importance of these genes in the signal transduction of the Notch pathway (Donoviel et al. 1999; Herreman et al. 1999). The Notch receptors, NOTCH1, NOTCH2 and NOTCH4 were also upregulated on these surfaces at both time points. Notch signaling is not only known to be important for osteogenic differentiation, but has also been shown to be instrumental for both BMP2-induced osteoblast differentiation and BMP signaling itself (Nobta et al. 2005). Given that we have previously demonstrated that SLA and modSLA surfaces induce BMP2 secretion (Vlacic-Zischke et al. 2011), it is likely that activation of the Notch pathway enables the coordination of other pathways leading to osteogenic differentiation.

The results from this study revealed increased expression of transcription factors of the Wnt pathway, NFATC1, NFATC2, NFATC3, and NFATC4. These belong to the nuclear factor of activated T-cells (NFAT) family of transcription factors (Crabtree & Olson 2002). The NFAT transcriptional activation is prompted by stimulation of calcineurin via Wnt molecules such as WNT5A (Saneyoshi et al. 2002). Interestingly, there was no differential regulation of the key molecule of the canonical Wnt signaling pathway, CTNNB1. This finding is in agreement with previous studies using the SLA and modSLA surfaces, which demonstrated the activation of the non-canonical calcium-dependent Wnt pathway (Olivares-Navarrete et al. 2010a; Olivares-Navarrete et al. 2011a,b). We also observed the upregulation of several receptors of the frizzled family: FZD1, FZD3, FZD5, FZD6, FZD8, and FZD9. As in the case of canonical Wnt signaling, the non-canonical Wnt ligands signal through the frizzled family of receptors; however, this is independent of the LRP5 and LRP6 co-receptors (Seifert & Mlodzik 2007; Slusarski & Pelegri 2007). We did find upregulation of the LRP5 co-receptor on both the modSLA and SLA surfaces at 24 hours; however, the Ct values were particularly high, and hence, the

significance of this finding is questionable. LRP6 did not show a significant increase in expression in response to the modified surfaces, and therefore, it is unclear whether there is any activation/inhibition of the canonical Wnt signaling pathway. Olivares-Navarrete et al.'s work in 2010 indicated that the canonical Wnt signaling pathway is important in the early phase of osteo-differentiation, whereas the non-canonical Wnt/Ca^{2+} pathway is critical in the later stages of differentiation on modSLA and SLA surfaces (Olivares-Navarrete et al. 2010b). However, their later study in 2011 (Olivares-Navarrete et al. 2011a) showed that the canonical Wnt signaling does not play a role in osteogenic differentiation on micro-structured surfaces. Wang et al.'s recent work (Wang et al. 2012) discusses the activation of the canonical Wnt/β-catenin pathway and not the non-canonical pathway as an important regulator of osteogenic differentiation on micropitted/nanotubular titanium surfaces. These observations could possibly be attributed to the time-points (day 3 and day 7) for their study.

The TGFβ/BMP pathway activation was manifested through upregulation of the receptors BMPR2 and TGFBR2 at 24 hours on both modSLA and SLA. Vlacic et al's whole genome microarray based study (2011) showed upregulation of several genes of the TGFβ/BMP following 72 hours of *in vitro* culture on the modSLA and SLA surfaces. Our recent work describing the microRNA expression profiles on modSLA and SLA surfaces explored the possibility of potential regulation of the TGFβ/BMP and Wnt/Ca^{2+} pathways on these surfaces (Chakravorty et al. 2012). The coordinated stimulation of TGFβ, Wnt, and the Notch pathways on the modified titanium implant surface is possibly responsible for their improved osteogenic and osseointegration properties. Based on the results of the study, we summarized the cascade of molecular events (Figure 6-7) to illustrate the interactions between these pathways leading to the upregulation of osteogenic transcription factors like Runt-related transcription factor 2 (Runx2) and osterix (Osx). The activation of the three signaling pathways (TGFβ, Wnt and Notch) is synchronized with each other, leading to a condition prone to osteogenesis. The immediate interaction of BCs with the topographically modified titanium implant surfaces stimulates them to over-express ligands and receptors for these pathways and this initiates the downstream chain of events. The increased expression of ligands BMP2, BMP6, and GDF15 at 24 hours, described in this study strengthens the findings we previously reported (increased

expression of ligands BMP2, BMP6 and WNT5A) (Chakravorty et al. 2012). Binding of the ligands with their receptors directs the activation of downstream mediators. Therefore, switching-on the TGFβ/BMP pathway leads to activation of the receptor-regulated SMADs (R-SMADs) that along with the common-mediator SMAD (co-SMAD) translocate into the nucleus. Similarly, the canonical Wnt/β-catenin activation causes translocation of the active de-phosphorylated form of β-catenin into the nucleus. Concerted activity of the TGFβ/BMP and canonical Wnt/β-catenin cascade leads to activation of Runx2 (Lin & Hankenson 2011). The non-canonical Wnt/Ca^{2+} pathway causes activation of the Nuclear factor of activated T-cells (NFATs) molecules which conglomerates with another transcription factor, osterix (Osx) (Koga et al. 2005), that in turn is under the regulation of Runx2. Notch pathway is known to induce Osx expression (Engin et al. 2008). The subsequent inter-play between the osteogenic transcription factors eventually leads to osteogenic differentiation and osseointegration.

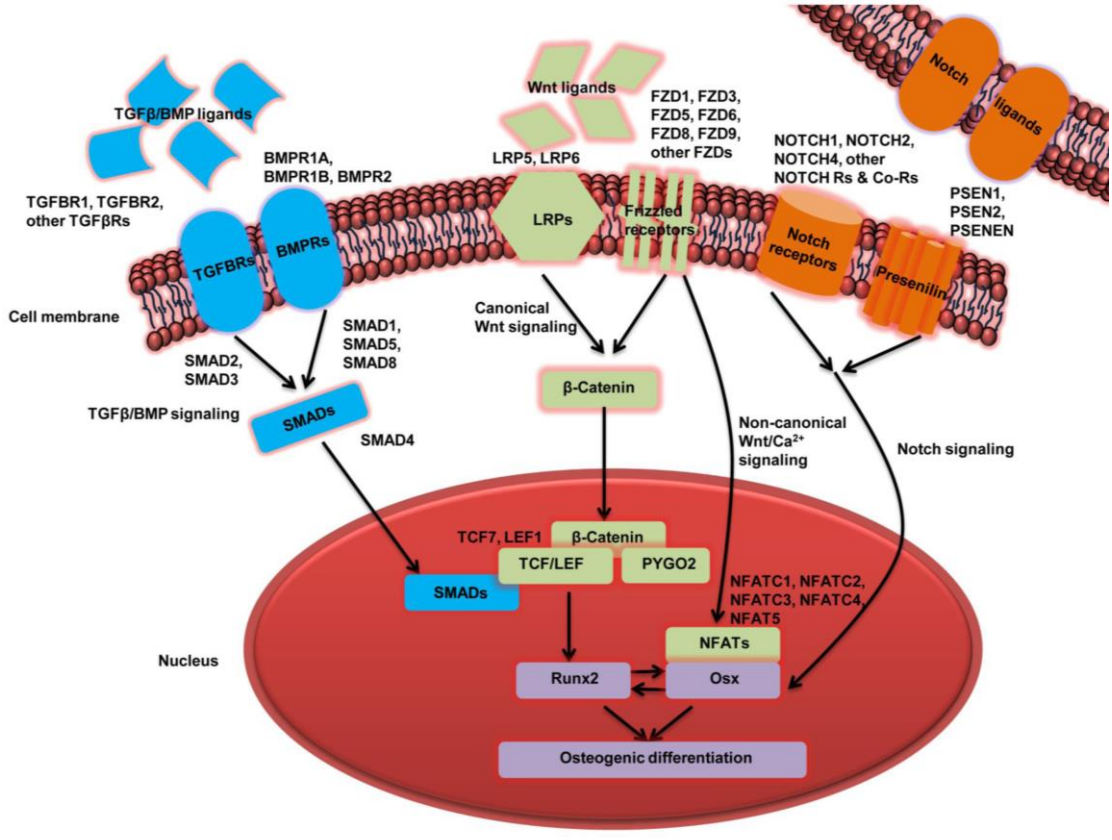

Figure 6-7: Schematic diagram representing the inter-relationship and cross-talk between TGFβ/BMP, Wnt, and Notch signaling pathways, that leads to osteogenic differentiation on the modified titanium implant surfaces (modSLA and SLA).

Comparison of the gene expression pattern on the different discs between the two time-points illustrated the importance of the early cellular response to topographical cues. The majority of the genes showing differential expression between 72 and 24 hours were downregulated at 72 hours. This suggests that the early activation of the cell signaling pathways on titanium surfaces occurs within the first 24 hours. The gene expression of TGFβ/BMP receptors like BMPR2, BMPR1B, and TGFBR3 was downregulated on all surfaces at 72 hours, possibly as a consequence of negative feedback control of gene expression due to translational repression. Translational repression has been shown to be more efficient in controlling the sequence of gene expression (Swain 2004), and our observations could be the result of the temporal feedback. The NFATC molecules (NFATC2 and NFATC3) were also shown to be downregulated at 72 hours compared to 24 hours, possibly indicating early modulation of the Wnt/Ca^{2+} signaling cascade on the implant surfaces. The downregulation of the Notch pathway was reflected in decreased receptor gene expression (NOTCH2 on modSLA and NOTCH4 on the SLA surface). It is noteworthy that these same receptors were seen to be upregulated on the surfaces at 24 hours (also at 72 hours when compared with SMO surfaces). Although the differentially regulated genes on the modified surfaces were upregulated at 72 hours when compared to the control, the relatively lower expression at 72 hours (when compared to 24 hours) provides insight into the temporal sequence of the gene expression associated with osteogenic differentiation in response to surface micro-roughness.

The osteogenic influence of the modified surfaces was demonstrated by confirming the upregulation of the osteogenic markers, integrin-binding sialoprotein (IBSP) and osteocalcin (BGLAP) at 24 and 72 hours, compared with smooth surfaces. Furthermore, we also showed that the modified surfaces stimulated the expression of the pro-osteogenic differentiation factors BMP2, BMP6, and GDF15, in keeping with previous reports (Vlacic-Zischke et al. 2011). The mineralization potential of modSLA and SLA surfaces was confirmed by earlier and higher Alizarin Red S staining and calcium content, as well as changes in osteoblast cell morphology in the form of increased cellular processes and secretory granules. These findings demonstrate that the activation of the pro-osteogenic cell signaling pathways by modSLA and SLA surfaces leads to enhanced osteogenic differentiation and matrix

mineralization and provide mechanistic insight into the superior osseointegration on the modSLA and SLA surfaces that is observed *in vivo*. The correlation between the accelerated expression of the TGFβ/BMP, Wnt, and Notch signaling pathways and the superior osteogenic properties of modSLA and SLA surfaces, as described in this study, emphasize the importance of these signaling pathways in bone formation, and therefore, modulation of these pathways using chemical and biological modulators may result in improved bone formation in demanding clinical conditions.

This study also showed that the vast majority of the statistically significant changes in gene expression were found in the comparison of both modSLA and SLA with SMO, but not between SLA and modSLA. This suggests that surface micro-roughness, common to both SLA and modSLA, rather than the distinguishing features of modSLA (nano-roughness, hydrophilicity, reduced surface contamination), is predominantly responsible for promoting osteogenic differentiation. Further, it implies that hydrophilicity may accelerate clinical osseointegration by also influencing biological mechanisms other than those directly associated with osteogenesis, such as indirectly promoting bone formation via an immunomodulatory effect on the inflammatory response (Hamlet et al. 2012).

6.5 CONCLUSIONS

The results of the study show that the pro-osteogenic cues of the modSLA and SLA surfaces promote the early activation of TGFβ/BMP, Wnt (especially the Wnt/Ca^{2+} pathway), and Notch pathways, which are likely to be responsible for the subsequent accelerated differentiation of the osteoprogenitor cells. The differences in the gene expression pattern between the modSLA and SLA surfaces were subtle, indicating that the surface micro-roughness feature that is common to both surfaces is primarily responsible for the activation of TGFβ/BMP, Wnt, and Notch pathways early in the process of osteogenic differentiation.

6.6 SUPPLEMENTARY MATERIAL

The expression pattern of keys genes involved in signal transduction on modSLA and SLA surfaces were compared with the control SMO surfaces at each time-point (24 hours and 72 hours). Expression patterns were also compared between modSLA and SLA surfaces (Figure 6-8 and 6-9). Furthermore, the relative

expression of genes for each type of disc at 72 hours was compared with the expression at 24 hours (Figure 6-10).

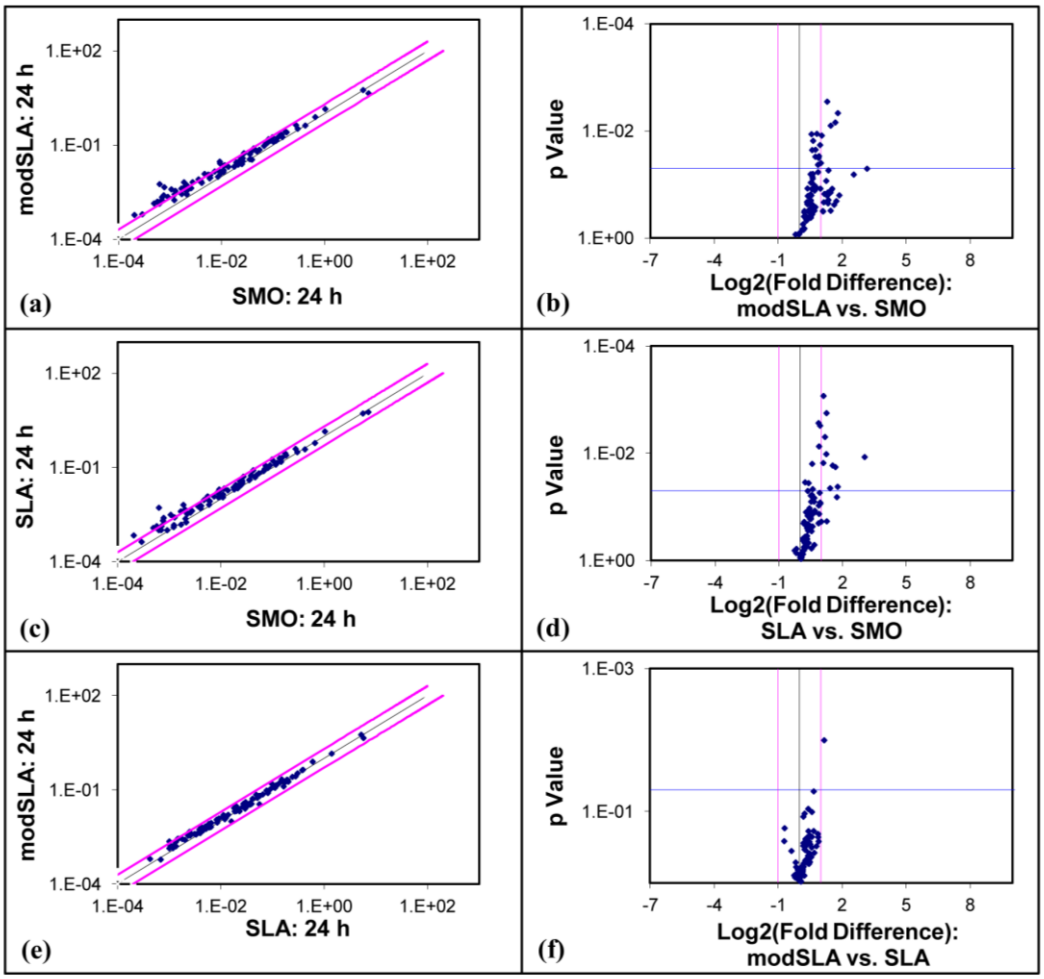

Figure 6-8: Relative gene expression profile of human alveolar bone derived cells on modSLA, SLA, and smooth (polished) (SMO) titanium surfaces after 24 hours of culture. (a: Relative expression on modSLA vs. SMO; b: Volcano plot – modSLA vs. SMO; c: Relative expression on SLA vs. SMO; d: Volcano plot – SLA vs. SMO; e: Relative expression on modSLA vs. SLA; f: Volcano plot – modSLA vs. SLA. The black line indicates a fold change of 1, pink line indicates 2 fold change and the horizontal blue line in the graph indicates p-value = 0.05).

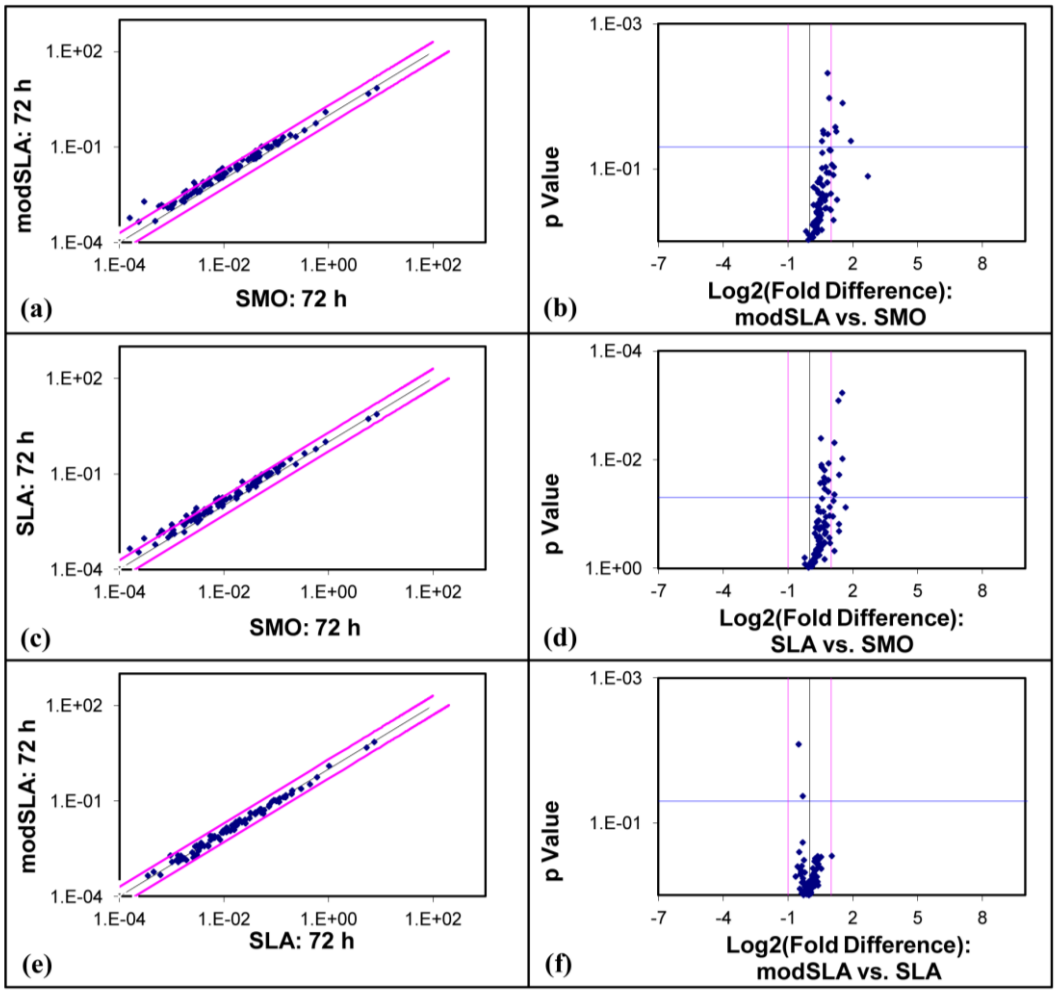

Figure 6-9: Relative gene expression profile of human alveolar bone derived cells on modSLA, SLA, and smooth (polished) (SMO) titanium surfaces after 72 hours of culture. (a: Relative expression on modSLA vs. SMO; b: Volcano plot – modSLA vs. SMO; c: Relative expression on SLA vs. SMO; d: Volcano plot – SLA vs. SMO; e: Relative expression on modSLA vs. SLA; f: Volcano plot – modSLA vs. SLA. The black line indicates a fold change of 1, pink line indicates 2 fold change and the horizontal blue line in the graph indicates p-value = 0.05).

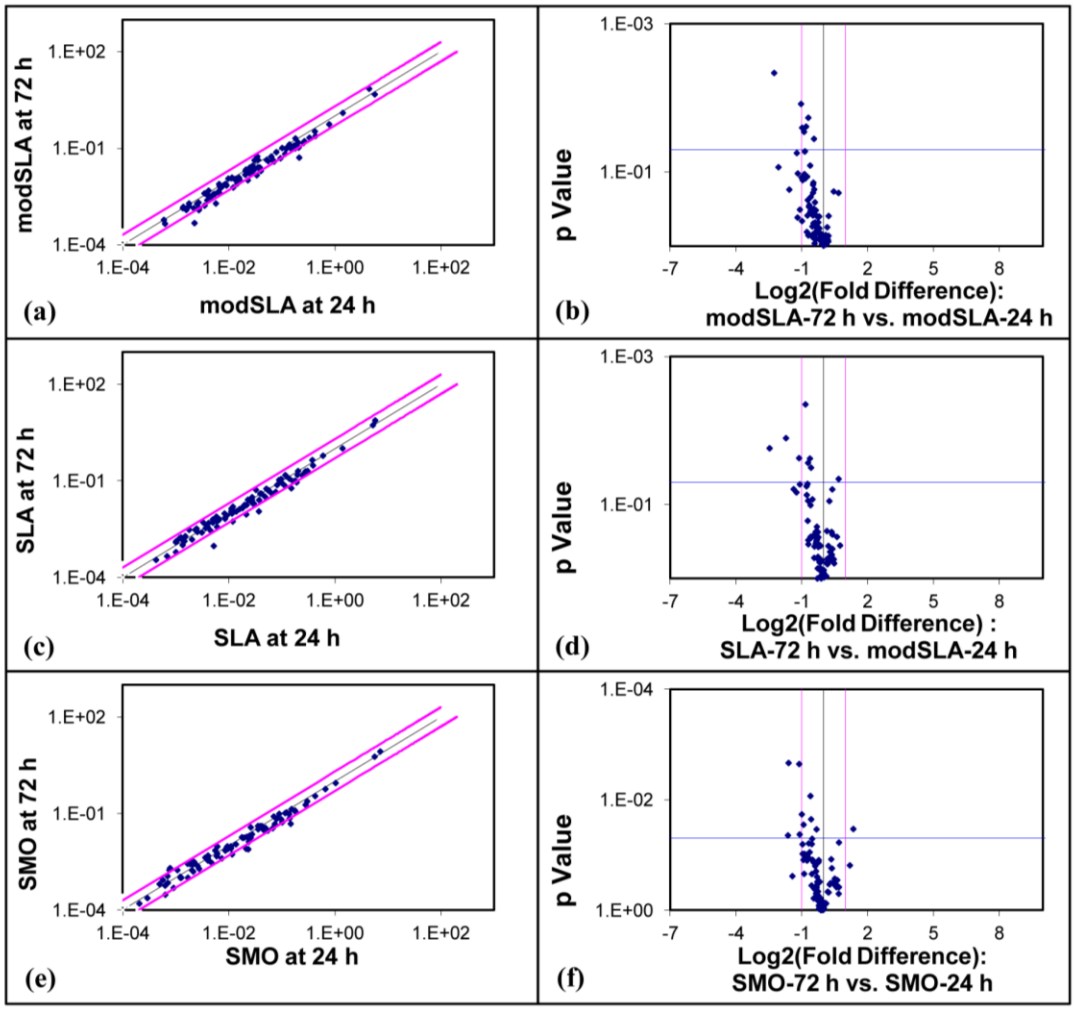

Figure 6-10: Relative gene expression profile of human alveolar bone derived cells on modSLA, SLA and SMO (polished) titanium surface. (a: Relative expression on modSLA 72 hours vs. 24 hours; b: Volcano plot – modSLA 72 hours vs. 24 hours; c: Relative expression on SLA 72 hours vs. 24 hours; d: Volcano plot – SLA 72 hours vs. 24 hours; e: Relative expression on SMO 72 hours vs. 24 hours; f: Volcano plot – SMO 72 hours vs. 24 hours. The black line indicates a fold change of 1, pink line indicates 2 fold change and the horizontal blue line in the graph indicates p-value = 0.05).

6.7 REFERENCES

Bagno, A., Piovan, A., Dettin, M., Chiarion, A., Brun, P., Gambaretto, R., Fontana, G., Di Bello, C., Palù, G. & Castagliuolo, I. (2007) Human osteoblast-like cell adhesion on titanium substrates covalently functionalized with synthetic peptides. *Bone* **40**: 693-699.

Bornstein, M. M., Valderrama, P., Jones, A. A., Wilson, T. G., Seibl, R. & Cochran, D. L. (2008) Bone apposition around two different sandblasted and acid-etched titanium implant surfaces: a histomorphometric study in canine mandibles. *Clinical Oral Implants Research* **19**: 233-241.

Bosshardt, D. D., Salvi, G. E., Huynh-Ba, G., Ivanovski, S., Donos, N. & Lang, N. P. (2011) The role of bone debris in early healing adjacent to hydrophilic and hydrophobic implant surfaces in man. *Clinical Oral Implants Research* **22**: 357-364.

Brett, P. M., Harle, J., Salih, V., Mihoc, R., Olsen, I., Jones, F. H. & Tonetti, M. (2004) Roughness response genes in osteoblasts. *Bone* **35**: 124-133.

Buser, D., Broggini, N., Wieland, M., Schenk, R. K., Denzer, A. J., Cochran, D. L., Hoffmann, B., Lussi, A. & Steinemann, S. G. (2004) Enhanced bone apposition to a chemically modified SLA titanium surface. *Journal of Dental Research* **83**: 529-533.

Buser, D., Nydegger, T., Oxland, T., Cochran, D. L., Schenk, R. K., Hirt, H. P., Snetivy, D. & Nolte, L. P. (1999) Interface shear strength of titanium implants with a sandblasted and acid-etched surface: a biomechanical study in the maxilla of miniature pigs. *Journal of Biomedical Materials Research* **45**: 75-83.

Buser, D., Schenk, R. K., Steinemann, S., Fiorellini, J. P., Fox, C. H. & Stich, H. (1991) Influence of surface characteristics on bone integration of titanium implants. A histomorphometric study in miniature pigs. *Journal of Biomedical Materials Research* **25**: 889-902.

Chakravorty, N., Ivanovski, S., Prasadam, I., Crawford, R., Oloyede, A. & Xiao, Y. (2012) The microRNA expression signature on modified titanium implant surfaces influences genetic mechanisms leading to osteogenic differentiation. *Acta Biomaterialia* **8**: 3516-3523.

Crabtree, G. R. & Olson, E. N. (2002) NFAT signaling: Choreographing the social lives of cells. *Cell* **109** (Suppl): S67-79.

Donos, N., Hamlet, S., Lang, N. P., Salvi, G. E., Huynh-Ba, G., Bosshardt, D. D. & Ivanovski, S. (2011a) Gene expression profile of osseointegration of a hydrophilic compared with a hydrophobic microrough implant surface. *Clinical Oral Implants Research* **22**: 365-372.

Donos, N., Retzepi, M., Wall, I., Hamlet, S. & Ivanovski, S. (2011b) In vivo gene expression profile of guided bone regeneration associated with a microrough titanium surface. *Clinical Oral Implants Research* **22**: 390-398.

Donoviel, D. B., Hadjantonakis, A. K., Ikeda, M., Zheng, H., Hyslop, P. S. & Bernstein, A. (1999) Mice lacking both Presenilin genes exhibit early embryonic patterning defects. *Genes & Development* **13**: 2801-2810.

Engin, F., Yao, Z., Yang, T., Zhou, G., Bertin, T., Jiang, M. M., Chen, Y., Wang, L., Zheng, H., Sutton, R. E., Boyce, B. F. & Lee, B. (2008) Dimorphic effects of Notch signaling in bone homeostasis. *Nature Medicine* **14**: 299-305.

Galli, C., Piemontese, M., Lumetti, S., Manfredi, E., Macaluso, G. M. & Passeri, G. (2012) The importance of Wnt pathways for bone metabolism and their regulation by implant topography. *European Cells & Materials Journal* **24**: 46-59.

Gregory, C. A., Gunn, W. G., Peister, A. & Prockop, D. J. (2004) An Alizarin red-based assay of mineralization by adherent cells in culture: Comparison with Cetylpyridinium chloride extraction. *Analytical Biochemistry* **329**: 77-84.

Haase, H. R., Ivanovski, S., Waters, M. J. & Bartold, P. M. (2003) Growth hormone regulates osteogenic marker mRNA expression in human periodontal fibroblasts and alveolar bone-derived cells. *Journal of Periodontal Research* **38**: 366-374.

Hamlet, S., Alfarsi, M., George, R. & Ivanovski, S. (2012) The effect of hydrophilic titanium surface modification on macrophage inflammatory cytokine gene expression. *Clinical Oral Implants Research* **23**: 584-590.

Han, P., Wu, C., Chang, J. & Xiao, Y. (2012) The cementogenic differentiation of periodontal ligament cells via the activation of Wnt/beta-catenin signalling pathway by Li(+) ions released from bioactive scaffolds. *Biomaterials* **33**: 6370-6379.

Hemming, M. L., Elias, J. E., Gygi, S. P. & Selkoe, D. J. (2008) Proteomic profiling of gamma-secretase substrates and mapping of substrate requirements. *PLoS Biology* **6**: e257.

Herreman, A., Hartmann, D., Annaert, W., Saftig, P., Craessaerts, K., Serneels, L., Umans, L., Schrijvers, V., Checler, F., Vanderstichele, H., Baekelandt, V., Dressel, R., Cupers, P., Huylebroeck, D., Zwijsen, A., Van Leuven, F. & De Strooper, B. (1999) Presenilin 2 deficiency causes a mild pulmonary phenotype and no changes in amyloid precursor protein processing but enhances the embryonic lethal phenotype of Presenilin 1 deficiency. *Proceedings of the National Academy of Sciences of the United States of America* **96**: 11872-11877.

Ito, T., Sawada, R., Fujiwara, Y. & Tsuchiya, T. (2008) FGF-2 increases osteogenic and chondrogenic differentiation potentials of human mesenchymal stem cells by inactivation of Tgf-beta signaling. *Cytotechnology* **56**: 1-7.

Ivanovski, S., Hamlet, S., Retzepi, M., Wall, I. & Donos, N. (2011b) Transcriptional profiling of "guided bone regeneration" in a critical-size calvarial defect. *Clinical Oral Implants Research* **22**: 382-389.

Ivanovski, S., Hamlet, S., Salvi, G. E., Huynh-Ba, G., Bosshardt, D. D., Lang, N. P. & Donos, N. (2011a) Transcriptional profiling of osseointegration in humans. *Clinical Oral Implants Research* **22**: 373-381.

Kaether, C., Haass, C. & Steiner, H. (2006) Assembly, trafficking and function of gamma-secretase. *Neuro-Degenerative Diseases* **3**: 275-283.

Koga, T., Matsui, Y., Asagiri, M., Kodama, T., de Crombrugghe, B., Nakashima, K. & Takayanagi, H. (2005) NFAT and Osterix cooperatively regulate bone formation. *Nature Medicine* **11**: 880-885.

Lai, H. C., Zhuang, L. F., Zhang, Z. Y., Wieland, M. & Liu, X. (2009) Bone apposition around two different sandblasted, large-grit and acid-etched implant

surfaces at sites with coronal circumferential defects: an experimental study in dogs. *Clinical Oral Implants Research* **20**: 247-253.

Lang, N. P., Salvi, G. E., Huynh-Ba, G., Ivanovski, S., Donos, N. & Bosshardt, D. D. (2011) Early osseointegration to hydrophilic and hydrophobic implant surfaces in humans. *Clinical Oral Implants Research* **22**: 349-356.

Lin, G. L. & Hankenson, K. D. (2011) Integration of BMP, Wnt, and Notch signaling pathways in osteoblast differentiation. *Journal of Cellular Biochemistry* **112**: 3491-3501.

Liu, L., Ling, J., Wei, X., Wu, L. & Xiao, Y. (2009) Stem cell regulatory gene expression in human adult dental pulp and periodontal ligament cells undergoing odontogenic/osteogenic differentiation. *Journal of Endodontics* **35**: 1368-1376.

Mak, K. K., Chen, M. H., Day, T. F., Chuang, P. T. & Yang, Y. (2006) Wnt/beta-catenin signaling interacts differentially with Ihh signaling in controlling endochondral bone and synovial joint formation. *Development* **133**: 3695-3707.

Mao, X., Peng, H., Ling, J., Friis, T., Whittaker, A. K., Crawford, R. & Xiao, Y. (2009) Enhanced human bone marrow stromal cell affinity for modified poly(l-lactide) surfaces by the upregulation of adhesion molecular genes. *Biomaterials* **30**: 6903-6911.

Mareddy, S., Dhaliwal, N., Crawford, R. & Xiao, Y. (2010) Stem cell-related gene expression in clonal populations of mesenchymal stromal cells from bone marrow. *Tissue Engineering Part A* **16**: 749-758.

Nobta, M., Tsukazaki, T., Shibata, Y., Xin, C., Moriishi, T., Sakano, S., Shindo, H. & Yamaguchi, A. (2005) Critical regulation of Bone Morphogenetic Protein-induced osteoblastic differentiation by Delta1/Jagged1-activated Notch1 signaling. *The Journal of Biological Chemistry* **280**: 15842-15848.

Olivares-Navarrete, R., Hyzy, S. L., Hutton, D. L., Dunn, G. R., Appert, C., Boyan, B. D. & Schwartz, Z. (2011a) Role of non-canonical Wnt signaling in osteoblast maturation on microstructured titanium surfaces. *Acta Biomaterialia* **7**: 2740-2750.

Olivares-Navarrete, R., Hyzy, S. L., Hutton, D. L., Erdman, C. P., Wieland, M., Boyan, B. D. & Schwartz, Z. (2010a) Direct and indirect effects of microstructured titanium substrates on the induction of mesenchymal stem cell differentiation towards the osteoblast lineage. *Biomaterials* **31**: 2728-2735.

Olivares-Navarrete, R., Hyzy, S. L., Park, J. H., Dunn, G. R., Haithcock, D. A., Wasilewski, C. E., Boyan, B. D. & Schwartz, Z. (2011b) Mediation of osteogenic differentiation of human mesenchymal stem cells on titanium surfaces by a Wnt-integrin feedback loop. *Biomaterials* **32**: 6399-6411.

Olivares-Navarrete, R., Hyzy, S.L., Wieland, M., Boyan, B. D. & Schwartz, Z. (2010b) The roles of Wnt signaling modulators Dickkopf-1 (Dkk1) and Dickkopf-2

(Dkk2) and cell maturation state in osteogenesis on microstructured titanium surfaces. *Biomaterials* **31**: 2015-2024.

Roccuzzo, M., Bunino, M., Prioglio, F. & Bianchi, S. D. (2001) Early loading of sandblasted and acid-etched (SLA) implants: a prospective split-mouth comparative study. *Clinical Oral Implants Research* **12**: 572-578.

Saneyoshi, T., Kume, S., Amasaki, Y. & Mikoshiba, K. (2002) The Wnt/Calcium pathway activates NFAT and promotes ventral cell fate in Xenopus embryos. *Nature* **417**: 295-299.

Schwartz, Z., Lohmann, C. H., Sisk, M., Cochran, D. L., Sylvia, V. L., Simpson, J., Dean, D. D. & Boyan, B. D. (2001) Local factor production by MG63 osteoblast-like cells in response to surface roughness and 1,25-(OH)2D3 is mediated via protein kinase C- and protein kinase A-dependent pathways. *Biomaterials* **22**: 731-741.

Seifert, J. R. & Mlodzik, M. (2007) Frizzled/PCP signalling: a conserved mechanism regulating cell polarity and directed motility. *Nature Reviews Genetics* **8**: 126-138.

Slusarski, D. C. & Pelegri, F. (2007) Calcium signaling in vertebrate embryonic patterning and morphogenesis. *Developmental Biology* **307**: 1-13.

St-Jacques, B., Hammerschmidt, M. & McMahon, A. P. (1999) Indian Hedgehog signaling regulates proliferation and differentiation of chondrocytes and is essential for bone formation. *Genes & Development* **13**: 2072-2086.

Swain, P. S. (2004) Efficient attenuation of stochasticity in gene expression through post-transcriptional control. *Journal of Molecular Biology* **344**: 965-976.

Taniguchi, Y., Karlstrom, H., Lundkvist, J., Mizutani, T., Otaka, A., Vestling, M., Bernstein, A., Donoviel, D., Lendahl, U. & Honjo, T. (2002) Notch receptor cleavage depends on but is not directly executed by Presenilins. *Proceedings of the National Academy of Sciences of the United States of America* **99**: 4014-4019.

Tsutsumi, S., Shimazu, A., Miyazaki, K., Pan, H., Koike, C., Yoshida, E., Takagishi, K. & Kato, Y. (2001) Retention of multilineage differentiation potential of mesenchymal cells during proliferation in response to FGF. *Biochemical and Biophysical Research Communications* **288**: 413-419.

Vlacic-Zischke, J., Hamlet, S. M., Friis, T., Tonetti, M. S. & Ivanovski, S. (2011) The influence of surface microroughness and hydrophilicity of titanium on the up-regulation of TGFβ/BMP signalling in osteoblasts. *Biomaterials* **32**: 665-671.

Wall, I., Donos, N., Carlqvist, K., Jones, F. & Brett, P. (2009) Modified titanium surfaces promote accelerated osteogenic differentiation of mesenchymal stromal cells in vitro. *Bone* **45**: 17-26.

Wang, W., Zhao, L., Ma, Q., Wang, Q., Chu, P. K. & Zhang, Y. (2012) The role of the Wnt/beta-catenin pathway in the effect of implant topography on MG63 differentiation. *Biomaterials* **33**: 7993-8002

Wennerberg A., Galli S. & Albrektsson T. (2011) Current knowledge about the hydrophilic and nanostructured SLActive surface. *Clinical, Cosmetic and Investigational Dentistry* **3**: 59–67.

Wennerberg, A., Svanborg, L. M., Berner, S. & Andersson, M. (2013) Spontaneously formed nanostructures on titanium surfaces. *Clinical Oral Implants Research* **24:** 203-209

Wieland, M., Textor, M., Chehroudi, B. & Brunette, D. M. (2005) Synergistic interaction of topographic features in the production of bone-like nodules on Ti surfaces by rat osteoblasts. *Biomaterials* **26**: 1119-1130.

Xiao, Y., Haase, H., Young, W. G. & Bartold, P. M. (2004) Development and transplantation of a mineralized matrix formed by osteoblasts in vitro for bone regeneration. *Cell Transplantation* **13**: 15-25.

Xiao, Y., Qian, H., Young, W. G. & Bartold, P. M. (2003) Tissue engineering for bone regeneration using differentiated alveolar bone cells in collagen scaffolds. *Tissue Engineering* **9**: 1167-1177.

Zamurovic, N., Cappellen, D., Rohner, D. & Susa, M. (2004) Coordinated activation of Notch, Wnt, and Transforming Growth Factor-beta signaling pathways in Bone Morphogenic Protein 2-induced osteogenesis. Notch target gene Hey1 inhibits mineralization and Runx2 transcriptional activity. *The Journal of Biological Chemistry* **279**: 37704-37715.

Zhao, G., Raines, A. L., Wieland, M., Schwartz, Z. & Boyan, B. D. (2007) Requirement for both micron- and submicron scale structure for synergistic responses of osteoblasts to substrate surface energy and topography. *Biomaterials* **28**: 2821-2829.

Zinger, O., Zhao, G., Schwartz, Z., Simpson, J., Wieland, M., Landolt, D. & Boyan, B. (2005) Differential regulation of osteoblasts by substrate microstructural features. *Biomaterials* **26:** 1837-1847.

6.8 ACKNOWLEDGEMENTS

Dr. Nishant Chakravorty is supported by QUT scholarship. The modSLA, SLA, and SMO discs were supplied by Institut Straumann. This project is partly supported by the ITI foundation and Australian Dental Research Foundation. We thank Dr. Sanjleena Singh for helping us with SEM and AFM work.

Chapter 7: The microRNAs, miR-26a & miR-17 and TGFβ/BMP & Wnt/Ca^{2+} pathways relationship

The miR-26a and miR-17 mediated cell signaling cross-talks guide osteogenic differentiation and osseointegration

Nishant Chakravorty, Anjali Jaiprakash, Ross Crawford,

Adekunle Oloyede, Saso Ivanovski & Yin Xiao

(Manuscript in preparation)

Suggested Statement of Contribution of Co-Authors for Thesis by Publication

Contributors	Statement of contribution
Nishant Chakravorty	Involved in the conception and design of the project. Performed laboratory experiments and wrote the manuscript.
Anjali Jaiprakash	Assisted in performing the experiments.
Ross Crawford	Involved in the conception and design of the project. Assisted in reviewing the manuscript.
Adekunle Oloyede	Involved in the conception and design of the project. Assisted in reviewing the manuscript.
Saso Ivanovski	Involved in the conception and design of the project, manuscript preparation and reviewing.
Yin Xiao	Involved in the conception and design of the project, manuscript preparation and reviewing.

Principal Supervisor Confirmation

I have sighted email or other correspondence from all co-authors confirming their certifying authorship

Prof. Yin Xiao		**10th July, 2014**
Name	**Signature**	**Date**

Abstract

Superior osseointegration and *in vitro* osteogenic differentiation properties of micro-roughened titanium implant surfaces, like the sand-blasted, large grit, acid-etched (SLA) and its successor, the chemical modified hydrophilic SLA (modSLA) surfaces, have provided us with critical molecular cues pertaining to the process of osteogenesis. Our previous studies have demonstrated the upregulation of the pro-osteogenic TGFβ/BMP & Wnt/Ca^{2+} cell signaling pathways and a simultaneous downregulation of microRNAs with putative targets in these pathways, on the modSLA and SLA surfaces compared with smooth polished (SMO) surfaces. The present study aimed at exploring the influence of two such miRNAs (miR-26a & miR-17) on the TGFβ/BMP & Wnt/Ca^{2+} pathways during osteogenesis. Osteogenic differentiation studies on human osteoblast-like SAOS-2 cells overexpressing miR-26a & miR-17, showed lower expression of TGFβ/BMP & Wnt/Ca^{2+} genes and osteogenic markers. Osteo-inhibitory effects of intrinsic miR-26a & miR-17 were also demonstrated by inducing osteo-differentiation in presence of pro-inflammatory cytokine, TNFα. The higher expression of miR-26a & miR-17, coupled with lower expression of TGFβ/BMP and Wnt/Ca^{2+} pathways, in presence of TNFα, strengthened the correlations between them and osteoinhibition. Dual luciferase reporter assays confirmed WNT5A and SMAD1 as targets for miR-26a; and PPP3R1, NFAT5 and BMP2 as targets for miR-17, establishing the role of miR-26a and miR-17 in the regulation of TGFβ/BMP and Wnt/Ca^{2+} pathways. Further, exploring the cross-talk between the TGFβ/BMP & Wnt/Ca^{2+} pathways using recombinant human BMP2 and KN-93 (Wnt/Ca^{2+} pathway inhibitor), demonstrated a positive influence of the TGFβ/BMP pathway on the activation of the Wnt/Ca^{2+} pathway. Finally, the study observed an accelerated mineralization and osteogenic differentiation on polished titanium surfaces upon the use of inhibitors for miR-26a and miR-17 (i-miR-26a and i-miR-17), thereby highlighting the impact of suppressing miRNAs that inhibit the pro-osteogenic TGFβ/BMP & Wnt/Ca^{2+} pathways. Therefore, the study concluded an intricate miRNA modulated control of cell signaling pathways that guide osteogenesis in pro-osteogenic environments. Synthetic miRNA modulators are novel clinical options to achieve superior osseointegration especially in compromised conditions.

7.1 INTRODUCTION

Small non-coding RNA molecules, known as microRNAs (miRNAs) (approximately 22 nucleotides residues in length) have been recently identified as important regulators of genetic mechanisms leading to translational repression and gene silencing [1]. MicroRNAs have been found to be critical in the developmental stages of organisms and are differentially expressed in different tissues [2]. Such RNAs are therefore considered vital for the initiation and propagation of various biological processes. They are considered as key regulators of the cellular development and differentiation process [3] and have been shown to influence the process of bone formation [4] and osseointegration [5].

Osseointegration is a dynamic biological process that eventually leads to a functional union of orthopedic and dental implants with the surrounding bone tissue. The clinically established micro-roughened titanium implant surfaces, like the sand-blasted, large-grit, acid-etched (SLA) and its successor, the chemically modified, modSLA surfaces, are known to have improved osseointegration and bone formation compared with smooth and polished (SMO) surfaces [6, 7]. Osseointegration is known to occur either via new bone formation on the implant surface from surrounding bone (distance osteogenesis), or by direct deposition of new bone on the surface of the implant (contact osteogenesis) as seen commonly on micro-roughened surfaces [8]. Therefore, the micro-rough SLA and modSLA surfaces provide interesting cues regarding the molecular regulation process during bone formation. Gene expression and cell signaling studies on SLA and modSLA surfaces have demonstrated early stimulation of the pro-osteogenic TGFβ/BMP and Wnt/Ca^{2+} cell signaling pathways [9-12]. Recently, we have demonstrated differential regulation of several microRNAs on these surfaces. Several of the miRNAs downregulated on the modSLA and SLA surfaces compared with SMO surfaces have been shown to have predicted targets in the TGFβ/BMP and Wnt/Ca^{2+} pathways [13].

The microRNAs, miR-26a and miR-17 have been recently described to modulate the process of osteogenic differentiation and bone formation [4, 14]. These microRNAs were found to be downregulated on modSLA and SLA surfaces compared with SMO surfaces after 24 hours of culture of osteoprogenitor cells [13]. Although, both miR-26a and miR-17 are seen to have several putative targets in the TGFβ/BMP and Wnt/Ca^{2+} signaling pathways; yet their role in the functional

regulation of these pathways during the process of osteogenic differentiation hasn't been explored. The aim of this study was to explore the role of these microRNAs in modulation of the TGFβ/BMP and Wnt/Ca^{2+} pathways during the process of osteogenic differentiation and to further study the inter-relationship between these two cell signaling pathways.

7.2 MATERIALS AND METHODS

7.2.1 Titanium implant surfaces

All the titanium discs used for this study (modSLA, SLA and SMO) were provided by Institut Straumann (Basel, Switzerland) and were manufactured from grade II commercially pure titanium. Briefly, the SLA surfaces were prepared by sand-blasting the titanium surface with corundum (250-500 μm) and etched with acid – hot solution of hydrochloric/sulfuric acids. The modSLA surfaces were obtained by rinsing the SLA discs in a nitrogen environment and stored in isotonic saline solution at a pH=4-6. The process is known to produce a hydrophilic surface with reduced carbon contamination on the surface [15]. Polished titanium surfaces with smooth mirror-finish were categorized as SMO surfaces.

7.2.2 MicroRNA mimics and inhibitors

Synthetic microRNA mimics - miR-26a (mature ID: miR-26a-5p) and miR-17 (mature ID: miR-17-5p); and negative control (miR-NC) were purchased from Ambion® (Life Technologies - Applied Biosystems, Mulgrave, VIC, Australia). The synthetic miRNA inhibitors for miR-26a-5p (i-miR-26a) and miR-17-5p (i-miR-17) and negative control (i-miR-NC) were obtained from Sigma Aldrich Pty Ltd. (Castle Hill, NSW, Australia).

7.2.3 Cytokines, growth factors and cell signaling modulators

The pro-inflammatory cytokine, recombinant human Tumor Necrosis Factor-α (TNFα) was purchased from Gibco® (Life Technologies - Applied Biosystems, Mulgrave, VIC, Australia). Recombinant human bone morphogenetic protein-2 (HumanKine^{TM} BMP2) and KN93, an inhibitor of Ca^{2+}/calmodulin-dependent protein kinases II (CAMKII-the read-out of the Wnt/Ca^{2+} pathway) were obtained from Sigma Aldrich Pty Ltd. (Castle Hill, NSW, Australia).

7.2.4 Cell culture

Human alveolar bone derived osteoprogenitor cells (BCs) were collected from healthy volunteers. Cells were cultured from redundant tissues following third molar extraction surgery as described previously [16-18]. BCs (5×10^4 cells/disc) were exposed to modSLA, SLA, and SMO surfaces (six discs of each kind were used) for 6 and 24 hours and cultured as discussed in details in our earlier reports [12, 13]. Human osteoblast-like SAOS-2 cells were used to study the role of miR-26a and miR-17 during osteogenic differentiation. Osteogenic differentiation was induced by supplementing the standard culture media (Dulbecco's Modified Eagle's Medium (DMEM) + 10% fetal bovine serum (FBS) and antibiotics – 100 U/ml penicillin/100 μg/ml streptomycin) with 100 nM dexamethasone, 0.2 mM L-ascorbic acid and 10 mM β-glycerophosphate (standard osteogenic media). Cytokine experiments were conducted by supplementing osteogenic media with TNFα (0.5 ng/ml) and comparing them with controls without cytokines. The inter-relationship between TGFβ/BMP and the non-canonical Wnt/Ca^{2+} pathways were studied on BCs cultured in standard media with/without HumanKine™ BMP2 and KN93, and compared with appropriate controls.

7.2.5 Transfections

MicroRNA mimics and inhibitors were transfected using X-tremeGENE HP DNATransfection Reagent (Roche Diagnostics Australia Pty Limited, Castle Hill, NSW, Australia). Briefly, miRNA-mimics/inhibitors (30 pmoles) were mixed with the transfection reagent in Opti-MEM® I Reduced Serum Media (Life Technologies - Applied Biosystems, Mulgrave, VIC, Australia) (in absence of antibiotics), and incubated for 30 minutes at room temperature before adding to the cells. After six hours, the transfection mixes were replaced with standard osteogenic media. Transfection protocol was confirmed by transfecting positive control microRNA (miR-1) (Pre-miR™ hsa-miR-1 miRNA Precursor Positive Control from Ambion® by Life Technologies - Applied Biosystems, Mulgrave, VIC, Australia) and observing the downregulation of Twinfilin-1 (PTK9) gene by quantitative real-time polymerase chain reaction (qPCR). Further, the transfection efficiencies were tested by qPCR for miR-26a and miR-17.

7.2.6 TGFβ/BMP and Wnt/Ca^{2+} pathway interactions

The interaction between TGFβ/BMP and Wnt/Ca^{2+} pathways was studied using stimulants and inhibitors for these pathways. Recombinant human BMP2 (HumanKine^{TM} BMP2) is known to activate the BMP pathway, and leads to phosphorylation of the intra-cellular transducer molecules for the pathway (SMADs). The chemical, KN93 is known to inhibit the Wnt/Ca^{2+} pathway read-out, Ca^{2+}/calmodulin-dependent protein kinase (CAMKII). Human osteoprogenitor cells were cultured in standard media and supplemented with HumanKine^{TM} BMP2 (10 ng/ml) and/or KN93 (10 μM).

7.2.7 Dual luciferase reporter gene constructs

The predicted targets in the TGFβ/BMP and Wnt/Ca^{2+} pathways for miR-26a and miR-17 (based on TargetScan predictions as described in our previous work [13]), were cloned into the pmirGLO Dual-Luciferase miRNA Target Expression Vector (Promega Australia, Alexandria, NSW, Australia). The predicted target regions for the genes were cloned between the SacI and XbaI regions in the pmirGLO vector such that the potential target is inserted 3' of the firefly luciferase gene (SacI and XbaI restriction enzymes purchased from Genesearch Pty Ltd., Arundel, QLD, Australia). The ligated products were transformed into Alpha-Select Silver Efficiency Competent Cells obtained from Bioline (Aust) Pty Ltd (Alexandria, NSW, Australia). The genes considered for experimental target validation are detailed in Table 7-1. Following the transformations, single colonies were picked and cultured in Luria Broth (LB)/Ampicillin (100 μg/ml). Plasmids were extracted after 16 hours of culture using Nucleospin Plasmid extraction kit (Macherey Nagel GmbH & Co. KG, Dueren, Germany). The plasmids sequences were verified by sequencing at the Australian Genome Research Facility Ltd (AGRF) (University of Queensland, Brisbane, Australia).

Table 7-1: TGFβ/BMP and Wnt/Ca^{2+} pathway genes predicted as targets for miR-26a and miR-17 and chosen for the experimental target validation using luciferase assay.

Gene	Position on 3'UTR	Predicted consequential pairing of target region (top) and miRNA (bottom) (TargetScan predictions)
Targets on TGFβ/BMP2 and Wnt/Ca^{2+} pathways predicted for miR-26a		
WNT5A	Position 1350-1357 of WNT5A 3' UTR	5' ...AAACUGUUCCCAGUGUACUUGAA... ||| ||||||| 3' UCGGAUAGGACCUAAUGAACUU
PLCB1	Position 2412-2419 of PLCB1 3' UTR	5' ...UAAUAAUAUUAAUAUUACUUGAA... ||||||| 3' UCGGAUAGGACCUAAUGAACUU
PPP3CB	Position 617-624 of PPP3CB 3' UTR	5' ...CCAGGCAGGCUCUCUUACUUGAA... ||||||| 3' UCGGAUAGGACCUAAUGAACUU
PPP3R1	Position 386-392 of PPP3R1 3' UTR	5' ...GGCUUUAAUUUAAUAUACUUGAU... ||||||| 3' UCGGAUAGGACCUAAUGAACUU
SMAD1	Position 103-109 of SMAD1 3' UTR	5' ...AAGGAGCCUUGAUAAUACUUGAC... ||| ||||||| 3' UCGGAUAGGACCUA--AUGAACUU
SMAD4	Position 1034-1040 of SMAD4 3' UTR	5' ...GUUUGGAUAUUUUUGUACUUGAU... ||||||| 3' UCGGAUAGGACCUAAUGAACUU
Targets on TGFβ/BMP2 and Wnt/Ca^{2+} pathways predicted for miR-17		
PLCB1	Position 2001-2007 of PLCB1 3' UTR	5' ...AAUCAUUCUACUUUU-GCACUUUG... ||| ||||||| 3' GAUGGACGUGACAUUCGUGAAAC
PPP3R1	Position 193-200 of PPP3R1 3' UTR	5' ...CAAUAACUCAGUGUAGCACUUUA... ||||||| 3' GAUGGACGUGACAUUCGUGAAAC
NFAT5	Position 5813-5820 of NFAT5 3' UTR	5' ...CCCUAUUGAUAUUAUGCACUUUA... ||||||| 3' GAUGGACGUGACAUUCGUGAAAC
BMP2	Position 93-99 of BMP2 3' UTR	5' ...CCCCACCCCAGUUGACACUUUAA... |||||| 3' GAUGGACGUGACAUUCGUGAAAC

7.2.8 Luciferase assays

Hep2 (HeLa derivative) cells were used for the luciferase assays. The cells were co-transfected with 10 pmoles of either miR-26a/miR-17 or miR-NC mimic and 50 ng of their predicted gene plasmids, using X-tremeGENE HP DNA Transfection Reagent (Roche Diagnostics Australia Pty Limited, Castle Hill, NSW, Australia). The protocol was similar to miRNA mimics transfections as described above. Briefly, the plasmid and miRNA mimic were incubated for 30 minutes with the transfection reagent separately in Opti-MEM® I Reduced Serum Media (Life Technologies - Applied Biosystems, Mulgrave, VIC, Australia) (in absence of antibiotics). This mix was used to incubate Hep2 cells for 6 hours, following which the media was replaced with standard culture media. Luciferase assays were performed after 24 hours using the Dual-Glo® Luciferase Assay System (Promega Australia, Alexandria, NSW, Australia) as per the manufacturer's protocol. The firefly luciferase activity was measured using a luminometer and was normalized using the the Renilla luciferase internal control.

7.2.9 Quantitative real-time polymerase chain reaction (qPCR)

cDNA for the detection of mRNAs (gene expression) was prepared from RNA templates by reverse transcription using DyNAmo^{TM} cDNA Synthesis Kit (Finnzymes Oy., Vantaa, Finland) according to the manufacturer's protocol. For the detection of microRNAs, cDNA was prepared using the miRCURY LNA^{TM} Universal RT microRNA PCR (Exiqon A/S, Vedbaek, Denmark). The mRNA expression levels for genes of the TGFβ/BMP and Wnt/Ca^{2+} pathways and the miRNAs, miR-26a and miR-17, were investigated. The full list of genes and primers used for detection of mRNAs are shown in Table 7-2. The microRNA primers sets were purchased from Exiqon A/S (Vedbaek, Denmark) (miRCURY LNA^{TM} Universal RT microRNA PCR LNA^{TM} PCR primer sets: hsa-miR-26a-Product No. 204724; hsa-miR-17-Product No. 204771 and U6 snRNA-Product No. 203907). Quantitative real time PCR (qPCR) reactions were performed using ABI PCR machines (ABI Prism 7900HT Sequence Detection System, ABI Prism 7000 Sequence Detection System and ABI Prism 7300 Sequence Detection System - Applied Biosystems). Consistency with the starting amount of RNA (≥100 ng) was maintained for each part of the study. The reactions were incubated at 95 °C for 10 minutes for 1 cycle, and then 95 °C (15 seconds), 60 °C (for 1 minute) for 40 cycles.

PCR reactions were validated by observing the presence of a single peak in the dissociation curve analysis. The housekeeping gene, glyceraldehyde-3-phosphate-dehydrogenase (GAPDH) was used as an endogenous reference gene for analysis of mRNAs using the Comparative Ct (Cycle of threshold) value method. The ΔC_T value was obtained by subtracting the average Ct value of the endogenous references selected from the test mRNA Ct value of the same samples. U6 snRNA (hsa, mmu, rno) was used as the reference miRNA gene for analysis of miRNA expressions. The relative levels of expression of mRNAs and miRNAs were compared between the samples using the Student's *t*-test. The critical value for significance was set at $p<0.05$. Fold changes were calculated relative to the control sample in each case.

Table 7-2: List of gene primers used for the study.

Gene name	Forward primer (5'→3')	Reverse primer (5'→3')
WNT5A	TCTCAGCCCAAGCAACAAGG	GCCAGCATCACATCACAACAC
FZD6	GCGGAGTGAAGGAAGGATTAG	ACAAGCAGAGATGTGGAACC
FZD2	GTGCCATCCTATCTCAGCTACA	GACCAGGTGAGGATCCAGAG
BMP2	CGCAGCTTCCACCATGAAGAATC	CCTGAAGCTCTGCTGAGGTG
BMP6	CAGGAGCATCAGCACAGAGAC	GCTGAAGCCCCATGTTATGCTG
BMPR1A	CCTGGGCCTTGCTGTTAAATTCA	TCCACGATCCCTCCTGTGAT
SMAD1	GTATGAGCTTTGTGAAGGGC	TAAGAACTTTATCCAGCCACTGG
SMAD4	CTCCAGCTATCAGTCTGTCAG	CCCGGTGTAAGTGAATTTCAAT
SMAD5	TCATCATGGCTTTCATCCCACC	GCTCCCCAACCCTTGACAAA
GAPDH	TCAGCAATGCCTCCTGCAC	TCTGGGTGGCAGTGATGGC

7.2.10 Western Blotting

To assess for the activation of the TGFβ/BMP and Wnt/Ca^{2+} pathways, cells were first washed with cold PBS and then lysed with Hepes-Triton protein lysis buffer (20 mM Hepes, 2 mM EGTA, 1% Triton X-100, 10% Glycerol, pH=7.4). The lysis buffer was supplemented with appropriate dilutions of protease inhibitor (cOmplete ULTRA Tablets, Mini, EDTA-free, EASYpack - Roche Diagnostics Australia Pty Limited, Castle Hill, NSW, Australia) and phosphatase inhibitors (PhosSTOP Phosphatase Inhibitor Cocktail Tablets - Roche Diagnostics Australia Pty Limited, Castle Hill, NSW, Australia). The total protein concentration was calculated by using the BCA Protein Assay Kit (bicinchoninic acid) (Thermo

Scientific Pierce Protein Biology Products, Rockford, Illinois, USA). The protein samples were fractionated by gel electrophoresis in 10% polyacrylamide gels under reducing conditions and were transferred to nitrocellulose membranes. The membranes were blocked with 5% bovine serum albumin (BSA) and probed with primary antibodies overnight at 4 °C. The next day, the blots were washed with Tris Buffered Saline-Tween (TBST) and then probed with their appropriate secondary antibodies. The blots were again washed (three times) with TBST and then imaged either using enhanced chemiluminescence (ECL) or fluorescence based methods. The antibodies used for the study are listed in Table 7-3.

Table 7-3: List of antibodies used for Western Blots.

Protein	Dilution	Source	Product Code
Phospho-CAMKII (Thr 286)	1:1000	Cell Signaling Technology, Inc., Danvers, MA, USA	#3361
CAMKII (pan)(D11A10) Rabbit mAb	1:1000	Cell Signaling Technology, Inc., Danvers, MA, USA	#4436
Phospho-Smad1 (Ser463/465)/Smad5 (Ser463/465)/ Smad8 (Ser426/428)	1:1000	Cell Signaling Technology, Inc., Danvers, MA, USA	#9511
Smad1/5/8 (N-18)	1:200	Santa Cruz Biotechnology, Inc, Dallas, TX, USA	sc-6031-R
GAPDH Antibody (0411)	1:2000	Santa Cruz Biotechnology, Inc, Dallas, TX, USA	sc-47724

7.2.11 Alkaline phosphatase activity and Alizarin-Red S staining

Intracellular ALP activity was determined with the Quantichrom™ Alkaline Phosphatase Assay Kit (Gentaur Belgium BVBA, Kampenhout, Belgium), a p-nitrophenyl phosphate (pNP-PO_4) based assay. Osteoblastic cells were rinsed twice with PBS, and lysed in 200µl of 0.2% Triton X-100 in MilliQ water, followed by 20 minutes agitation at room temperature. A 50 µl sample was then mixed with a 100 µl working solution and absorbance was measured after 5 min at 405 nm in a microplate reader. Extracellular matrix deposition was determined by fixing the cells in 4% paraformaldehyde and staining with a 1% Alizarin-Red S solution.

7.3 RESULTS

7.3.1 Expression of miR-26a & miR-17 and key BMP and Wnt/Ca^{2+} genes on modified titanium implant surfaces

qPCR based evaluation of the pattern of expression of the microRNAs on the modified titanium surfaces compared with SMO surfaces following 6 hours of exposure of BCs showed lower expression of miR-26a and miR-17 on modSLA and SLA surfaces (modSLA<SLA<SMO) (Figure 7-1). The expression of the genes: BMP2, BMP6 (TGFβ/BMP pathway), WNT5A and FZD6 (Wnt/Ca^{2+} pathway) were

seen to be higher on modSLA and SLA surfaces (modSLA and SLA > SMO surfaces) following 24 hours of culture of BCs on modSLA, SLA, and SMO surfaces (Figure 7-1).

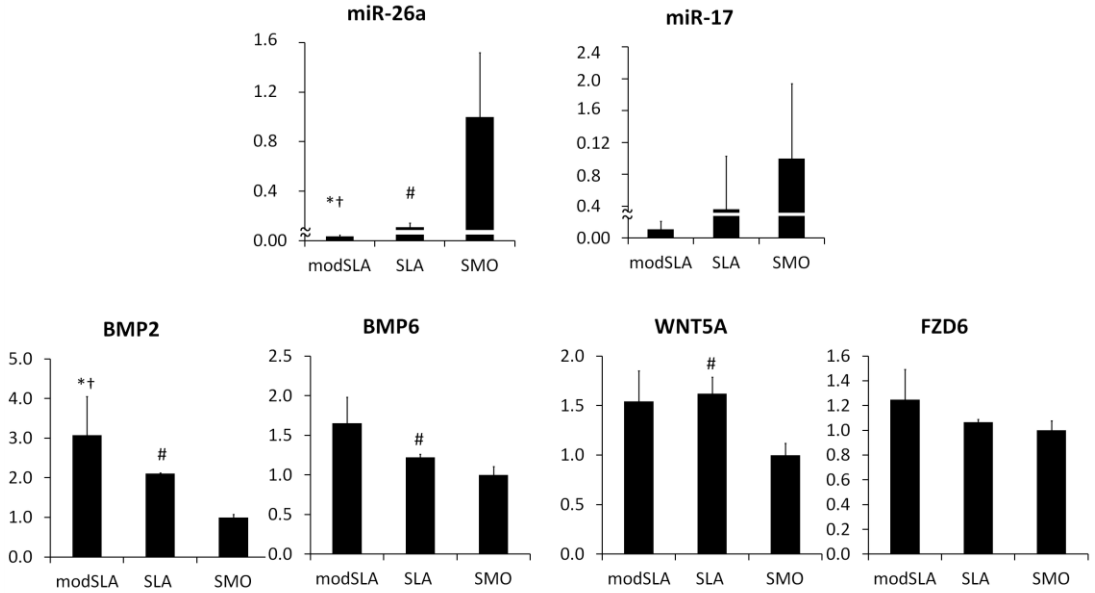

Figure 7-1: qPCR expression analysis of miR-26a & miR-17 and genes of TGFβ/BMP and Wnt/Ca^{2+} pathway on modSLA, SLA & SMO surfaces. (y-axis: relative fold changes to SMO)(*: $p<0.05$, modSLA vs. SMO; #: $p<0.05$, SLA vs. SMO; $p<0.05$, †: $p<0.05$, modSLA vs. SLA). Lower expression of miR-26a and miR-17 on modSLA and SLA surfaces compared with SMO surfaces was observed (6 hours exposure). This was associated with increased expression of TGFβ/BMP (BMP2, BMP6) and Wnt/Ca^{2+} (WNT5A, FZD6) genes (24 hours exposure) on modSLA and SLA surfaces.

7.3.2 Effect of osteo-inhibitory environment on expression of miR-26a & miR-17 and TGFβ/BMP & Wnt/Ca^{2+} genes

Osteo-inhibitory environment was created by supplementing osteogenic media with the pro-inflammatory cytokine - TNFα (0.5 ng/ml) and was used to culture osteoblast-like SAOS-2 cells. Osteogenic media without any cytokine supplementation was used as control for these experiments. Inhibition in osteogenic differentiation was confirmed by observing reduced ALP activity and Alizarin Red S staining in presence of cytokine (Figure 7-2A). qPCR analysis demonstrated higher expression of miR-26a and miR-17 in presence of TNFα during osteogenic differentiation (Figure 7-2B). This was coupled with decreased expression of BMP2 and WNT5A (key ligands for the TGFβ/BMP and Wnt/Ca^{2+} pathways, respectively) (Figure 7-2B). Reduced expression of SMAD4 and SMAD5 was also observed in presence of cytokines (Figure 7-2B).

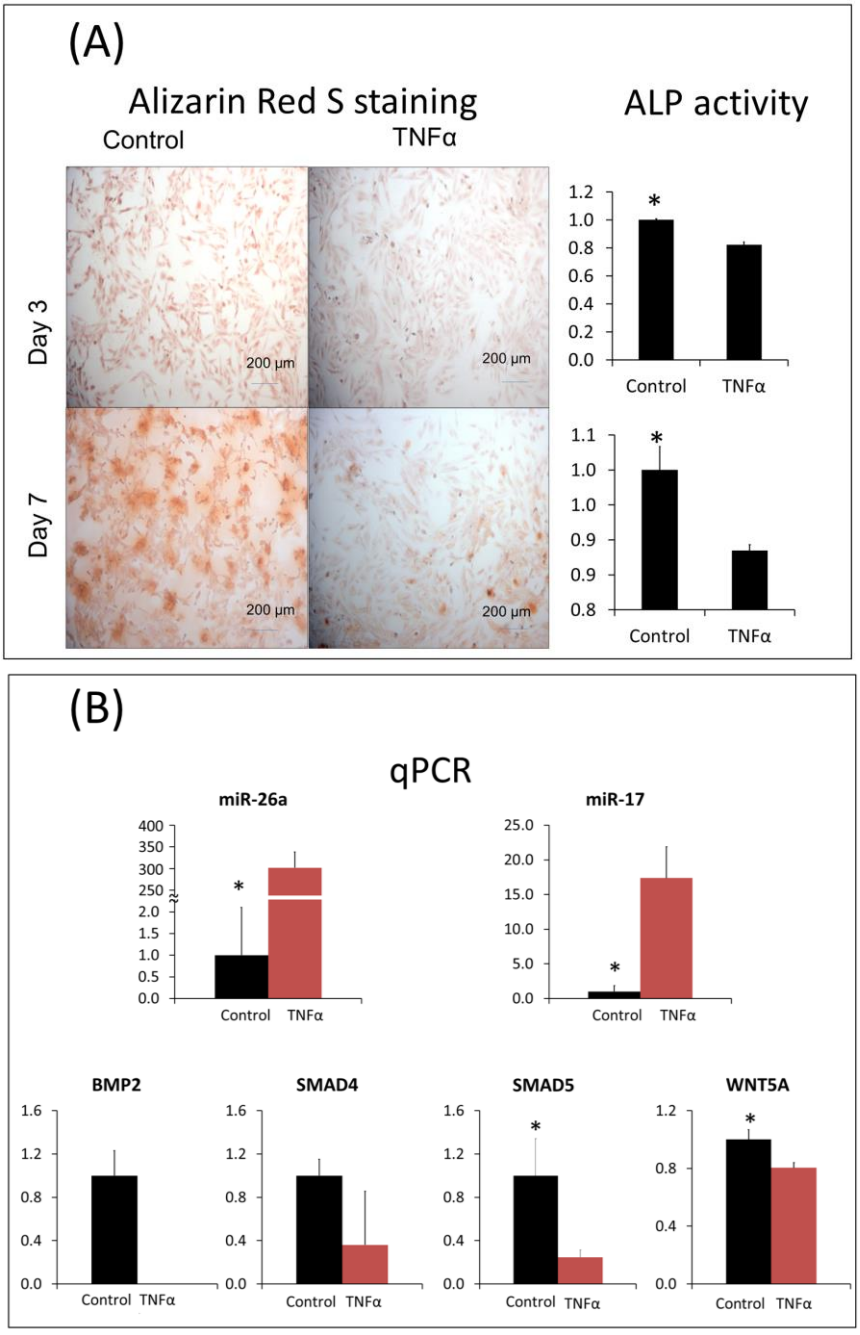

Figure 7-2: Effect of osteo-inhibitory environment on expression of miR-26a & miR-17 and TGFβ/BMP and Wnt/Ca^{2+} genes (A) Alizarin Red S staining and ALP activity levels after 3 & 7 days of culture in osteogenic media (OM) (Control) or in presence of OM+TNFα 0.5 ng/ml (TNFα) confirm OM+TNFα as osteoinhibitory environment. (*: $p<0.05$, Control vs. TNFα). (B) qPCR expression analysis of miR-26a & miR-17 and genes of TGFβ/BMP and Wnt/Ca^{2+} pathway in osteo-inhibitory environment (OM+TNFα 0.5 ng/ml: designated as TNFα) compared to OM (Control). Higher expression of miR-26a and miR-17, simultaneous with lower expression of BMP2, SMAD4, SMAD5 (TGFβ/BMP) and WNT5A (Wnt/Ca^{2+}) was observed in OM+TNFα (y-axis: relative fold changes to Control) (*: $p<0.05$, Control vs. TNFα) following 3 days of culture.

7.3.3 Over-expression of miR-26a and miR-17 and their effect on TGFβ/BMP and Wnt/Ca^{2+} pathway

Synthetic miRNA mimics, miR-26a and miR-17 were transfected into human osteoblast-like, SAOS-2 cells and osteogenic differentiation was induced. The mRNA expression pattern of important genes of the TGFβ/BMP and Wnt/Ca^{2+} pathway was examined (Figure 7-3). qPCR analysis showed a significantly decreased expression of the WNT5A (representative ligand for the non-canonical Wnt/Ca^{2+} pathway) in miR-26a and miR-17 samples after 24 hours of transfection of the miRNAs. The differences persisted even after 3 days of culture. The non-canonical receptor, FZD2 was seen to have lower expression within 24 hours of transfection with miR-17, and subsequently all the test samples showed higher expression (except for miR-17 at day 14). A sharp decline in the expression of FZD2 was observed in miR-26a overexpressing cells after 72 hours. There were no other noteworthy differences observed at other time-points, except at day 14, where it showed significantly reduced expression with miR-26a and miR-17 samples compared to miR-NC. BMP2 was significantly downregulated in miR-17 overexpressing cells at day 1 and 3 (compared with miR-NC). The expression of BMP2 wasn't appreciable at day 14 in miR-17 transfected samples. BMP2 expression was decreased when miR-26a was overexpressed (significant differences were observed after three days). miR-26a and miR-17 samples showed higher expression of BMP2 at day 7. BMPR1A showed decreased expression within one day of miR-26a overexpression, although higher expression was observed at later time-points (day 7 and day 14). Decreased expression levels were observed with miR-17 transfections compared with miR-NC almost at each time-point. BMPR2 and SMAD4 demonstrated similar trends, except at day 1 with miR-17 overexpression. SMAD1 showed reduced expressions with miR-26a and miR-17 samples (especially at days 1 and 3).

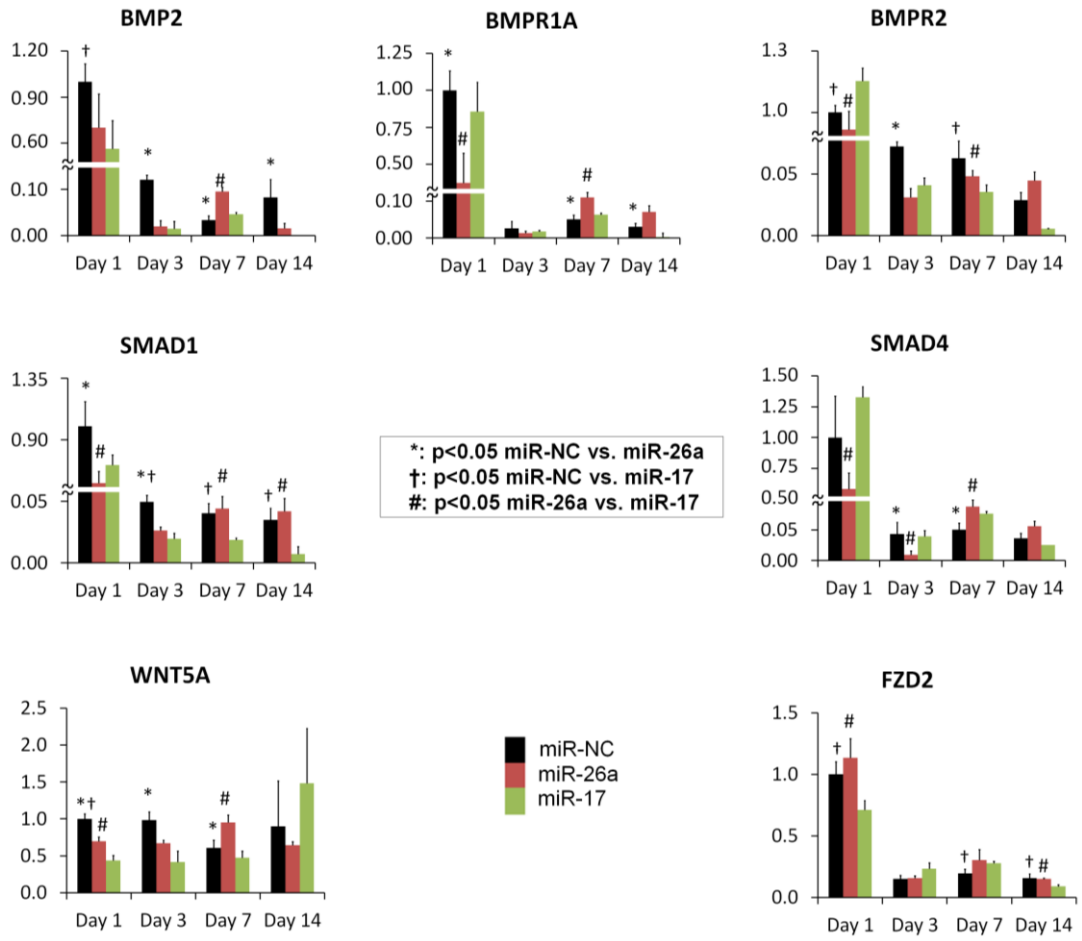

Figure 7-3: qPCR expression analysis of genes of the TGFβ/BMP (BMP2, BMPR1A, BMPR2, SMAD1, and SMAD4) and Wnt/Ca^{2+} pathway (WNT5A, FZD2) after transfecting cells with miR-mimics and inducing osteogenic differentiation (miR-NC: negative control)(y-axis: fold change relative to miR-NC day 1). Lower expression of the genes was observed in miR-26a and miR-17 overexpressing cells compared to miR-NC (especially after 1 and 3 days of culture in OM following transfection).

The effects of overexpressing miR-26a and miR-17 on the cell signaling pathways were further tested at the level of protein expression. The read-outs of the Wnt/Ca^{2+} (phospho-CAMKII and pan-CAMKII) and TGFβ/BMP pathway (phospho-SMAD1/5/8 and total SMAD1/5/8) were observed (Figure 7-4). A relatively lower expression of phospho-CAMKII was observed in cells transfected with miR-26a samples compared with miR-NC (at day 1 and day 3). Lower expression of phospho-CAMKII and pan-CAMKII was also observed with miR-17 cells at day 1; however, the expression levels seemed to improve in these samples by day 3. The expression of phospho-CAMKII was seen to be lower even at day 3 in miR-26a transfected cells. However, this wasn't overtly obvious with miR-17 at that time-point. The

expression of phospho-SMAD1/5/8 was significantly lower in miR-17 expressing cells (both at day 1 and day 3) indicating a decreased activation of the TGFβ/BMP pathway.

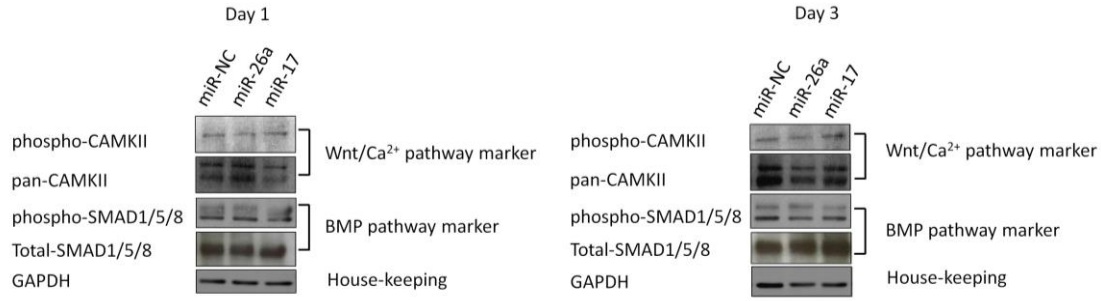

Figure 7-4: Western Blots following 1 and 3 days of transfecting miR-26a and miR-17. Phospho-CAMKII and pan-CAMKII are read-outs for the Wnt/Ca^{2+} pathway; and phospho-SMAD1/5/8 is the read-out for the activation of TGFβ/BMP pathway. Lower expression of read-outs of Wnt/Ca^{2+} and TGFβ/BMP pathways was observed following miR-26a and miR-17 transfections.

The effects of miR-26a and miR-17 over-expression on mineralization and osteogenic differentiation of cells was also studied (Figure 7-5). A lower Alizarin Red S staining was noted in miR-26a and miR-17 transfected cells in comparison with miR-NC (day 7 and day 14). Alkaline phosphatase (ALP) activity in the transfected samples was also assessed at days 1, 3, 7 and 14. The miR-26a and miR-17 over-expressing cells were seen to have lower ALP activity (normalized to total protein) relative to miR-NC at each time-point. miR-26a was seen to have a relatively higher activity compared to miR-17 at day 7; however, it showed a drop at day 14.

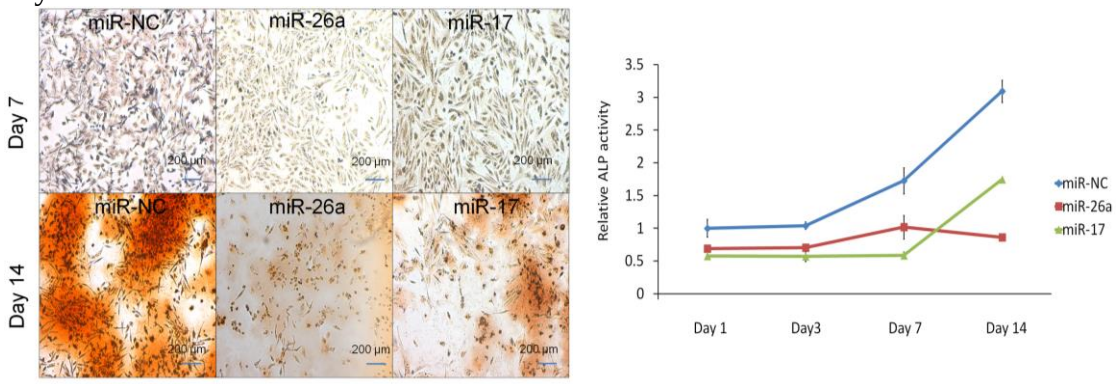

Figure 7-5: Osteogenic differentiation following miR-26a and miR-17 transfections. Alizarin Red S staining images after 7 and 14 days of culturing miRNA-mimic transfected SAOS-2 cells in osteogenic media (OM) (miR-NC: Negative Control; miR-26a & miR-17). Reduced matrix deposition was observed in miR-26a and miR-17 transfected cells when compared with miR-NC controls at each time-point demonstrating inhibition of osteogenic differentiation in miR-26a & miR-17 transfected cells. ALP activity also demonstrated similar features. The ALP activity values were consistently lower in miR-26a and miR-17 transfected cells.

7.3.4 Target validation experiments

Bioinformatics based target predictions using the online tool, TargetScan with a focus on the Wnt/Ca^{2+} and TGFβ/BMP pathways (according to KEGG pathway [19] based map), predicted several targets for the miR-26a and miR-17. The details of this sorting and predictions can be found in our previous work [13]. The miRNAs and their potential targets with their seed matching regions are shown in Table 7-1. The predicted target regions were cloned into the pmirGLO Dual-Luciferase vector (target region inserted 3' of the firefly luciferase gene). The different clones were co-transfected with the predicted miRNAs separately into Hep2 cells. The clones were also co-transfected with miR-NC (as a negative control). The luciferase activities (Firefly-F and Renilla-R) were tested after 24 hours of transfections and the ratios were calculated (F/R).

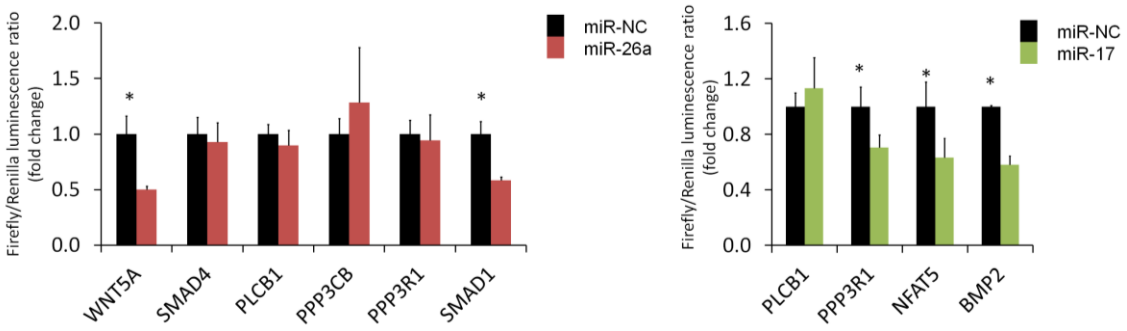

Figure 7-6: Target validation experiments for miR-26a and miR-17 using Dual-luciferase reporter assays. Lower relative firefly luminescence in miR-26a/miR-17 compared to miR-NC asserted WNT5A and SMAD1 as targets for miR-26a and PPP3R1, NFAT5 and BMP2 as targets for miR-17 (Fold changes in F/R ratios for miR-26a/miR-17 relative to miR-NC F/R ratios).

Fold changes were calculated as Ratio=$(F/R)_{miR\text{-}26a/miR17}/(F/R)_{miR\text{-}NC.}$ Ratios <1, were also noted as the negative reciprocal of the ratio (-1/Ratio). The WNT5A (FC: -2, p=0.007) (Wnt/Ca^{2+} pathway) and SMAD1 (FC: -1.7, p=0.004) (TGFβ/BMP pathway) showed statistically significant decline in F/R ratios with miR-26a. PPP3R1 (FC: -1.4, p=0.038), NFAT5 (FC: -1.5, p=0.048) (Wnt/Ca^{2+} pathway) and BMP2 (FC: -1.7, p=0.0004) (TGFβ/BMP pathway) showed significantly lower F/R ratios (miR-17/miR-NC). The relative Firefly/Renilla luciferase ratios (miR-26a or miR-17/miR-NC co-transfections) are shown in Figure 7-6.

7.3.5 TGFβ/BMP and Wnt/Ca^{2+} cross-talk

To test whether the Wnt/Ca^{2+} pathway and the TGFβ/BMP pathway influence each other's expression, activation and inhibition strategies were used. The impact of Wnt/Ca^{2+} pathway inhibition on the activation of the TGFβ/BMP pathway was tested using KN93 (selective Ca^{2+}/calmodulin-dependent protein kinase II inhibitor). Cells were stimulated with Humankine^{TM} recombinant BMP2 for 60 minutes and 120 minutes in the absence and presence of KN93. Simultaneously, un-stimulated controls (with and without KN93) were tested for activation of TGFβ/BMP pathway. No difference was observed in the level of expression of phospho-SMAD1/5/8 in presence or absence of KN93 (Figure 7-7A).

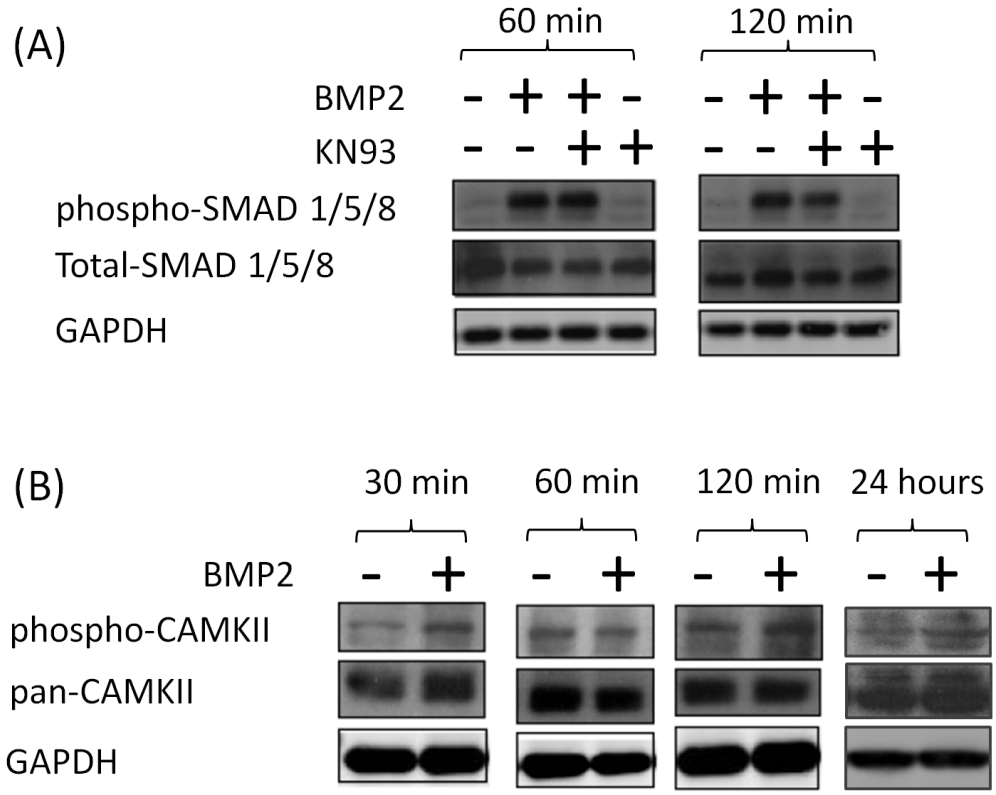

Figure 7-7: The TGFβ/BMP & Wnt/Ca^{2+} pathway cross-talk. (A) Human osteoprogenitor cells were stimulated with recombinant human BMP2 in presence or absence of KN93 (inhibitor of Wnt/Ca^{2+} pathway). Presence of KN93 did not change the level of activation of the TGFβ/BMP pathway (activation of phospho-SMAD1/5/8 - the read-out for the pathway). (B) Effect of stimulation of the TGFβ/BMP pathway on the activation of phospho-CAMKII and pan-CAMKII (read-outs for the Wnt/Ca^{2+} pathway). Higher expression of Wnt/Ca^{2+} pathway read-outs was observed when osteoprogenitor cells were stimulated with BMP2.

Therefore, inhibition of the Wnt/Ca^{2+} pathway did not seem to affect the activation/inhibition of the TGFβ/BMP pathway. Further, the influence of the activation of TGFβ/BMP pathway on the Wnt/Ca^{2+} pathway activation was also tested. Human osteoprogenitor cells were stimulated with recombinant human BMP2 (10 ng/ml), and the expression of phospho- and pan-CAMKII was evaluated using Western Blot. The expression of CAMKII was seen to increase in cells following stimulation with BMP2 indicating a positive influence of BMP2 stimulation on Wnt/Ca^{2+} pathway (Figure 7-7B).

7.3.6 Inhibition of miR-26a and miR-17 improves osteogenic differentiation on smooth surfaces

Synthetic inhibitors of miR-26a (i-miR-26a) and miR-17 (i-miR-17) were transfected into SAOS-2 cells and exposed to SMO (smooth/polished) titanium surfaces. A negative control miRNA inhibitor (i-miR-NC) was also transfected into SAOS-2 cells and incubated on SMO surfaces. qPCR analysis of BMP2 (TGFβ/BMP pathway) and WNT5A (Wnt/Ca^{2+} pathway) showed higher expression in i-miR-26a and i-miR-17 transfected cells (Figure 7-8A). The effect on the expression BMP2 seemed more prominent at day 1. In contrast to this, i-miR-26a and i-miR-17 were seen to have more striking effects on WNT5A at day 3. Osteogenic differentiation was initiated and the effects of inhibition of miR-26a and miR-17 on the mineralization and ALP activity on SMO surface (indicators of osteoblastic differentiation) were evaluated. Higher Alizarin Red S staining demonstrated increased deposition of calcified matrix with i-miR-26a and i-miR-17 after 7 days of culture on SMO surfaces (Figure 7-8B). A higher ALP activity was observed in i-miR-26a and i-miR-17 transfected cells cultured on SMO surfaces (Figure 7-8C). The results implied an accelerated osteogenic differentiation especially at an early stage following inhibition of miR-26a and miR-17.

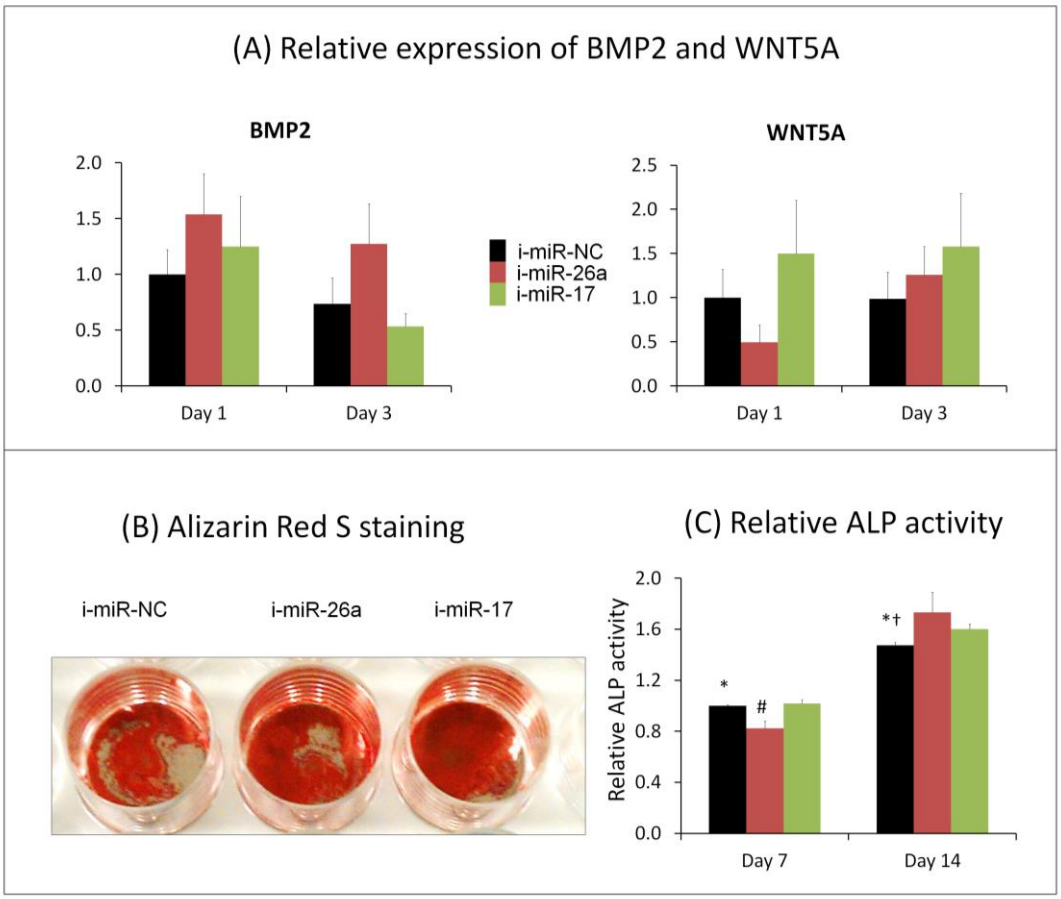

Figure 7-8: Effects of inhibitors of miR-26a (i-miR-26a) and miR-17 (i-miR-17) on smooth polished (SMO) surfaces. (A) Relative expression of BMP2 (TGFβ/BMP pathway) and WNT5A (Wnt/Ca^{2+} pathway) following transfection of i-miR-26a and i-miR-17 transfected cells on SMO surfaces. Higher expression BMP2 and WNT5A was observed with i-miR-26a and i-miR-17 (y-axis: fold change relative to i-miR-NC day 1). (B) Alizarin Red-S staining after 7 days of transfection with i-miR-26a and i-miR-17 and culturing on polished titanium surfaces (SMO) in osteogenic media. Higher staining was observed with i-miR-26a and i-miR-17 indicating enhanced osteogenic differentiation when miR-26a and miR-17 are inhibited. (C) Relative ALP activity on SMO surfaces in presence of i-miR-26a and i-miR-17 (y-axis: fold change to i-miR-NC day 7) (*: $p<0.05$ i-miR-NC vs. i-miR-26a; †: $p<0.05$ i-miR-NC vs. i-miR-17; #: $p<0.05$ i-miR-26a vs. i-miR-17).

7.4 DISCUSSION

Micro-roughened titanium implant surfaces like the topographically modified, SLA and the chemically modified hydrophilic, modSLA surfaces, have become established as dental implants with improved osseointegration properties compared with their smooth and polished counterparts. Several studies have been investigating the molecular mechanisms involved in improved osseointegration properties of these surfaces [9-13, 20-23]. Osseointegration, like any other biological process occurs as

a culmination of a complex cascade of genetic interactions, involving sequential pattern of activation of cell signaling pathways. MicroRNAs regulate the expression of genes at the translational level [1] and thus control the activation and repression of cell signaling processes involved in differentiation of cells and tissues.

Our recent studies have observed an early expression of cell signaling pathway molecules like the TGFβ/BMP and Wnt/Ca^{2+} on these surfaces and correlated them with the expression of microRNAs [12, 13]. Further, the microRNAs, miR-26a and miR-17 were found to have key cell signaling ligands of the Wnt/Ca^{2+} and TGFβ/BMP pathways as potential targets (miR-26a-WNT5A and miR-17-BMP2). These pathways are known to be activated during the process of osteogenic differentiation and osseointegration [24]. This study aimed at investigating the role of miR-26a and miR-17 in the early regulation of the key pro-osteogenic TGFβ/BMP and Wnt/Ca^{2+} signaling pathways during the process of osteogenesis. The study further explored the interaction of the TGFβ/BMP and Wnt/Ca^{2+} pathways to get an insight into how these pathways influence each other during osteogenesis.

The expression of miR-26a and miR-17 on modSLA, SLA, and SMO surfaces was tested using qPCR method. The relative lower expression of miR-26a and miR-17 on modSLA and SLA surfaces (compared with SMO), was evident within 6 hours of exposure of human osteoprogenitor cells to the titanium surfaces. This observation was in agreement with our previous study, where these miRNAs were seen to be downregulated on the modSLA and SLA surfaces compared with SMO following 24 hours of exposure [13]. Furthermore, the study also confirmed the higher expression of the key molecules of the TGFβ/BMP (BMP2 and BMP6) and Wnt/Ca^{2+} (WNT5A and FZD6) pathway genes. These findings are in agreement with the higher expression of TGFβ/BMP and Wnt/Ca^{2+} pathways on the topographically modified titanium surfaces as demonstrated in several studies [9-13].

The modSLA and SLA surfaces, by virtue of their micro-roughened topography and their ability to induce “contact osteogenesis” [25], are regarded as pro-osteogenic platforms akin to the bone micro-topography and are considered as physiologically relevant substrates to study the process of osteogenesis [12, 13]. We postulated that the miRNA and mRNA expression patterns on these surfaces are possibly a result of the pro-osteogenic response on these surfaces and tested whether these molecules are differentially regulated in osteo-inhibitory environments. To test

this supposition, osteogenic differentiation of osteoblastic cells was induced in absence (controls) or presence of TNFα - a pro-inflammatory cytokine that is known to create osteo-inhibitory conditions [26]. The osteo-inhibitory effect of pro-inflammatory cytokines was confirmed by observing relatively lower deposition of calcified matrix in presence of TNFα. The microRNAs, miR-26a and miR-17 were seen to be upregulated in presence of TNFα within 3 days. Simultaneously, the TGFβ/BMP (BMP2, SMAD4, SMAD5) and Wnt/Ca^{2+} pathway genes (especially WNT5A) were seen to be downregulated. The non-canonical Wnt/Ca^{2+} receptor FZD2 demonstrated variable expression and wasn't very conclusive. However, FZD2 was seen to be downregulated over the course of time between day 3 and day 7. Previously, Liu et al. had demonstrated the inhibition of Wnt/Ca^{2+} signaling pathway in inflammatory conditions [27] and this corroborates with our observations. They had also discussed higher expression and activation of Wnt/β-catenin pathway in inflammatory conditions. The expression of some of the members of the Wnt/β-catenin pathway genes was explored in this study as well; however, the results weren't conclusive to establish a trend (either activation/inhibition). The inhibition of TGFβ/BMP pathway in inflammatory conditions has been recorded in several studies [28-30].

The effects of miR-26a and miR-17 over-expression in osteoblastic cells were examined subsequently. Synthetic miR-mimics were transfected using chemical-based methods to induce transient transfections, such that we may be able to explore their impact on the TGFβ/BMP and Wnt/Ca^{2+} pathways. Comparisons between the miR-NC samples and untransfected controls did not show any significant differences and hence strengthened the suitability of the experimental model and study comparisons. Therefore, to keep all parameters consistent, subsequent comparisons were made with miR-NC as the control. The miRNA mimics were transfected and osteogenic differentiation was induced following transfections. Gene and protein expression, ALP activity and Alizarin Red S staining were performed at different time-points. The effects of miR-26a and miR-17 on the cell signaling pathways were most evident at the earlier time-points (days 1 and 3). The later time-points (days 7 and 14) were found to have relatively higher gene expression for most of the molecules. This could possibly be attributed to the fact that the initial inhibitory effect of the miRNAs on the signaling pathways becomes unmasked. These

unmasked cells, in presence of osteogenic supplements start expressing the pro-osteogenic signaling molecules. Pro-osteogenic cell signaling processes peak during the early stages of differentiation and start waning following the initial highs, leading to lower expression of signaling molecules with a synchronized increase in expression of differentiation markers. The diminution in cell signaling molecules over a time-course during osteogenesis has been reported previously [12, 14]. Therefore, the relative higher expression of cell signaling molecules observed at later time-points in miR-26a and miR-17 overexpressing cells is possibly because the unmasked cells, in presence of osteogenic supplements start expressing the pro-osteogenic signaling molecules at a later time-point and this is observed to be higher compared to miR-NC, where the signaling peaks have started waning. The early inhibition of the pro-osteogenic TGFβ/BMP and Wnt/Ca^{2+} pathways was clearly seen to delay the process of osteogenic differentiation (Figure 7-5).

The early impact of miR-26a and miR-17 on TGFβ/BMP and Wnt/Ca^{2+} pathways was evident at the level of the protein read-outs for the pathways. Activation of the TGFβ/BMP pathway leads to phosphorylation of SMAD1/5/8 and therefore, decreased levels of phospho-SMAD1/5/8 indicate a reduced activation of the pathway [31, 32]. The Ca^{2+}/calmodulin-dependent protein kinase (CAMKII) is a molecule that gets activated upon stimulation of the Wnt/Ca^{2+} pathways. Upon activation of the non-canonical Wnt pathway, Ca^{2+}/calmodulin activates the protein CAMKII, which soon becomes auto-phosphorylated. CAMKII (including phospho-CAMKII) is established as a read-out of the non-canonical Wnt/Ca^{2+} pathway [33]. Over-expressing miR-26a and miR-17 demonstrated reduced activation of both of the pathways. Lower activation of CAMKII was observed with both miR-26a and miR-17 at days 1 and 3 (especially phospho-CAMKII with miR-26a and pan-CAMKII with miR-17 – Figure 7-4). The phosphorylation of SMAD1/5/8 was also seen to be reduced with miR-26a and miR-17 (Figure 7-4).

Targetscan's seed-based algorithm [34] predicted several targets genes in the TGFβ/BMP and Wnt/Ca^{2+} pathways (Table 7-1). Experimental validation of these potential targets indicated WNT5A and SMAD1 as targets for miR-26a and PPP3R1, NFAT5 and BMP2 as targets for miR-17, thereby confirming that their influence on the TGFβ/BMP and Wnt/Ca^{2+} pathways is actually via an RNA-interference mediated mechanism. Targeting the key ligands for both of the pathways (WNT5A

and BMP2) implies an inhibition of the initiation for the pathways. This coupled with the decreased expression of the read-outs of the pathways (CAMKII and phospho-SMADs) confirmed the regulation of both of the cell signaling pathways by miR-26a and miR-17. Inhibition of osteogenic differentiation following transient transfections with miR-26a and miR-17 further elaborates the significance of early activation of the TGFβ/BMP and Wnt/Ca^{2+} pathways in the process of osteogenesis. Previously, other groups have reported the regulation of lineage commitment between osteogenesis and adipogenesis by miR-17 targeting BMP2 [35]; and miR-26a has been shown to modulate osteogenic response by targeting SMAD1 [14]. Although, a couple of studies have discussed the promotion of osteogenic differentiation with miR-26a [36, 37], other reports have discussed its negative influence on osteogenesis [4, 14]. Studies showing improved osteogenesis have either reported an increased expression of miR-26a at a late time-point during differentiation [36], or had a sustained delivery of miR-26a using an *in vivo* delivery system [37]. Further, this *in vivo* study had also described higher mineralization in mesenchymal stem cells (BMMSCs) with miR-26a mimic. This could possibly be attributed to the sustained high levels of miR-26a as observed in transfected samples in their study, as opposed to a steady decline in the fold-change levels of miR-26a (between miR-26a transfected and negative controls) in our study. The increasing levels of the expression of genes of TGFβ/BMP and Wnt/Ca^{2+} pathways at later time-points (miR-26a compared with controls) as observed in here are also in agreement with this. Moreover, the protein expression of osteogenic markers, RUNX2 and OCN do not seem to differ much between mimics and controls in their study [37]. Although, the RUNX2 and OCN gene expression were seen to be higher in miR-26a mimic, yet on a time-course analysis for the mimic, it was seen to be gradually decreasing between 2 and 14 days.

The dual-luciferase reporter assay technique incorporating putative short target sequences (based on bioinformatics-based predictions) is an established model for target validation experiments for miRNAs [38]. Target predictions for miR-26a and miR-17 were performed using the online tool, TargetScan and only the targets showing these miRNAs as “representative miRNAs” (based on the context scores calculated) were chosen for analysis. These putative targets were screened for genes of the TGFβ/BMP and Wnt/Ca^{2+} pathways. The details for this analysis maybe found

in our previous work [13]. The target regions for miR-26a and miR-17 were inserted 3' of the firefly luciferase gene of pmirGLO Dual-Luciferase miRNA Target Expression vector. A significant drop in firefly luciferase signal (luminescence was normalized to the Renilla internal control) was observed with miR-17-PPP3R1, miR-17-NFAT5, miR-17-BMP2, miR-26a-WNT5A and miR-26a-SMAD1 and therefore both of the miRNAs were seen to have targets in TGFβ/BMP and Wnt/Ca^{2+} pathways.

The results from the study substantiated that the repression of the TGFβ/BMP and Wnt/Ca^{2+} pathways delays the process of osteogenesis. Activation of TGFβ/BMP pathway during osteogenesis has been established for long [39]. The role of Wnt/Ca^{2+} pathway in osteogenic differentiation is being unraveled only recently [27]. To explore the relationship between these two pathways, the TGFβ/BMP cascade was stimulated using BMP2 in presence and absence of KN93. KN93 is a potent inhibitor of the non-canonical Wnt/Ca^{2+} pathway [40]. No difference in the level of phosphorylation of SMAD1/5/8 was observed in presence or absence of KN93, indicating that the TGFβ/BMP pathway is independent of the stimulation of Wnt/Ca^{2+} pathway. In contrast to this, stimulation with BMP2 was seen to increase the level of expression of CAMKII (Figure 7-7). This indicates a positive influence of the TGFβ/BMP pathway on the activation of the Wnt/Ca^{2+} pathway. Other studies have also suggested that the non-canonical Wnt/Ca^{2+} pathway is activated following the stimulation of the TGFβ/BMP pathway [41, 42]. In fact, the non-canonical Wnt ligand, WNT5A is known to be under the influence of BMP2 guided pathways during osteogenesis [41]. Although, a previous study by Olivares–Navarrete et al. had described the stimulation of BMP2 and BMP4 when cultures on micro-roughened modSLA and SLA surfaces were supplemented with WNT5A [20]; however, unlike in this study, they did not explore the effects of blocking the Wnt/Ca^{2+} pathway. Their findings could possibly be attributed to stimulation of the BMP molecules via other WNT5A-guided mechanisms beyond the Wnt/Ca^{2+} pathway. Indeed, a more detailed exploration of these interactions with more sophisticated techniques like gene knock-out models in the future, may divulge greater details regarding the complex interactions between the two pathways.

Finally, the study observed an accelerated mineralization and osteogenic differentiation along with relatively higher expression of BMP2 and WNT5A on

polished titanium surfaces upon the use of i-miR-26a and i-miR-17 (inhibitors), thereby highlighting the impact of eliminating the inhibitors of the pro-osteogenic signaling pathways in the early phase of differentiation.

7.5 CONCLUSION

Modulation of pro-osteogenic cell signaling pathways, TGFβ/BMP and Wnt/Ca^{2+} by microRNAs is imperative in the process of osteogenic differentiation *in vitro* and osseointegration *in vivo.* miR-26a and miR-17 mimics were seen to repress the expression of several key molecules of the TGFβ/BMP and Wnt/Ca^{2+} pathways in the early phase of osteogenic differentiation and thereby delaying the osteogenic processes. The use of synthetic inhibitors (i-miR-26a and i-miR-17) during early phase of osteodifferentiation on polished titanium surfaces was found to accelerate the process of osteogenesis. It is concluded that the use of modulators for miR-26a and miR-17 may be considered to improve osseointegration of titanium surfaces, which may be more beneficial in clinically demanding situations, like in regions with compromised bone formation thereby allowing faster osseointegration.

7.6 REFERENCES

[1] Bartel DP. MicroRNAs: target recognition and regulatory Functions. Cell 2009;136:215-33.

[2] Xu P, Vernooy SY, Guo M, Hay BA. The Drosophila microRNA miR-14 suppresses cell death and is required for normal fat metabolism. Current Biol 2003;13:790-5.

[3] Shivdasani RA. MicroRNAs: regulators of gene expression and cell differentiation. Blood 2006;108:3646-53.

[4] Lian JB, Stein GS, van Wijnen AJ, Stein JL, Hassan MQ, Gaur T, et al. MicroRNA control of bone formation and homeostasis. Nat Rev Endocrinol 2012;8:212-27.

[5] Palmieri A, Pezzetti F, Avantaggiato A, Lo Muzio L, Scarano A, Rubini C, et al. Titanium acts on osteoblast translational process. J Oral Implantol 2008;34:190-5.

[6] Buser D, Schenk RK, Steinemann S, Fiorellini JP, Fox CH, Stich H. Influence of surface characteristics on bone integration of titanium implants. A histomorphometric study in miniature pigs. J Biomed Mater Res 1991;25:889-902.

[7] Buser D, Broggini N, Wieland M, Schenk RK, Denzer AJ, Cochran DL, et al. Enhanced bone apposition to a chemically modified SLA titanium surface. J Dent Res 2004;83:529-33.

[8] Osborn J, Newesely H. Dynamic aspects of the implant-bone interface. In: Heimke G, editor. Dental implants: Materials and Systems: München: Carl Hanser Verlag; 1980. p. 111-23.

[9] Vlacic-Zischke J, Hamlet SM, Friis T, Tonetti MS, Ivanovski S. The influence of surface microroughness and hydrophilicity of titanium on the up-regulation of TGFbeta/BMP signalling in osteoblasts. Biomaterials 2011;32:665-71.

[10] Olivares-Navarrete R, Hyzy SL, Hutton DL, Dunn GR, Appert C, Boyan BD, et al. Role of non-canonical Wnt signaling in osteoblast maturation on microstructured titanium surfaces. Acta Biomater 2011;7:2740-50.

[11] Ivanovski S, Hamlet S, Salvi GE, Huynh-Ba G, Bosshardt DD, Lang NP, et al. Transcriptional profiling of osseointegration in humans. Clin Oral Implants Res 2011;22:373-81.

[12] Chakravorty N, Hamlet S, Jaiprakash A, Crawford R, Oloyede A, Alfarsi M, et al. Pro-osteogenic topographical cues promote early activation of osteoprogenitor differentiation via enhanced TGFbeta, Wnt, and Notch signaling. Clin Oral Implants Res 2014;25:475-86.

[13] Chakravorty N, Ivanovski S, Prasadam I, Crawford R, Oloyede A, Xiao Y. The microRNA expression signature on modified titanium implant surfaces influences genetic mechanisms leading to osteogenic differentiation. Acta Biomater 2012;8:3516-23.

[14] Luzi E, Marini F, Sala SC, Tognarini I, Galli G, Brandi ML. Osteogenic differentiation of human adipose tissue-derived stem cells is modulated by the miR-26a targeting of the SMAD1 transcription factor. J Bone Miner Res 2008;23:287-95.

[15] Hamlet S, Alfarsi M, George R, Ivanovski S. The effect of hydrophilic titanium surface modification on macrophage inflammatory cytokine gene expression. Clin Oral Implants Res 2012;23:584-90.

[16] Haase HR, Ivanovski S, Waters MJ, Bartold PM. Growth hormone regulates osteogenic marker mRNA expression in human periodontal fibroblasts and alveolar bone-derived cells. J Periodontal Res 2003;38:366-74.

[17] Xiao Y, Haase H, Young WG, Bartold PM. Development and transplantation of a mineralized matrix formed by osteoblasts in vitro for bone regeneration. Cell Transplant 2004;13:15-25.

[18] Xiao Y, Qian H, Young WG, Bartold PM. Tissue engineering for bone regeneration using differentiated alveolar bone cells in collagen scaffolds. Tissue Eng 2003;9:1167-77.

[19] Kanehisa M, Goto S. KEGG: Kyoto encyclopedia of genes and genomes. Nucleic Acids Res 2000;28:27-30.

[20] Olivares-Navarrete R, Hyzy SL, Park JH, Dunn GR, Haithcock DA, Wasilewski CE, et al. Mediation of osteogenic differentiation of human mesenchymal stem cells

on titanium surfaces by a Wnt-integrin feedback loop. Biomaterials 2011;32:6399-411.

[21] Olivares-Navarrete R, Hyzy SL, Hutton DL, Erdman CP, Wieland M, Boyan BD, et al. Direct and indirect effects of microstructured titanium substrates on the induction of mesenchymal stem cell differentiation towards the osteoblast lineage. Biomaterials 2010;31:2728-35.

[22] Olivares-Navarrete R, Raz P, Zhao G, Chen J, Wieland M, Cochran DL, et al. Integrin alpha2beta1 plays a critical role in osteoblast response to micron-scale surface structure and surface energy of titanium substrates. Proc Natl Acad Sci U S A 2008;105:15767-72.

[23] Olivares-Navarrete R, Hyzy S, Wieland M, Boyan BD, Schwartz Z. The roles of Wnt signaling modulators Dickkopf-1 (Dkk1) and Dickkopf-2 (Dkk2) and cell maturation state in osteogenesis on microstructured titanium surfaces. Biomaterials 2010;31:2015-24.

[24] Deng ZL, Sharff KA, Tang N, Song WX, Luo J, Luo X, et al. Regulation of osteogenic differentiation during skeletal development. Front Biosci 2008;13:2001-21.

[25] Berglundh T, Abrahamsson I, Lang NP, Lindhe J. De novo alveolar bone formation adjacent to endosseous implants. Clin Oral Implants Res 2003;14:251-62.

[26] Wahl EC, Aronson J, Liu L, Fowlkes JL, Thrailkill KM, Bunn RC, et al. Restoration of regenerative osteoblastogenesis in aged mice: modulation of TNF. J Bone Miner Res 2010;25:114-23.

[27] Liu N, Shi S, Deng M, Tang L, Zhang G, Ding B, et al. High levels of beta-catenin signaling reduce osteogenic differentiation of stem cells in inflammatory microenvironments through inhibition of the noncanonical Wnt pathway. J Bone Miner Res 2011;26:2082-95.

[28] Zhu NL, Li C, Huang HH, Sebald M, Londhe VA, Heisterkamp N, et al. TNF-alpha represses transcription of human Bone Morphogenetic Protein-4 in lung epithelial cells. Gene 2007;393:70-80.

[29] Yamazaki M, Fukushima H, Shin M, Katagiri T, Doi T, Takahashi T, et al. Tumor necrosis factor alpha represses bone morphogenetic protein (BMP) signaling by interfering with the DNA binding of Smads through the activation of NF-kappaB. J Biol Chem 2009;284:35987-95.

[30] Li Y, Li A, Strait K, Zhang H, Nanes MS, Weitzmann MN. Endogenous TNFalpha lowers maximum peak bone mass and inhibits osteoblastic Smad activation through NF-kappaB. J Bone Miner Res 2007;22:646-55.

[31] Kretzschmar M, Liu F, Hata A, Doody J, Massague J. The TGF-beta family mediator Smad1 is phosphorylated directly and activated functionally by the BMP receptor kinase. Genes Dev 1997;11:984-95.

[32] Massague J. How cells read TGF-beta signals. Nat Rev Mol Cell Biol 2000;1:169-78.

[33] Kuhl M, Pandur P. Measuring CamKII activity in Xenopus embryos as a read-out for non-canonical Wnt signaling. Methods Mol Biol 2008;468:173-86.

[34] Lewis BP, Burge CB, Bartel DP. Conserved seed pairing, often flanked by adenosines, indicates that thousands of human genes are microRNA targets. Cell 2005;120:15-20.

[35] Li H, Li T, Wang S, Wei J, Fan J, Li J, et al. miR-17-5p and miR-106a are involved in the balance between osteogenic and adipogenic differentiation of adipose-derived mesenchymal stem cells. Stem Cell Res 2013;10:313-24.

[36] Trompeter HI, Dreesen J, Hermann E, Iwaniuk KM, Hafner M, Renwick N, et al. MicroRNAs miR-26a, miR-26b, and miR-29b accelerate osteogenic differentiation of unrestricted somatic stem cells from human cord blood. BMC Genomics 2013;14:111.

[37] Li Y, Fan L, Liu S, Liu W, Zhang H, Zhou T, et al. The promotion of bone regeneration through positive regulation of angiogenic-osteogenic coupling using microRNA-26a. Biomaterials 2013;34:5048-58.

[38] Jin Y, Chen Z, Liu X, Zhou X. Evaluating the microRNA targeting sites by luciferase reporter gene assay. Methods Mol Biol 2013;936:117-27.

[39] Huang W, Yang S, Shao J, Li YP. Signaling and transcriptional regulation in osteoblast commitment and differentiation. Front Biosci 2007;12:3068-92.

[40] Kaneuji T, Ariyoshi W, Okinaga T, Toshinaga A, Takahashi T, Nishihara T. Mechanisms involved in regulation of osteoclastic differentiation by mechanical stress-loaded osteoblasts. Biochem Biophys Res Commun 2011;408:103-9.

[41] Nemoto E, Ebe Y, Kanaya S, Tsuchiya M, Nakamura T, Tamura M, et al. Wnt5a signaling is a substantial constituent in bone morphogenetic protein-2-mediated osteoblastogenesis. Biochem Biophys Res Commun 2012;422:627-32.

[42] Choi YH, Choi JH, Oh JW, Lee KY. Calmodulin-dependent kinase II regulates osteoblast differentiation through regulation of Osterix. Biochem Biophys Res Commun 2013;432:248-55.

Chapter 8: General Discussion

8.1 INTRODUCTION

Osseointegration is a biological phenomenon that results in the structural and functional integration of an implant surface with the surrounding bone. This process shapes the structural framework and eventually helps in healing a fractured bone to regain its original shape. Implants are also known to provide the foundation for restoration of missing parts of the skeleton, as in case of dental implants. Implants are routinely used in cosmetic dentistry and have become the mainstream modality to restore lost or damaged parts of teeth. Since the inception of the concept of osseointegration by Prof. Brånemark in the 1950s and -60s [1, 2], titanium has remained the material of choice for dental implants, owing to its properties like high strength-to-weight ratio, resistance to corrosion and inertness to body fluids. The continued search to achieve faster and better osseointegration has lead researchers to experiment with various structural and topographical modifications. Micro-roughened titanium implants are known to osseointegrate better compared with their machined and polished counterparts [3].

Research on the topographical modifications of titanium led to the development of the sand-blasted, large grit, acid-etched (SLA) dental implants by Institut Straumann AG (Waldenburg, Switzerland). *In vivo* and *in vitro* experimental evidences have proven its superior osseointegration and bone formation properties compared with smooth surfaces [4, 5] and it remains the gold standard in implant dentistry since its introduction in the clinics in 1994. Subsequently, Straumann designed another modification of the SLA surface to achieve higher wettability, and created the chemically modified hydrophilic, modSLA (also known as SLActive®) surface. The hydrophilic modification is known to improve osseointegration further [6] and achieve faster healing *in vivo* [7]. Both SLA and modSLA implants have been known to have a similar surface architecture, when visualized using scanning electron microscope (SEM) and atomic force microscope (AFM) [8, 9].

Micro-roughened titanium surfaces like the SLA and modSLA surfaces are known to induce osseointegration by the principle of “contact osteogenesis” wherein new bone formation occurs directly on the implant surface as described by Osborn and Newesley [10, 11] and therefore, serve as interesting models to study osteogenic differentiation and osseointegration. Although, several studies have reported the improved osseointegration and bone formation properties of modified surfaces, the

underlying molecular mechanisms responsible for the improved osteogenic properties have been difficult to identify. Previous studies on the modSLA and SLA surfaces had demonstrated differential regulation of several genes on them; however, an organized study identifying and describing the molecular sequence of events was missing. Therefore, this PhD project used a structured approach to study the regulation of key molecular cascades on these surfaces, by microRNAs that are known to modulate gene expression in biological processes. The project subsequently studied the regulation of the two most consistently activated pro-osteogenic cell signaling pathways (TGFβ/BMP and Wnt/Ca^{2+} pathways) by two miRNAs (miR-26a and miR-17) that were observed to be differentially regulated on the modSLA and SLA surfaces compared with SMO surfaces.

8.2 THE STUDIES

MicroRNAs are small RNA molecules that influence patterns of gene expression and eventually mediate various biological processes, like osseointegration, by translational repression and gene silencing [12]. MicroRNAs, by virtue of their functional mechanisms, come in action immediately before gene expression. Therefore, in order to determine the microRNAs modulating the molecular mechanisms for improved osteogenic effects of modSLA and SLA surfaces, it was important to identify an early time-point that demonstrated a pro-osteogenic genetic profile on the modSLA and SLA surfaces compared with SMO (smooth polished) titanium surfaces. Although, several studies had demonstrated the early modulation of gene expression on the topographically modified titanium implants like, modSLA and SLA surfaces [9, 13, 14], yet none of the studies looked into the initial interactions of osteogenic cells with these topographically modified implant surfaces and how these interactions lead to the generation of a pro-osteogenic niche. Therefore the first part of this project aimed at exploring the early interactions of osteoprogenitor cells with SLA surfaces using a whole genome transcriptomic profile in comparison with SMO surfaces.

The study wanted to assess the early course of molecular events and microarray technology with its potential to measure the expression levels of large numbers of genes simultaneously, was considered as one of the most adept techniques to evaluate these changes at the transcriptome level. Experimental observations from our group have shown that osteoblasts, like other adherent cells,

attach to the substrates within the first three hours of exposure; and therefore, the earliest molecular events guiding them towards osteogenic differentiation were expected to happen after 3 hours. This prompted us to analyze the microarray gene expression pattern firstly after 3 hours of exposure to the titanium surfaces and subsequently at 24 hours. The differentially expressed genes were categorized into functional clusters using the Database for Annotation, Visualization and Integrated Discovery (DAVID) [15] and Ingenuity Pathways Analysis (IPA) tool (Ingenuity® Systems, www.ingenuity.com, Redwood City, CA, USA) to find the genetically enriched biological processes.

The microarray study revealed a clearly evident pro-osteogenic response on SLA surfaces compared with SMO surfaces after 24 hours of exposure, and this wasn't obvious at 3 hours. This observation laid the foundation for the next stage of the project where the microRNA expression profile was investigated. The temporal comparisons for SLA and SMO surfaces (especially 3 hours) in the microarray study revealed a pro-angiogenic and immunomodulatory response on the SLA surfaces that wasn't observed on the SMO surface. These interactions indicate a preparatory phase before the actual process of osteogenesis. Previous studies using endothelial progenitor cells and macrophage-like cells had also demonstrated similar pro-angiogenic [16] and immunomodulatory effects [17] on topographically modified surfaces. Similar effects using osteoprogenitor cells as observed here recognize the contributory role of osteogenic cells on these "pre-osteogenic" biological processes. Enrichment of pro-osteogenic clusters after 24 hours of exposure confirmed the early osteogenic response of topographically modified titanium surfaces. A striking observation from this part of the work was the upregulation of the bone morphogenetic protein-2 (BMP2) gene (fold change=5.7) (SLA compared with SMO), which is known to activate the functioning of the TGFβ/BMP pathway - a pathway known to be instrumental in the osteogenic differentiation process [18, 19]. This was substantiated even in the subsequent studies, where TGFβ/BMP pathway in general and the BMP2 molecule in particular were found to be consistently upregulated on the modified titanium surfaces [8, 9].

The study also confirmed higher deposition of minerals (calcium and phosphorus) in cultures on SLA surfaces compared with SMO surfaces and this was indicative of higher osteogenic differentiation on modified surfaces. Improved *in vitro* osteogenic differentiation may be considered as a reflection of the ameliorated

in vivo osseointegration properties of topographically modified surfaces compared to SMO surfaces.

The second part of the project focused on investigating the role of microRNAs in the process of osteogenic differentiation on micro-roughened surfaces. As described above, the microarray expression analysis established a clear pro-osteogenic genetic profile on modified titanium surfaces compared with SMO surfaces following 24 hours of exposure. To study whether the differential gene expression on topographically modified titanium surfaces is an outcome of the microRNA regulation, this part of the project explored the microRNA expression profile on the modified titanium implant surfaces in comparison with SMO surfaces following 24 hours of exposure. The chemically modified hydrophilic titanium (modSLA) surface was included in the study owing to the further improvement in osseointegration (compared to SLA) as demonstrated in recent studies [7, 20-22].

The microRNA study, firstly affirmed the higher expression of key genes already known to be differentially expressed on the modSLA and SLA surfaces compared with SMO surfaces [13, 23, 24], in order to ascertain the pro-osteogenic response of modSLA and SLA surfaces at 24 hours. BMP2, BMP6, ACVR1 (TGFβ/BMP pathway), WNT5A, FZD6 (Wnt/Ca^{2+} pathway), ITGB1 and ITGA2 (integrins) showed higher expression on modSLA and SLA surfaces compared with SMO surfaces after 24 hours of exposure. Subsequently, the microRNA expression profile on modSLA, SLA and SMO surfaces was evaluated. The Human Cell Development & Differentiation miRNA PCR Array (SABiosciences, Frederick, Maryland, USA) was selected as the panel of microRNAs to be tested for this purpose. Using this array enabled us to specifically study the microRNAs that are known to be instrumental in the process of cell differentiation. Moreover, studying a select panel of miRNAs allowed the use of a PCR-based technique which is more stringent rather than a microarray [25]. Further, the miRNA expressions were normalized to the mean expression of three endogenous small RNA controls - SNORD47, SNORD44, and RNU6-2, allowing for more stringent comparisons.

Analysis of the expression profile for the microRNAs revealed several miRNAs to be down-regulated on the modSLA and SLA surfaces compared with SMO surfaces. It is worth noting that majority of the miRNAs found to be down-regulated were common to both modSLA and SLA. Similar observation was made for the miRNAs that were upregulated on the micro-roughened surfaces. Among the

different miRNAs upregulated on modSLA and SLA, eight were common to both. Relatively minor differences were observed between the expression profile on modSLA and SLA surfaces, with a general trend towards lower expression on modSLA surfaces compared with SLA surfaces. These findings were further strengthened when the activation of cell signaling genes was studied in the subsequent part of the project. Both of the modified surfaces were seen to have higher expression of key regulatory genes of pro-osteogenic cell signaling pathways, (specifically the TGFβ/BMP, non-canonical Wnt/Ca^{2+} and Notch pathways) compared with the smooth surface. Only minor differences in the gene expression were observed between modSLA and SLA surfaces. These observations suggest that the surface micro-roughness feature of modSLA and SLA surfaces has a greater role to play in the pro-osteogenic molecular interactions of osteoprogenitor cells with titanium surfaces. The superior osseointegration of modSLA compared with SLA as seen in *in vivo* settings could possibly be due the interaction of cells that do not belong to osteogenic lineage (e.g. blood cells), which come in contact with the surfaces earlier than the MSCs and osteoblasts.

The microRNA expression profile study further explored the correlation between the downregulation of miRNAs and the upregulation of TGFβ/BMP and non-canonical Wnt/Ca^{2+} pathways on modSLA and SLA surfaces, using bioinformatics-based prediction models (TargetScan). TargetScan is an online bioinformatics tool that can predict targets for miRNAs by identifying potential binding sites in the mRNA 3' UTR region. TargetScan was specifically chosen as the prediction tool owing to its context score assigning algorithm for miRNAs, which according to Witkos et al., is the only existing model that correlates well even at the protein level [26]. They further commented that among the various target prediction tools, TargetScan with a precision of 51% and a sensitivity of 12% is the only tool, besides PicTar, whose prediction results match well at the *in vivo* level as well. TargetScan predictions demonstrated several genes of the TGFβ/BMP and non-canonical Wnt/Ca^{2+} pathways to be putative targets for the downregulated miRNAs and hence a potential regulation of these pathways during the process of bone formation on micro-roughened surfaces emerged as a possible reason for their superior osteogenicity. As Notch pathway genes were also seen to be upregulated on the micro-roughened surfaces, a potential regulation of the Notch pathway was also explored; however no noteworthy findings were observed. This possibly indicates the

role of “non-miRNA” mediated mechanisms for the stimulation of this pathway during osteogenesis on micro-roughened surfaces. The target predictions also revealed several inhibitors of osteogenesis as potential targets for the upregulated miRNAs, suggesting other pro-osteogenic mechanisms that get triggered following the interaction of micro-rough surfaces with osteoblastic cells. The findings from this part of the study advocated for further in-depth functional studies to be under-taken to understand the molecular regulation of pro-osteogenic cell signaling pathways by microRNAs during osteogenesis.

The existing literature and empirical findings from the project were suggestive of the differential regulation of several genes belonging to various cell signaling pathways and especially the TGFβ/BMP and Wnt/Ca^{2+} pathways [13, 24, 27-29]. However, none of the previous studies had used a comprehensive approach to explore the cell signaling pathways stimulated on the topographically modified surfaces. Further, as described above, the previous part of the project had observed downregulation of several miRNAs that had putative targets in the TGFβ/BMP and Wnt/Ca^{2+} pathways. Thus, the next part of the project aimed to identify the response of key cell signaling pathways in osteoprogenitor cells, following 24 and 72 hours exposure to modSLA & SLA surfaces in comparison with SMO surfaces. For this purpose, human alveolar osteoprogenitor cells were cultured on modSLA, SLA, and SMO surfaces for 24 and 72 hours. A PCR-based array technique (Human Stem Cell Signaling PCR Array - SABiosciences, Frederick, MD, USA) with its potential to examine the expression of a large set of genes from relatively small quantities of experimental samples allowed us to investigate the activation and upregulation of various cell signaling pathways simultaneously.

The key regulatory genes from the TGFβ/BMP, Wnt (especially the non-canonical Wnt/Ca^{2+}) and Notch pathways were upregulated on the modified surfaces. The findings correlated with higher expression of osteogenic markers on modSLA and SLA surfaces. These findings demonstrated that the activation of the pro-osteogenic cell signaling pathways on modSLA and SLA surfaces leads to enhanced osteogenic differentiation and provided a mechanistic insight into the superior osseointegration properties of modSLA and SLA surfaces as seen *in vivo*. Enhanced osteogenic differentiation on the modified surfaces was confirmed by the higher mineralization on modSLA and SLA surfaces. Further, the comparisons between 24 and 72 hours showed a relative lower expression of cell signaling pathway genes at

72 hours on all the surfaces, which further justified our 24 hour time-point for studying the microRNA expression profile. Pro-osteogenic molecular responses are thus shown to be triggered early during the interaction of osteoblastic cells with modified surfaces. Therefore, miRNAs guiding these changes need to respond early in this process as well. The results from the miRNA expression profiling study confirmed this conjecture. Further, phenotypic changes in osteoprogenitor cells cultured on titanium surfaces for 24 and 72 hours showed increase in the number of surface granules, possibly indicating increased protein synthesis. This could additionally mean that the cells start exhibiting more maturing phenotypes to prepare and nurture the osteogenic niche. As discussed above, the relatively minor differences between the modSLA and SLA surfaces further reinforced the fact that topographical modifications of implant surfaces have a greater impact on their osteogenic properties, than chemical alterations.

Although, the initial parts of this project demonstrated that several of the microRNAs showing lower expression on modSLA and SLA surfaces (compared with SMO) have putative targets in the TGFβ/BMP and Wnt/Ca^{2+} pathways that correlated well with the higher expression of these pathways; yet studies confirming the functional regulation of these two pathways by miRNAs during osteogenesis were still lacking. Therefore, the final part of the project explored the regulatory role of two microRNAs (miR-26a and miR-17) on the TGFβ/BMP and Wnt/Ca^{2+} pathways during osteogenesis. The microRNAs, miR-26a and miR-17 were specifically selected for the following reasons:

- Both miR-26a and miR-17 were observed to be downregulated on the modSLA and SLA surfaces compared with SMO.
- The microRNAs, miR-26a and miR-17 were found to have putative targets in TGFβ/BMP and Wnt/Ca^{2+} pathways.
- More importantly, miR-26a was seen to be potentially targeting the key non-canonical Wnt/Ca^{2+} pathway ligand, WNT5A and miR-17 was found to target the key TGFβ/BMP ligand, BMP2.

This study used synthetic miRNA mimics owing to concerns with expression levels for miRNAs achieved with plasmid-based techniques. Moreover, the primary purpose of the study was to investigate the early effects of miRNAs on the cell signaling pathways and so transient transfections with miRNA mimics were suitable for the purpose. In order to investigate deeper into the molecular signaling during

osteogenic differentiation, the study explored the cross-talk between the two cell signaling pathways as well.

The expression of miR-26a and miR-17 on the modified titanium surfaces following 6 hours of culturing confirmed a lower expression on modSLA and SLA surfaces compared to SMO surfaces. This was seen to guide the higher expression of important molecules of the TGFβ/BMP (BMP2 and BMP6) and Wnt/Ca^{2+} pathways (WNT5A and FZD6) at 24 hours. These findings substantiate the previous findings of the project as described earlier. The regulatory role of miR-26a and miR-17 on the cell signaling pathways was evaluated subsequently using synthetic miRNA mimics. Inducing osteogenic differentiation in human osteoblast-like SAOS-2 cells following transfection of these miRNAs, demonstrated delayed mineralization and ALP activity compared to negative controls. Simultaneously, the TGFβ/BMP and Wnt/Ca^{2+} pathways showed reduced expression in miR-26a and miR-17 transfected cells suggesting an inhibitory impact on both pathways. This strengthens the supposition that early downregulation of miRNAs on modSLA and SLA surfaces potentially release the inhibitory effects on the signaling pathways, thereby inducing their expression. Luciferase target confirmation assays confirmed several molecules of the two pathways as targets for miR-26a and miR-17. Further, the TGFβ/BMP & Wnt/Ca^{2+} pathway cross-talk experiments suggest that the Wnt/Ca^{2+} pathway acts downstream to the TGFβ/BMP pathway. Finally, the study using inhibitors of miR-26a & miR-17 showed higher osteogenic differentiation on polished titanium surfaces suggesting an accelerated osteogenic differentiation; and thereby demonstrated the potential of enhancing osteogenesis and possibly osseointegration especially in regions with compromised bone.

Figure 8-1 summarizes the overall study design and the key findings of the project. All the findings of the project taken together indicate towards an intricate miRNA modulated control of the TGFβ/BMP and Wnt/Ca^{2+} cell signaling pathways during osteogenesis. The initial interactions of osteoblastic cells seem to have a complementary role in preparation of the cellular niche by stimulating vascular and immunological processes, in an effort to make the environment conducive for osteogenic differentiation. Following the initial activity, the early events on modified surfaces clearly show the triggering of "pro-osteogenic" mechanisms and stimulation of the osteogenic differentiation process. Thus, miRNAs having inhibitory action on the "pro-osteogenic" cell signaling pathways (specifically the TGFβ/BMP and

Wnt/Ca^{2+}) tend to get suppressed on the modSLA and SLA surfaces and this possibly withdraws the inhibitory effects on molecular processes. Subsequently, pro-osteogenic cell signaling pathways - especially TGFβ/BMP and Wnt/Ca^{2+} are activated early on the modified surfaces and this probably culminates in an accelerated osteogenic response on the micro-roughened surfaces. Extrinsic modulation of miRNAs, like miR-26a and miR-17 as described in the last part of the project could possibly regulate the cell signaling pathways and help in superior osteogenesis/osseointegration in clinically challenging situations.

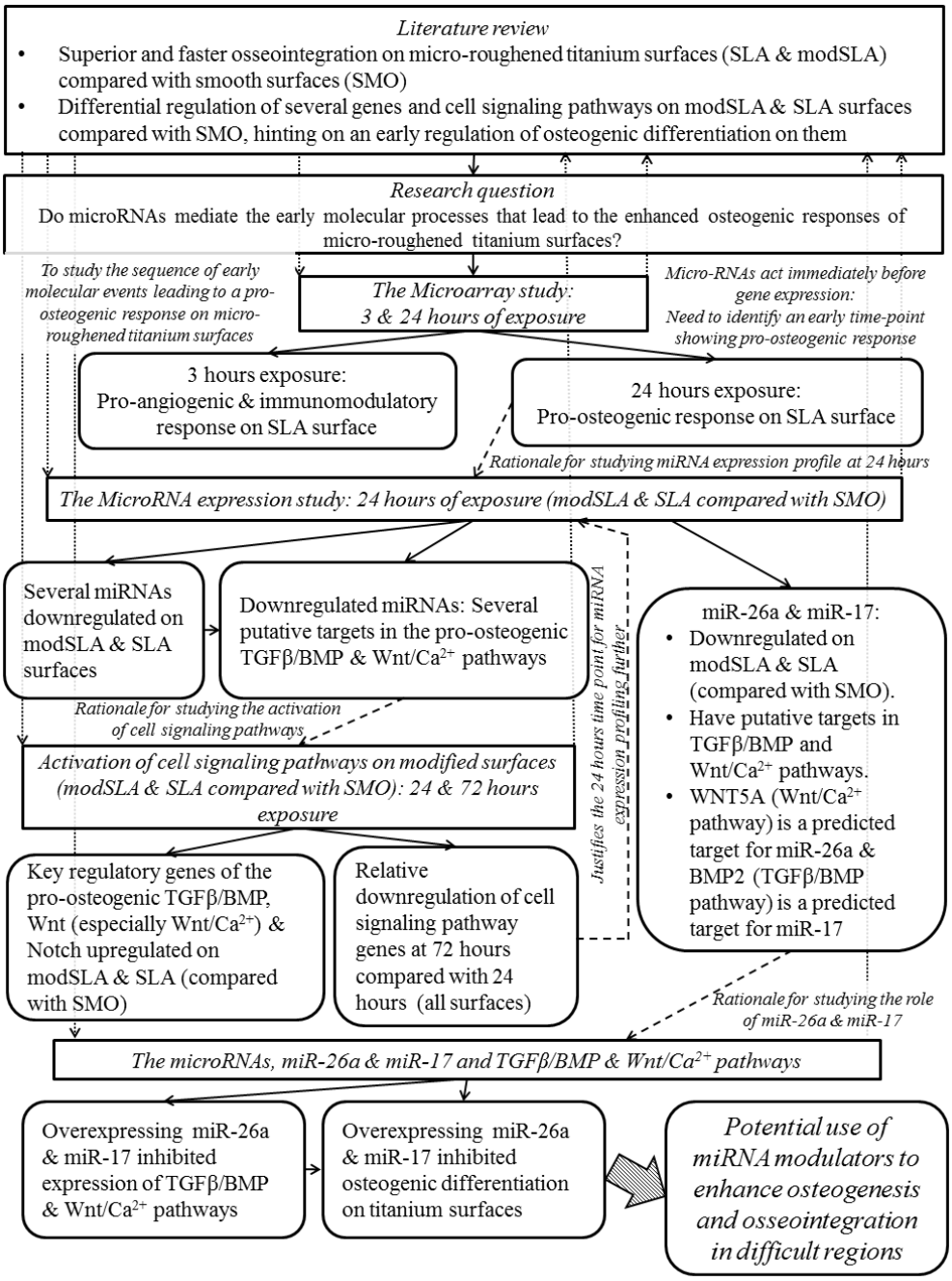

Figure 8-1: Flow-diagram describing the key findings of the project

8.3 LIMITATIONS & FUTURE DIRECTIONS

The findings of this project are based on *in vitro* experimental models using osteogenic cells (osteoprogenitor and osteoblast-like SAOS-2 cells), developed to understand the molecular regulation of osteogenesis as observed in laboratory settings. Osseointegration is a complex biological process that occurs as a culminating event, following the interaction of different types of cells present in the implant bed. The implant bed is populated not only by osteogenic cells (osteoprogenitor, osteoblasts and osteocytes) but also by cells of the hematopoietic origin (osteoclasts and blood cells). The results from this PhD project specifically identify the role of interaction of osteogenic cells with topographically modified implant surfaces. Although, osseointegration, being the process of structural and functional integration of implant surfaces with the surrounding bone, is highly dependent on these interactions, nevertheless we cannot rule out the possible influence of other cells, which may be more important to explain the superior osseointegration of modSLA compared with SLA surfaces as observed in clinical settings. As the primary aim of this project was to understand the pro-osteogenic mechanisms involved in osteogenesis, especially on topographically modified implant surfaces, this project did not focus on the other cell types. Further, it should be noted that the limited range of sample types used (modSLA, SLA and SMO) may restrain the generalization of the conclusions drawn.

Primary osteoprogenitor cells used in the studies were established after culturing redundant tissues obtained following third molar extraction surgery using methods described previously [30]. Using primary cells ensures the use of physiologically relevant cells and it is expect that the data obtained are more pertinent. However, primary cells are prone to inter-subject variability and the observations may vary with different cell types. Nevertheless, the essence of the findings should not be undermined, as they identify some of the critical trends observed as a result of the interactions with implant surfaces and the use of biological replicates made the findings more stringent. Subsequently, the study moved on to investigate the molecular regulation of the cell signaling pathways by microRNAs in human osteoblast-like SAOS-2 cells as primary human osteoprogenitor cells are difficult to transfect and inconsistent in their expression of exogenously administered genes. Moreover, such modulations by external agents are

expected to be consistent in all cell types. This PhD project used synthetic microRNA mimics to study their role in osteogenesis. It may be interesting to study the impact of sustained inhibition of these microRNAs using modalities that can induce stable and persistent transfections.

MicroRNAs are known to have several potential targets and may regulate more than one gene. This project has focused on the influence of miR-26a and miR-17 on the TGFβ/BMP and Wnt/Ca^{2+} pathways. It is possible that these microRNAs have influence on several other genes and proteins that may be important for osteogenesis. One of the future directions should aim for other potential targets of these miRNAs. Besides, miR-26a and miR-17, the microRNA expression profiling study found several other microRNAs that are differentially regulated. Their role in osseointegration remains to be investigated. A special area of focus maybe the miRNAs found to be upregulated on the modSLA and SLA surfaces (compared with SMO), as inhibitors of osteogenesis were found to be putative targets for some of these upregulated miRNAs. Further, pathway analysis of all the predicted targets of the differentially regulated miRNAs could identify other molecular pathways that maybe of significance. The third part of the project found a consistent upregulation of the Notch pathway genes on the modified titanium surfaces. The relevance of this finding has not been explored here. Experimental designs to study the role of Notch pathway in osseointegration and its interactions are needed in the future.

To understand the biological and clinical relevance of the findings of this project, we need to investigate the molecular events in an *in vivo* setting. An animal model for osseointegration, for example a mouse or rat model, needs to be developed in the future to study the modulation of the molecular events. Inhibitors of miR-26a and miR-17 may be used in this model to observe their effects on osseointegration. To study the influence of the TGFβ/BMP and Wnt/Ca^{2+} in an *in vivo* setting, synthetic enhancers (like recombinant BMP2 and WNT5A) and inhibitors (like Dorsomorphin for BMP pathway and KN93 for Wnt/Ca^{2+} pathway) of these pathways maybe used following placement of titanium implants. The *in vivo* animal model will help us in understanding the relevance of the inhibition of miR-26a and miR-17 in a biologically relevant situation and perhaps will be able to lay the foundation for their prospective use in clinical settings.

8.4 REFERENCES

[1] Brånemark R, Brånemark PI, Rydevik B, Myers RR. Osseointegration in skeletal reconstruction and rehabilitation: a review. J Rehabil Res Dev 2001;38:175-81.

[2] Brånemark PI, Hansson BO, Adell R, Breine U, Lindstrom J, Hallen O, et al. Osseointegrated implants in the treatment of the edentulous jaw. Experience from a 10-year period. Scand J Plast Reconstr Surg Suppl 1977;16:1-132.

[3] Wennerberg A, Albrektsson T. Suggested guidelines for the topographic evaluation of implant surfaces. Int J Oral Maxillofac Implants 2000;15:331-44.

[4] Buser D, Schenk RK, Steinemann S, Fiorellini JP, Fox CH, Stich H. Influence of surface characteristics on bone integration of titanium implants. A histomorphometric study in miniature pigs. J Biomed Mater Res 1991;25:889-902.

[5] Gotfredsen K, Wennerberg A, Johansson C, Skovgaard LT, Hjorting-Hansen E. Anchorage of TiO2-blasted, HA-coated, and machined implants: an experimental study with rabbits. J Biomed Mater Res 1995;29:1223-31.

[6] Abdel-Haq J, Karabuda CZ, Arisan V, Mutlu Z, Kurkcu M. Osseointegration and stability of a modified sand-blasted acid-etched implant: an experimental pilot study in sheep. Clin Oral Implants Res 2011;22:265-74.

[7] Buser D, Broggini N, Wieland M, Schenk RK, Denzer AJ, Cochran DL, et al. Enhanced bone apposition to a chemically modified SLA titanium surface. J Dent Res 2004;83:529-33.

[8] Chakravorty N, Ivanovski S, Prasadam I, Crawford R, Oloyede A, Xiao Y. The microRNA expression signature on modified titanium implant surfaces influences genetic mechanisms leading to osteogenic differentiation. Acta Biomater 2012;8:3516-23.

[9] Chakravorty N, Hamlet S, Jaiprakash A, Crawford R, Oloyede A, Alfarsi M, et al. Pro-osteogenic topographical cues promote early activation of osteoprogenitor differentiation via enhanced TGFbeta, Wnt, and Notch signaling. Clin Oral Implants Res 2014;25:475-86.

[10] Osborn J, Newesely H. Dynamic aspects of the implant-bone interface. In: Heimke G, editor. Dental implants: Materials and Systems: München: Carl Hanser Verlag; 1980. p. 111-23.

[11] Berglundh T, Abrahamsson I, Lang NP, Lindhe J. De novo alveolar bone formation adjacent to endosseous implants. Clin Oral Implants Res 2003;14:251-62.

[12] Bartel DP. MicroRNAs: target recognition and regulatory functions. Cell 2009;136:215-33.

[13] Vlacic-Zischke J, Hamlet SM, Friis T, Tonetti MS, Ivanovski S. The influence of surface microroughness and hydrophilicity of titanium on the up-regulation of TGFbeta/BMP signalling in osteoblasts. Biomaterials 2011;32:665-71.

[14] Brett PM, Harle J, Salih V, Mihoc R, Olsen I, Jones FH, et al. Roughness response genes in osteoblasts. Bone 2004;35:124-33.

[15] Dennis G, Jr., Sherman BT, Hosack DA, Yang J, Gao W, Lane HC, et al. DAVID: Database for Annotation, Visualization, and Integrated Discovery. Genome Biol 2003;4:P3.

[16] Ziebart T, Schnell A, Walter C, Kammerer PW, Pabst A, Lehmann KM, et al. Interactions between endothelial progenitor cells (EPC) and titanium implant surfaces. Clin Oral Investig 2013;17:301-9.

[17] Refai AK, Textor M, Brunette DM, Waterfield JD. Effect of titanium surface topography on macrophage activation and secretion of proinflammatory cytokines and chemokines. J Biomed Mater Res A 2004;70:194-205.

[18] Aubin JE, Liu F, Malaval L, Gupta AK. Osteoblast and chondroblast differentiation. Bone 1995;17:77S-83S.

[19] Malaval L, Liu F, Roche P, Aubin JE. Kinetics of osteoprogenitor proliferation and osteoblast differentiation in vitro. J Cell Biochem 1999;74:616-27.

[20] Zhang Y, Andrukhov O, Berner S, Matejka M, Wieland M, Rausch-Fan X, et al. Osteogenic properties of hydrophilic and hydrophobic titanium surfaces evaluated with osteoblast-like cells (MG63) in coculture with human umbilical vein endothelial cells (HUVEC). Dent Mater 2010;26:1043-51.

[21] Schwarz F, Herten M, Sager M, Wieland M, Dard M, Becker J. Histological and immunohistochemical analysis of initial and early subepithelial connective tissue attachment at chemically modified and conventional SLA®titanium implants. A pilot study in dogs. Clin Oral Investig 2007;11:245-55.

[22] Rupp F, Scheideler L, Olshanska N, de Wild M, Wieland M, Geis-Gerstorfer J. Enhancing surface free energy and hydrophilicity through chemical modification of microstructured titanium implant surfaces. J Biomed Mater Res A 2006;76:323-34.

[23] Wall I, Donos N, Carlqvist K, Jones F, Brett P. Modified titanium surfaces promote accelerated osteogenic differentiation of mesenchymal stromal cells in vitro. Bone 2009;45:17-26.

[24] Olivares-Navarrete R, Hyzy SL, Park JH, Dunn GR, Haithcock DA, Wasilewski CE, et al. Mediation of osteogenic differentiation of human mesenchymal stem cells on titanium surfaces by a Wnt-integrin feedback loop. Biomaterials 2011;32:6399-411.

[25] Wang X. A PCR-based platform for microRNA expression profiling studies. RNA 2009;15:716-23.

[26] Witkos TM, Koscianska E, Krzyzosiak WJ. Practical Aspects of microRNA target prediction. Curr Molecular Med 2011;11:93-109.

[27] Donos N, Hamlet S, Lang NP, Salvi GE, Huynh-Ba G, Bosshardt DD, et al. Gene expression profile of osseointegration of a hydrophilic compared with a hydrophobic microrough implant surface. Clin Oral Implants Res 2011;22:365-72.

[28] Ivanovski S, Hamlet S, Retzepi M, Wall I, Donos N. Transcriptional profiling of "guided bone regeneration" in a critical-size calvarial defect. Clin Oral Implants Res 2011;22:382-9.

[29] Ivanovski S, Hamlet S, Salvi GE, Huynh-Ba G, Bosshardt DD, Lang NP, et al. Transcriptional profiling of osseointegration in humans. Clin Oral Implants Res 2011;22:373-81.

[30] Haase HR, Ivanovski S, Waters MJ, Bartold PM. Growth hormone regulates osteogenic marker mRNA expression in human periodontal fibroblasts and alveolar bone-derived cells. J Periodontal Res 2003;38:366-74.

Chapter 9: Concluding Remarks

MicroRNAs are considered important for regulation of gene expression patterns. However, this layer of network for gene regulation during the process of osteogenesis on implant surfaces has received scant attention so far. The findings of this PhD project described an intricate modulation of the molecular pathways by microRNAs following the interaction of osteogenic cells with topographically modified titanium surfaces. The topographical cues from modSLA and SLA surfaces enable us to reveal the microRNAs that get differentially regulated to give rise to the pro-osteogenic effects of these surfaces. Further, the studies confirmed the stimulation of pro-osteogenic TGFβ/BMP and Wnt/Ca^{2+} pathways on these surfaces that lead to their subsequent improved osteogenic differentiation. Finally, the last part of the project discusses the functional studies using miR-26a and miR-17. The study further demonstrates the ability of modulating these miRNAs to induce an early stimulation of the TGFβ/BMP and Wnt/Ca^{2+} pathways and ultimately achieve an accelerated osteogenesis.

This PhD project forms the ground-work to use therapeutic microRNA modulators to improve osseointegration on different types of implant surfaces. Moreover, the pro-osteogenic effects of modSLA and SLA surfaces have enabled us to study the early molecular events during bone formation in an *in vitro* setting (without using chemical supplements) and consequently provided us with important clues regarding the process of bone formation in general. Therefore, this PhD project also reveals potential clinical targets to improve bone formation in compromised conditions.

MicroRNAs are interesting therapeutic targets that have started coming to limelight recently. Modified antisense miRNA oligonucleotides (AMOs) (also known as "antagomirs") are being used for different purposes like gene target validation and experimental therapy models [1] and maybe considered as future therapeutic options to enhance clinical outcomes in orthopedics and implant dentistry. Different types of AMOs are known, however the ones designed with locked nucleic acids (LNAs) have been used to effectively knock-down miRNAs in *in vivo* settings [2]. The use of AMOs provides us with interesting models to work with, especially in animal models for our future studies. Another modality used to inhibit endogenously expressed microRNAs is "microRNA sponge". MicroRNA

sponges are tandem repeats of mRNA binding sites that can act as decoys to which the endogenous microRNAs can bind [2]. The current project findings encourage us to explore the possibility of using microRNA modulators, like antagomirs and/or miRNA sponges that can be coated on to titanium implant surfaces. Implants coated with such modulators with potential to release them in the early phases of healing, may be able to achieve faster osseointegration especially in regions where osseointegration is difficult to achieve, for example the posterior maxilla.

In summary, this PhD project has been able to establish the critical role of microRNAs in the early molecular response of osteoprogenitor cells following exposure to topographically modified titanium surfaces that leads to their improved osteogenicity. Further, the project demonstrated the regulation of the two crucial pro-osteogenic cell signaling pathways (TGFβ/BMP and Wnt/Ca^{2+}) by miR-26a and miR-17 during the process of osteogenic differentiation. It is expected that the results of this project form the ground-work for future research projects to enhance bone formation in general and osseointegration of implant surfaces in specific.

REFERENCES

[1] Davis S, Lollo B, Freier S, Esau C. Improved targeting of miRNA with antisense oligonucleotides. Nucleic Acids Res 2006;34:2294-304.

[2] Hu R, Li H, Liu W, Yang L, Tan YF, Luo XH. Targeting miRNAs in osteoblast differentiation and bone formation. Expert Opin Ther Targets 2010;14:1109-20.

Appendices

Appendix-1:

List of microRNAs profiled using the Human Cell Development & Differentiation miRNA PCR Array (SABiosciences, Frederick, Maryland, USA).
http://www.sabiosciences.com/mirna_pcr_product/HTML/MAH-103A.html

miR-106b	miR-488	miR-214	miR-133b
let-7e	miR-215	miR-21	miR-520g
miR-20b	miR-24	miR-18b	miR-33a
miR-125a-5p	miR-192	miR-345	miR-124
miR-125b	miR-18a	let-7c	miR-208a
miR-122	miR-100	miR-26a	miR-142-5p
miR-155	miR-9	miR-101	miR-370
miR-126	miR-137	miR-17	miR-150
miR-22	miR-452	miR-129-5p	miR-128
miR-92a	miR-15a	miR-96	miR-15b
miR-141	miR-134	miR-183	miR-130a
miR-378	miR-103	miR-210	miR-127-5p
miR-10a	miR-424	miR-223	miR-498
miR-182	miR-20a	let-7a	let-7b
miR-302a	let-7i	miR-518b	miR-302c
miR-93	miR-222	miR-194	miR-219-5p
miR-1	miR-99a	miR-503	let-7g
miR-181a	miR-206	miR-218	miR-375
miR-146b-5p	miR-195	let-7d	miR-7
let-7f	miR-132	miR-205	miR-146a
miR-196a	miR-16	miR-10b	miR-371-3p
miR-301a	miR-23b	miR-185	miR-142-3p

Appendix-2:

Signal transduction genes profiled using the Human Stem Cell Signaling PCR Array (SABiosciences, Frederick, Maryland, USA).
http://www.sabiosciences.com/rt_pcr_product/HTML/PAHS-047A.html

Pluripotency Maintenance Pathway:
Receptors: IL6ST (GP130), LIFR.
Transcription Factor: STAT3.

Fibroblast Growth Factor (FGF) Signaling Pathway:
Receptors: FGFR1, FGFR2, FGFR3, FGFR4.
Transcription Factor: CDX2.

Hedgehog Signaling Pathway:
Receptors & Co-Receptors: PTCH1, PTCHD2, SMO.
Transcription Factors & Co-Factors: GLI1, GLI2, GLI3, SUFU.

Notch Signaling Pathway:
Receptors & Co-Receptors: NCSTN, NOTCH1, NOTCH2, NOTCH3, NOTCH4, PSENEN, PSEN1, PSEN2.
Transcription Factor: RBPJL.

TGFβ Superfamily Signaling Pathway:
Receptors & Co-Receptors: ACVRL1, ACVR1, ACVR1B, ACVR1C, ACVR2A, ACVR2B, AMHR2, BMPR1A, BMPR1B, BMPR2, ENG, LTBP1, LTBP2, LTBP3, LTBP4, RGMA, TGFBR1, TGFBR2, TGFBR3, TGFBRAP1.
Transcription Factors & Co-Factors: EP300, SMAD1, SMAD2, SMAD3, SMAD4, SMAD5, SMAD6, SMAD7, SMAD9, CREBBP, E2F5, RBL1, RBL2, SP1, ZEB2.

Wnt Signaling Pathway:
Receptors: FZD1, FZD2, FZD3, FZD4, FZD5, FZD6, FZD7, FZD8, FZD9, LRP5, LRP6, VANGL2.
Transcription Factors & Co-Factors: BCL9, BCL9L, CTNNB1, LEF1, NFAT5, NFATC1, NFATC2, NFATC3, NFATC4, PYGO2, TCF7L1, TCF7L2, TCF7.